Geol.

JOURNAL OF PETROLOGY

VOLUME 1 NUMBER 3

OCTOBER 1960

OXFORD AT THE CLARENDON PRESS

JOURNAL OF PETROLOGY

Editors

T. F. W. BARTH (Oslo); C. E. TILLEY (Cambridge)
L. R. WAGER (Oxford); H. S. YODER (Washington)

Managing Editors

G. M. BROWN (Oxford); S. R. NOCKOLDS (Cambridge)

Honorary Advisory Board

C. R. BURRI (Zürich)
C. W. CORRENS (Göttingen)
H. VON ECKERMANN (Stockholm)
A. B. EDWARDS (Melbourne)
P. ESKOLA (Helsinki)
L. HAWKES (London)
I. E. HAWLEY (Kingston, Ont.)
H. H. HESS (Princeton)
D. S. KORZHINSKY (Moscow)
H. KUNO (Tokyo)
W. T. PECORA (Washington)
E. RAGUIN (Paris)
H. H. READ (London)
A. RITTMANN (Catania)
F. J. TURNER (Berkeley, Calif.)

It is the aim of the editors to provide, in the *Journal of Petrology*, a place for the publication of original researches in the whole range of subjects which fall within a liberal definition of petrology. The subjects will thus include the physics and chemistry of rocks, their mineralogy and textures, and certain aspects of petrology which involve the dating of rocks by natural radioactivity. Quantitative studies of rock-forming minerals, experimental physical chemistry relevant to petrology, and parts of isotope geology, will appropriately find a place. Regional studies, unless they lead to results fundamental to the science of petrology, will not usually be considered suitable to the journal.

The journal is being published at first in 400-page volumes consisting of three numbers per year, in February, June, and October. The subscription price for three consecutive numbers is 80*s*. ($12 in the U.S.A. and Canada), post free. Single numbers cost 30*s*. net. Orders may be placed with any bookseller or sent direct to the publishers.

OXFORD UNIVERSITY PRESS

AMEN HOUSE · LONDON · E.C.4

The Geochemistry of Scapolite

Part II. Trace Elements, Petrology, and General Geochemistry

by DENIS M. SHAW

Department of Geology, McMaster University, Hamilton, Ontario, Canada

ABSTRACT

Fifty scapolites have been analysed spectrographically for numerous elements. Average concentrations (p.p.m.) were as follows: B 25, Be 9·3, Ga 33, Ti 82, Li 56, Cu 4·4, Zr 59, Mn 57, Sr 1,800, Pb 45, Ba 120, Rb 20. The following were seldom or never detected: Cr, Ni, Co, Mo, Sn, V, Sc, Ag, Y, La. The major elements Ca, Na, K were also determined. The distribution of the trace elements can be explained by isomorphous substitution, but no detailed correlation of trace elements with each other or with major elements was found.

Refractive indices were determined and the relation between average index and per cent Me was examined: correlation was poor, which may in part be attributed to analytical error.

Examination of scapolite parageneses shows that scapolite characteristically occurs in the upper amphibolite facies or the pyroxene hornfels facies: it is not restricted to these and may occur in any facies from zeolitic to granulitic and in any hornfels facies. The elements generally concentrated in scapolite include Ca, Na, C, Cl, S, H, B, Be, Li, Sr, Pb. The presence of C, Cl, S, H testify to genesis in the presence of high partial pressure of CO_2, Cl_2, SO_3, H_2O (or related compounds), that is in pneumatolytic, pegmatitic, or hydrothermal environments. The concentration of B, Be, Li can also be attributed to these conditions.

The source of the elements concentrated in scapolite must in part be common rocks. In a limited contact zone, the nearby magma supplied some elements, but where regional scapolitization has taken place the presence of magma is less clear. Many common rocks or rock series contain all the necessary constituents, but some particular conjunction of conditions is necessary for scapolite to form, or it would be more common.

INTRODUCTION

THE general mineralogy and major element composition of the scapolite family was discussed in Part I (this *Journal*, pp. 218–60). In the present paper the results of spectrographic analysis of about 50 scapolites for certain major, minor, and trace elements will be discussed, with a concluding section devoted to problems of general geochemistry and petrology. Author references not included in the bibliography at the end of this paper were given in Part I.

TRACE AND MAJOR ELEMENTS

Analytical methods

Five different spectrographic methods were used, all making use of the Stallwood jet. They will be referred to as follows:

(i)	Palladium–graphite method	Shaw (in press)
(ii)	Argon–oxygen method	Shaw, Wickremasinghe, & Yip (1958)
(iii)	Caesium carbonate method	Shaw, Wickremasinghe, & Weber (1960)
(iv)	Lithium carbonate method	Filby (1957)
(v)	Lanthanum–graphite method	Shaw (1957*a*)

[Journal of Petrology, Vol. 1, Part 3, pp. 261–85, 1960]

0233.3

Each method except the last was developed specifically for the analysis of scapolite, but they have also proved satisfactory for the analysis of a wide variety of silicate minerals and rocks. The equipment and certain steps in the procedure were the same in each method and are summarized in the following.

The spectrograph was a Jarrel-Ash Co. 21-ft grating instrument, Wadsworth mount, using the first-order spectrum with dispersion of 5·2 Å/mm. The sample

TABLE 1

Spectral line symbols and wavelengths

Element	*Å*	*Int. std.*	*E* (%)	*G*-1 (p.p.m.)	*W*-1 (p.p.m.)	*Element*	*Å*	*Int. std.*	*E* (%)	*G*-1 (p.p.m.)	*W*-1 (p.p.m.)
B	2497·733	Pd *B*	19	nd	tr	Mn *A*	2576·104	Pd *B*	—	—	—
Be *A*	2348·610	Pd *B*	—	tr	nd	Mn *B*	2801·064	Pd *A*	11	200	—
Be *B*	3131·072	Pd *B*	14	tr	nd	Mn *C*	3212·884	Pd *A*	9	300	780
Ga *A*	2943·637	Pd *A*	12	16	8	Y *A*	3216·682	Pd *A*	13	—	—
Ga *B*	2943·637	In *A*	—	37	26	Y *B*	3242·280	Pd *A*	11	—	—
Ga *C*	4172·056	In *A*	—	30	29	Na *A*	3302·323	In *B*	5	3·44%*	2·10%*
Cr	4254·346	Pd *A*	14	tr	100	Na *B*	6160·760	Cs	9	3·27%*	—
Mg *A*	2776·690	Pd *A*	9	2,100	—	Na *C*	8183·270	Cs	—	—	—
Mg *B*	2781·417	Pd *A*	12	2,100	—	Ca	4302·527	La	6	—	—
Ti *A*	3349·406	Pd *A*	9	—	—	Sr *A*	4607·331	Pd *A*	13	250	150
Ti *B*	3354·635	Pd *A*	11	—	—	Sr B‡	4607·331	La	—	290	255
Ti *C*	3321·588	Pd *A*	8	1,500	5,200	Sr C§	4607·331	La	—	—	—
Ti *D*	3346·728	Pd *A*	6	1,300	5,000	Pb *A*	3683·471	In *A*	—	54	tr
Li *A*	3232·610	In *A*	—	—	—	Pb *B*	4057·820	In *A*	—	58	tr
Li *B*	6707·844	Cs	5	26	12	K *A*	4044·140	In *B*	10	5·66%‖	—
Li *C*	6103·642	Cs	—	—	—	K *B*	6938·980	Cs	5	7·4%‖	—
Ni	3414·765	Pd *A*	8	tr	54	K *C*	7698·979	Cs	—	—	—
Mo	3193·973	Pd *A*	12	tr	nd	Ba *A*	4554·042	Pd *A*	13	—	120
Cu *A*	3273·962	Pd *A*	15	9·5	—	Ba *B*‡	4554·042	La	—	1,150	170
Cu *B*	3273·962	In *A*	—	15	—	Ba C§	4554·042	La	—	—	—
Zr	3391·975	Pd *A*	14	145	86	Rb	7800·227	Cs	5	283	24

Pd *A* 3258·780 Å
Pd *B* 2476·418
In *A* 3256·090
In *B* 2932·624 Å
La 4920·971
Cs 6983·488

* Na_2O. † CaO. ‡ Analyst R. H. Filby. § Analyst D. M. Shaw. ‖ K_2O.

was tamped in a plain crater (1·5 by 6 mm) graphite electrode (National Carbon Co., 'Special' Grade) of $\frac{1}{8}$-in. diameter, which was burned as the anode. The counter-electrode was a similar $\frac{1}{8}$-in. graphite rod. The arc-gap was 5 mm and the d.c. potential on open circuit was 230 V. The arc was focused on the slit (width 30 μ) using a standard optical system consisting of a spherical lens, a diaphragm of 1-cm aperture serving as a secondary source, and a pair of crossed cylindrical lenses. A rotating step-sector with log intensity ratio 0·2 was adjacent to the slit. The Eastman–Kodak plates were developed for 3 min (types S.A. 1 and III-F) or 4 min (types I-L and I-N) in D-19 developer at 20° C. Line blackness and background were measured on an A.R.L. densitometer. Plate calibration curves were constructed for each spectral line. Calculations of the ratio of log intensity analysis line to internal standard line (corrected for background), referred to as dY, were made on a conventional calculating board. Samples were analysed in triplicate, with one exposure on each of three pairs of plates.

Other details and spectral lines used are given in Tables 1 and 2, where lines have been given suffixes *A*, *B*, &c., to prevent confusion. To construct the working curves several series of artificial standards were made using Johnson–Matthey 'Specpure' chemicals: these standards approximated in bulk composition to scapolite or granite, and contained from 3 to 1,000 p.p.m. of trace elements, and greater amounts of more abundant elements. In the case of major elements, analysed natural materials (G-1, W-1, N.B.S. Standards, analysed minerals) were used as well as synthetic standards wherever possible.

TABLE 2

Spectrographic procedures

	Pd–*graphite method*	*Argon–oxygen method*	Cs_2CO_3 *method*	Li_2CO_3 *method*	La–*graphite method*
Slit length	6 mm	4 mm	11 mm	5 mm	6 mm
Intensity reduction screens*	one	none	none	none	one
Filter	none	none	Corning No. 3486 yellow	none	none
Current (A)	6½†	6	5	6½†	7†
Exposure (sec.)	85	95	100	120	80
Gas	air	argon/oxygen = 1/1	air	air	air
Gas flow rate	1 l./min	5 l./min	1 l./min	1 l./min	1 l./min
Emulsion and range	SA-1 2,200–3,550 Å III-F 3,550–4,900 Å	SA-1 2,900–4,250 Å	I-L or I-N 5750–8,250 Å	III-F 2,900–4,200 Å	III-F 3,900–5,200 Å
Sample	1 part mineral to 1 part graphite containing 0·1 per cent $PdCl_2$	5 parts mineral, 1 part graphite, and 4 parts KCl containing 0·025 per cent In_2O_3	2 parts mineral, 1 part Cs_2CO_3, 1 part graphite	1 part mineral, 9 parts Li_2CO_3 containing 1% In_2O_3	1 part mineral, 9 parts of a mixture of graphite, KCl, La_2O_3 in ratio 1885/100/15
Internal standard lines	Pd *A* 3258·780Å Pd *B* 2476·418 Å	In *A* 3256·090Å	Cs 6983·488 Å	In *B* 2932·624 Å	La 4920·971 Å
Elements determined	B, Be, Ga, Cr, Mg, Ti, Ni, Mo, Cu, Zr, Mn, Y, Sr, Ba	Ga, Li, Cu, Pb	Li, Na, K, Rb,	Na, K	Ca, Sr, Ba
Other elements sought	Li, Sn, Co, V, Sc, Ag, La	Sn			

* One, two, or three 100-mesh screens could be used for intensity reduction, in addition to the step-sector.

† Current started at 3½ A and increased during the first 10 sec of arcing.

Reproducibility was usually evaluated in terms of the relative error (*E*), i.e. the ratio of the standard deviation for triplicate analysis to the amount present, expressed in per cent. The figures obtained are included in Table 1 and range from about 4 to 23 per cent, averaging perhaps 10 per cent. Values of *E* were not calculated in method (ii) but were probably a little better than 10 per cent. Wherever possible the standard rocks G-1 and W-1 were analysed to check accuracy: the results (averages of at least 8 runs) are also included in Table 1, and will be discussed in the following. It may be noted here that in general the

TABLE 3

Element determinations using more than one spectral line

	Be			Ga				Mg			Ti				
	A	*B*	*R*	*A*	*B*	*C*	*R*	*A*	*B*	*R*	*A*	*B*	*C*	*D*	*R*
CA 1	3·2	5·4	5·4	17·0	51	31·0	29·0	4,500	4,200	4,350	tr	78			78·0
CA 30	1·1	1·6	1·6	12·0	47	42·0	28·0	1,300	1,250	1,280	45·0	55			50·0
CA 51	14·0	18·0	18·0	48·0	88	99·0	71·0	440	370	410	9·5				9·5
CA 56	5·1	8·2	8·2	23·0	63	47·0	39·0	490	520	510		110			110·0
CA 61	3·8	6·2	6·2	20·0	53	55·0	37·0	2,100	1,950	2,000	*†				*
CA 63 A	3·6	6·8	6·8	21·0	47	37·0	32·0	640	640	640	21·0				21·0
CA 74 B	4·3	7·7	7·7	15·0	62	34·0	32·0	500	520	510	*				*
CA 83	2·2	3·9	3·9	15·0	49	30·0	27·0	2,300	2,250	2,300	24·0				24·0
Q 7	3·6	4·5	4·5	9·0	31	12·0	15·0	1,800	1,800	1,800		87			87·0
Q 11 A	3·6	6·5	6·5	21·0	60	43·0	36·0	1,900	2,000	2,000	27·0	tr			27·0
Q 12 B	3·0	4·4	4·4	18·0	55	42·0	33·0	1,250	1,300	1,300	36·0	36·0			36·0
Q 13 A	3·7	6·9	6·9	17·0	56	66·0	39·0	310	310	310	*				*
Q 16 D	4·2	8·4	8·4	16·0	36	64·0	33·0	120	tr	120		110			110·0
Q 19 D	4·0	5·0	5·0	26·0	63	41·0	39·0	210	190	200	38·0	47			43·0
Q 23 F	2·2	2·2	2·2	22·0	45	61·0	38·0	220	210	220	44·0	60			52·0
Q 24	35·0	37·0	37·0	31·0	80	78·0	55·0	1,100	1,150	1,150	39·0	48			44·0
Q 24 C	21·0	34·0	34·0	27·0	83	72·0	52·0	290	260	280	45·0	47			46·0
Q 26	13·0	24·0	24·0	44·0	108		65·0	tr	tr	tr	12·0				12·0
Q 27	8·6	10·0	10·0	26·0	63	55·0	43·0	3,500	3,100	3,300	tr				tr
Q 30	5·2	8·6	8·6	26·0	93	84·0	57·0	3,200	2,900	3,100	11·0				11·0
Q 31 B	5·4	9·6	9·6	22·0	70	69·0	46·0	1,100	1,100	1,100	20·0				20·0
Q 31 C	4·6	7·0	7·0	29·0	93	54·0	51·0	620	580	600		540	490	530	520·0
Q 85	5·4	8·4	8·4	7·8	41	22·0	20·0		1·1%	1·1%	32·0				32·0
Q 87 A	5·6	6·9	6·9	34·0	73	40·0	45·0	1,550	1,500	1,550	tr				tr
M 728	17·0	25·0	25·0	21·0	60	36·0	35·0	590	580	590		640	590	540	590·0
M 730	0·9	tr	0·9	6·4	29	12·0	13·0	3,500	4,000	3,800		320	170	210	230·0
M 731	4·9	8·4	8·4	13·0	40	42·0	27·0	600	620	610	35·0	36			36·0
M 733	*	*	*	21·0	49	53·0	36·0	1,550	1,600	1,600	9·9				9·9
M 1162	2·9	4·8	4·8	6·0	31	35·0	20·0	310	250	280		100	120	90	100·0
A	2·3	4·1	4·1	2·9	20	7·0	8·2	510	530	520		130			130·0
B	8·1	6·6	6·6	26·0	65	88·0	51·0	540	540	540		480	420	460	450·0
ON 1	5·7	9·0	9·0	9·8	33	21·0	18·0	3,000	2,850	2,900	11·0				11·0
ON 3 B	3·0	5·1	5·1	21·0	68	44·0	39·0	1,000	1,000	1,000	51·0	60			56·0
ON 4	7·4	11·0	11·0	8·3	31	26·0	18·0	4,100	3,800	4,000	11·0				11·0
ON 5	4·8	5·6	5·6	15·0	35	38·0	26·0	310	300	310	31·0	32			32·0
ON 6	16·0	29·0	29·0	36·0	87	48·0	52·0	tr	tr	tr	11·0				11·0
ON 7	2·7	4·5	4·5	14·0	41	51·0	30·0	1,050	1,000	1,000	tr				tr
ON 8	0·5	tr	tr	9·8	28	16·0	16·0	100	tr	100	tr				tr
ON 20	4·5	7·6	7·6	15·0	43	38·0	28·0	250	tr	250	tr				tr
ON 27	3·0	3·4	3·4	27·0	51	33·0	35·0	350	tr	350		120			120·0
ON 28	1·9	3·8	3·8	4·7	20	24·0	13·0	tr	tr	tr	18·0				18·0
ON 29	11·0	20·0	20·0	15·0	59	46·0	34·0	930	970	950	36·0	30			33·0
ON 37	2·1	2·9	2·9	29·0	76	76·0	53·0	2,150	2,100	2,100	21·0				21·0
ON 44	—‡	—	—	—	—	—	—	—	—	—	—	—	—	—	—
ON 45	20·0	28·0	28·0	2·9	9	12·0	6·7	730	670	700		120	100		110·0
ON 47	2·1	3·5	3·5	tr	12	16·0	14·0	340	300	320	75·0	68			72·0
ON 48	17·0	22·0	22·0	13·0			13·0	100		100	10·0				10·0
ON 49	4·8	7·2	7·2	8·5	24	31·0	18·0	tr	tr	tr	21·0				21·0
ON 50	1·9	3·4	3·4	3·2	21	25·0	13·0	tr	tr	tr	36·0	31·0			34·0
ON 53		1·4	1·4	6·2	16	18·0	12·0	610	540	580		600	510	650	590·0

All figures are averages of triplicate analyses, and are expressed in p.p.m., except for Na and K which are in weight per cent. † means not detected. ‡ means not determined.

TABLE 3 (*contd.*)

	Li				Cu			Mn				Y		
	A	*B*	*C*	*R*	*A*	*B*	*R*	*A*	*B*	*C*	*R*	*A*	*B*	*R*
CA 1	69		44	44·0	tr	3·0	2·0	57	79		68	*†	*	*
CA 30	96		57	57·0	2·9	6·0	4·5	27	43		35	*	*	*
CA 51	120		84	84·0	tr	1·0	1·0	28	46		37	*	*	*
CA 56	57	30·0		30·0	2·0	5·0	3·5	47	50		49	*	*	*
CA 61	93			93·0	1·8	12·0	6·9	36	47		52	*	*	*
CA 63 A	81		58	58·0	2·6	5·0	3·8	43	58		51	*	*	*
CA 74 B	110		82	82·0	2·5	6·0	3·8	60	81		71	*	*	*
CA 83	100		64	64·0	1·7	5·0	3·4	43	59		51	*	*	*
Q 7	tr	26·0		26·0	2·6	4·0	3·3	40	52		46	*	*	*
Q 11 A	tr	12·0		12·0	1·1	4·5	2·8	42	39		41	*	*	*
Q 12 B	57	24·0		24·0	2·2	5·0	3·6	26	39		33	*	*	*
Q 13 A	tr	21·0		21·0	1·7	5·0	3·4	33	30		32	*	*	*
Q 16 D	57	41·0		41·0	1·1	2·0	1·6	39	39		39	*	*	*
Q 19 D	62	50·0		50·0	1·3	3·0	2·2	27	40		34	*	*	*
Q 23 F	tr	36·0		36·0	tr	1·0	1·0	46	79		63	*	*	*
Q 24	80			80·0	14·0	33·0	24·0	82	105		94	4·3	tr	4·3
Q 24 C	110			110·0	5·5	12·0	8·8	64	83		74	*	*	*
Q 26	160		100	100·0	tr	1·7	1·4	48	65		57	*	*	*
Q 27	tr	24·0		24·0	1·5	3·0	2·3	94	100		97	*	*	*
Q 30	120		64	64·0	1·1	3·0	2·1	40	48		44	*	*	*
Q 31 B	100		50	50·0	4·3	6·0	5·2	37	35		36	*	*	*
Q 31 C	120		56	56·0	1·1	6·0	3·6	28	42		35	13·0	tr	13·0
Q 85	tr		53	53·0	1·4	3·0	2·2	78	87		83	9·0	7·5	8·3
Q 87 A	tr	24·0		24·0	2·4	4·0	3·2	25	48		37	*	*	*
M 728		17·0		17·0	3·1	8·0	5·6	36	30		33	*	*	*
M 730	tr		35	35·0	3·3	9·0	6·2	44	54		49	*	*	*
M 731	tr	27·0		27·0	2·0	5·0	3·5	49	58		54	*	*	*
M 733	120		71	71·0	3·0	6·0	4·5	20	33		27	*	*	*
M 1162	tr	13·0		13·0	3·0	7·0	5·0	48	56		52	*	*	*
A	tr		35	35·0	2·2	5·0	3·6	78	73		76	*	*	*
B	tr		86	86·0	2·7	7·0	4·9	38	56		47	11·0	tr	11·0
ON 1	tr	8·2		8·2	tr	4·0	2·5	13	26		20	*	*	*
ON 3 B	65	20·0		20·0	tr	4·0	2·5	44	73		59	*	*	*
ON 4	tr	8·8		8·8	tr	2·0	1·5	19	30		25	*	*	*
ON 5		5·2		5·2	tr.	1·0	1·0	68	100		84	3·6	2·2	2·9
ON 6	170		185	185·0	2·6	6·0	4·3	38	47		43	*	*	*
ON 7	130		115	115·0	tr	3·0	2·0	42	60		51	*	*	*
ON 8	tr		50	50·0	8·3	17·0	13·0			160	160	3·8	4·6	4·2
ON 20	160		106	106·0	5·2	8·0	6·6	22	18		20	*	*	*
ON 27	52	30·0		30·0	3·0	4·0	3·5	41	42		42	*	*	*
ON 28	tr	45·0		45·0	tr	3·0	3·0	165	130		150	*	*	*
ON 29	370		235	240·0	1·8	6·0	3·9	42	43		43	*	*	*
ON 37	84	33·0		33·0	12·0	28·0	20·0	46	74		60	*	*	*
ON 44	—‡	—	—	—	—	—	—	—	—	—	—	—	—	—
ON 45	tr	2·5		2·5	2·3	4·0	3·2	50	48		49	*	*	*
ON 47	tr	20·0		20·0	1·3	8·0	4·7	48	42		45	*	*	*
ON 48			160	160·0	2·8		2·8	140	170		160	*	*	*
ON 49	tr		52	52·0	2·1	5·0	3·6		> 200		> 200	3·2	3·1	3·2
ON 50	tr		50	50·0	tr	4·0	4·0		> 200		> 200	*	*	*
ON 53	tr		45	45·0	tr	3·0	3·0	70			70	*	*	*

All figures are averages of triplicate analyses, and are expressed in p.p.m., except for Na and K which are in weight per cent. † means not detected. ‡ means not determined.

TABLE 3 (*contd.*)

	Na			Sr				Pb			Ba				K		
	A	*B*	*R*	*A*	*B*	*C*	*R*	*A*	*B*	*R*	*A*	*B*	*C*	*R*	*B*	*C*	*R*
CA 1	5·2	4·0	4·6		2,500	2,500	2,500	26	24	25	79	130	82	82			—
CA 30	5·8	4·4	5·1		2,100	1,900	1,900	99	92	96		185	150	150		0·45	0·45
CA 51	7·5	6·4	7·0	550	720	780	780	26	23	25	130	70	87	87	1·4	0·69	1·0
CA 56	4·3	3·5	3·9		2,550	2,700	2,700	54	47	51	70	115	90	80		0·37	0·37
CA 61	6·9	—‡	6·9		1,650	1,450	1,450	52	45	49		385	400	400			—
CA 63A	5·8	5·6	5·7		3,200	2,900	2,900	47	42	45	100	190	130	120	1·7	0·86	1·3
CA 74B	4·8	3·5	4·2		2,500	2,500	2,500	72	61	67	120	270	210	210		0·39	0·39
CA 83	4·9	3·7	4·3		2,700	2,600	2,600	69	68	69		170	130	130		0·58	0·58
Q 7	3·6	3·6	3·6		2,250	2,100	2,100	110	100	105	16	64	30	23		0·35	0·35
Q 11 A	6·8	4·0	5·4		2,900	2,900	2,900	10	7	9	120	160	160	160		0·44	0·44
Q 12 B	3·7	3·1	3·4		2,700	2,600	2,600	68	73	71	57	130	100	80		0·37	0·37
Q 13 A	5·8	3·5	4·7		2,050	2,000	2,000	23	22	23	58	88	58	58	1·2	0·78	1·0
Q 16 D	5·9	5·2	5·6		2,350	2,200	2,200	14	tr	tr	54	90	65	60	1·7	0·71	1·2
Q 19 D	6·6	4·4	5·5		1,800	1,700	1,700	92	93	93	70	120	93	82	1·6	0·86	1·2
Q 23 F	3·9	2·8	3·4		6,000	3,100	3,100	95	93	94		185	150	150		0·58	0·58
Q 24	—	—	—	340			340	52	47	50	17			17			—
Q 24 C	5·4	—	5·4	240	400	320	280	35	33	34	14	31	14	14			—
Q 26	5·3	3·7	4·5		1,450	1,600	1,600	50	47	49	100	110	98	99	2·3	0·66	1·5
Q 27	5·4	6·4	5·9		1,250	1,100	1,100	69	54	62	28	59	34	31	2·2	0·66	1·4
Q 30	5·5	5·2	5·4	440	1,200	1,050	1,050	27	14	21	60	135	100	80	1·2	1·1	1·2
Q 31 B	6·9	5·2	6·1		1,300	1,150	1,150	25	20	23	55	82	61	58	1·4	0·95	1·2
Q 31 C	6·2	4·2	5·2		1,800	1,300	1,300	tr	tr	tr	90	140	98	98		0·51	0·51
Q 85	—	2·8	2·8		2,600	3,300	3,300	107	90	99	73	77	98	86	1·5	0·37	0·93
Q 87 A	4·9	3·6	4·3		3,500	3,700	3,700	38	33	36	43	70	51	47	1·5	0·76	1·1
M 728	3·2	2·3	2·8	440	820	1,150	1,150	57	52	55	27	54	24	26		0·32	0·32
M 730	2·2	1·1	1·7		1,060	920	920	*†	*	*		110	95	95	2·0	0·76	1·4
M 731	6·6	3·7	5·2		2,200	2,500	2,500	80	77	79		260	240	240	1·6	0·71	1·2
M 733	6·0	7·8	6·9		—	2,800	2,800	11	14	13			145	145	1·7	0·71	1·2
M 1162	4·5	4·0	4·3		2,500	2,200	2,200	48	43	46		390	350	350		0·45	0·45
A	2·7	1·2	2·0		3,550	5,100	5,100	70	61	66	115	120	120	120		0·37	0·37
B	4·4	2·0	3·2	200			200	67	66	67	10	20		10			—
ON 1	6·2	6·2	6·2		1,100	1,350	1,350	34	37	36		700	580	580	1·7	0·86	1·3
ON 3 B	6·0	5·1	5·6		2,200	2,800	2,800	40	38	39		375	170	170		0·91	0·91
ON 4	7·7	6·4	7·1		2,100	1,900	1,900	35	31	33		490	560	560	1·9	0·61	1·3
ON 5	5·8	6·7	6·3		3,300		3,300	17	14	16	110	180		150	1·2		1·2
ON 6	6·4	5·6	6·0	470	1,400	950	950	36	29	33	65	93	62	64	1·0	0·61	0·80
ON 7	6·3	5·6	6·0		2,450	2,900	2,900	53	48	51		270	180	180	0·91	0·86	0·89
ON 8	8·7	8·9	8·8	125			125	115	110	110	19	20		19	2·2	1·2	1·7
ON 20	3·6	2·0	2·8		1,360	1,350	1,350	21	17	19	83	125	90	87	1·7	0·63	1·2
ON 27	3·9	2·4	3·2		1,700	1,500	1,500	12	9	11		210	170	170		0·48	0·48
ON 28	—	4·4	4·4			1,250	1,250	83	91	87			115	115		0·44	0·44
ON 29	2·2	1·4	1·8	100			100	12	10	11	7·7	20	10	10		0·32	0·32
ON 37	5·5	6·2	5·9	350	830	600	600	49	34	42	31	51	31	31		0·71	0·71
ON 44	—	—	—	—	—	tr	tr	—	—	—			tr	tr			—
ON 45	—	0·64	0·64		—	1,250	1,250	tr	tr	tr			115	115		0·41	0·41
ON 47	—	1·1	1·1		—	1,800	1,800	16	13	15			280	280		0·27	0·27
ON 48	—	1·7	1·7		—	2,000	2,000	—	—	—	18		36	27		0·08	0·08
ON 49	—	3·3	3·3		—	920	920	49	50	50	38		48	43		0·58	0·58
ON 50	—	4·6	4·6		—	1,200	1,200	71	74	73			110	110		0·37	0·37
ON 53	—	1·8	1·8	760	—		760	tr	tr	tr	40			40		0·10	0·10

All figures are averages of triplicate analyses, and are expressed in p.p.m., except for Na and K which are in weight per cent. † means not detected. ‡ means not determined.

results agree fairly well with other estimates: they are usually better on G-1, which is to be expected because the spectrographic standards were close to granite in composition.

Where an element was determined by more than one method or line the results are given in Table 3: the results from different estimations do not always agree as well as might be wished, because of experimental bias. The representative value (*R* in Table 3) was an average, a weighted average, or was obtained by a choice. Wherever possible *R* was obtained after assessment of the results on G-1

TABLE 4

Comparison of chemical and spectrographic analyses for Mg, Ti, Mn (*p.p.m.*), Na_2O, *and* K_2O (*wt. per cent*)

Element	*XXX* M 730	*XXXI* Q 85	*XXXII* Q 19 D	*XXXIII* Q 87 A	*XXXIV* ON 6 A	*XXXV* ON 8
Mg (chem.)	2,770	6,030	121	1,085	181	181
Mg (spec.)	3,800	11,000	200	1,500	tr	100
Ti (chem.)	420	180	180	120	60	60
Ti (spec.)	230	32	43	tr	11	tr
Mn (chem.)	80	80	tr	tr	nd	80
Mn (spec.)	49	83	34	37	43	160
Na_2O (chem.)	2·44	3·82	6·40	6·86	8·55	10·50
Na_2O (Na *A*)	3·0	—	8·9	6·6	8·6	11·7
Na_2O (Na *B*)	1·45	3·7	5·9	4·9	7·6	12·0
K_2O (chem.)	2·21	1·01	1·16	0·87	1·08	1·16
K_2O (K *C*)	0·92	0·60	1·04	0·92	0·74	1·45
K_2O (K *B*)	2·4	1·8	1·9	1·8	1·2	2·6

The analysis numbers XXX–XXXV refer to the data of Table 7 in Part I.

and W-1, compared with the best estimates of other workers (taken from a compilation kindly made available by Dr. M. Fleischer, U.S. Geological Survey). The *R* values are included in Table 6 along with results for elements on which only one line was used. Brief discussion of some elements follows.

Be. The reproducibility for Be *A* was much inferior to Be *B* and the working curve showed less sensitivity. The chosen value is Be *B*.

Ga. The results on Ga *B* and *C* are always about 2 or 3 times those on *A*. The probable Ga contents of G-1 and W-1 (20 and 15 p.p.m.), however, are closer to the results on *A*. The representative value was accordingly taken as the weighted average $(2A+B+C)/4$.

Cr. Estimates of Cr in G-1 and W-1 are 8–60 p.p.m. and 70–170 p.p.m. respectively: no precise determinations were available for comparison. The figure of 100 p.p.m. in W-1 seems acceptable.

Mg. Results on the two lines agree quite well and *R* is the average. The lines are too intense in W-1 but the average in G-1 is 2,100 p.p.m. This gives 0·35 per cent M O, to compare with the 0·39 per cent recommended by Fairbairn (1953) suggesting that Mg *R* may be too low. The writer's six chemically analysed

scapolites (see Part I) are compared with several spectrographic determinations in Table 4: in four cases the spectrographic values of Mg are higher than the chemical determinations.

Ti. Ti *A* is much more sensitive than the other lines: where results were obtained on more than one line the average was taken for *R*. The values for G-1 and W-1 gave 0·242 and 0·852 per cent TiO_2, to compare with 0·25 and 1·1 per cent (Fairbairn, 1953): the agreement is satisfactory for G-1 but comparison of the determinations in Table 4 shows poor agreement. The chemical results, however, were close to the limits of detection, and should be given little weight.

Li. Results on Li *A* were close to the sensitivity limit and were always higher than *B* or *C*. Wherever possible Li *A* is ignored, since the G-1 and W-1 values on *B* (26 and 12 p.p.m.) agree well with the best estimates (21 and 13 p.p.m.; Smales & Webster, 1958).

Ni. Ni could not be measured in G-1: the value in W-1 (54 p.p.m.) is below the best estimate (73 p.p.m.; Smales, 1955).

Co. G-1 gave no detectable Co but W-1 gave 35 p.p.m., which is lower than Smales's estimate of 49 p.p.m. (1955).

Cu. *A* and *B* were averaged to obtain *R*, since the figures for G-1 (9·5 and 15 p.p.m.) were close to other workers' values (9·5 to 18 p.p.m.).

V. Using V 3102 Å and Pd *B* the figures for G-1 and W-1 were 12 and 120 p.p.m. The former seems satisfactory but the latter may be too low. However, V is often determined using V 3185 Å, which is subject to Ca interference in samples such as W-1.

Zr. For G-1 the figure of 145 p.p.m. is lower than most determinations (range 100-600 p.p.m.), but is fairly close to Degenhardt's (1957) value of 162 p.p.m. The figure of 86 p.p.m. for W-1 agrees well with Degenhardt (85 p.p.m.).

Mn. Mn *A* and *B* agree fairly well and were averaged: *C* was only measured on one sample, in which *A* and *B* were too intense. The agreement between chemical and spectrographic results in Table 4 is reasonable, since the former gives figures close to the detection limit. The average for G-1 gives 320 p.p.m. MnO, which is higher than the recommended 270 p.p.m. (Fairbairn, op. cit.): on the other hand, W-1 has 1,000 p.p.m. MnO, which is lower than the recommended 1,700 p.p.m.

Sc. Using Sc 4246 Å and Pd *A* the values for G-1 and W-1 were tr. and 17 p.p.m.: both seem satisfactory.

Y. *A* and *B* were averaged for *R*. Owing to Fe and Ti interference neither line could be estimated in G-1 and W-1.

Na. Agreement is generally poor between the chemical and spectrographic figures (converted to weight per cent) in Table 4, but the estimate of 3·27 per cent Na_2O in G-1 agrees well with the recommended 3·25 per cent (Fairbairn, op. cit.). *R* is the average of *A* and *B*.

Ca. The figures were obtained from a working curve constructed from artificial standards, G-1 and W-1, and the six analysed scapolites.

Sr. *B* and *C* refer to the same spectra, using different working curves. Sr *C* included G-1 (250 p.p.m.) and additional artificial standards to *B*. Usually *C* is taken as the best estimate (*R*), but for low values *A*, or the average of *A* and *C*, were used. The best figures for Sr in G-1 and W-1 are probably 230 and 180 p.p.m.

Pb. *A* and *B* agree well and were averaged. The value of 56 p.p.m. in G-1 is in good agreement with recent data.

K. No values were obtained on K *A*. The results on *B* and *C* disagree seriously and the comparisons in Table 4 are very discouraging. The value of 7·4 per cent K_2O in G-1 is much higher than Fairbairn's figure of 5·42 per cent. It was not feasible to recalibrate the method and repeat the analyses since most of the samples had been exhausted.

It was decided to retain the figures (*R* is the average of *B* and *C*), since the order of magnitude should be correct. Also the estimates of per cent Me (later) would be of more value if K is taken into account, even if the figures are suspect, than if it is ignored completely.

Ba. The data for Ba *B* and *C* are related as for Sr *B* and *C*. For Ba *C* the standards used included G-1 and W-1 (taken as 1,150 and 120 p.p.m.). Usually Ba *C* was taken as the best value but in some cases *A* was used, or the average of *A* and *C*.

Rb. 283 p.p.m. in G-1 is rather high: the best value is in the range 214-54 p.p.m. (Smales, 1955, 1958). The value of 24 p.p.m. in W-1 compares well with the range of 21–29 p.p.m. (idem).

To summarize, the results appear to be satisfactory for all elements except Mg, Na, and K. The Mg values are not likely to be seriously in error and the uncertainty in Na is difficult to assess, since the agreement between the determined and recommended values on G-1 is good. The uncertainty is more acute because Na is a major element. The results on K would not normally be worth reporting, but they have been included for reasons given above.

Samples

About 60 scapolites and scapolite-bearing rocks were chosen and from these 50 clean samples were prepared and analysed. In a very few cases the scapolite was of gem-quality and only required crushing: most, however, required very careful heavy liquid and electromagnetic separation along the lines described in Part I, where the difficulties of completely removing feldspar, calcite, &c., were also discussed. Every sample was checked by grain-counting at the time of refractive index determination, and any sample where foreign grains amounted to more than 1 per cent was rejected. Also rejected were a few scapolites which were seriously altered: the majority were quite fresh although occasionally stained a little by limonite.

The majority of the scapolites were collected by the writer and were constituents of rocks of the Precambrian Grenville province of Quebec and Ontario.

TABLE 5

Scapolite specimen localities

No.	*Locality*	*Rock Type*
CA 1	27-VII, Grand Calumet Twp., Quebec	Scapolite–pyroxene granulite
CA 30	25-VII, ditto	Scapolite–pyroxene gneiss
CA 51	30-VII, ditto	Pegmatitic skarn
CA 56	13-North Range, ditto	Scapolite–pyroxene gneiss
CA 61	12-North Range, ditto	Pegmatitic skarn
CA 63 A	31-VI, ditto	RA pegmatitic skarn
CA 74 B	32-VIII, ditto	Scapolite–pyroxene gneiss
CA 83	28-IX, ditto	Pegmatitic skarn
Q 7	19-V, Huddersfield Twp., Quebec	Scapolite–pyroxene–amphibole gneiss
Q 11 A	20-IV, ditto	Pegmatitic skarn
Q 12 B	19/20-V, ditto	Scapolite–pyroxene–calcite gneiss
Q 13 A	30-IV, ditto	Scapolite–pryoxene gneiss
Q 16 D	16/17-V, ditto	ditto
Q 19 D	22-V, ditto	Scapolite–pyroxene marble
Q 23 F	26/27-VIII, ditto	Single crystal from pegmatitic skarn
Q 24	38-II, Clapham Twp., Quebec	Scapolite–pyroxene granite
Q 24 C	ditto	Scapolite–pyroxene granite
Q 26	28-III, ditto	Single crystal from pegmatitic skarn
Q 27	29-V, Huddersfield Twp., Quebec	Pegmatitic skarn
Q 30	3-XIII, Clarendon Twp., Quebec	Scapolite–pyroxene gneiss
Q 31 B	ditto	Scapolite–epidote gneiss
Q 31 C	ditto	Scapolite–pyroxene granulite
Q 85	26-IV, Huddersfield Twp., Quebec	Pegmatitic skarn
Q 87 A	16/17-V, ditto	RA pegmatitic skarn
M 728	St. Laurence Co., New York	Scapolite–pyroxene–calcite pegmatitic aggregate
M 730	Grenville, Quebec	Single crystal (fluorescent)
M 731	Sebastopol, Ontario	Scapolite–calcite–apatite pegmatitic skarn
M 733	Lowe, Quebec	Coarse bladed scapolite aggregate
M 1162	Renfrew Co., Ontario	Vuggy aggregate of scapolite prisms
A	Unknown	Single crystal
B	Unknown	Single crystal with pyroxene
ON 1	34-VIII, Brudenell, Twp., Ontario	Single crystal with graphite
ON 3 B	13-XVI, Lyndoch Twp., Ontario	Prismatic aggregate with pyroxene
ON 4	25-XV, ditto	Single crystal
ON 5	Glendower Iron Mine, Bedford Twp., Ontario	Single crystal from calcareous gneiss
ON 6	13-XVI, Monmouth Twp., Ontario	Scapolite–pyroxene granulite
ON 7	32-XVII, ditto	Large single crystal from calcareous gneiss
ON 8	2½ miles east Gooderham, Glamorgan Twp., Ont.	Single crystal from syenite pegmatite
ON 20	13-XVI, Monmouth Twp., Ontario	Scapolite marble
ON 27	Olmsteadville, New York	Pegmatitic skarn
ON 28	Madagascar	Yellow gem crystal
ON 29	Pargas, Finland	Scapolite–pyroxene aggregate
ON 37	17-VI, Glamorgan Twp., Ontario	Scapolite–pyroxene–calcite skarn
ON 44	Pianura, Italy (ROM M-5432)	Prisms in tuff (?)
ON 45	Monte Somma, Italy (ROM M-9122)	Prisms in lava
ON 47	Slyudyanka, Siberia, U.S.S.R. (ROM M-18778)	Large single crystal
ON 48	Campolungo, Switzerland (ROM M-16589)	Pale yellow single gem crystal
ON 49	Minas Geraes, Brazil (ROM M-20030)	Glassy single gem crystal
ON 50	Tsarasaotra, Madagascar (ROM M-12109)	Pale yellow single gem crystal
ON 53*	Near Trooper Lake, Glamorgan Twp., Ontario	Calcareous gneiss

Twp. means Township; RA means radioactive; ROM refers to catalogue numbers in the Royal Ontario Museum Collections. The figures, e.g. 27-VII, mean Lot 27, Concession or Range VII.

* ON 53 is the same material as analysis No. XIV in Part I.

TABLE 6

Spectrochemical analyses of scapolities

rA	0·23 B	0·35 Be	0·62 Ga	0·63 Cr	0·66 Mg	0·68 Ti	0·68 Li	0·69 Ni	0·70 Mo	0·72 Cu	0·79 Zr	0·80 Mn	0·92 Y	0·97 Na	0·99 Ca	1·12 Sr	1·20 Pb	1·33 K	1·34 Ba	1·47 Rb
Sensitivity	10	0·5	1	5	100	5	1	1	5	1	5	10	2	0·3%	1%	10	10		10	1
CA 1	8·4	5·4	29·0	7·6	4,350	78·0	44·0	tr	*	2·0	*	68	*	4·6	6·5	2,500	25	—	82	20·0
CA 30	9·8	1·6	28·0	*	1,280	50·0	57·0	*	*	4·5	50·0	35	*	5·1	5·2	1,900	96	0·45	150	4·6
CA 51	32·0	18·0	71·0	tr	410	9·5	84·0	tr	*	1·0	*	37	*	7·0	4·9	780	25	1·0	87	17·0
CA 56	tr	8·2	39·0	*	510	110·0	30·0	*	*	3·5	39·0	49	*	3·9	10·0	2,700	51	0·37	80	17·0
CA 61	51·0	6·2	37·0	*	2,000	*	93·0	*	*	6·9	tr	42	*	6·9	3·1	1,450	49	—	400	—
CA 63 A	tr	6·8	32·0	*	640	21·0	58·0	*	*	3·8	*	51	*	5·7	6·5	2,900	45	1·3	120	11·0
CA 74 B	tr	7·7	32·0	*	510	*	82·0	*	*	3·8	*	71	*	4·2	9·0	2,500	67	0·39	210	18·0
CA 83	12·0	3·9	27·0	*	2,300	24·0	64·0	*	*	3·4	*	51	*	4·3	11·5	2,600	69	0·58	130	15·0
Q 7	22·0	4·5	15·0	*	1,800	87·0	26·0	*	*	3·3	6·8	46	*	3·6	12·5	2,100	105	0·35	23	22·0
Q 11 A	tr	6·5	36·0	*	2,000	27·0	12·0	*	*	2·8	37·0	41	*	5·4	7·9	2,900	9	0·44	160	27·0
Q 12 B	22·0	4·4	33·0	*	1,300	36·0	24·0	*	*	3·6	*	33	*	3·4	10·5	2,600	71	0·37	80	30·0
Q 13 A	13·0	6·9	39·0	*	310	*	21·0	*	*	3·4	tr	32	*	4·7	5·5	2,000	23	1·0	58	15·0
Q 16 D	tr	8·4	33·0	*	120	110·0	41·0	*	*	1·6	19·0	39	*	5·6	5·9	2,200	tr	1·2	60	11·0
Q 19 D	19·0	5·0	39·0	*	200	43·0	50·0	*	*	2·2	16·0	34	*	5·5	8·3	1,700	93	1·2	82	13·0
Q 23 F	tr	2·2	38·0	*	220	52·0	36·0	*	*	1·0	*	63	*	3·4	11·5	3,100	94	0·58	150	11·0
Q 24	tr	37·0	55·0	*	1,150	44·0	80·0	*	*	24·0	*	94	4·3	—	—	340	50	—	17	—
Q 24 C	tr	34·0	52·0	*	280	46·0	110·0	*	*	8·8	*	74	*	5·4	6·0	280	34	—	14	—
Q 26	16·0	24·0	65·0	*	tr	12·0	100·0	*	*	1·4	*	57	*	4·5	6·2	1,600	49	1·5	99	39·0
Q 27	20·0	10·0	43·0	*	3,300	tr	24·0	tr	*	2·3	tr	97	*	5·9	5·7	1,100	62	1·4	31	22·0
Q 30	11·0	8·6	57·0	*	3,100	11·0	64·0	*	12	2·1	tr	44	*	5·4	7·9	1,050	21	1·2	80	17·0
Q 31 B	tr	9·6	46·0	*	1,100	20·0	50·0	*	*	5·2	7·3	36	*	6·1	7·1	1,150	23	1·2	58	18·0
Q 31 C	37·0	7·0	51·0	*	600	520·0	56·0	*	*	3·6	18·0	35	13·0	5·2	9·5	1,300	tr	0·51	98	12·0
Q 85	36·0	8·4	20·0	*	1·1%	32·0	53·0	*	*	2·2	60·0	83	8·3	2·8	10·2	3,300	99	0·93	86	64·0
Q 87 A	14·0	6·9	45·0	*	1,550	tr	24·0	*	*	3·2	7·3	37	*	4·3	7·9	3,700	36	1·1	47	9·8
M 728	93·0	25·0	35·0	*	590	590·0	17·0	*	*	5·6	19·0	33	*	2·8	11·5	1,150	55	0·32	26	14·0
M 730	270·0	tr	13·0	*	3,800	230·0	35·0	*	*	6·2	4·0	49	*	1·7	11·2	920	*	1·4	95	130·0
M 731	tr	8·4	27·0	*	610	36·0	27·0	*	*	3·5	*	54	*	5·2	10·0	2,500	79	1·2	240	15·0
M 733	tr	*	36·0	*	1,600	9·9	71·0	*	*	4·5	*	27	*	6·9	13·0	2,800	13	1·2	145	8·0
M 1162	33·0	4·8	20·0	*	280	100·0	13·0	*	*	5·0	*	52	*	4·3	8·9	2,200	46	0·45	350	12·0
A	37·0	4·1	8·2	*	520	130·0	35·0	*	*	3·6	*	76	*	2·0	14·3	5,100	66	0·37	120	12·0
B	8·0	6·6	51·0	*	540	450·0	86·0	*	*	4·9	570·0	47	11·0	3·2	—	200	67	—	10	23·0
ON 1	17·0	9·0	18·0	*	2,900	11·0	8·2	*	*	2·5	*	20	*	6·2	4·8	1,350	36	1·3	580	27·0
ON 3 B	14·0	5·1	39·0	*	1,000	56·0	20·0	*	*	2·5	tr	59	*	5·6	8·4	2,800	39	0·91	170	5·6
ON 4	16·0	11·0	18·0	*	4,000	11·0	8·8	3·5	*	1·5	40·0	25	*	7·1	5·7	1,900	33	1·3	560	15·0
ON 5	19·0	5·6	26·0	tr	310	32·0	5·2	*	*	1·0	130·0	84	2·9	6·3	—	3,300	16	1·2	150	16·0
ON 6	39·0	29·0	52·0	tr	tr	11·0	185·0	*	*	4·3	*	43	*	6·0	5·9	950	33	0·80	64	24·0
ON 7	tr	4·5	30·0	*	1,000	tr	115·0	*	*	2·0	*	51	*	6·0	6·7	2,900	51	0·89	180	8·5
ON 8	30·0	tr	16·0	*	100	tr	50·0	tr	*	13·0	*	160	4·2	8·8	3·4	125	110	1·7	19	6·5
ON 20	120·0	7 6	28·0	*	250	tr	106·0	*	*	6·6	*	20	*	2·8	13·0	1,350	19	1·2	87	19·0
ON 27	66·0	3·4	35·0	*	350	120·0	30·0	*	*	3·5	27·0	42	*	3·2	14·0	1,500	11	0·48	170	27·0
ON 28	tr	3·8	13·0	*	tr	18·0	45·0	*	*	3·0	*	150	*	4·4	—	1,250	87	0·44	115	4·4
ON 29	tr	20·0	34·0	*	950	33·0	240·0	*	*	3·9	*	43	*	1·8	12·5	100	11	0·32	10	67·0
ON 37	16·0	2·9	53·0	*	2,100	21·0	33·0	*	*	20·0	*	60	*	5·9	7·1	600	42	0·71	31	11·0
ON 44	—	—	—	—	—	—	—	—	—	—	—	—	—	—	3·3	tr	—	—	tr	—
ON 45	tr	28·0	6·7	*	700	110·0	2·5	*	*	3·2	6·2	49	*	0·64	—	1,250	tr	0·41	115	6·5
ON 47	18·0	3·5	14·0	*	320	72·0	20·0	tr	*	4·7	*	45	*	1·1	—	1,800	15	0·27	280	5·4
ON 48	5·9	22·0	13·0	*	100	10·0	160·0	*	*	2·8	*	160	*	1·7	—	2,000	—	0·08	27	4·6
ON 49	7·1	7·2	18·0	*	tr	21·0	52·0	*	*	3·6	*	> 200	3·2	3·3	—	920	50	0·58	43	5·8
ON 50	6·4	3·4	13·0	*	tr	34·0	50·0	*	*	4·0	*	> 200	*	4·6	—	1,200	73	0·37	110	3·4
ON 53	96·0	1·4	12·0	*	580	590·0	45·0	*	*	3·0	16·0	70·0	*	1·8	—	760	tr	0·10	40	6·6

All figures are averages of triplicate analyses, and are expressed in p.p.m. except for Na, Ca, and K which are in weight per cent. The Ca values in Q 19 D, Q 85, Q 87 A, M 730, and ON 8 were determined chemically.

The rocks were calcareous gneisses, and pegmatitic skarns, pods and veins within such gneisses. Accompanying minerals included augite, calcite (usually salmon-pink), sphene, phlogopite or biotite, various amphiboles, quartz, and feldspars. Associated pelitic rocks demonstrated the metamorphic grade to be the sillimanite grade of the amphibolite facies. Parallel studies of pyroxene and calcite have been carried out and the petrology will be discussed elsewhere. A few

samples from localities outside Canada were available and include four gem-quality specimens (ON 28, 48, 49, 50).

Although there is considerable variation in composition and appearance of the gneisses, the same assemblages occur throughout and may be grouped together. From the point of view of paragenesis it is convenient to distinguish four groups of samples:

(*a*) calcareous gneisses of regional development,
(*b*) purple fluorite-bearing skarns: these are always radioactive, but so also are many skarns where fluorite is absent,
(*c*) gem deposits,
(*d*) volcanic contact action.

It is, however, questionable whether the first three correspond to any real differences in origin. Sample localities are given in Table 5.

GENERAL INTERPRETATION

Table 6 contains the results of spectrographic analysis of 50 scapolites. The figures for Ca, Na, and K are given in weight per cent, while the remainder are in parts per million (p.p.m.). Ionic radii for six-fold coordination (Ahrens' values) in the usual valence state are included, together with the spectrographic sensitivity. The symbol tr indicates a line too weak to measure, whereas * indicates that the element was sought but not found; —means that the element was not sought. For the sake of completeness six Ca values determined chemically and used as standards are included. The following elements were not detected in any scapolite (sensitivity in brackets in p.p.m.): Co (3), V (10), Sc (3), Ag (1), La (100), Sn (10).

When discussing the significance of trace elements in minerals, it cannot be immediately assumed that the elements in question occur in isomorphous substitution at structural sites. Elements may also occur in inclusions (solid or liquid), in adsorbed surface layers, discontinuities or imperfections, or in structural cavities. This has been discussed by Kutina (1957), Jedwab (1953), and other authors. The careful purification of the present samples only indicates that gross impurities were excluded: the possibility of submicroscopic inclusions and of stain contamination remains. It may, however, be relevant to note that the four gem-quality samples were particularly clear and glassy but contain a similar trace-element suite to the other samples. Surface and sorption effects cannot be readily assessed.

Indirect evidence, however, suggests that isomorphous replacement explains the occurrence of most elements. For if it may be assumed that a supply of all the elements was available at the time of crystallization of the parent rocks, then it should be noticed that the more prominent trace elements are those which would be expected to substitute for the major elements Al, Ca, Na, and K, i.e. Ga, Mn, Sr, Pb, Ba, Rb. By contrast Mg and Fe are not important constituents of scapolite and the trace elements which normally follow them (e.g. Cr, Ni, Co,

V, Cu, Zr, Sc) are absent or at low concentration. In accompanying pyroxenes and amphiboles these elements, however, are all more prominent. On the whole it appears that scapolite has selected certain trace elements and excluded others and the selection is best explained in terms of isomorphous replacement. The significance of several elements (e.g. B, Be, Li), however, remains in question and will be dealt with shortly. For further discussion the data in Table 6 is

TABLE 7

A summary of trace elements in scapolite compared with crustal abundances and some plagioclase feldspars (p.p.m.)

	Scapolite		*Crust*		*Plagioclase*					
Element	*Range*	*Mean*	*C*‖	*Reference*	*A*	*B*	*C*	*D*	*E*	*F*
B	< 10–270	25	3	Goldschmidt (1937)	–†	–	*‡			
Be	< 0·5–37	9·3	2	Sandell (1952)	*	*	*			
Ga	6–71	33	19	Shaw (1957)	29	30	71			
Cr	<5–8	x§	100	Shaw (1954)	*	7	2			
Ti	< 5–590	82	4,400	Goldschmidt (1937)	–	–	–			
Li	2–240	56	29	Horstmann (1957)	9	7	2			
Ni	< 1–4	x	80	Sandell & Goldich (1943)	*	6	2			
Co	< 3	x	23	ditto	*	8	*			
Mo	< 5–12	x	1	Kuroda & Sandell (1954)	*	*	*			
Sn	< 10	x	2	Onishi & Sandell (1957)	–	–	–			
Cu	1–24	4·4	70	Sandell & Goldich (1943)	–	50	170			
V	< 10	x	100	Shaw (1954)	3	16	7			
Zr	< 5–570	59	156	Degenhardt (1957)	70	70	5			21
Mn	20– > 200	57	1,000	Green (1953)	*	140	87			
Sc	< 3	x	15	Shaw (1954)	*	*	*			
Ag	< 1	x	0·1	Goldschmidt (1937)	*	*	*			
Y	< 2–13	x	40	Fleischer (1955)	*	*	*			
Sr	< 100–5100	1,800	450	Turekian & Kulp (1956)	760	2,700	2,500		210	
La	< 100	x	20	Green (1953)	*	*	*			
Pb	< 10–110	45	15	Wedepohl (1956)	20	9	*	14		
Ba	10–580	120	250	Green (1953)	150	840	260			
Rb	3–130	20	120	Horstmann (1957)	*	120	*			

The scapolite means are minima, since they include analyses marked tr or * in Table 6, except in the case of Zr where no analyses marked * were included.

Column A: average of 6, Howie (1955).
B: average of 9, Nockolds and Mitchell (1948).
C: average of 6, Wager & Mitchell (1951).
Column D: average of 8, Wedepohl (1956).
E: average of 7, Turekian & Kulp (1956).
F: average of 5, Degenhardt (1957).

† no data. ‡ not detected.
§ no mean computed. ‖ crustal abundance.

summarized in ranges and averages in Table 7 along with crustal abundances and analyses of some plagioclase feldspars for comparison.

By comparison with the crust of the earth it is seen that scapolite is usually enriched in B, Be, Ga, Li, Sr, and Pb, but is impoverished in the other elements studied. By comparison with plagioclase, scapolite is notably richer in B, Be, Li, and Pb. Recalling the major elements discussed in Part I it may be added that scapolite is usually enriched in Al, Ca, Na, C, Cl, and S, with respect to the crust. It should perhaps be mentioned that enrichment must be considered on a relative basis: thus the absolute Be content is very low, but the enrichment is none the less valid.

Behaviour of individual elements

Boron has a small radius and is more likely to form BO_3^{-3} anions than substitute directly for an element such as Si^{+4}. In scapolite the presence of BO_3^{-3} radicles would present no problem, behaving in a similar way to CO_3^{-2} and substituting at an anion site. The possibility must, however, be borne in mind that contamination by tourmaline may have taken place. Tourmaline was only recorded in one or two of the parent rock samples, but in many other localities scapolite and tourmaline occur together. The average B content of tourmaline is about 3 per cent, so a B content of 30 p.p.m. could be caused by the presence of 0·1 per cent tourmaline in the sample, or 1 grain in 1,000. Tourmaline contrasts markedly with scapolite in immersion oils and none was detected: contamination could therefore have only taken place on a submicroscopic scale. In any event the presence of B contrasts sharply with plagioclase, and it occurs in almost all the scapolites examined, although the gem varieties contain much less than the average. Whatever its structural significance, it may be presumed to have been concentrated from the same source as other volatile components of scapolite.

Beryllium is seldom detected in common silicates and its ubiquitous presence in scapolite is interesting. The range in concentration is narrow and it presumably occurs as Be^{+2} (radius 0·35 Å) replacing Si^{+4} (radius 0·42 Å) in oxygen-coordinated tetrahedra. The geochemistry of Be is not well known, but geological evidence indicates that Be concentrations only become notable in pneumatolytic–pegmatitic conditions: this is in accord with the usual interpretation of the conditions of formation of scapolite, whether in limited contact zones or on a regional scale.

Gallium may be expected to occur as Ga^{+3}, substituting for Al^{+3} (radius 0·51 Å), both being somewhat enriched over the crustal averages.

The elements Cr, Ni, Co, Mo, Sn, and V need little comment. As mentioned above, they customarily follow Mg and Fe, both of which are unimportant as major constituents. Similarly, Ti is greatly depleted by comparison with the crust, and the values recorded may represent substitution for Al and Si, contamination by submicroscopic sphene (present in almost every source rock), or oxide stain.

Lithium is unexpectedly high, and its location is difficult to find. On the basis of radius (0·68 Å) it is rather large to substitute for Al^{+3} (0·51 Å) and rather small for Na^{+1} (0·97 Å). It usually follows Mg and Fe and undoubtedly accompanies them in scapolite also. The average Mg content of the scapolites is 1,420 p.p.m., which gives a Li/Mg ratio of $39 \div 10^3$. This figure is much higher than the values of 0·1–4·0 obtained by Nockolds & Mitchell (1948) for a series of differentiated calc–alkalic rocks from the Garabal Hill–Glen Fyne complex: however, their results showed a clear increase of the ratio towards the latest stages of differentiation. The figure of 39 would suggest an extrapolation into pegmatitic–hydrothermal conditions, again in accord with views on scapolite

genesis. The source of the Li will be considered later, but the enrichment in scapolite contrasts with plagioclase: this may imply a richer source in the loci of scapolite genesis, or a greater ease of accommodation in the structure, or both. If the source were unusually rich in Li (the same argument applies to B, Be, Sr, or Pb), the element may simply be trapped in lattice cavities, crystal imperfections, and surface adsorption, falling into the category of an *élément typochimique* (Jedwab, op cit.) which gives information on the environment of formation rather than on structural mineralogy. The source of the scapolites is, however, very diverse and no Li minerals were encountered in the rocks. The significance of Li is thus obscure, but its presence may testify to similarity in conditions of genesis of all the scapolites examined.

Copper requires no comment beyond pointing out that the very low content testifies to freedom from contamination from sulphides (present in many of the rocks), equipment, and chemicals. There is less Cu in most scapolites than in Reagent grade chemicals, yet it is hard to believe that Cu was negligible in the environment of formation. The author would rather regard the data as indicating to what degree a mineral can exclude a trace element which cannot be accommodated.

Zirconium was not detected in most analyses, but occurs in 23, with most figures up to 60 p.p.m. and two high values of 125 and 570 p.p.m. The latter almost certainly indicate contamination by zircon, which was present in many of the parent rocks. Neglecting these two, the overall average would be about 7 p.p.m. Such small amounts may again accompany the minor Mg and Fe: it should be noted, however, that Zr occurs in plagioclase.

Manganese is a ubiquitous constituent, shows a narrow concentration range, and is clearly less abundant than in the usual crustal rocks. It is well known that Mn^{+2} can replace Ca^{+2} in various minerals and presumably that also takes place in scapolite. Some Mn may be present in oxide stain, but this can largely be discounted since the four gem varieties (free from stain and visible inclusions) ON 28, 48, 49, 50 are richer in Mn than usual (150, 160, $>$ 200, $>$ 200 p.p.m. respectively): the reason for this enrichment is not obvious.

Yttrium was measurable in a few specimens: it may be present in isomorphous replacement (following Ca?) or in occasional inclusions of rare-earth minerals.

Strontium shows notable enrichment in scapolite and plagioclase compared with the crust as a whole. This is to be expected in view of the similarity in radii and crystal chemistry of Sr^{+2} and Ca^{+2}. The situation is similar for lead, which shows about the same degree of enrichment in scapolite, although a lesser degree in plagioclase. Barium, however, shows an opposite behaviour, i.e. it is impoverished in scapolite but concentrated in plagioclase. Rubidium is also depleted in scapolite, and its average concentration in plagioclase is apparently low. These relations are not easily explained, since Ba^{+2} and Rb^{+1} (radii 1·34, 1·47 Å) tend to follow K^{+1} (radius 1·33 Å), and K_2O is generally more abundant in scapolite (up to at least 3·6 per cent) than in plagioclase (Emmons

et al, 1953, show the range in K_2O in 18 plagioclase specimens to be 0·19–0·62 per cent). Thus one might expect rather greater Ba and Rb contents: Pb, however, has a radius (1·20 Å) intermediate between Ca^{+2} and K^{+1} and may therefore be expected to enter scapolite more readily, as is the case.

The low Rb concentrations are particularly puzzling because other elements (B, Be, Li) appear to have concentrations testifying to pegmatitic–hydrothermal conditions of genesis, and Rb might also be expected to concentrate in a similar manner. The relationship of K to Rb cannot be profitably discussed, in view of the unsatisfactory K analyses, but inspection of the data suggests no constancy of the Rb/K ratio.

Relationships between elements

In most series of igneous minerals there are clear relationships between the major structure-forming elements and the camouflaged minor elements. These are expressed by concomitant increases or decreases in pairs of elements with similar properties, and clearly result from the dynamic history of a magma expressed by the effects of fractional crystallization: for example, Li^{+1} usually follows Mg^{+2} but increases (relatively) as the latter decreases throughout a sequential series of differentiated minerals from a given source.

The scapolites under discussion here are in a different category. They represent a metamorphic–metasomatic origin, do not contain any sequential series, and include diverse and unconnected localities and ages. Accordingly one might not expect the same regularities of relative distribution, especially because the scapolites were phases of different assemblages, each of which may be presumed to have formed by simultaneous recrystallization. The elements entering a given scapolite would therefore depend on:

(*a*) the supply of elements in the original rocks,
(*b*) the supply of elements in any mobile phase,
(*c*) the additional mineral phases crystallizing contemporaneously,
(*d*) the crystal chemical features of scapolite.

The last point has already been discussed to some extent, and the previous three will be dealt with in a general paper on the geochemistry of the Quebec and Ontario scapolite skarns. At the present time it is sufficient to indicate that geochemical coherence might be expected to be less marked than in igneous rocks.

Nevertheless, in the scapolites available, which range from 20 to 85 per cent meionite (Me) it was expected that some sympathetic variations between major elements (e.g. Ca, Na, K) and trace elements would appear beyond the generalities discussed in the last section. To examine this the data of Table 6 were plotted in a series of binary diagrams such as per cent Ca vs. p.p.m. Sr, K vs. Rb, &c. It was surprising to find an almost complete lack of any relationship between pairs of major and trace elements on the scale of individual

analyses. The same results were obtained on plotting trace elements against each other and against per cent Me.

It may be concluded that

(*a*) the unrelated parentage of individual scapolites makes detailed comparison pointless,

(*b*) in a given environment the intake of favourable trace elements into scapolite resembles the action of blotting-paper, and the mineral appears to take in whatever is available, in competition with other minerals (this applies to major elements also, and is in accord with thermo-dynamical requirements),

(*c*) not enough is known of the detailed conditions of formation of these or any other scapolites to investigate the question of whether some of the fluctuating major/trace element ratios might reflect varying *PT* conditions.

Attempts were also made to relate trace element content to colour, grain-size, geographic locality, and type of occurrence, with conspicuous lack of success. The only definite correlation obtained was with the gem varieties which, as already mentioned in part, have low B, Mg, Ti, and Rb, and high Mn. The significance of this is uncertain, but it is unlikely that it only reflects greater freedom from contamination.

Unfortunately it was only possible to isolate enough of ON 44 to confirm that it was Ca-poor; this sample is from the original locality from which marialite was named, and it is noteworthy that it contains 3·3 per cent Ca, corresponding to about 20 per cent Me. As mentioned in Part I it is unlikely that pure marialite exists in nature.

ON 45 from Monte Somma, Vesuvius, shows a similar trace element suite to scapolites from regionally developed rocks, suggesting a similarity of conditions of genesis.

CORRELATION OF MAJOR ELEMENTS AND OPTICAL PROPERTIES

The refractive indices (n_o and n_e) of the scapolites were determined by immersion methods, using sodium light and applying the usual temperature corrections to the indices of the oils. A standard set of oils was used and individual oils were occasionally checked with an Abbé refractometer. The results are believed correct to within 0·001 and are given in Table 8 along with atomic per cent meionite. The latter was calculated as the ratio of atomic Ca/(Ca+Na+K), using the analyses in Table 6. The results are plotted in Fig. 1, which shows the relationship between the average index n_m and per cent Me. For comparison, the chemically analysed samples are shown with a cross, and the determinative curve from Part I is also included.

The points on Fig. 1 conform roughly with the determinative curve and show a general increase in n_m with per cent Me. The scatter is, however, considerable and is certainly due in part to analytical errors (the effect of the doubtful K

TABLE 8

Composition and refractive indices of 50 scapolites

Sample number	n_e	n_o	*dn*	n_m	% *Me*	*Sample number*	n_e	n_o	*dn*	n_m	% *Me*
CA 1	1·548	1·566	0·018	1·557	44	M 730	1·555	1·587	0·032	1·571	70*
CA 30	1·550	1·566	0·016	1·558	36	M 731	1·548	1·568	0·020	1·558	49
CA 51	1·546	1·564	0·018	1·555	27	M 733	1·544	1·558	0·014	1·551	50
CA 56	1·552	1·572	0·020	1·562	58	M 1162	1·552	1·578	0·026	1·565	52
CA 61	1·546	1·562	0·016	1·554	21	A	1·555	1·586	0·031	1·571	78
CA 63 A	1·548	1·565	0·017	1·557	36	B	1·552	1·584	0·032	1·568	—
CA 74 B	1·550	1·569	0·019	1·560	55	ON 1	1·542	1·558	0·016	1·550	29
CA 83	1·549	1·568	0·019	1·559	59	ON 3 B	1·550	1·566	0·016	1·558	45
Q 7	1·558	1·584	0·026	1·571	65	ON 4	1·546	1·560	0·014	1·553	29
Q 11 A	1·549	1·567	0·018	1·558	45	ON 5	1·549	1·569	0·020	1·559	—
Q 12 B	1·553	1·575	0·022	1·564	62	ON 6	1·547	1·560	0·013	1·554	34*
Q 13 A	1·551	1·571	0·020	1·561	38	ON 7	1·544	1·560	0·016	1·552	38
Q 16 D	1·548	1·566	0·018	1·557	36	ON 8	1·541	1·549	0·008	1·545	19*
Q 19 D	1·551	1·569	0·018	1·560	48*	ON 20	1·557	1·582	0·025	1·570	69
Q 23 F	1·556	1·581	0·025	1·569	64	ON 27	1·550	1·577	0·027	1·564	70
Q 24	—	—	—	—	—	ON 28	1·552	1·570	0·018	1·561	—
Q 24 C	1·551	1·571	0·020	1·561	39	ON 29	1·552	1·589	0·037	1·571	78
Q 26	1·552	1·572	0·020	1·562	40	ON 37	1·550	1·571	0·021	1·561	39
Q 27	1·550	1·568	0·018	1·559	32	ON 44	—	—	—	—	—
Q 30	1·549	1·567	0·018	1·558	43	ON 45	1·561	1·598	0·037	1·580	—
Q 31 B	1·548	1·566	0·018	1·557	38	ON 47	1·560	1·592	0·032	1·576	—
Q 31 C	1·549	1·567	0·018	1·558	50	ON 48	1·553	1·586	0·033	1·570	—
Q 85	1·557	1·581	0·024	1·569	66*	ON 49	1·552	1·574	0·022	1·563	—
Q 87	1·550	1·568	0·018	1·559	46*	ON 50	1·549	1·569	0·020	1·559	—
M 728	1·553	1·586	0·033	1·570	69	ON 53	1·553	1·584	0·031	1·569	—

* Per cent Me obtained from chemical analyses listed in Table 7, Part I.

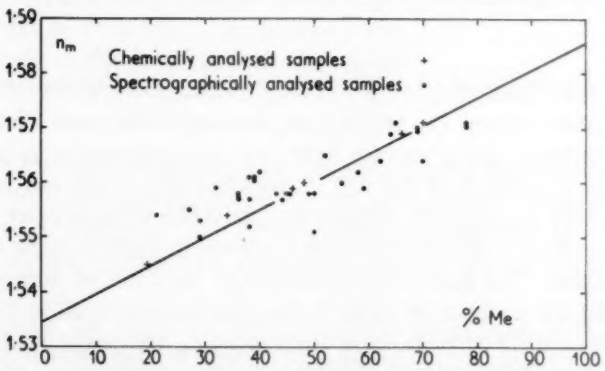

FIG. 1. Variation of n_m with per cent Me in 50 scapolites.

analyses, however, is small). One or two points (e.g. M 733) deviate from the line by about 20 per cent Me and it is unlikely that the errors are of such magnitude. One of the conclusions of Part I was that there is a straight-line relation between n_m and per cent Me: the present results throw some doubt on that hypothesis but the matter cannot be resolved at present.

A plot of birefringence (*dn*) against per cent Me shows a similar scatter of points, but with the same tendency for *dn* to increase with per cent Me.

GENERAL GEOCHEMISTRY AND PETROLOGY

Papers discussing the genesis of scapolite have been reviewed in Part I. It is sufficient here to summarize the main modes of occurrence as follows:

(*a*) in blocks ejected from volcanoes and by contact volcanic action,
(*b*) in contact skarns or tactites, where sedimentary marbles have been influenced by nearby plutonic bodies,
(*c*) in altered igneous rocks, especially gabbro and diabase, by the effect of hydrothermal or pneumatolytic fluids (possibly also by ground-water action, as claimed by Lacroix in the Pyrenees),
(*d*) in metamorphic rocks of regional distribution, especially marbles, greenstones, calcareous gneisses, and granulites, but also in pelitic and psammitic varieties,
(*e*) in fissure-fillings (veins) in various regionally metamorphosed rocks,
(*f*) in metamorphosed salt deposits (Serdyuchenko, 1955: seen only in abstract).

It is evident from the literature that scapolite can coexist with a wide variety of common minerals, and there are few rock types in which it has not been found: however, it seems unable to form in sedimentary environments. It is typically metamorphic and is not a product of primary magmatic crystallization.

There is a general tendency for scapolite and plagioclase to be mutually exclusive and many authors have described progressive replacement of feldspar by scapolite. However, the two minerals are not always antipathetic and there are numerous examples of metamorphic rocks in which scapolite and feldspar appear to be in equilibrium. There are relatively few instances where the composition of both scapolite and coexisting plagioclase are known, but 18 examples were found and are plotted in Fig. 2 which shows the per cent Me versus per cent An. It is clear that there is no linear relation, and scapolite is not always richer in Ca than coexisting plagioclase as claimed by Barth (1952, p. 284). The same conclusion was reached by Turner & Verhoogen (1951, p. 390).

Turning to the conditions necessary for the formation of scapolite, it is evident that it is most prevalent in rocks which recrystallized in the *upper amphibolite facies*. Most of the writer's samples discussed previously come from the Precambrian Grenville province of Quebec and Ontario, and occur in sequences where intercalated pelitic horizons are common. These usually

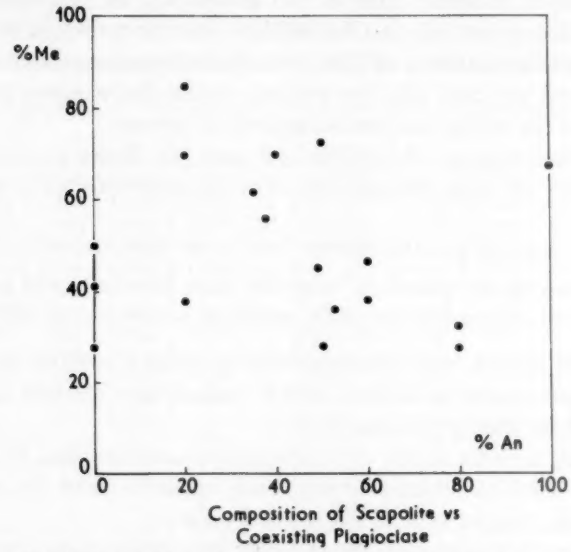

FIG. 2. Composition of scapolite versus coexisting plagioclase.

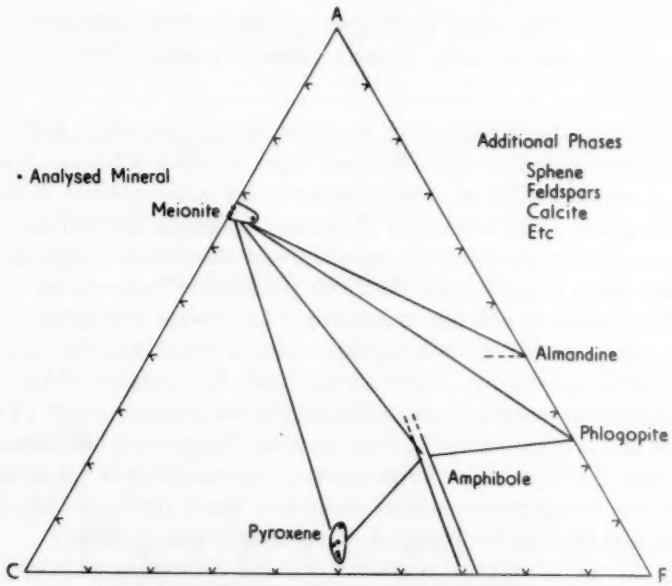

FIG. 3. *ACF* diagram for scapolite assemblages.

contain sillimanite and testify to the metamorphic grade. The characteristic calcareous assemblage is

scapolite–pyroxene–sphene

with or without amphibole, phlogopite or garnet, and commonly including calcite, quartz, and feldspars. These assemblages are shown in an *ACF* plot in Fig. 3 using the six analysed scapolites (Nos. XXX–XXXV) from Part I, and six analysed pyroxenes which will be discussed elsewhere. It should be noted that the pyroxenes are low in Al and thus show no eclogitic affinities. Various additional assemblages occur, but the association scapolite–pyroxene–sphene is of world-wide distribution in rocks of many ages. Since, however, the assemblage is not confined to the upper amphibolite facies, it is perhaps too broad to be worth introducing as a separate facies name, even though it appears to represent a particular conjunction of geological conditions.

It is evident that scapolite is by no means confined to a narrow range in metamorphic conditions, but can occur in almost any grade of metamorphism. This is partially obscured by the fact that plagioclase, which plays such an important role in estimating metamorphic grade, is often absent from scapolitic assemblages.

Examples, however, from the *epidote–amphibolite facies* include Glen Meran, Scotland, where the assemblage scapolite–feldspar–pyroxene–epidote–zoisite–garnet–vesuvianite–muscovite–uralite was found (Flett, 1907), the Leventina, where scapolite–calcite–biotite–plagioclase–zoisite–muscovite–quartz rocks form veins (Preiswerk, 1917), and Kiruna, Sweden, where scapolite–biotite–hornblende–epidote–plagioclase assemblages are found (Sundius, 1915).

Kiruna also provides examples of the *green–schist facies*, with similar assemblages including chlorite and sericite: in the Tessin, Jakob (1931) has described a similar occurrence, and at Laxford Bridge, Scotland, there occurs an assemblage of scapolite–epidote–quartz–albite (Flett, op. cit.).

Veins cutting a diabase at French Creek, Pennsylvania, contain scapolite associated with prehnite and heulandite (Tomlinson, 1943) which indicates the *zeolite facies*.

The association of scapolite with aluminous augite, hornblende, and magnesian garnet in the Shai Hills, Ghana, has been taken as evidence of recrystallization in the *granulite–eclogite facies* (von Knorring & Kennedy, 1958).

The ejected blocks of the Laacher See (Brauns, 1914) contain scapolite associated with sanidine, and indicate the *sanidinite facies*. The occurrences in the Oslo district of Norway (Goldschmidt, 1911) are in contact rocks of the *pyroxene hornfels facies*.

In some of the examples of regional scapolitization (e.g. Kiruna) the formation of scapolite has post-dated the main recrystallization. This, plus the fact that some of the assemblages quoted above contain a large number of minerals, suggests that in some cases the conditions for equilibrium did not obtain. Even

so, there remains abundant evidence that scapolite can form (stably or metastably) in all facies from zeolitic to granulitic to sanidinite. This is roughly equivalent to a temperature and pressure range of 200–1,100° C and 0–10,000 kg/cm² (it should be recalled that Himmelbauer found the beginning of melting at room pressure to be close to 1,100° C), and covers the whole field of metamorphic and anatectic conditions. One might therefore expect scapolite to be much more widespread than in fact it is. In point of fact its complex constitution limits its field of occurrence to conditions where not only temperature and pressure, but also composition is suitable.

Until adequate synthesis studies have been carried out it is only possible to speculate on the necessary conditions. However, it is evident that the materials of plagioclase are first necessary, whether they exist in the rock or are introduced from outside: it is unlikely that ferromagnesian minerals play any direct role in scapolite genesis, and claims that scapolite can replace hornblende or pyroxene are probably erroneous textural interpretations. In addition the anions Cl^{-1}, SO_4^{-2}, CO_3^{-2}, and OH^{-1} are usually present in every scapolite. Water is subordinate, however, and of uncertain significance (see Part I) and it is evident that the principal requirement for scapolite to form is a diminution of p-H_2O and concomitant increase in one or all of p-CO_2, p-Cl_2, p-SO_3. Numerous scapolites contain negligible SO_3, and one or two apparently contain little Cl_2. Relatively high p-CO_2 is therefore a prime requirement, but is clearly not sufficient in itself, otherwise scapolite would be a much more common mineral in marbles than is the case. In most scapolites Cl_2 is about as abundant as CO_2, and p-Cl_2 must therefore be significant. The possibility must also be considered that K_2O is a necessary component, but in any event most rocks contain an adequate amount.

There is also a remote possibility that some of the enriched trace elements (B, Be, Li, Sr, Pb) might be essential constituents in the sense of stabilizing the structure. This has proved to be the case in another mineral synthesized in the laboratory,[1] and many minerals can grow more readily in the presence of catalysts. The hypothesis could be readily investigated.

The above discussion of volatile partial pressures corresponds in a general manner with the concepts of contact and regional pneumatolytic metamorphism developed by Lacroix, Sundius, and others, summarized in the six modes of occurrence listed at the beginning of this section. The distribution of several trace elements discussed in the previous section also agrees with the similar concept of pegmatitic–hydrothermal environments, whether or not directly related to magmatic activity.

The problem of the source of the elements concentrated in scapolite, i.e. Ca, Na, CO_2, Cl, SO_3, H_2O, B, Be, Li, Sr, Pb, must now be discussed. Most rocks and geological environments contain H_2O, which can be disregarded. Where scapolite forms in calcareous rocks there is clearly a source of CO_2 and Ca. Sulphur

[1] R. I. Harker (abstract presented at the 1958 Ann. Meeting, Geol. Soc. America) found small amounts of Al and F necessary for the synthesis of tilleyite.

is present in all rocks in the form of sulphides, and Cl is widely distributed in both igneous and sedimentary rocks (see Correns, 1956) in amounts ranging up to about 0·1 per cent. B is widely spread in some igneous and most sedimentary rocks, where it is well known to concentrate in the ocean and in marine sediments. Sr, Li, and Pb are widespread in most kinds of rock, but Sr is often enriched in limestones. Little is known about the quantitative distribution of Be, but there is no reason to expect any unusual concentrations in sediments.

All the components of scapolite are therefore present to some degree in a variety of geological environments. The problems of supply mostly centre on the question of how much comes from the parent rock and how much is introduced from elsewhere. It is evident that an impure marine limestone would contain an adequate amount of all the elements required, except perhaps Na, Be, Li, and Pb (Na is commonly present in interstratal waters, however), for a certain amount of scapolite to form during regional metamorphism. A shale, by contrast, might lack CO_2, Ca, and Sr, and a gabbro or greenstone would need CO_2, B, Be, Li, Sr, and Pb. It should perhaps again be stressed, however, that adequate supply of the necessary elements is not the only condition, otherwise scapolite would be more commonly encountered.

The volumetric extent of some scapolitized areas should be emphasized. In the Mt. Isa district of Queensland, Edwards & Baker (1953) calculated that the formation of scapolite in three narrow belts of rock a few miles long necessitated about 500 million tons of chlorine alone. In Ontario, Quebec, and New York State scapolitic rocks are abundant throughout an area of over 80,000 square miles. Another large region containing widespread scapolite is the Kiruna district of Sweden. Both in the last case and at Mt. Isa the scapolitization appears to be related on a regional scale with the emplacement of iron and base-metal ore-bodies. By contrast, other regions showing similar ores do not always show scapolitization.

In the case of limited contact-zones, such as Laacher See, Oslo, and Vesuvius, the participating magmas were obviously the source of any elements absent from the country rocks. Where a regional development of scapolite has taken place there are in every case numerous associated bodies of igneous (or at any rate plutonic) rock, which could have conceivably been the source of metasomatic fluids. However, it is possible that some of these plutonic rocks have themselves been formed by anatectic or metasomatic processes, and it is likely that such large segments of the crust have suffered considerable redistribution of material. It is possible, for example, that in the Grenville province the formation of scapolite was part of a more widespread plutonic metasomatic metamorphism, which also led to the development of anatectic syenite, granite, and migmatites, and concentrated particular elements into the widespread deposits of magnetite, apatite, phlogopite, talc, corundum, lead, zinc, rare-earths, and radio-active minerals. In such a case the addition of elements from elsewhere could only be assessed if the average composition of the whole region

were to be compared with other segments of the crust, and this is not yet possible.

An additional or complementary possibility is that regional scapolitization has only taken place where the original sedimentary–volcanic sequences had significant intercalations of evaporite minerals such as halite, gypsum, and anhydrite. Such beds would be potent sources of Cl, S, B, Na, Ca, and possibly Sr, and might in addition be expected to disappear to a large degree during plutonic metamorphism. The possibility has been considered by Serdyuchenko (1955), and Brown & Engel (1956) have found these minerals to be present in the Grenville rocks of the Adirondacks as primary minerals.

In summary, scapolite appears to have formed stably or metastably in a wide range of *PT* conditions during metamorphism coupled with pegmatitic, pneumatolytic, or hydrothermal action. Since scapolite, although common in certain environments, does not occur in the majority of metamorphic rocks, it may be concluded that unusually high concentrations of certain components are necessary for its formation. These undoubtedly include CO_2, Cl_2, and in some cases SO_3, and were presumably in a fluid phase which was no doubt also rich in H_2O: the role of water is uncertain but small amounts are incorporated in scapolite. The fluid phase in some cases is clearly of magmatic origin, but in other cases it may have been derived from rocks undergoing metamorphic differentiation or anatexis. Experimental studies are necessary before more positive interpretation can be made.

ACKNOWLEDGEMENTS

Acknowledgements of financial aid through research grants from the National Research Council of Canada, the Geological Survey of Canada, and the Penrose Fund of the Geological Society of America are gratefully expressed: other acknowledgements were already given in Part I.

REFERENCES

BARTH, T. E. W., 1952. *Theoretical petrology*. John Wiley & Sons: New York.

BROWN, J. S., & ENGEL, A. E. J., 1956. Revision of Grenville stratigraphy and structure in the Balmat–Edwards district, north-west Adirondacks, New York. *Bull. geol. Soc. Amer.* **67**, 1599–1622.

CORRENS, C. W., 1956. The geochemistry of the halogens, in *Physics and chemistry of the earth*, vol. **2**. Pergamon Press: London.

DEGENHARDT, H., 1957. Untersuchungen zur geochemischen Verteilung des Zirkoniums in der Lithosphäre. *Geochim. et Cosmochim. Acta*, **11**, 279–309.

EMMONS, R. C., *et al.*, 1953. Selected petrogenetic relationships of plagioclase. *Mem. geol. Soc. Amer.* **52**.

FAIRBAIRN, H. W., 1953. Precision and accuracy of chemical analysis of silicate rocks. *Geochim. et Cosmochim. Acta*, **4**, 143–56.

FILBY, R. H., 1957. Spectrographic methods for the determination of Na, K and Ca in minerals, and their application to some scapolites. Unpublished M.Sc. thesis, McMaster University.

FLEISCHER, M., 1955. Estimates of the abundances of some chemical elements and their reliability. *Geol. Soc. Amer., Spec. Pap.* **62**, 145–54.

GOLDSCHMIDT, V. M., 1937. Geochemische Verteilungsgesetze der Elemente. IX. Die Mengenverhältnisse der Elemente und der Atom-Arten. *Skr. norske Vidensk. Akad., I. Mat.-nat. Kl.*, No. **4.**

GREEN, J., 1953. Geochemical table of the elements for 1953. *Bull. geol. Soc. Amer.* **64,** 1001–12.

HORSTMAN, E. L., 1957. The distribution of Li, Rb and Cs in igneous and sedimentary rocks. *Geochim. et Cosmochim. Acta*, **12,** 1–28.

HOWIE, R. A., 1955. The geochemistry of the charnockite series of Madras, India. *Trans. roy. Soc. Edinb.* **62,** 725–68.

JEDWAB, J., 1953. Sur la définition des éléments typochimiques. *Bull. Soc. belge Géol. Pal. Hydr.* **62,** 173–9.

KURODA, P. K., & SANDELL, E. B., 1954. Geochemistry of Mo. *Geochim. et Cosmochim. Acta*, **6,** 35–63.

KUTINA, J., 1957. Zur Frage des kristallchemischen und typochimischen Elemente. *Heidelberg. Beitr. Min.* **6,** 204–14.

NOCKOLDS, S. R., & MITCHELL, R. L., 1948. The geochemistry of some Caledonian plutonic rocks: a study in the relationship between the major and trace elements of igneous rocks and their minerals. *Trans. roy. Soc. Edinb.* **61,** 533–75.

ONISHI, H., & SANDELL, E. B., 1957. Meteoritic and terrestrial abundance of Sn. *Geochim. et Cosmochim. Acta*, **12,** 262–70.

SANDELL, E. B., 1952. The Be content of igneous rocks. Ibid. **2,** 211–16.

—— & GOLDICH, S. S., 1943. The rarer metallic constituents of some American igneous rocks. *J. Geol.* **51,** 99–115 and 167–89.

SHAW, D. M., 1954. Trace elements in pelitic rocks. Part I. Variation during metamorphism. *Bull. geol. Soc. Amer.* **65,** 1151–66.

—— 1957*a*. Some aspects of the determination of Ba in silicate rocks. *Spectrochim. Acta*, **10,** 125–7.

—— 1957*b*. The geochemistry of Ga, In, Tl—a review, in *Physics and chemistry of the earth*, vol. **2.** Pergamon Press: London.

—— WICKREMASINGHE, O. C., & YIP, C., 1958. A simple device for the spectrographic analysis of minerals in an inert atmosphere using the Stallwood jet. *Spectrochim. Acta.* **13,** 197–201.

—— —— & WEBER, J. N., 1960. Spectrochemical determination of Li, Na, K in rocks and minerals using the Stallwood jet. *Anal. Chim. Acta*, **22,** 398–400.

SMALES, A. A., 1955. Some trace-element determinations in G-1 and W-1 by neutron activation. *Geochim. et Cosmochim. Acta*, **8,** 300.

—— & WEBSTER, R. K., 1958. The determination of Rb by the method of stable isotope dilution. *Anal. Chim. Acta*, **18,** 582–6.

—— —— 1958. The determination of Li in rocks by the method of stable isotope dilution. *Anal. Chim. Acta*, **18,** 587–95.

TUREKIAN, K. K., & KULP, J. L., 1956. The geochemistry of Sr. *Geochim. et Cosmochim. Acta*, **10,** 245–96.

TURNER, F. J., & VERHOOGEN, J., 1951. *Igneous and metamorphic petrology*. McGraw-Hill Inc.: New York.

WAGER, L. R., & MITCHELL, R. L., 1951. The distribution of trace-elements during strong fractionation of basic magma—a further study of the Skaergaard intrusion, East Greenland. *Geochim. et Cosmochim. Acta*, **1,** 129–208.

WEDEPOHL, K. H., 1956. Untersuchungen zur Geochemie des Bleis. Ibid. **10,** 69–148.

Diabase–Granophyre Relations in the Endion Sill, Duluth, Minnesota

by W. G. ERNST

Geophysical Laboratory, Carnegie Institution of Washington, Washington, D.C., U.S.A.

ABSTRACT

The gently dipping 1,500-ft thick Endion sill intrudes Keweenawan flows at Duluth, Minnesota. In a general way, from the bottom to the top of the body, there is a gradual transition from diabase through intermediate rock (granodiorite) to granophyre (adamellite). These latter two rock types together constitute about 40 per cent of the exposed mass. Fractional crystallization of basaltic magma produced a great thickness of basic and intermediate rock types which accumulated predominantly in the lower portions of the sill, and probably in the end-stage production of an aqueous, salic, alkalic liquid. It is proposed that, due to initial inclination of the sill, part of this salic fraction migrated up dip, accumulated and reacted with portions of the diabase and intermediate rock, and completed crystallization at the presently exposed level. Alternatively, much or all of the Endion sill granophyre may represent a separate intrusion unrelated to differentiation of the earlier diabase. In either case the sill is composite. Bulk compositions of cryptoperthites indicate both granophyre and intermediate rock crystallized at magmatic temperatures.

Compositional uniformity of the clinopyroxene and lack of iron enrichment in felsic portions of the Endion sill may be the result of accumulation of H_2O and the presumed maintenance of nearly constant partial oxygen pressure during crystallization. This mechanism would furthermore account for inferred late magmatic solid solution between alkali feldspar and $KFe^{3+}Si_3O_8$, with subsequent subsolidus exsolution of haematite.

INTRODUCTION

SCHWARTZ & SANDBERG (1940) described three large sills (the Endion, Northland, and Lester River sills) which intrude Keweenawan flows at Duluth, Minnesota. These bodies are diabase in the lower portions and grade upward to rocks of granitic composition. Schwartz & Sandberg considered a number of hypotheses to explain the origin of the rock series and concluded (1940, pp. 1136–7) that ' . . . many factors had some effect, but that differentiation within each sill accounts for the major part of the segregation of the rock in each of the three sills into two distinct facies'.

The Endion sill was selected for further investigation because it is the largest of the bodies previously studied, and because two fairly complete stratigraphic sections are available; moreover, ubiquitous replacement textures and the abundance of alkali feldspar in the granophyre suggested the possibility of post-magmatic origin for felsic portions of the intrusive.

METHODS OF INVESTIGATION

Two traverses were made across the sill, one along the shore of Lake Superior, the other along Tischer (Congdon) Creek. Outcrops along these traverses and

[Journal of Petrology, Vol. 1, Part 3, pp. 286–303, 1960]

additional scattered exposures within the city were located on aerial photographs and on the 7½-min series Duluth quadrangle topographic sheet (1953). These observations together with data from mapping by Schwartz & Sandberg (1940, pl. 1) and by Taylor (1956, pl. 1) are the basis for Fig. 1 of this report.

Forty-six thin sections representing 37 different rocks were available for petrographic work. Modal analyses were performed on 27 slides; mineral proportions visually estimated on the others are in good agreement with Rosiwal analyses of contiguous rocks. Pyroxene compositions were determined by combined 2V and γ index measurements (Poldervaart, 1947; Hess, 1949). The anorthite contents of plagioclase cores were determined on a four-axis universal stage using a modified Rittman zone method (Emmons, 1943, pp. 115–33) and charts published by Kennedy (1947). Due to normal zoning, plagioclase bulk compositions are probably 10–20 per cent less calcic than the measured cores, as deduced by comparison with normative plagioclase. Thermal state of the plagioclase was determined by X-ray analysis (Tuttle & Bowen, 1950; Smith & Yoder, 1956). The plagioclase is of the low-temperature 'Bushveld type', hence optical determination of composition should be reasonably accurate; anorthite values arrived at by X-ray and optical methods are within 10 per cent An of each other. In any case, *relative* proportions of the anorthite molecule in plagioclases of the various Endion sill rock types are indicated by the optical determinations. Seventeen thin sections were etched and stained (Rosenblum, 1956) to test for potash-bearing feldspar. Symmetry and compositions of the alkali feldspars were determined by X-ray techniques (Goldsmith & Laves, 1954; Bowen & Tuttle, 1950; Orville, 1958). Homogenization of cryptoperthite is described in the section on alkali feldspars.

FIELD RELATIONS

Lake shore section

Immediately below the base of the Endion sill is a layer of baked felsite 2 ft thick which in turn is underlain by a basalt flow. The extrusives strike N. 17° W., and dip 19° NE., and at this locality the contact with diabase appears concordant. Using this attitude, the sill is calculated to be approximately 1,505 ft thick along the shore of Lake Superior. Within 5 ft of the basal contact, the Endion sill is a moderately fine-grained rock, plagioclase laths 1 mm in length being clearly visible. It grades rapidly upward to coarse-grained massive diabase containing grey-green plagioclase laths and tablets up to 10 mm in length (5-mm average). Ophitic pyroxene, magnetite–ilmenite, and variable amounts of serpentine and chlorite are visible with a hand lens. A few hundred feet above the lower contact, several inclusions of anorthositic gabbro were found in typical diabase. At about the middle of the sill, diabase gradually gives way to mottled reddish-black rock of diabasic texture, here termed intermediate rock; this material contains red alkali feldspar and minor quartz in addition to minerals common in the diabase. Continuing up-section, intermediate rock grades imper-

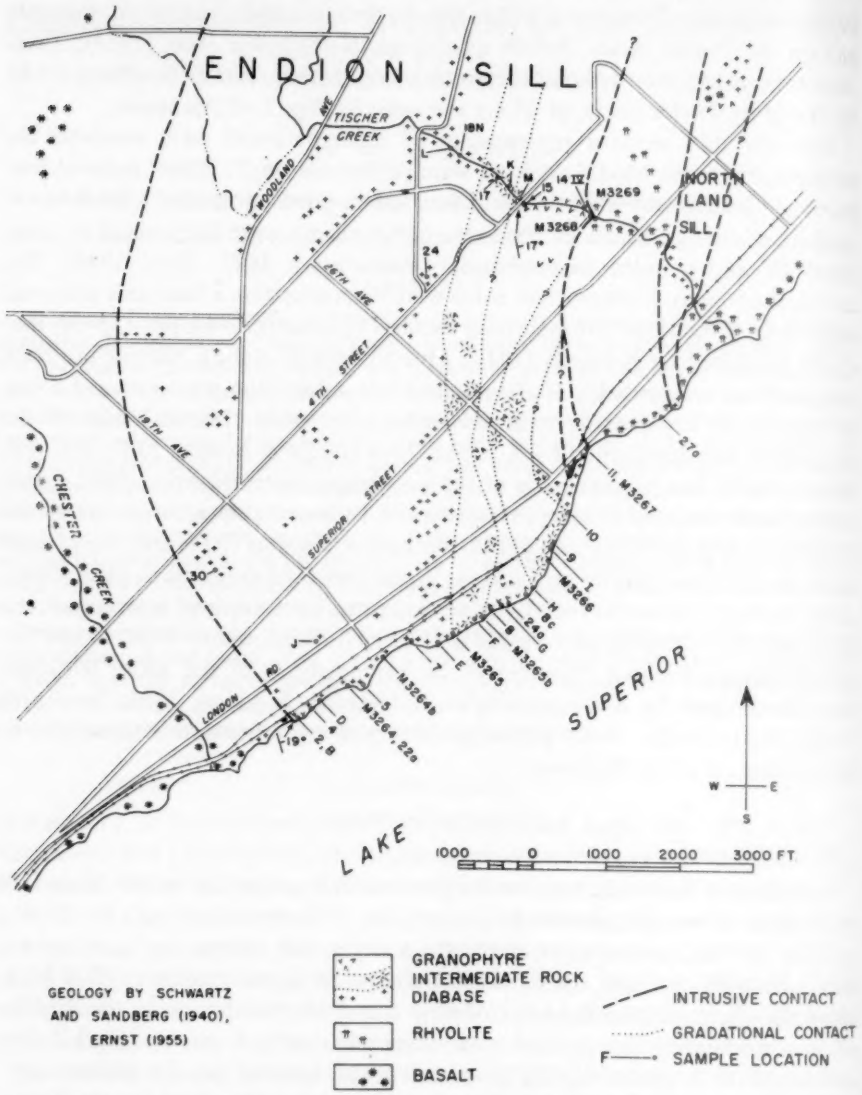

FIG. 1. Areal geology of the Endion sill. Map symbols are in accord with usage of the Minnesota Geological Survey.

ceptibly into granophyre, a brick-coloured felsic unit composed chiefly of red alkali feldspar, plagioclase laths, quartz, chlorite, and magnetite–ilmenite. Some alteration products are pseudomorphous after amphibole. Still farther up-section the granophyre passes continuously through intermediate rock to somewhat altered diabase, the latter becoming increasingly fine-grained as the top of the

sill is approached. Directly overlying the upper fine-grained diabase is a second layer of granophyre about 25 ft thick. The contact between these two rock types is fairly distinct but irregular in detail; the granophyre contains abundant inclusions of fine-grained diabase. The contact between the upper granophyre and overlying recrystallized rhyolite appears gradational and cannot be located precisely. Still higher in the section recrystallized rhyolite passes by degree into unmetamorphosed banded felsite.

Sinuous dikelets of fine-grained granophyre several inches thick and irregular patches of medium-grained granophyre are present in basic portions of the Endion sill. These bodies very locally exhibit aureoles of feldspathized diabase. Several chilled basalt dikes cut all rock types, both in this section and that exposed along Tischer Creek.

Creek section

In the area shown in Fig. 1 of this report, the basal contact of the Endion sill is located accurately only at the shore of Lake Superior; however, mapping to the north by Schwartz & Sandberg (1940, pl. 1) and by Taylor (1956, pl. 1) has provided enough control to locate this contact as shown. Using a dip of 19°, the calculated thickness of the sill in the Tischer Creek area is 1,475 ft. The upper half of the Endion sill, including its contact with overlying rhyolite, is exposed by Tischer Creek. Outcrops along the stream are discontinuous and are moderately weathered. The rocks range from medium-grained diabase (plagioclase laths average about 3 mm in length) upward through intermediate rock to granophyre at the sill roof. Near the contact with overlying rhyolite the grain size diminishes slightly, and several inclusions (up to 4 ft in diameter) of fine-grained altered basalt or diabase are present. The overlying felsite seems virtually unmetamorphosed, and the contact may be located within a few feet.

Miscellaneous outcrops

Scattered exposures within the city exhibit the various rock types of the sill. Three miles north of the mapped area Taylor (1956, p. 59 and pl. 1) shows diabase intruding anorthositic gabbro. Taylor (p. 48) considers this latter type to represent an early stage in the crystallization of the Duluth complex. The diabase which intrudes the anorthositic gabbro lies along strike of the Endion sill, and may be its extension. If so, and considering the anorthositic gabbro inclusions noted in description of the lake shore section, the Endion sill post-dates at least part of the Duluth gabbro sequence.

PETROGRAPHY

Modes of the various rock types are presented in Tables 1 and 2. Most samples show extensive deuteric alteration. The chemical analyses of Endion sill and associated rocks (Schwartz & Sandberg, 1940, table 1) are reproduced in Table 3 with corresponding norms. Modes and chemical analyses of Endion sill rock

TABLE 1

Modes of Endion sill and associated rocks exposed along the shore of Lake Superior

Sample No.	*Strat**	*Qtz*	*Alkali feldspar*	*Plag*	*Core*	*Px*	*Ol*	*Ores*	*Alt†*	*Total mafics*	*Rock types*
2	5	3·7	4·2	44·9	An 52	12·7	—	11·2	23·3	47·2	diabase
B	10	3·2	8·6	41·7	An 51	11·9	—	8·6	26·0	46·5	diabase
4	73	5·0	8·5	39·4	An 60	19·5	—	8·5	19·1	47·1	diabase
D	130	1	7	52	An 54	8	—	4	28	48	diabase
M3264	218	—	0·7	51·3	An 64	18·0	3·1	6·4	20·5	48·0	diabase
22a	218	—	tr.	55	An 64	15	—	5	25	45	diabase
5	280	1·7	5·1	47·9	An 62	15·6	—	5·5	24·2	45·3	diabase
M3264b	405	—	5·5	55·6	An 63	—	—	6·3	32·6	38·9	diabase
7	533	0·8	8·7	51·5	An 64	14·2	—	9·1	15·7	39·0	diabase
E	685	1	6	60	An 45	10	—	7	16	33	dioritic diabase
M3265	727	10·0	14·2	38·8	An 50	—	—	5·2	31·8	37·0	intermediate rock
F	820	8	20	38	An 36	7	—	7	20	34	intermediate rock
M3265b	846	9·5	19·9	33·7	An 43	10·8	—	6·9	19·2	36·9	intermediate rock
8	903	12·0	33·6	24·3	An 36	—	—	3·1	27·0	30·1	granophyre
G	935	14	25	37	An 29	—	—	11	13	24	granophyre
24a	965	15	35	25	An 28	—	—	3	22	25	granophyre
8c	1,072	15·2	41·6	15·5	An 36	—	—	12·6	15·1	27·7	granophyre
H	1,125	13·1	37·7	18·5	An 38	0·7	—	4·7	25·3	30·7	granophyre
M3266	1,220	14·6	40·0	25·7	An 42	4·2	—	2·6	12·9	19·7	granophyric intermediate rock
I	1,250	8·0	35·9	17·9	An 32	11·5	—	4·9	21·8	38·2	granophyric intermediate rock
9	1,265	7·5	12·5	42·5	An 44	10	—	5	22·5	37·5	intermediate rock
10	1,340	7·7	13·1	37·4	An 45	9·7	—	7·8	24·3	41·8	intermediate rock
11	1,505	19·9	44·8	14·9	An 30	—	—	8·4	12·0	20·4	granophyre
M3267	1,505	17·1	42·7	25·5	An 29	—	—	4·2	10·5	14·7	granophyre
27a	1,787	25	72		?	—	—	3	tr.	3	rhyolite

* Strat = distance above base of sill in feet.
† Alt = mafic alteration products.
Location of samples shown in Fig. 1.

TABLE 2

Modes of Endion sill and associated rocks exposed along Tischer (Congdon) Creek and within the city of Duluth

Sample No.	*Strat**	*Qtz*	*Alkali feldspar*	*Plag*	*Core*	*Px*	*Ol*	*Ores*	*Alt†*	*Total mafics*	*Rock types*
30	100	—	tr.	48·9	An 65	9·4	14·3	7·5	19·9	51·1	diabase
J	280	tr.	2	50	An 57	15	—	8	25	48	diabase
L	820	3·2	20·2	38·7	An 54	5·8	—	5·7	26·4	37·9	granophyric diabase
24	840	3·1	9·8	38·2	An 55	19·6	—	11·0	18·3	48·9	diabase
18N	870	6·5	10·8	40·7	An 55	11·9	—	8·2	21·9	42·0	diabase
17	1,005	11·1	16·9	34·4	An 50	14·1	—	5·8	17·7	37·6	intermediate rock
K	1,100	7·5	19·1	31·0	An 48	10·1	—	7·0	25·3	42·4	intermediate rock
M	1,150	10	30	35	An 25	5	—	5	15	25	granophyre
15	1,180	13·2	31·5	22·9	An 25	8·6	—	3·5	20·3	32·4	granophyre
141V	1,382	15·2	43·0	14·4	An 36	tr.	—	5·9	21·5	27·4	granophyre
M3268	1,459	19·1	32·3	26·7	An 31	tr.	—	6·2	15·7	21·9	granophyre
M3269	1,480	30	65		?	—	—	5	tr.	5	rhyolite

* Strat = distance above base of sill in feet.
† Alt = mafic alteration products.
Location of samples shown in Fig. 1.

TABLE 3

Analysed Endion sill and associated rocks (Schwartz & Sandberg, 1940)

	M3264	M3264b	M3265b	M3266	M3267	M3268	M3269
SiO_2	47·25	—	52·42	61·46	—	61·07	75·48
Al_2O_3	15·00	—	12·66	13·22	—	13·66	12·30
Fe_2O_3	2·64	5·97	3·90	3·08	4·53	3·04	2·54
FeO	11·09	9·37	9·55	5·42	2·57	5·54	0·36
MgO	6·52	—	3·74	2·00	—	2·48	tr.
CaO	8·40	—	5·16	2·96	—	2·36	0·14
Na_2O	2·52	2·03	3·01	3·33	3·50	3·40	3·43
K_2O	0·81	1·17	2·44	4·30	4·59	4·10	5·17
H_2O+	1·63	—	2·00	1·24	—	1·79	0·24
H_2O-	0·35	—	0·80	0·32	—	0·45	0·04
TiO_2	2·89	—	2·66	1·37	—	1·37	0·21
P_2O_5	0·56	—	1·14	0·40	—	0·48	0·02
MnO	0·21	—	0·25	0·18	—	0·15	0·02
CO_2	—	—	—	0·53	—	0·20	—
TOTAL	99·87		99·73	99·81		100·09	99·95
Niggli molecular norms (calculated by present author)							
Q	—		8·5	15·3		15·3	33·4
Or	5·0		15·5	26·5		25·0	31·5
Plag	52·0		43·5	40·3		40·5	32·0
	An 55		An 35	An 22		An 21	An 2
Px	34·0		21·6	11·6		12·8	—
Ol	0·6		—	—		—	—
Ores	7·1		8·2	5·5		5·3	3·1
Ap	1·3		2·7	0·8		1·1	—

Location of samples shown in Fig. 1.

Analyses of M3264 and M3269 performed by S. S. Goldich; all others by R. W. Perlich, Rock Analysis Laboratory, University of Minnesota.

types are similar to those of gabbro, granodiorite, and granophyre exposed elsewhere in the Duluth region. Endion sill granophyre tends to have a higher modal proportion of mafic minerals than separate granophyre intrusions described by Taylor (1956, table 6). The intermediate rock contains smaller amounts of lime, and both intermediate rock and granophyre contain less Fe_2O_3 and generally less SiO_2 than corresponding types from the Enger Tower area (Goldich *et al.*, 1956, table 6).

Stated $\pm$ errors in mineral compositions for plagioclase, clinopyroxene, and olivine in this section, and for alkali feldspar in the following section are subjective evaluations and reflect the author's relative degree of confidence in reliability of the determinations.

Diabase

Diabase is the most abundant rock type in the Endion sill. Its lath-shaped plagioclase shows normal continuous zoning with cores ranging from $An_{73\pm5}$ to $An_{50\pm5}$. Large calcic crystals have been fractured or broken and are surrounded by more sodic rims. Poikilitic subcalcic clinopyroxene ($Wo_{35\pm5}En_{10\pm5}Fs_{25\pm5}$) is

commonly preserved, but to some extent is altered to chlorite, sphene, magnetite–ilmenite, and fine-grained uralite; the violet hue of the pyroxene suggests the presence of TiO_2. Euhedral olivine ($Fo_{62\pm2}$ in sample 30) was apparently an essential constituent in most specimens, but it is now largely replaced by intergrowths of chlorite, talc, iddingsite, magnetite–ilmenite, and serpentine. In several specimens, small amounts of interstitial alkali feldspar and quartz are graphically intergrown. The alkali feldspar rims plagioclase and in part replaces it along cleavage traces or irregular seams.

Intermediate rock (granodiorite)

Although megascopically similar to diabase, the intermediate rock displays a red and black mottling due to irregular distribution of granophyric material. The red colour results from the clouding of alkali feldspar by minute hematite flakes. Diabasic texture is preserved. Plagioclase laths are gradationally zoned, with cores ranging from $An_{50\pm5}$ to $An_{36\pm5}$; they are armoured and irregularly replaced by rusty alkali feldspar. Alkali feldspar is generally less than one-third of the total feldspar. Interstitial myrmekitic–graphic quartz+alkali feldspar, remnant sub-calcic titanaugite (compositionally similar to that found in the diabase) and alteration products (pseudomorphous after clinopyroxene) are the other important constituents. Significance of the mantled feldspars is not clear: textures suggest partial replacement of plagioclase by alkali feldspar, but the occurrence of interstitial quartz and alkali feldspar in the same specimen seems to indicate late magmatic crystallization.

Textural and mineralogic variations of intermediate rock towards diabase on one hand, and granophyre on the other, are common in the Endion sill.

Granophyre (adamellite)

This rock is composed chiefly of plagioclase and red alkali feldspar in roughly equal proportions, quartz, moderate amounts of mafic alteration products (in part pseudomorphous after amphibole), and relic subcalcic titanaugite (violet hue) of the composition $Wo_{40\pm5}En_{35\pm5}Fs_{25\pm5}$. The cores of weakly zoned plagioclase laths range from $An_{38\pm5}$ to $An_{25\pm5}$; these remnants are extensively armoured and irregularly replaced by alkali feldspar. In addition, much red alkali feldspar is graphically intergrown with quartz.

Variations in mineralogy of the Endion sill along the shore of Lake Superior and along Tischer Creek are illustrated in Figs. 2 and 3.

THE ALKALI FELDSPAR

As shown by Tables 1 and 2, large amounts of alkali feldspar are present in felsic rock types of the Endion sill. Several determinations of $2V$ performed by P. M. Orville gave an angle of approximately $80° \perp(010)$, suggesting that the material (which is optically homogeneous) is a low-temperature form. The

author was unable to separate the alkali feldspar from intergrown quartz and plagioclase. X-ray investigation of the felsic fraction of both granophyre and intermediate rock indicates that the potash-rich phase is uniformly monoclinic with composition close to pure $KAlSi_3O_8$. This material is intimately associated

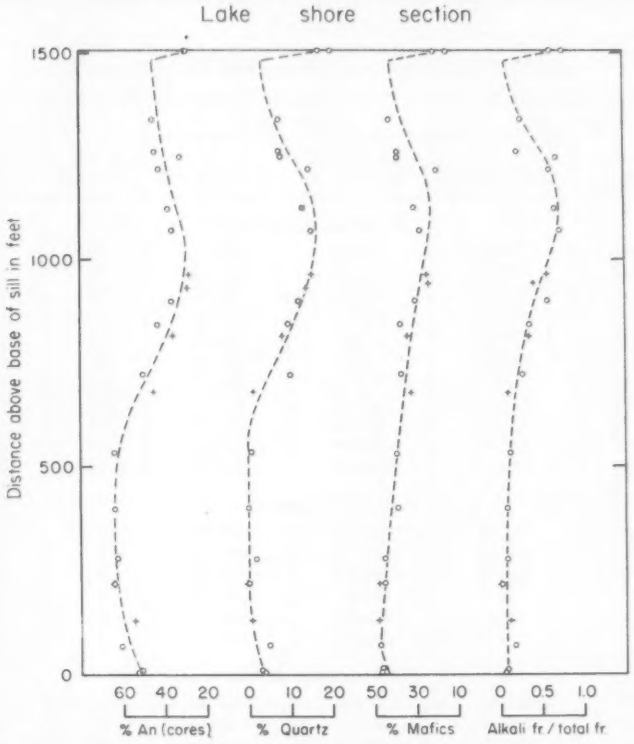

FIG. 2. Stratigraphic section through the Endion sill along the shore of Lake Superior. Crosses indicate estimated modal percentages. Note scale values.

with relatively sodic plagioclase, and lack of solid solution suggests that these feldspars completed recrystallization at subsolidus temperatures. It would be tempting to account for the abundance and composition of the alkali feldspar by means of a process of low-temperature feldspathization—an explanation in accord with ubiquitous replacement textures (and mantling) previously described.

Because plagioclase laths could not be separated from their alkali feldspar mantles, it was not known if these rims were composed solely of $KAlSi_3O_8$ or whether submicroscopic lamellae of sodic plagioclase were present in addition to the orthoclase. Therefore heating experiments were conducted to determine whether or not the mantles were cryptoperthitic. It was expected that if cryptoperthite were present it would homogenize rapidly, while reaction between

discrete plagioclase laths and alkali feldspar mantles and irregular replacement patches would be slow but relatively continuous. Heat treatment of felsic fractions of Endion sill rocks at 1,050° C caused compositional change (homogenization) of the alkali feldspar, as deduced by X-ray analysis. Rate studies were performed on Endion sill and other samples (described below) in order to select

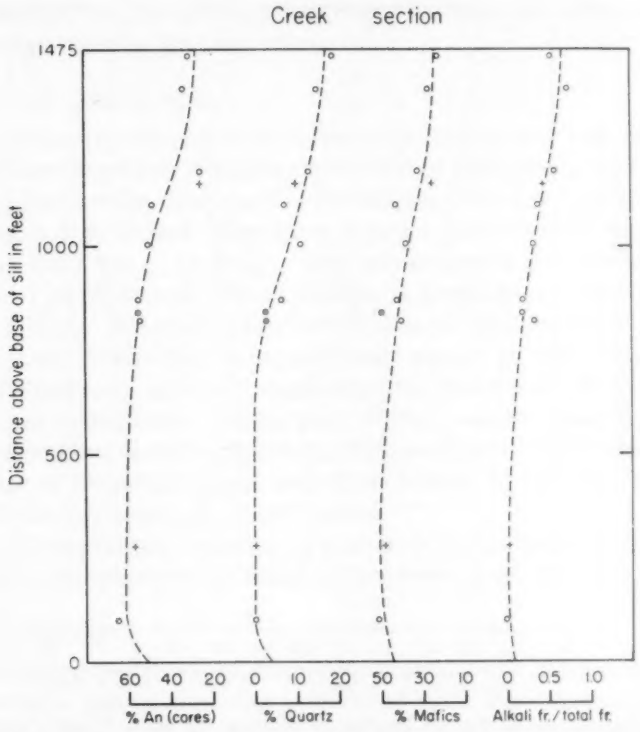

FIG. 3. Stratigraphic section through the Endion sill along Tischer Creek and including miscellaneous exposures within the city of Duluth. Crosses indicate estimated modal percentages. Note scale values.

the minimum time in which homogenization could be obtained at this temperature without significant contamination of the alkali feldspar by its interaction with the separate plagioclase crystals.

Endion sill samples (all of which contained quartz) show no sign of melting in runs as long as 1,138 min at 1,050° C. Partial fusion would be expected above ~960° C (Tuttle & Bowen, 1958, p. 83) if given sufficient time. No change in the red colour of the alkali feldspar is observed. (The experiments were carried out in air, and were well within the haematite field of stability.) Endion sill and other feldspar samples were sized and the 28–45 mesh fraction (0·589–0·322 mm) was employed for experiments. Endion sill material finely ground to minus

100 mesh (< 0.147 mm) yields the same results as the coarse fraction, suggesting that the rate of reaction between separate plagioclase and alkali feldspar grains is not affected appreciably by particle size. Rate study data are summarized in Table 4.

TABLE 4

Rate study on homogenization of alkali feldspar

Duration in minutes	*No. of readings*	*Alkali feldspar*		*Plagioclase*	
		2θave (20$\bar{1}$)*	*Stand. error of the mean*	*2θave* (20$\bar{1}$)*	*Stand. error of the mean*
		Endion sill sample H			
0	10	21·000	0·0089	22·018	0·0058
5	12	21·119	0·0174	21·992	0·0106
11	10	21·121	0·0120	21·942	0·0072
25	10	21·182	0·0058	21·913	0·0116
26†	10	21·251	0·0056	21·887	0·0076
63†	10	21·264	0·0064	21·924	0·0073
100	10	21·240	0·0153	21·861	0·0126
180†	10	21·298	0·0048	21·876	0·0114
330	12	21·276	0·0109	21·863	0·0067
956	10	21·253	0·0096	21·868	0·0071
1138†	10	21·278	0·0085	21·887	0·0089
		Spencer sample I			
0	8	20·913	0·0027	22·138	0·0050
10	8	21·269	0·0040	22·111	0·0251
25	8	21·286	0·0041	21·992	0·0468
55	8	21·286	0·0048	—	—
125	8	21·288	0·0035	—	—
939	6	21·283	0·0048	—	—
		Orville sample 57–109			
0	10	20·977	0·0032	22·060	0·0043
20	8	21·021	0·0043	22·027	0·0096
248	12	21·020	0·0076	21·980	0·0097
427	10	21·025	0·0038	21·923	0·0074
991	12	21·049	0·0038	21·865	0·0179

* Cu $K\alpha = 1{\cdot}5418$; reflection determined by difference from $KBrO_3$ internal standard (101) = 20·205° 2θ.

† −100-mesh powder; all others 28–75 mesh fraction.

Fig. 4*a* gives curves for the change in composition of feldspar versus time for the felsic fraction of a typical sample of Endion sill granophyre (sample H). Within 60 min at 1,050° C, the alkali feldspar is completely homogenized; with continued heating a negligible compositional change occurs in both alkali feldspar and plagioclase. The X-ray composition of the homogenized alkali feldspar is $Or_{68\pm3}$. The change in composition of the potassic phase is accompanied by a complementary change in plagioclase composition; concomitantly plagioclase decreases in relative amount, as indicated by X-ray intensities, as the alkali feldspar increases. These phenomena reflect the fact that, prior to

heating, two plagioclase phases are present: (1) optically visible primary laths (oligoclase-andesine) which contain moderate amounts of the Or molecule, and (2) subsolidus exsolution cryptoperthite (albite) which contains almost no potash; when the cryptoperthite plagioclase is resorbed during homogenization, the primary laths remain and their composition and proportion are measured.

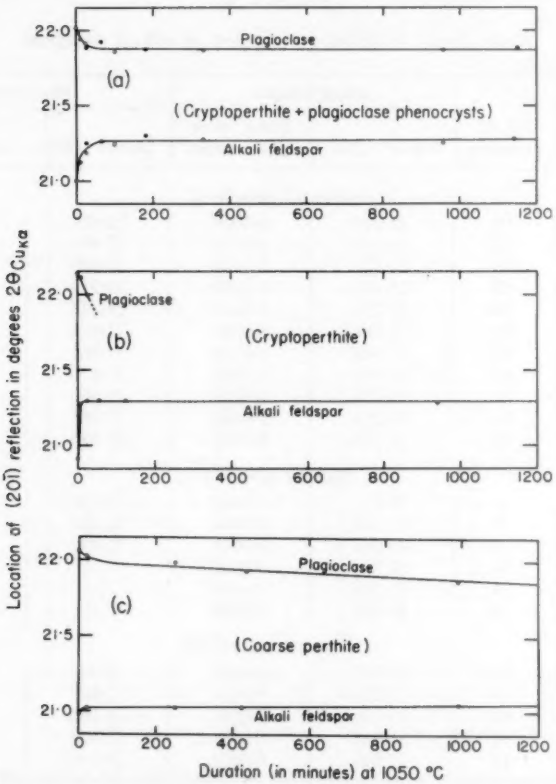

FIG. 4. Homogenization of cryptoperthite at 1,050° C (dry) as a function of heating duration. (20$\bar{1}$) reflections measured by difference from (101) peak of $KBrO_3$ ($2\theta = 20{\cdot}205°$ Cu $K\alpha$) as described by Orville (1958). Open circles represent 28–45 mesh samples, closed circles indicate powder of −100 mesh. (*a*) Endion sill alkali feldspar+plagioclase+quartz (sample H); (*b*) Spencer orthoclase+albite cryptoperthite (sample I); (*c*) Orville coarse orthoclase+albite perthite (sample 57–109). See text for discussion of homogenization rate curves; Table 4 summarizes results of heating experiments.

For comparison, rate experiments were performed on samples of known cryptoperthite and very coarse perthite (approximating the condition of separate orthoclase and plagioclase grains). Fig. 4*b* shows the very rapid homogenization of Spencer (1937) cryptoperthite (sample I) at 1,050° C obtained from H. S. Yoder. All original plagioclase is cryptoperthitic and is completely eliminated by homogenization. X-ray composition of the alkali feldspar is $Or_{69\pm3}$.

Fig. 4*c* illustrates compositional changes at 1,050° C of both phases of a

coarse perthite (sample 57–109) obtained from P. M. Orville. From the rate study it is inferred that a small amount of submicroscopic perthite (homogenized within 20 min) is initially present in the sample; this observation is supported by the discrepancy between modal composition, Or_{81}, and chemically analysed bulk composition, Or_{72} (P. M. Orville, personal communication). Reaction between the coarse alkali feldspar and plagioclase lamellae is reflected in compositional migration (determined by X-ray analysis) of both phases during prolonged heating. Here the reaction between potash-rich feldspar and plagioclase grains is much greater than in Endion sill material for a corresponding duration of heating. Plagioclase of the coarse perthite is albite and that of the Endion sill is oligoclase-andesine; presumably the rate of reaction between plagioclase and alkali feldspar is dependent on composition.

Although termed cryptoperthite on the basis of optical homogeneity, Endion sill alkali feldspars fall within the orthoclase-microperthite group as defined by MacKenzie & Smith (1956, p. 406). Heat treatment of this material (sample H) at 700° C induced partial homogenization in 150 min; continued heating caused a very slow but measurable increase in homogenization with time. Similar experiments performed by P. M. Orville (personal communication) resulted in complete homogenization of Spencer sample I, but caused no change in the coarse perthite (sample 57–109). The present writer tentatively suggests that at 700° C, although cryptoperthite homogenizes readily, homogenization of fine-grained 'microperthite' (submicroscopic) is exceedingly sluggish; on this premiss, alkali feldspars of the Endion sill appear to be a mixture of crypto- and fine-grained microperthite.

X-ray analysis of heated samples indicates that alkali feldspar of the Endion sill is compositionally about $Or_{62\pm5}$ in the intermediate rock and $Or_{67\pm5}$ in the granophyre (the remainder being plagioclase near the albite end member). Judging from the relatively uniform composition in individual samples, cryptoperthites doubtless crystallized initially as a homogeneous phase. Investigations of Bowen & Tuttle (1950, fig. 3) demonstrated that an alkali feldspar of this composition is stable only above temperatures of the order of 600° C; presence of the anorthite molecule in the exsolved plagioclase phase increases the temperature of the solvus (Yoder *et al.*, 1957), so 600° C may be considered as a low-temperature limit for crystallization of Endion sill alkali feldspar. Thus emplacement of the Endion sill intermediate rock and granophyre was essentially a high-temperature process.

Partial replacement of early plagioclase laths by alkali feldspar can be explained by fractionation of the magma; with decreasing temperature, the melt must have migrated from a two-feldspar field to a region where magma was in equilibrium with alkali feldspar alone. This migration is a complicated process, and involves solvus-solidus relations in the magma. Referring to the system Or–Ab–An (–SiO_2–H_2O), Stewart (1956, pp. 99–124) has described such relations in detail.

At low P_{H_2O} the point of tangency between solvus and solidus in the system Or–Ab–An ($-SiO_2$–H_2O) lies on the Or side of the critical point on the feldspar solvus. (A solvus critical point is the point at which coexisting phases become identical in composition.) Mantling and replacement of plagioclase by alkali feldspar in Endion sill rocks probably were produced as follows. As temperature decreased towards that of the point of tangency, the composition of alkali feldspar changed rapidly, relative to the composition of plagioclase, and for appropriate bulk compositions the condensed assemblage plagioclase+alkali feldspar+liquid (+quartz) was placed in a region where only alkali feldspar and liquid (+quartz) could coexist; hence there was reaction to form additional alkali feldspar at the expense of both plagioclase and melt (yielding replacement and armouring textures). At still lower temperatures, for salic compositions under consideration the solvus and solidus no longer intersected; regardless of the position of critical points on the solvus, melt was in equilibrium with alkali feldspar alone, and earlier solids were armoured by alkali feldspar (+quartz).

Alternatively, observed feldspar textures could have resulted from devolatilization during later stages in crystallization of the Endion magma. This mechanism is considered less probable than that described above. With periodic egress of vapour, large-scale rhythmic banding should have occurred; the gradual elevation of vapour pressure between these cycles might be expected to have caused reprecipitation of plagioclase, yielding rapakivi texture. The effect of relatively continuous loss of volatiles should have been that of diminution of grain size during end stages of crystallization, but observed alkali feldspar mantles and myrmekitic intergrowths are as coarse-grained as the plagioclase laths.

Although at low P_{H_2O} the point of tangency between solvus and solidus is on the Or side of the critical point of the solvus, at several thousand bars water pressure, the locus of this intersection is thought to lie on the opposite side of the solvus critical point (Stewart, in press), and rapakivi textures are to be expected. With P_{H_2O} in excess of about 6,000 bars, solvus and solidus intersect over the entire range of feldspar compositions, and cotectic crystallization of two feldspars results (H. S. Yoder, personal communication). Considering the experimental evidence, feldspar textures developed in the Endion sill suggest that during later stages of crystallization, water pressure was of the order of $1{,}000 \pm 500$ bars (which corresponds to a depth of intrusion of roughly 1–3 miles, provided P_{H_2O} approximates P_{total}).

DISCUSSION

In preceding sections it has been demonstrated that the Endion sill is composed of a gradational sequence of magmatic rock types (Tables 1 and 2, Figs. 2 and 3 and discussion of alkali feldspars). This succession is fundamentally similar to the diabase– and gabbro– granophyre association found in many places throughout the world. Studies by Wager & Deer (1939), Walker (1940), Cornwall (1951 *a*, *b*), Hotz (1953), Taylor (1956), Goldich *et al.* (1956), and

Bayley (1959) all lend support to the hypothesis that such associations are genetic and result from fractional crystallization. It has been suggested (Grout, 1947, p. 51) that differentiation of basaltic magma yields a maximum of about 10 per cent granite by volume, provided a suitable mechanism for separating solid and liquid phases is operative. Fig. 1 indicates that the Endion sill in known exposures contains about 20 per cent intermediate rock (granodiorite) and an equal amount of granophyre (adamellite). From consideration of the chemistry of Endion sill rock types (Table 3), fractional crystallization of basaltic magmas *in situ* is totally inadequate to produce the observed series. Therefore, either the magma was (1) more salic than ordinary basaltic rocks of the Duluth complex, or (2) significant addition of granitic material and/or replacement of diabase occurred during emplacement of the sill.

Modes of the fine-grained basal contact of the Endion sill (samples 2 and B) indicate that the primary magma was basalt. Corroborating evidence may be cited in the analysis given by Schwartz & Sandberg (1940, table 1, sample 8) for the overlying Northland sill which is only 31 ft thick and is uniformly fine grained where the sample was taken. It is probable that this analysis represents relatively undifferentiated basaltic magma similar to that of the Endion sill. Therefore change in bulk composition of the intrusive undoubtedly took place after the onset of crystallization. Field relations along Lake Superior and the pronounced mineralogic and chemical dissimilarity between granophyre and rhyolite shown in Tables 1–3 (see also Schwartz & Sandberg, 1940, fig. 4) indicate the former cannot be a recrystallized phase of the latter. Assimilation of rhyolite and subsequent differentiation in place was found inadequate by Schwartz & Sandberg (1940, pp. 1165–6), who showed that the bulk composition of the sill cannot be represented by combination of rhyolite and diabase. The absence of rhyolitic inclusions to some extent supports their argument. (The only inclusions are of mafic rock types.)

Plagioclase crystals in the Endion sill are gradationally zoned and their albite contents reach a maximum in the felsic, alkali feldspar-rich upper portions of the sill; concomitantly the mafic/felsic ratio diminishes. It is apparent that crystal fractionation did occur, and this process doubtless gave rise to moderate amounts of aqueous, salic, alkalic melt near the end stages of crystallization. This residuum was concentrated in the upper portions of the sill, for although solidification proceeded from both roof and floor, most of the early crystals accumulated along the bottom of the sill due to gravitative settling.

Sandberg (1938, p. 822) has given evidence (fanning of dips) that the Lake Superior basin was subsiding during accumulation of the Keweenawan flows. Consequently the Endion sill must have been emplaced as a gently inclined sheet. In response to the gradient produced by the small initial inclination of the sill, tenuous salic magma (derived by differentiation of the diabase) may have migrated up-dip, reacted locally with permeable portions of the still warm diabase to produce additional intermediate rock and granophyre, and concentrated

and solidified towards the up-dip termination of the body. Where fracturing was minor, the liquid was contained within the sill proper, or rose along fissures to solidify between the upper chilled diabase and the overlying rhyolite (as inferred from the lake shore section). In regions of more extensive fracturing, the diabasic roof may have sunk into the granophyric magma, displacing it

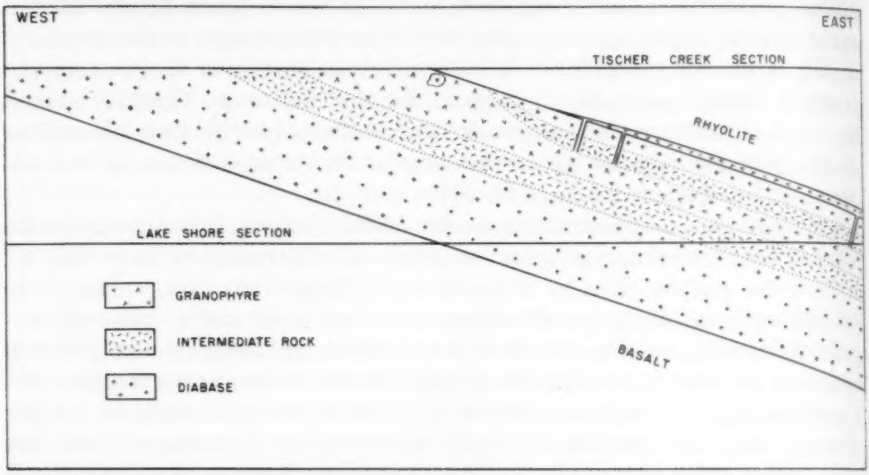

FIG. 5. Diagrammatic cross-section through Endion sill. Note medial granophyre as indicated by lake shore section.

upwards (as inferred from the creek section). These relations are diagrammatically illustrated in Fig. 5. According to this hypothesis, a large section of diabase with little associated granophyre and intermediate rock should be present down-dip from the present level.

Alternatively, it may be suggested that the granophyre represents a separate, unrelated body which was intruded into the late crystallizing portion (intermediate rock) of the original sill. In this case, relatively continuous mineralogic variations illustrated in Figs. 2 and 3 may be explained through a process of uniform reaction between diabase (and some of the intermediate rock) and the intrusive granitic magma. Because felsic rocks of the Endion sill exhibit the effects of both differentiation and reaction, it is difficult to decide whether or not the granophyre and diabase are genetically related. Under either hypothesis the sill is composite; the disproportionate masses of intermediate rock and granophyre displayed in the mapped area are a consequence of up-dip movement and accumulation of salic melt. The first hypothesis is preferred because internal sill contacts and mineralogic discontinuities between diabase and granophyre are totally absent in the Endion sill. However, it should be noted that separate intrusions of granophyre are abundant in the Duluth area (Taylor, 1956).

Similar anomalous proportions of granophyre and gabbro developed on a

larger scale elsewhere in the region. Grout *et al.* (1959, pp. 45–46, also pl. 2) have indicated approximately equal outcrop areas of felsic and mafic rock types in portions of the north-eastern tongue of the Duluth complex. Granophyre is considered to have crystallized late in the magmatic cycle, and these authors have tentatively suggested that salic magma migrated eastward and accumulated at a stage when the gabbro was largely solid.

Influence of volatiles on the course of crystallization

The occurrence of primary amphibole (now represented by alteration products) in the granophyre suggests that the late crystallizing magma contained moderate amounts of water. Osborn (1959) has postulated that residual concentration of iron is inhibited during crystallization of volatile-rich magmas in which dissociation of water maintains partial oxygen pressure at a relatively constant value. Table 3 shows that felsic members of the Endion sill rock sequence do not exhibit iron enrichment relative to the mafic rocks. Stabilized P_{O_2} would explain the lack of variation in clinopyroxene composition: as exemplified by the system MgO–FeO–Fe_2O_3–SiO_2 (Muan & Osborn, 1956), at constant partial oxygen pressure the ratio $FeO+Fe_2O_3/FeO+Fe_2O_3+MgO$ of the liquid remains almost fixed during solidification, so that successively precipitated pyroxenes would be of nearly identical composition.

The problem of clouded red feldspars

Uniform clouding of alkali feldspar of the Endion sill and the lack of red inclusions in the graphically intergrown (cotectic) quartz rule out the possibility that intratelluric haematite was simply engulfed by late-stage feldspar. More probably alkali feldspar contained minor amounts of the iron orthoclase molecule, which exsolved on cooling. Dry experiments by Faust (1936) and hydrothermal investigation of 'ferriannite' by Wones (1959) indicate that $KFe^{3+}Si_3O_8$ is stable at magmatic temperatures only at relatively high oxidation states. Assuming nearly constant P_{O_2}, the *relative* state of oxidation increases as temperature declines, and the residual Endion sill magma probably passed through the magnetite stability field towards the P_{O_2}–T region where magnetite and haematite coexist; this explains why only late crystallizing feldspars could contain appreciable iron orthoclase. Subsolidus experiments by Rosenqvist (1951, p. 73) showed that less Fe_2O_3 is incorporated in the feldspar lattice at low temperatures than at high temperatures; he further pointed out that change of bulk composition to a higher alumina content could cause exsolution of haematite at constant temperature. Endion sill rocks, however, show no mineralogical evidence of late Al_2O_3 enrichment. If expelled as iron orthoclase, this exsolved phase must have decomposed to haematite and potash+silica (presumably leached away); if expelled as haematite, the structural sites were filled by incoming alumina, with Fe_2O_3 occupying lattice defects. In either case, only small amounts of exsolution would be necessary to impart a red colour to the alkali feldspar.

ACKNOWLEDGEMENTS

The writer is indebted to S. S. Goldich who interested the writer in the problem and suggested numerous improvements in the manuscript, and to R. B. Taylor, G. M. Schwartz, and W. C. Phinney, all of the University of Minnesota, who read the manuscript at one stage or another. The constructive criticism of H. S. Yoder, H. J. Greenwood, and P. M. Orville of the Geophysical Laboratory, D. B. Stewart of the U.S. Geological Survey, and O. F. Tuttle of the Pennsylvania State University, is also appreciated.

Financial support was obtained from the Minnesota Geological Survey and the Geophysical Laboratory.

REFERENCES

Bayley, R. W., 1959. A metamorphosed differentiated sill in northern Michigan. *Amer. J. Sci.* **257**, 408–30.

Bowen, N. L., & Tuttle, O. F., 1950. The system $NaAlSi_3O_8$–$KAlSi_3O_8$–H_2O. *J. Geol.* **58**, 489–511.

Cornwall, H. R., 1951*a*. Differentiation in magmas of the Keweenawan series. *J. Geol.* **59**, 151–72.

—— 1951*b*. Differentiation in lavas of the Keweenawan series and the origin of the copper deposits of Michigan. *Bull. geol. Soc. Amer.* **62**, 159–202.

Emmons, R. C., 1943. The universal stage. *Mem. geol. Soc. Amer.* **8**.

Ernst, W. G., 1955. *The petrology of the Endion sill, Duluth, Minnesota.* Unpubl. M.Sc. thesis, Univ. Minnesota.

Faust, G. T., 1936. The fusion relations of iron-orthoclase. *Amer. Min.* **21**, 735–63.

Goldich, S. S., Taylor, R. B., & Lucia, F. J., 1956. Geology of the Enger Tower area, Duluth, Minnesota. *Guidebook Ser., geol. Soc. Amer.*, Field Trip No. 1, 67–90.

Goldsmith, J. R., & Laves, F., 1954. The microcline-sanidine stability relations. *Geochim. et Cosmochim. Acta*, **5**, 1–19.

Grout, F. F., 1947. Origin of granite. *Mem. geol. Soc. Amer.* **28**, 45–53.

—— Sharp, R. F., & Schwartz, G. M., 1959. The geology of Cook County, Minnesota. *Bull. Minn. geol. Surv.* **39**, 163 p.

Hess, H. H., 1949. Chemical composition and optical properties of common clinopyroxenes. *Amer. Min.* **34**, 621–66.

Hotz, P. E., 1953. Petrology of granophyre in diabase near Dillsburg, Pennsylvania. *Bull. geol. Soc. Amer.* **64**, 675–704.

Kennedy, G. C., 1947. Charts for correlation of optical properties with chemical composition of some common rock-forming minerals. *Amer. Min.* **32**, 561–73.

MacKenzie, W. S., & Smith, J. V., 1956. The alkali feldspars. III. An optical and X-ray study of high-temperature feldspars. *Amer. Min.* **41**, 405–27.

Muan, A., & Osborn, E. F., 1956. Phase equilibria at liquidus temperatures in the system MgO–FeO–Fe_2O_3–SiO_2. *J. Amer. Ceram. Soc.* **39**, 121–40.

Orville, P. M., 1958. Feldspar investigations. *Yearbook Carnegie Inst.* No. **57**, 206–9.

Osborn, E. F., 1959. Role of oxygen pressure in the crystallization and differentiation of basaltic magma. *Amer. J. Sci.* **257**, 609–47.

Poldervaart, A., 1947. The relationship of orthopyroxene to pigeonite. *Miner. Mag.* **28**, 164–72.

Rosenblum, S., 1956. Improved technique for staining potash feldspars. *Amer. Min.* **41**, 662–4.

Rosenqvist, I. T., 1951. Investigations in the crystal chemistry of silicates. III. The relation haematite microcline. *Norsk geol. Tidsskr.* **29**, 65–76.

Sandberg, A. E., 1938. Section across Keweenawan lavas at Duluth, Minnesota. *Bull. geol. Soc. Amer.* **49**, 795–830.

Schwartz, G. M., & Sandberg, A. E., 1940. Rock series in diabase sills at Duluth, Minnesota. *Bull. geol. Soc. Amer.*, **51**, 1135–72.

Smith, J. R., & Yoder, H. S., 1956. Variation in X-ray powder diffraction patterns of plagioclase feldspars. *Amer. Min.* **41**, 632–47.

SPENCER, E., 1937. The potash-soda-feldspars. I. Thermal stability. *Miner. Mag.* **24,** 453–94.

STEWART, D. B., 1956. *Rapakivi granite of the Deer Isle region, Maine.* Unpubl. Ph.D. thesis, Harvard Univ.

—— *in press.* Rapakivi granite from eastern Penobscot Bay, Maine. *XX Int. geol. Congr.*

TAYLOR, R. B., 1956. The Duluth gabbro complex, Duluth, Minnesota. *Guidebook Ser., geol. Soc. Amer.*, Field Trip No. 1, 42–66.

TUTTLE, O. F., & BOWEN, N. L., 1950. High-temperature albite and contiguous feldspars. *J. geol.* **58,** 572–83.

—— —— 1958. Origin of granite in the light of experimental studies in the system $NaAlSi_3O_8$–$KAlSi_3O_8$–SiO_2–H_2O. *Mem. geol. Soc. Amer.* **74.**

WAGER, L. R., & DEER, W. A., 1939. Geological investigations in East Greenland. *Medd. Grønland,* **105,** No. 4.

WALKER, F., 1940. Differentiation of the Palisade diabase, New Jersey. *Bull. geol. Soc. Amer.* **51,** 1059–1106.

WONES, D. R., 1959. Biotites. *Yearbook Carnegie Inst.* No. **58,** 132.

YODER, H. S., STEWART, D. B., & SMITH, J. R., 1957. Ternary feldspars. *Yearbook Carnegie Inst.* No. **56,** 206–14.

Chemical Analyses of Two Pantellerites

by E. G. ZIES

Geophysical Laboratory, Carnegie Institution of Washington, Washington, D.C., U.S.A.

IT is almost fifty years since the appearance of H. S. Washington's now classic paper on the Volcanoes and Rocks of Pantelleria (Washington, 1913, 1914). The analyses of a group of rocks which he called Hyalopantellerites aroused considerable interest on account of their 'large excess of soda (Na_2O), expressed as sodium metasilicate, over alumina and ferric oxide' (Washington, 1913, p. 707). Attention has in the last years again been directed toward this relationship (Tuttle & Bowen, 1958, pp. 84–89; Chayes, 1960; Tuttle, 1960). At the suggestion of Dr. F. Chayes the writer undertook to analyse again two samples of the Hyalopantellerites. Fortunately, many of Dr. Washington's rock samples are now in the Petrographic Reference Collection in the U.S. National Museum in Washington, D.C.[1]

In view of Washington's ability as an analyst it seemed at first somewhat presumptuous to analyse these samples. Although the summations of his analyses are low by 0·6 per cent, an amount which he usually considered sufficient to warrant a rating of other than superior (Washington, 1917, p. 21), he nevertheless had sufficient confidence in their correctness to include them in his compilation of superior analyses. This circumstance suggested that some constituent or constituents had been overlooked. The constituent chlorine[2] is nowadays usually determined in rocks of a rhyolite composition and this was sought at once. Table 1 shows 0·76 per cent Cl was found in No. 2000 and 0·37 per cent in No. 2007. Both values are greater than usually found in such rocks, the former so much so that one suspects contamination by sea-water; if so, much of the Cl would be extractable by water. This, however, is not the case; only 0·03 per cent of the sample was extracted by H_2O. There seems no doubt that the Cl is in the glassy portion of the rock. 'Contamination' by sea-water, if operative at all, must have occurred during cooling of the hot lava.

It is not amiss to give here a few details of the method used in estimating Cl content. Five grammes of the rock powder, crushed to pass 100 mesh to the

[1] The samples selected are designated by Washington (1913, p. 706) as *A* and *D*, and carry the Museum numbers P.R.C. 2000 and P.R.C. 2007. These specimens match closely the descriptions given by Washington (1913, pp. 705–7). P.R.C. 2000 contains about 12 per cent of phenocrysts, mostly sanidine, set in a nearly glassy matrix; cossyrite amounts to less than 4 per cent of the whole by volume, most of it as microlites in the groundmass. P.R.C. 2007 consists of about 2 per cent sanidine phenocrysts, and less than 0·1 per cent of all other crystalline matter, set in a clear brown glass. In both specimens the index of the glass is 1·516, unusually high for rhyolite. But these are unusual rhyolites.

[2] Referred to subsequently as Cl with no implication that we are dealing with free chlorine.

[Journal of Petrology, Vol. 1, Part 3, pp. 304–8, 1960]

linear inch, was agitated in water in a glass beaker at 40° C with a magnetic stirrer, allowed to settle for 2 h, and filtered by decantation through a fine-pored glass-fritted Gooch crucible. In order to avoid production of an undue amount of flour, which may readily take up moisture on grinding, the rock was crushed by tamping, in a large steel Ellis mortar, with frequent sifting through a 100-mesh sieve.

The residue after filtration was allowed to air-dry, which by capillarity often brings chlorides within the particles to the surface. It was extracted with H_2O as before and filtered. A repetition of the drying and extraction yielded no further Cl. The filtrate was chilled in order to prevent precipitation of SiO_2 by the subsequent acidification with HNO_3; the Cl was precipitated in the usual manner with $AgNO_3$, filtered through a fritted Gooch, dried, and weighed.[1] The precipitate was dissolved on the Gooch with dilute ammonia and the residue again dried at 140° C and weighed.

A further check was obtained by reprecipitation of AgCl from the solution. The value obtained by difference agreed quite well with that obtained from the weighed reprecipitated AgCl. It will also be noted that if the equivalent value for Cl obtained by me is added to Washington's analysis of No. 2000 the summation is much closer to the theoretical 100 per cent. In the second sample not as much Cl was found as in the first, but Washington evidently did not determine the MnO content of this specimen. When both the MnO and the equivalent Cl are added to his analysis its total also approaches closely the theoretical 100 per cent.

As a further precaution, a blank was run by fusing a very pure quartz with Na_2CO_3 and carrying the operation through in the same manner as for the samples. The value of the blank was $< 0{\cdot}01$ per cent Cl. During all the work pertaining to Cl all sources of HCl were removed from the laboratory.

The amount of Cl shown evidently demands that one recalculate Washington's norms, but it seemed best first to re-analyse the rocks. The new alkali analyses were run in duplicate by the J. Lawrence Smith method, which Washington also used. It will be seen from Table 2 that the duplicates agree quite well, and, what is even more important, do not differ much from the results obtained by Washington. Within my experience the values obtained by the somewhat more expeditious flame photometer method would differ very little from these results. As a matter of fact, there is still a tendency to use the J. L. S. as an umpire method for determining the alkalis in rocks. The $CaCO_3$ used in the J. L. S. sintering was specially prepared and analysed by the writer; it contains $SiO_2 < 0{\cdot}02$ per cent, $R_2O_3 < 0{\cdot}01$ per cent, and a negligible amount of Na_2O and K_2O. The residues left after aqueous extraction of the alkalis, together with the $CaCO_3$ recovered from the extract, were used for a check determination of SiO_2.

[1] From this point onward all analytical methods used are given in detail in Hillebrand *et al.* (1953). The procedures described there were rigorously followed even though frequently time-consuming.

The analyses of No. 2000 by Washington and by me, with the exception, of course, of Cl, differ very little indeed with respect to the major constituents, but there is a significant difference with respect to TiO_2, which was determined in the new analysis by means of a photoelectric colorimeter.

It is not too surprising that our values for this minor element should differ, for the colorimetric method used by Washington was dependent on visual discrimination of differences in intensity of colour, which for the greenish-yellow region of the spectrum can be very poor. It also should be noted that ZrO_2 was found by me and probably not looked for by Washington. It is definitely present in both samples. In each case the identity of the ZrP_2O_7, obtained in the course of the analysis, was determined by comparing its X-ray powder diffraction pattern with that obtained from ZrP_2O_7 prepared from a pure zirconium chloride.

In No. 2000 the value for alumina has not been significantly changed because the sum of my TiO_2 and ZrO_2 is about the same as Washington's TiO_2. This simply means that the weight of our R_2O_3 group, in which both constituents occur, was practically the same.

In addition to the previously unreported Cl and ZrO_2, and the lower TiO_2, the new analysis of the obsidian No. 2007 obviously differs considerably from Washington's in SiO_2 and Al_2O_3. The sum of the two constituents is practically the same in both analyses, which means that the sum of the SiO_2 and the R_2O_3 group should not differ greatly in the two analyses under discussion. It is conceivable, but hardly likely, that No. 2007 contains significant amounts of B_2O_3, which would be weighed in part with the SiO_2 and in part with the R_2O_3 group, and it is possible that the writer may have used a more vigorous treatment with HF than Washington to arrive at the weight-by-loss of the SiO_2. This operation would, of course, also drive off the B_2O_3 and thus indicate more SiO_2 than Washington found. It thus seemed desirable to determine SiO_2 on a separate sample by a method which would remove any B_2O_3 by volatization as methyl borate. The value of SiO_2 so obtained (see Table 2, col. 5) is nearly identical with that found before. As an added check, the Al_2O_3 was next determined directly, after removal of iron, titanium, and zirconium by cupferon. The weight of the Al_2O_3 (see also Table 2) was corrected for the small amount of coprecipitated P_2O_5. One must, at present, conclude that 'Homer nodded'.[1]

Below, in Table 1, are shown the analyses of the two Pantellerites as carried out by Washington and by myself. They are placed in juxtaposition in order to bring out the striking similarities and also the significant differences. In Table 2 are shown the values obtained for various constituents either in replicate or by different methods. In Table 3 are shown the norms obtained by the same method as detailed in Washington's monumental work (1917).

[1] In the years since Washington's analyses of these curious rocks were first published I have many times heard them criticized; Washington's own norm calculation tends to focus attention on the alkalis and this too is where the criticism has centred. It appears to have been completely misdirected.

TABLE 1. *Chemical analyses of Hyalopantellerites*

	P.R.C. No. 2000		*P.R.C. No. 2007*	
	*H. S. W.**	*E. G. Z.†*	*E. G. Z.†*	*H. S. W.**
SiO_2	69·91	69·81	69·56	67·85
Al_2O_3	8·58	8·59	11·27	12·87
Fe_2O_3	1·81	2·28	1·87	1·84
FeO	5·86	5·76	4·18	4·54
MgO	0·28	0·10	0·23	0·30
CaO	0·33	0·42	0·44	0·17
Na_2O	6·41	6·46	6·28	6·03
K_2O	4·71	4·49	4·60	4·83
H_2O+	0·22	0·14	0·13	0·13
H_2O-	0·13	0·05	0·02	0·02
TiO_2	0·75	0·45	0·47	0·83
ZrO_2	—	0·25	0·12	—
P_2O_5	0·16	0·13	0·10	0·08
SO_3	—	0·06	0·06	—
Cl–H_2O sol.	—	0·03	0·01	—
Cl–H_2O insol.	—	0·76	0·37	—
MnO	0·24	0·28	0·28	—
		100·06	99·99	
Less O for Cl		0·18	0·09	
	99·39	99·88	99·90	99·49

* Analyses by H. S. Washington—1914.
† Analyses by E. G. Zies—1960.

TABLE 2. *Hyalopantellerite P.R.C. 2007*

Results of analyses of various constituents either by replicates or by different methods

	General sample No. 1	*General sample No. 2*	*From alkali sample No. 1*	*From alkali sample No. 2*	*From methyl borate sample*	*Two samples for* Fe″	*Samples for* Cl	*Average*
SiO_2	69·65	69·46	69·60	69·50	69·59*	—	—	69·56
Total Fe as Fe_2O_3	6·44†	6·57†	—	—	6·65‡	6·52§	6·40†	6·52
FeO	—	—	—	—	—	(4·19 / 4·16)	—	4·18
Al_2O_3	11·38‖	11·24‖	—	—	—	11·20¶	—	11·27
Na_2O	—	—	6·22	6·33	—	—	—	6·28
K_2O	—	—	4·63	4·56	—	—	—	4·60
TiO_2	0·47	0·47	—	—	—	—	0·47	0·47
Cl	—	—	—	—	—	—	0·35, 0·37, 0·40	0·37

* Sodium carbonate fusion, acidified with HCl, evaporated to dryness and, in order to remove B_2O_3, treated twice under proper conditions with dry methyl alcohol saturated with dry HCl.
† By titration with $KMnO_4$.
‡ Weighed as Fe_2O_3 obtained after separation and further treatment of FeS in a tartrate solution.
§ By titration with $KMnO_4$ after proper treatment of the precipitate obtained in an acid solution by cupferon.
‖ By difference in the usual manner.
¶ Directly, after removal of all organic matter, double precipitation, and recovery of Al_2O_3 in the filtrates.

TABLE 3. *Norms of the chemical analyses*

	P.R.C. No. 2000		*P.R.C. No. 2007*	
	H. S. W.	*E. G. Z.*	*E. G. Z.*	*H. S. W.*
Q	28·38	28·07	21·34	15·36
Z	—	0·25	0·11	—
Or	27·80	26·56	27·17	28·36
Ab	17·82	19·20	32·57	39·30
Ac	5·08	6·61	5·41	5·54
Ns	7·08	5·14	2·70	1·22
Di	0·75	0·54	1·19	—
Hy	10·34	10·35	7·41	7·80
Wo	—	0·25	—	—
Il	1·37	0·85	0·90	1·52
Ap	0·34	0·30	0·24	0·34
Hl	—	1·30	0·63	—
Rest	0·35	0·25	0·21	0·15
	99·31	99·67	99·88	99·59

The work reported here amply confirms Washington's principal finding, viz., that these specimens contain a molar excess of alkalis over available R_2O_3, a phenomenon he chose to express in terms of the normative molecule *ns*. It does not, however, support his interesting further suggestion that '... in a general way, the amount of cossyrite present is correlated with that of sodium metasilicate in the norm' (1913, p. 707). Specimen P.R.C. 2000 contains at most 4 per cent of cossyrite by volume, and specimen P.R.C. 2007 probably less than 0·1 per cent, yet in the composition of each there is a pronounced excess of alkalis over available R_2O_3. There seems no escape from the conclusion that in these two specimens this excess is a characteristic of the glass itself. As we have seen, the glass must also contain most of the unusually abundant Cl found on analysis.

ACKNOWLEDGEMENTS

The U.S. National Museum kindly loaned all of Washington's Pantelleria collection to me for study, and gave me half of each of the specimens selected for analysis. This selection was based on examination of the whole suite by F. Chayes, who also provided the petrographic information given above and critically reviewed the manuscript. H. S. Yoder, Jr., prepared X-ray spectrograms from powders of three zirconium pyrophosphates.

REFERENCES

CHAYES, F., 1960. Occurrence of normative sodium metasilicate in Washington's tables. *Bull. geol. Soc. Amer.* **71**, 503–4.

HILLEBRAND, W. G., LUNDELL, G. E. F., BRIGHT, H. A., & HOFFMAN, J. Q., 1953. *Applied inorganic analysis*, 2nd ed., New York: J. Wiley & Sons, Inc.

TUTTLE, O. F., 1960. Occurrence of normative sodium metasilicate in Washington's tables. A reply. *Bull. geol. Soc. Amer.* **71**, 505.

—— & BOWEN, N. L., 1958. Origin of granite in the light of experimental studies in the system $NaAlSi_3O_8$–$KAlSi_3O_8$–SiO_2–H_2O. *Mem. geol. Soc. Amer.* **74**.

WASHINGTON, H. S., 1917. Chemical analyses of igneous rocks. *Prof. Pap. U.S. geol. Surv.* **99**.

—— 1913, 1914. The volcanoes and rocks of Pantelleria, *J. Geol.* **21**, 653–70, 683–713; and **22**, 1–27.

The Pyroxenes and Olivines from some Tertiary Acid Glasses

by I. S. E. CARMICHAEL

Department of Geology, Imperial College, London, England

ABSTRACT

The coexisting pyroxenes and olivines from nine British and Icelandic Tertiary porphyritic acid glasses have been separated and analysed chemically. Eight new analyses of augite and ferroaugites, one of orthopyroxene, and five of iron-rich olivines are presented, together with their optical properties. The trend of crystallization of the ferroaugites is discussed. New optical determinative curves for these ferroaugites and the iron-rich olivines are presented. The relationship of the pyroxenes and olivines to their analysed residual glasses is considered.

THE comparative study of the igneous pyroxenes has been largely confined to those which have crystallized during the cooling of basic magmas. Thus Muir (1951) and Brown (1957) have studied the pyroxenes from the Skaergaard intrusion, a slowly cooled representative of tholeiitic basalt magma. The pyroxenes of alkali-basalt intrusives have been described by Murray (1954) and Wilkinson (1957), whilst Kuno (1950, 1954, 1955) has described in great detail the pyroxene phases of the tholeiitic Japanese lavas. More recently Muir & Tilley (1957) have presented some results of their investigations on the pyroxenes of the Hawaiian tholeiitic lavas. So far as is known to the writer, the pyroxenes, or indeed the olivines, of the possible acid differentiates of tholeiitic magma have received scant attention. Muir (1951, p. 694) has determined the optical properties of a clinopyroxene from a Skaergaard transgressive granophyre, and Anwar (1955) and Bell (1959) have each described a ferrohedenbergite from Tertiary Skye granophyres. However, in view of the alteration which often affects the ferromagnesian silicates of the crystalline acid rocks, it was decided to confine this study to the pyroxenes and olivines which occur as phenocrysts in some of the acid glasses of the north Atlantic Tertiary volcanic province.

The present paper is concerned with the ferromagnesian silicate phenocrysts from ten Tertiary porphyritic glasses. Six come from the east coast of Iceland, where the glasses occur in association with the Thingmuli central volcano as an acid dyke (G. 151) and as a pitchstone margin of an acid lava (G. 87); in chilled margins of high-level acid intrusions at Sellatur (E. 868) (Walker, 1959, p. 379), at Bondolfur (P. 186), and at Skruthur (P. 258); and in the chilled margin of a dacitic lava at Rauthaskritha (IC. 3) (Hawkes, 1924). The pitchstones from the British Tertiary all come, with one exception, from the island of Arran, where they form dykes or dyke-like intrusions, and have been described by Tyrrell

[Journal of Petrology, Vol. 1, Part 3, pp. 309–36, 1960]

(1928, pp. 210–35). The Arran specimens come from behind the schoolhouse at Brodick (AC. 6), from Glen Shurig (AC. 7), and from the Tormore shore—named Judd's No. 1 dyke (AC. 12). The remaining pitchstone forms the Sgurr of Eigg (Harker, 1908, pp. 170–4) about which there has been considerable controversy concerning its origin. While the writer does not feel confident to proclaim on its mode of emplacement, it is felt that it is more likely to be a lava, and it will be considered as such here and subsequently.

The chemical analyses of the rocks, together with their residual glasses, are presented in Table 6 and are discussed in relation to the ferromagnesian silicate phenocrysts. A more extensive study of the pitchstones and the residual glasses, together with analyses of the felspar phenocrysts and the iron–titanium oxides, will be published later.

PETROGRAPHY

It is hoped to publish a more detailed account of the petrography of these glasses later, so that only a very brief summary mainly concerning the phenocrysts is offered here. Detailed descriptions of the Sgurr of Eigg pitchstone (Harker, 1908) and the particular Arran dykes with which this paper is concerned (Tyrrell, 1928) have already been published.

The pitchstone of Eigg contains abundant phenocrysts of alkali felspar which is commonly microperthitic, together with less frequent pale-coloured augite and colourless orthopyroxene, the orthopyroxene typically forming the larger crystals. Opaque iron ores also occur as microphenocrysts, the whole being set in a dull brown micro-crystalline glass with perlitic fracture. The pitchstone dyke from Tormore, Arran (AC. 12), contains scattered phenocrysts of lath-like plagioclase, commonly euhedral ferroaugite and very rare orthopyroxene which has once been observed to enclose partially resorbed olivine. The composition of the orthopyroxene is derived from the optical properties (No. 2A) $\alpha = 1{\cdot}727$; $\nu = 1{\cdot}743$; $2V_\alpha = 59°$ (Of. = 62 per cent). The glassy groundmass is pale in colour with spicules developed in bands defining the flow direction. The dyke at Brodick (AC. 6) presents a most striking display of scopulites within the glass, with phenocrysts of quartz and plagioclase together with rarer ferroaugite and a pale-coloured olivine. The Glen Shurig dyke (AC. 7) is the richest in ferromagnesian phenocrysts of all glasses examined, and they consist of olivine, orthopyroxene, and ferroaugite. The orthopyroxene almost invariably forms shapeless irregular cores to mantles of ferroaugite, which may also form stout independent crystals. The optical properties of these two pyroxenes (not analysed) and the derived compositions are as follows, the composition of the ferroaugite being determined from Fig. 3. Orthopyroxene (No. 10A) $\alpha = 1{\cdot}692$, $\beta = 1{\cdot}702$–$1{\cdot}706$, $\gamma = 1{\cdot}704$–$1{\cdot}709$, $2V_\alpha = 65°$ (Of. 32–37 per cent). Ferroaugite (No. 10) $\beta = 1{\cdot}728$, $2V_\gamma = 52°$, $\gamma \wedge c = 42°$ ($Ca_{42}Mg_{16}Fe_{42}$).

The glass is almost colourless and contains abundant birefringent spicules. Microphenocrysts of opaque iron oxides are ubiquitous in these Arran glasses,

as is the tendency for the ferromagnesian silicate phenocrysts to cluster either together or with plagioclase, but never with quartz.

The Icelandic glasses typically have fewer microlites in the glass, and are all devoid of quartz as a porphyritic element. Basaltic xenoliths, often in advanced stages of digestion, are not uncommon and are particularly frequent in P. 258 and G. 87. The acid lava from Rauthaskritha (IC. 3) contains scattered phenocrysts of plagioclase, infrequent olivine and rarer ferroaugite, the whole being set in a hyalopilitic glass with tiny rhombs of alkali felspar (Hawkes, 1924).

The acid lava from Thingmuli (G. 87), which rests in the centre of a zone of intense hydrothermal alteration, shows extremely well-developed perlitic texture in the pale-coloured glass. Enclosed in the glass are phenocrysts of plagioclase and ferroaugite, together with basaltic material which may remain coherent or may be scattered throughout the glass as independent minerals. The optical properties of the ferroaugite are as follows, the composition being derived from Fig. 3. Ferroaugite (No. 3) $\beta = 1{\cdot}717$, $2V_\gamma = 53°$ ($Ca_{43}Mg_{24}Fe_{33}$).

The glassy margins of the acid intrusions contain phenocrysts of plagioclase, together with one or more ferromagnesian silicates. Olivine is absent from one (E. 868) which has large phenocrysts of ferroaugite, together with opaque iron oxides enclosed in a glass of a pale brown colour. Ferroaugite with less frequent olivine, together with iron ores, plagioclase, and very rare orthopyroxene[1] are inset in pale brown glass with strongly developed flow banding, and characterize P. 186.

Weakly birefringent spherulites are abundantly developed in P. 258 and may surround many of the phenocrysts of plagioclase and ferroaugite, the latter having a peculiar spongy appearance suggestive of incipient recrystallization. Extremely rare olivine and microphenocrysts of opaque ores are contained in a pale brown glass with well-developed perlitic fracture. The Thingmuli acid dyke (G. 151) has phenocrysts of plagioclase, less abundant olivine and ferroaugite, and opaque iron oxides all set in a glassy microlitic groundmass with abundant tiny plagioclase laths which may often show flow texture.

The olivine phenocrysts from these glasses have many features in common. The olivine is well rounded, often embayed, and is only feebly idiomorphic. It is characteristically the largest of the ferromagnesian phenocrysts although it may show a considerable gradation in size. Fracture cracks, typical of the olivines, may contain small amounts of a deep green, weakly birefringent alteration product, as may the erratically developed cleavage. Microphenocrysts of opaque iron ore may be enclosed by the olivine phenocrysts or associated with them in crystal clusters.

Macroscopically the olivines are all amber in colour, and show a pale yellow coloration in thin section, with feeble pleochroism.

The ferroaugites and augite are green as macroscopic grains (cf. Skaergaard,

[1] As only one small crystal has been found in several thin sections, the presence of this pyroxene has, in the subsequent discussion, been arbitrarily neglected.

brown ferroaugites) and show a distinct pleochroism from green to pale brownish-green, which varies in intensity throughout the series. Twinning is usually simple, only rarely absent, and may be repeated. There is no microscopic evidence of exsolution although it is possible that the ferroaugite (Fig. 1, No. 2)

TABLE 1

Modal analyses (vol. per cent)

	Glass	*Plagio-clase*	*Alkali felspar*	*Quartz*	*Pyroxene*	*Olivine*	*Iron oxides*	*Basaltic xenoliths*
1R (EC. 20)	79·2	tr.	19·2	—	1·0	—	0·5	—
2R (AC. 12)	97·0	2·5	—	—	0·2	—	0·2	—
3R (G. 87)	94·3	2·5	—	—	0·3	—	0·1	2·8
4R (E. 868)	92·1	6·0	—	—	0·4	—	0·4	1·2
5R (AC. 6)	95·3	2·9	—	1·5	0·1	0·1	0·1	—
6R (G. 151)	89·0	8·1	—	—	1·6	0·7	0·6	—
7R (P. 258)	86·6	9·2	—	—	0·5	—	0·2	3·4
8R (P. 186)	89·6	8·9	—	—	0·8	0·2	0·3	0·2
9R (IC. 3)	96·2	3·4	—	—	0·2	0·2	0·1	—
10R (AC. 7)	83·4	9·4	—	4·8	1·5	0·6	0·3	—

For the key to these analyses see below

KEY TO TABLES 1–7:

1 Augite from pitchstone, Sgurr of Eigg (Harker, 1908, pp. 170–4). EC. 20.
1A Hypersthene from EC. 20.
1R Pitchstone. EC. 20.
1G Residual glass from EC. 20.
2 Ferroaugite from Judd's No. 1 dyke, Tormore shore, Arran (Tyrrell, 1928, pp. 218–35). AC. 12.
2R Pitchstone. AC. 12.
2G Residual glass from AC. 12.
3R Pitchstone margin of acid lava, Thingmuli, east Iceland. G. 87.
3G Residual glass from G. 87.
4 Ferroaugite from pitchstone margin of Sellatur plug, east Iceland (Walker, 1959, p. 379). E. 868.
4R Pitchstone. E. 868.
4G Residual glass from E. 868.
5 Ferroaugite from pitchstone, Brodick School, Arran (Tyrrell, 1928, pp. 210–35). AC. 6.
5B Ferrohortonolite from AC. 6.
5R Pitchstone. AC. 6.
5G Residual glass from AC. 6.
6 Ferroaugite from glassy margin of dyke, Thingmuli, east Iceland. G. 151.
6B Ferrohortonolite from G. 151.
6R Pitchstone. G. 151.
6G Residual glass from G. 151.
7 Ferroaugite from pitchstone margin of intrusion, Skruthur, east Iceland. P. 258.
7R Pitchstone. P. 258.
7G Residual glass from P. 258.
8 Ferroaugite from pitchstone margin of intrusion, Bondolfur, east Iceland. P. 186.
8B Ferrohortonolite from P. 186.
8R Pitchstone. P. 186.
8G Residual glass from P. 186.
9 Ferroaugite from pitchstone margin of dacite lava, Rauthaskritha, east Iceland (Hawkes, 1924). IC. 3.
9B Ferrohortonolite from IC. 3.
9R Pitchstone. IC. 3. (New analysis.)
9G Residual glass from IC. 3.
10B Ferrohortonolite from pitchstone, Glen Shurig, Arran (Tyrrell, 1928, pp. 210–35). AC. 7.
10R Pitchstone. AC. 7. (New Analysis.)
10G Residual glass from AC. 7.
C Ferrohedenbergite from granophyre, Meall Dearg, Skye (Anwar, 1955, p. 371).
E Ferrohortonolite from Beaver Bay diabase (Muir, 1954, p. 378).
F Ferrohortonolite from Skaergaard ferrogabbro (Deer & Wager, 1939, pp. 19–20).
G Calcian ferrohortonolite, Baruta, Nyiragongo (Sahama & Hytönen, 1958, p. 868).
H Fayalite from Skaergaard fayalite–quartz-gabbro (Deer & Wager, 1939, pp. 19–20).

Analyses 1 to 10G by I. S. E. Carmichael.
Analysis C by J. H. Scoon.
The pyroxene phenocrysts from Nos. 3R and 10R have been determined optically (see text).

may have extremely fine exsolution lamellae. The calcium-rich pyroxenes, which are of very variable size, may be idiomorphic but are commonly ill-shaped.

The orthopyroxenes show the normal very pale pink and green pleochroism, but are pale brown as macroscropic grains.

The modal analyses of the pitchstones are given in Table 1. Owing to the small size of many of the ferromagnesian minerals in some of the Arran dykes, particularly AC. 7 (No. 10R), it is not possible reliably to count them using a point counter, and the ferromagnesian content (Table 1), especially for AC. 7, is therefore low. The determined modal content of the ferromagnesian phenocrysts for all the pitchstones may perhaps best be considered as an order of magnitude, whereas the felspars and quartz, which are more evenly distributed throughout the glasses, are more easily and precisely determined.

Mineral Analyses

The pyroxene and olivine phenocrysts may frequently comprise less than 0·5 per cent of the glass (Table 1), and therefore up to 1½ kg of rock were crushed to –100 mesh for subsequent mineral separation. All the mineral samples were separated on the Frantz isodynamic separator and by repeated centrifuging in Clerici solution, and it was found that all the minerals that were successfully separated had a very small range of specific gravity. Final handpicking ensured more than 99·5 per cent purity. The separation of ferrohortonolites from ilmenite gave considerable trouble, the 15 per cent or so of contaminant being removed by handpicking.

The calcium-poor pyroxene was easily separated from the calcium-rich pyroxene in the centrifuge using Clerici solution, the invariable green colour of the augites and ferroaugites contrasting with the pale browns of the calcium-poor pyroxenes.

All analyses were made on a semi-micro scale, as many of the Icelandic specimens were very much smaller in bulk than is desirable for macro-analysis. The amount generally used for the main portion of a gravimetric analysis was between 100 and 200 mg. However, six were made on a total sample of less than 100mg, while No. 8B, the least, was 51 mg.

The pyroxene analyses (Table 2) have been recalculated into the standard formula $(WXY)_2Z_2O_6$ (Table 3), using the method described by Hess (1949, p. 625). Thus instead of making $Z = 2$ by adding arbitrary amounts of Al and, where necessary, Ti and Fe''' to Si, the cations were allotted to groups in accordance with the balance of charge on a cation for cation basis. This may, and frequently does, give a somewhat different picture of the cations likely to be in fourfold coordination from that given by the automatic addition of the relevant cations to the (Z) group.

The variation of Ca, Mg, and Fe'' of these pyroxenes is shown in Fig. 1, together with the composition (as Mg: Fe+Mn ratio) of their associated olivines where appropriate. These ferroaugites contain a minimum of 40 per cent Ca of

TABLE 2

Analyses and optical properties of pyroxenes

Refractive indices $\pm 0{\cdot}002$ $2V \pm 2°$

For the key to these analyses see Table 1

	1	1A	2	4	5	6	7	8	9	C
SiO_2	51·72	51·88	50·18	49·25	48·86	48·76	48·01	49·05	49·10	46·86
TiO_2	0·62	0·57	0·36	0·49	0·54	0·47	0·91	0·48	0·63	0·57
Al_2O_3	1·05	1·46	1·23	1·04	1·19	0·99	2·42	1·61	1·07	1·31
Fe_2O_3	2·40	2·55	1·75	2·03	1·93	3·36	2·21	1·85	3·17	2·24
FeO	7·56	16·80	17·22	19·54	20·44	19·42	20·32	21·40	21·97	26·91
MnO	1·27	1·88	0·79	1·28	0·90	0·73	1·23	0·98	0·98	0·83
MgO	15·12	22·37	9·30	7·42	7·05	5·93	5·07	4·52	3·70	2·32
CaO	19·84	2·19	19·29	19·09	18·99	19·47	19·92	19·32	18·86	18·45
Na_2O	0·32	0·23	0·33	0·24	0·48	0·66	0·39	0·57	0·92	0·25
K_2O	0·06	0·08	0·07	0·05	0·06	0·11	0·04	0·14	0·11	0·20
TOTAL	99·96	100·02	100·52	100·43	100·44	99·90	100·52	99·92	100·51	100·37*
β	1·697	—	1·715	1·724	1·724	1·726	1·727	1·726	1·732	1·741
γ	—	1·706	—	—	—	—	—	—	—	—
$2V$	55°(+)	60°(−)	52°(+)	51°(+)	50°(+)	51°(+)	56°(+)	52°(+)	53°(+)	53°–56°(+)
$\gamma \wedge c$	43°	—	42°	43°	41°	41°	—	42°	—	47°
Atomic per cent:										
Ca	40·1	4·4	40·6	40·5	40·6	42·5	43·9	43·4	42·6	41·1
Mg	42·5	62·6	27·2	21·9	20·9	18·0	15·6	14·1	11·7	7·2
Fe	17·3	33·0	32·2	37·6	38·5	39·5	40·5	42·5	45·7	51·7

* Includes H_2O^+ 0·19 per cent, H_2O^- 0·24 per cent.

TABLE 3

Formulae of the analysed pyroxenes (on the basis of six oxygens)

		1	1A	2	4	5	6	7	8	9	C
Z	Si	1·937	1·928	1·942	1·939	1·929	1·937	1·904	1·955	1·958	1·924
	Al	0·045	0·062	0·050	0·047	0·049	0·048	0·097	0·056	0·050	0·064
	Ti	0·013	0·007	—	0·009	—	0·010	—	—	—	0·002
WXY	Al	—	—	0·006	—	0·008	—	0·017	0·021	0·003	—
	Ti	0·001	0·006	0·009	0·003	0·012	0·002	0·021	0·012	0·014	0·013
	Fe^{3+}	0·068	0·071	0·051	0·062	0·057	0·100	0·067	0·058	0·096	0·069
	Fe^{2+}	0·236	0·523	0·558	0·643	0·674	0·645	0·674	0·714	0·733	0·923
	Mn	0·040	0·058	0·026	0·042	0·031	0·024	0·040	0·034	0·034	0·030
	Mg	0·844	1·238	0·537	0·435	0·415	0·351	0·300	0·268	0·221	0·143
	Ca	0·796	0·087	0·800	0·804	0·804	0·829	0·846	0·824	0·805	0·812
	Na	0·022	0·018	0·023	0·019	0·038	0·052	0·028	0·043	0·072	0·020
	K	0·002	0·004	0·002	0·002	0·002	0·005	0·002	0·005	0·005	0·010
	Z	1·995	1·996	1·992	1·995	1·978	1·995	2·001	2·011	2·008	1·990
	WXY	2·009	2·005	2·012	2·010	2·041	2·008	1·995	1·979	1·983	2·020
Per cent Al in Z		2·2	3·1	2·5	2·4	2·4	2·4	4·8	2·8	2·5	3·2
Per cent Ti in Z		0·6	0·3	—	0·4	—	0·5	—	—	—	0·1

total Ca+Mg+Fe, and this represents the maximum replacement of the larger Ca ion by the smaller Fe″+Mg ions. Greater replacement of Ca by Mg+Fe″ occurs in the calcic clinopyroxenes of the slowly cooled tholeiitic intrusives such as the Skaergaard intrusion (Fig. 2).

The amount and distribution of the other cations present features of interest, particularly when comparison is made with the ferroaugites of the Skaergaard

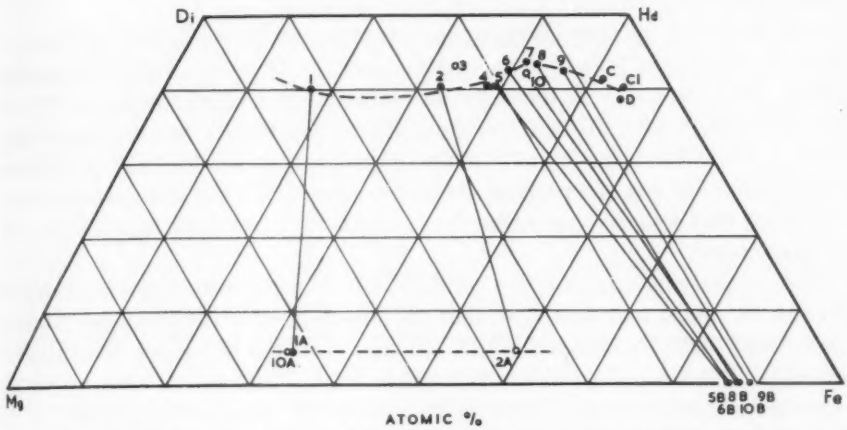

FIG. 1. Crystallization trend of calcium-rich and calcium-poor pyroxenes from some British and Icelandic Tertiary acid glasses. ● Analysed specimens (Nos. 1–9, augite and ferroaugites; No. 1A orthopyroxene; Nos. 5B–10B olivines). ○ Compositions of ferroaugites and orthopyroxenes derived from optical properties, and assuming that the orthopyroxenes have the same calcium content as No. 1A. Specimens C, C_1, and D are ferrohedenbergites from two Tertiary Skye granophyres (Anwar, 1955, Nos. C, C_1; Bell, 1959, No. D).

intrusion which provides the only source of comparable pyroxenes yet described. The Skaergaard ferroaugites have been described by Muir (1951), and Brown has indicated (op. cit., p. 515) that further work is in progress on the pyroxenes from the late stages of fractionation of the Skaergaard.

The MnO content of these pyroxenes, especially Nos. 1 and 1A (Table 2) is unusually high, and the average content of the ferroaguites (0·98 per cent) is in distinct contrast to the average (0·32 per cent) of the Skaergaard ferroaugites (Muir, 1951, Nos. 10, 11, 13–17). Distinct differences are also found in TiO_2 and Al_2O_3, the average values for these ferroaugites being 0·56 per cent and 1·4 per cent respectively, whereas the Skaergaard average values are 1·1 per cent TiO_2 and 2·0 per cent Al_2O_3.

Brown (1957, pp. 515–18) was able to establish a regular pattern of distribution of some of the minor cations between coexisting pyroxene phases and between successive pyroxenes formed during the early and middle stages of

fractionation of the Skaergaard intrusion. He noted that Al both in the (Z) group and (WXY) group decreased during fractionation, and accordingly the percentage of Al in the (Z) group of the calcium-rich pyroxenes decreased from 5·0 per cent to about 3·1 per cent in the most iron-enriched augites. Although these ferroaugites do not show a steady decrease, the average of 2·9 per cent Al in the (Z) group suggests that tetrahedrally coordinated Al may decrease even more with continued iron-enrichment. However, the ferroaugites described by Muir (1951, Nos. 10, 11, 13–17)[1] indicate that Al in the (Z) group does *per contra* increase with iron-enrichment, the average being 3·9 per cent Al in the (Z) group, with a maximum replacement of 6·6 per cent.

The two most iron-enriched augites described by Brown (1957, pp. 516–17, Nos. 9, 10) contain Ti in fourfold coordination, as do some of the ferroaugites (Muir, 1951, Nos. 11, 13, the latter also containing a small amount of Fe''' in the (Z) group)[1] and also the ferroaugite from the Beaver Bay diabase (Muir, 1954, p. 378).[1] The inclusion of Ti in the (Z) group is, as Brown (1957, p. 518) has pointed out, not due to a particularly high content of Ti, but to a low content of Al, which may also be responsible for fourfold Fe''', provided that the Na+K content is low.

Two of these ferroaugites also contain Ti in fourfold coordination (Table 3, Nos. 4, 6), and it may be shown that the ferroaugites of the Skaergaard noted above and these ferroaugites which contain Ti in the (Z) group have similar Fe+Mn/Fe+Mn+Mg ratios which range from 0·5 to 0·7. It seems possible that during fractionation Ti is accepted into the (Z) group due to paucity of Al only over a moderately narrow range of iron-enrichment (Muir, 1951, p. 698), and Ti may not again become tetrahedrally coordinated until the very last stages of fractionation (Table 3, No. C).

In these ferroaugites (Tables 2, 3) there is a general increase in the alkalis with iron-enrichment which is not shown by the Skaergaard ferroaugites (Muir, 1951, p. 699), and in respect of Na alone these ferroaugites (Table 3) are in contrast to the Skaergaard augites which decrease in Na with increasing iron-enrichment (Brown, 1957, p. 518).

The calcium-poor pyroxenes are enriched in Fe when compared to the coexisting calcium-rich pyroxenes (Fig. 1, Nos. 1A, 2A, and Table 2), the tie-lines being parallel, or almost so, to the pyroxene tie-lines of the slowly cooled tholeiitic magmas (Fig. 2). The calcium-poor pyroxene is also enriched in Al in the (Z) group, in relation to the coexisting calcium-rich pyroxene, and in this way is in contrast to the coexisting pyroxenes of the Skaergaard (Brown, 1957, p. 518).

It is unusual that such magnesian pyroxenes as Nos. 1 and 1A (Tables 2, 3) should have high Mn, and also have Ti in the (Z) group, and these features place these two pyroxenes apart from the pyroxenes of similar composition from basaltic and gabbroic environments.

The olivine analyses are given in Table 4 and their structural formulae in

[1] These analyses have been recomputed on the cation for cation basis of Hess (1949, p. 625).

Table 5. The new analyses show that about 5 per cent of the total iron content is present in the trivalent form, which is generally accounted unacceptable to the olivine structure. As the olivines were believed to be almost entirely free from visible opaque iron oxides, the reason for their trivalent iron presumably lies elsewhere. It is of interest, however, that the fayalite analysed by Deer & Wager (1939, p. 18) had a large number of minute orientated iron ore inclusions which were separated from the olivine before analysis. Thus it is conceivable that in-

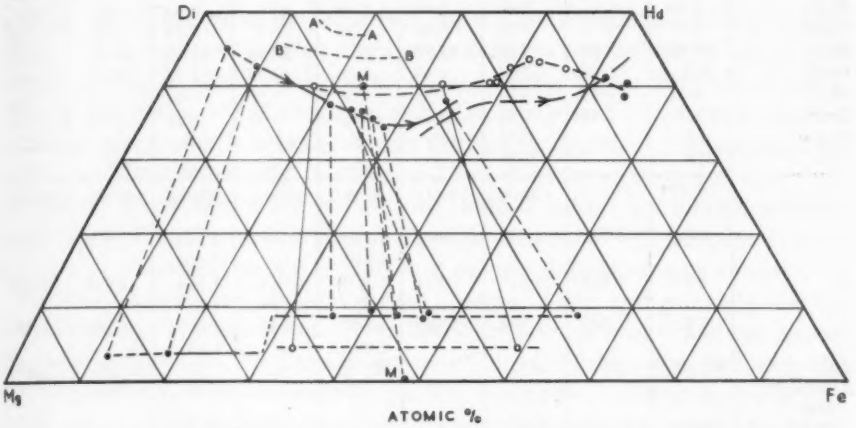

FIG. 2. Trends of crystallization from slowly cooled tholeiitic basalt magmas, with tie-lines between coexisting calcium-rich and calcium-poor pyroxenes. (Diagram slightly modified from Brown, 1957, fig. 3). ○ New analyses. ● Published analyses including the Skaergaard. →← Skaergaard augite trend of crystallization (Brown, 1957, fig. 2). – – → – Skaergaard ferroaugite trend (Muir, 1951, fig. 1). *M—M* coexisting augite and olivine from Camas Mor, Muck, gabbro dyke (Tilley, 1952). *A—A* augite trend of a differentiated teschenite sill (Wilkinson, 1957). *B—B* augite trend of the Garbh Eilean sill, Shiant Isles (Murray, 1954).

clusions do exist in these ferrohortonolites on a sub-microscopic scale. Repeated determinations of total iron by different methods gave comparable results, and the repeated ferrous iron determinations (Pratt's method) gave equally comparable results. A blank determination was made using ferrous ammonium sulphate, and slight oxidation did occur. A correction for this 'blank' would give a total content of 0·1 per cent ferric iron in the olivine.

At the suggestion of Dr. E. A. Vincent, the writer redetermined the ferrous iron of one olivine (Table 4, No. 10B), using the ammonium vanadate method of Wilson (1955) which resulted in the ferric iron content of the olivine falling from 3·80 per cent to 0·18 per cent. Unfortunately all the other olivine specimens had been used in the many repeated determinations by Pratt's method, but it is believed that the ferric iron content of Nos. 5B–9B (Table 4) would similarly fall, so that in the computation of the mineral formulae of Nos. 5B–9B (Table 5), the ferric iron has been converted to the ferrous equivalent and included with the determined figure.

TABLE 4

Analyses and optical properties of ferrohortonolites and fayalites

For the key to these analyses see p. 312, Table 1

Refractive Indices ±0·005, $2V \pm 2°$

	E	F	G	5B	6B	8B	10B	9B	H
SiO_2	30·42	31·85	31·58	30·13	30·62	30·21	30·96	30·13	30·15
TiO_2	1·20	0·01	0·28	0·73	0·59	0·48	0·39	0·51	0·20
Al_2O_3	0·50	trace	0·66	0·14	0·33	nil	0·02*	nil	0·07
Fe_2O_3	nil	0·11	3·26	2·88	2·98	2·57	0·18	2·30	0·43
FeO	57·62	58·64	52·97	58·90	58·21	59·56	61·60	60·31	65·02
MnO	n.d.	0·85	2·64	1·47	1·24	2·22	1·78	2·04	1·01
MgO	8·17	8·49	5·22	5·58	5·34	5·10	4·94	4·32	1·05
CaO	1·32	0·18	1·84	0·29	0·49	0·39	0·31	0·38	2·18
Na_2O	n.d.	—	0·54	n.d.	n.d.	n.d.	n.d.	n.d.	n.d.
K_2O	n.d.	—	0·53	n.d.	n.d.	n.d.	n.d.	n.d.	n.d.
TOTAL	99·62†	100·13	100·00‡	100·12	99·80	100·53	100·18	99·99	100·11
α	1·787	1·788	1·792	1·792	1·795–1·802	1·797	1·797–1·802	1·808	1·827
β	1·821	1·828	1·827	1·831	1·830–1·833	1·834–1·839	1·834–1·839	1·839	1·869
γ	1·838	1·840	1·844	1·846	1·842–1·846	1·849	1·843–1·847	1·854	1·879
$2V_\alpha$	58°–56°	58°	55°	55°	57°–53°	54°	55°	54°	48°
Atomic per cent:									
Mg	20·3	20·0	13·7	13·6	13·3	12·4	12·1	10·7	2·7
Fe + Mn	79·7	80·0	86·3	86·4	86·7	87·6	87·9	89·3	97·3

* Al_2O_3 by direct determination.
† Includes 0·18 per cent H_2O^+ and 0·21 per cent H_2O^-.
‡ Includes 0·38 per cent H_2O^+ and 0·10 per cent H_2O^-.

TABLE 5

Formulae of the analysed olivines on the basis of four oxygens, with Fe_2O_3 *recalculated to* FeO *for analyses* G *and* 5B *to* 9B

		E	F	G	5B	6B	8B	10B	9B	H
Z	Si	0·968	1·008	1·018	0·983	0·997	0·984	1·004	0·991	1·002
	Al	0·019	—	—	0·004	0·003	—	—	—	—
	Ti	—	—	—	0·014	—	0·010	—	0·010	—
XY	Al	—	—	0·006	—	0·009	—	—	—	0·003
	Ti	0·038	—	0·023	—	0·012	—	0·008	—	0·006
	Fe^{3+}	—	0·003	—	—	—	—	0·004	—	0·010
	Fe^{2+}	1·526	1·552	1·505	1·680	1·656	1·688	1·672	1·717	1·807
	Mn	—	0·023	0·072	0·041	0·033	0·061	0·049	0·057	0·030
	Mg	0·389	0·400	0·250	0·271	0·258	0·247	0·238	0·212	0·052
	Ca	0·044	0·006	0·064	0·010	0·017	0·014	0·012	0·014	0·078
Z		0·99	1·01	1·018	1·001	1·000	0·994	1·004	1·001	1·00
XY		2·00	1·98	1·974*	2·002	1·985	2·010	1·983	2·000	1·99

* Includes Na 0·031 per cent and K 0·23 per cent.

Deer & Wager (1939, p. 23) suggest that there is no replacement of Si by Al in the olivine series, but inspection of the analyses set down in Table 5 indicates an irregular fluctuation of Si instead of a steady decrease with iron-enrichment. This could be compensated by the inclusion of either Al or Ti, or perhaps both, in fourfold coordination. Thus the (Z) group has arbitrarily been made up to equal 2, although it is realized that this procedure is open to the same criticisms as have been noted above concerning the pyroxenes. Although Al can replace Si in tetrahedral coordination as in pyroxenes and felspars, there is no convincing evidence that it does so in the olivines in spite of the fluctuation of Si indicated above. It is considered that the uncertainty may not be resolved by the normal methods of Al_2O_3 determination in chemical analysis, where the Al_2O_3 figure is obtained by subtraction of total iron as Fe_2O_3, MnO, and TiO_2 from a weighed ammonia precipitate. It is believed that only an independent determination of Al_2O_3 will establish whether or not it exists in the olivine structure. One such determination has been made on No. 10B (Table 4) following a scheme outlined by Vincent (1954, p. 9) and resulted in an Al_2O_3 content of 0·02 per cent. Doubt, however, exists about the Al_2O_3 content of the remaining four new analyses.

The new olivine analyses show a high content of Mn and generally low Ca when compared with the olivines from the Skaergaard intrusion and the Beaver Bay diabase (Tables 4, 5). The Ca content of No. G (Tables 4, 5) has been discussed by Sahama & Hytönen (1958, pp. 870–1) who showed that the *d*-spacings of the plane (130) plotted above the olivine determinative curve (Yoder & Sahama, 1957, fig. 1). This was attributed to the high Ca content, but it appears to the writer that as Nos. E and H (Table 4) plot below the d_{130} curve (both of which have comparable amounts of Ca) it is to be doubted whether Ca alone is responsible. It is considered, therefore, that the iron-rich olivines may contain up to approximately 2 per cent CaO, but that they have normally less than 1 per cent and this would appear to be independent of the environment; No. G occurs in a melilite-bearing lava.

The olivines are always more enriched in Fe″+ Mn relative to Mg than are the coexisting ferroaugites (Fig. 1), and the pyroxene–olivine tie-lines are almost parallel to those of the Skaergaard intrusion (Muir, 1951, fig. 3).

THE CRYSTALLIZATION OF THE PYROXENES

A crystallization curve for the calcium-poor pyroxenes has been deduced by Kuno & Nagashima (1952), and subsequently modified by Brown (1957, fig. 5 and p. 541) who tied the crystallization curve to an experimentally determined temperature scale. This temperature scale is based on the results of Yoder & Tilley (1956, p. 170) who determined the temperature of pyroxene crystallization at various water-vapour pressures by melting an Hawaiian tholeiitic basalt lava. It is not possible, however, to deduce with any confidence the temperature of the liquidus of these two acid glasses in respect of their calcium-poor pyroxene phenocrysts. If the pyroxenes crystallized intratellurically, then the water-

vapour pressure may have been very much higher (and the pyroxene crystallization temperature lower) than the 500 kg/cm² which Tilley (1957, p. 331) has suggested attended the congelation of some of the Arran pitchstone dykes. Moreover, the effect of an enclosing acid melt on the crystallization temperature of these calcium-poor pyroxenes is unknown.

The crystallization trend[1] of the augite and ferroaugites of these acid glasses (Fig. 1) does not conform to the trends of the calcic pyroxenes of the tholeiitic layered intrusions (Fig. 2). The augite of the Sgurr of Eigg (No. 1) lies very near the augite trend of the slowly cooled tholeiitic bodies, but thereafter the trend of crystallization departs from those previously described. The exact location of the trend between Nos. 1 and 2 is unknown, but the trend undoubtedly flattens out (Fig. 1) and may run nearly parallel to the line of 40 per cent Ca (of total Ca, Mg, and Fe).

The composition of the augite (Fig. 2) of the Muck gabbro dyke (Tilley, 1952) would suggest that the crystallization curve between Nos. 1 and 2 may flatten out completely and become horizontal. Whether or not there is a slight curvature (Fig. 1) in the crystallization trend between Nos. 1 and 2 is not known, but the trend, which is a projection of the trace of the intersection of the solidus with the solvus surface on to the pyroxene basal composition triangle, is in marked contrast to the deeply concave (to the diopside–hedenbergite join) calcic limb of the pyroxene solvus of the slowly cooled tholeiitic magmas (Fig. 2) and it is possible that the solvus limb retains a curved surface under the different physico-chemical conditions of crystallization of these acid glasses. This weakly curved or straight calcic-pyroxene crystallization trend between Nos. 1 and 2 is akin to the essentially straight augite trend of the slowly cooled alkali-basalt magmas, although this alkali-basalt pyroxene trend is displaced towards, and lies very near, the diopside–hedenbergite join (Fig. 2) (Murray, 1954; Wilkinson, 1957).

The later rise of the crystallization trend towards the diopside–hedenbergite join is apparently not due to the absence of calcium-poor pyroxene, as pyroxene No. 4 (Fig. 1), which has no coexisting calcium-poor pyroxene, has the same Ca content as No. 2. This constancy of Ca content on crossing the limit of the two pyroxene field was found in the augites of the Skaergaard (Brown, 1957, p. 526). With further enrichment in iron the ferroaugite crystallization curve, having reached a maximum at 44 per cent Ca falls to the ferrohedenbergites of the two Skye granophyres (Anwar, 1955;[2] Bell, 1959). The successive rising and falling of the calcic pyroxene crystallization curve (Fig. 1) towards the diopside–hedenbergite join gives an indication of the complexity of form of the calcium-rich pyroxene solvus surface. The suggested pyroxene trend (Fig. 1) moves

[1] It may be disputed that a crystallization curve can reliably be drawn as these pyroxenes have not crystallized from successive fractions derived from a single differentiating parent. However, it is drawn within the restrictions noted in the text.

[2] The ferrohedenbergite from the Meall Dearg granophyre, Skye (Anwar, 1955), has been analysed twice; Anwar's analysis is No. C_1 (Fig. 1), and Scoon's analysis of a separate sample is No. C (Tables 1, 2; Fig. 1).

away from the hedenbergite corner, in contrast to the trend of the Skaergaard (Fig. 2) obtained by Muir (1951, fig. 1), but Brown (1957, p. 538, and a later personal communication, 1960) suggests that the Skaergaard ferroaugite trend does not move to the hedenbergite corner.

Brown (1957) offers a lucid summary of the hypotheses put forward to explain the cessation of crystallization of a calcium-poor pyroxene in the later stages of basaltic fractionation. He points out the difficulties which arise from the concept of a steeply-sided domed solvus falling beneath the crystallization surface with iron enrichment, which would result in the two pyroxene phases approaching one another in composition, along trend-lines which would be convex (cf. Fig. 2) to the clinoenstatite–clinoferrosilite and diopside–hedenbergite joins. In the hypothetical pyroxene equilibrium diagrams in which the augite in the one-pyroxene field is indicated as crystallizing at a liquidus minimum, and that in the two-pyroxene field on the calcic limb of a domed solvus (Muir, 1954, fig. 4), these pyroxenes (Fig. 1) indicate that, as in the Skaergaard, the minimum must be in the same position (with regard to Ca:(Mg+Fe) ratio) when it intersects the solvus as when it leaves it. It has been suggested (Brown, 1957, p. 527) that the liquidus minimum has moved during basaltic fractionation towards the calcic component, showing a change from Ca_{25} to Ca_{35}, and in the case of these pyroxenes there is apparently a further shift to Ca_{40}, this being the Ca per cent of the two pyroxenes (Fig. 1, Nos. 2, 4) which demarcate the limit of the two-pyroxene field. This shift of the liquidus minimum supports Muir's hypothesis (1954, pp. 384–6) that the limit of two-pyroxene crystallization is due to a migration of the pyroxene liquidus minimum.

It has also been suggested that, at the limit of the two-pyroxene field, a reaction relationship may exist between calcium-poor pyroxene and liquid to form a fayalitic olivine (Poldervaart & Hess, 1951, p. 479). The calcium-rich pyroxenes of these acid pitchstones at the stage of cessation of crystallization of the calcium-poor pyroxene are not immediately joined by a fayalitic olivine, for a small interval occurs (Fig. 1, Nos. 3, 4) where ferroaugite is the only crystallizing ferromagnesian silicate. It is possible, however, that this interval may be expanded or contracted by variation in the partial pressure of oxygen, the effects of which, in iron–magnesia–silica systems, have been summarized by Osborn (1959). Although there is no textural evidence of a reaction relationship of calcium-poor pyroxene to form a fayalitic olivine, natural acid melts on passing through the limit of two-pyroxene crystallization soon enter the stability field of fayalitic olivine which is found as a phenocryst in all successive porphyritic acid glasses.

The apparent absence of exsolution lamellae of a lime-poor pyroxene within many of the ferroaugites of the slowly cooled Skaergaard intrusion (Brown, 1957, p. 538) indicates a relatively large temperature interval between the liquidus minimum and the underlying solvus limb; exsolution of a lime-poor phase within comparable ferroaugites is apparently only brought about by conditions of regional metamorphism (Hess, 1949, Nos. 15, 17, 19).

The composition of the orthopyroxene, No. 10A (Fig. 1), and its mode of occurrence (p. 310) would suggest that it has crystallized much earlier than the associated ferroaugite (Fig. 1, No. 10). These two pyroxenes cannot have crystallized in equilibrium with one another.

THE CORRELATION OF CHEMICAL COMPOSITION WITH OPTICAL PROPERTIES

The clinopyroxenes

The estimation of the Ca:Mg:Fe ratio of the lime-rich clinopyroxenes may be made from the β refractive index and $2V_\gamma$ using the determinative charts and techniques of Hess (1949). Such optical properties have been determined for these ferroaugites (Table 2) and plotted as a group of curves in Fig. 3. When

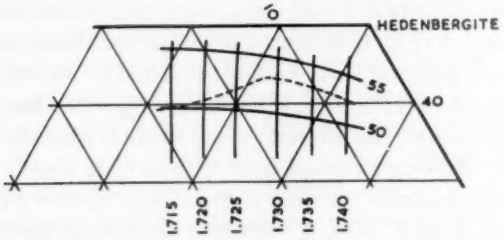

FIG. 3. Relationship between chemical composition and optical properties for the ferroaugites from some acid glasses. ⌒ Optic axial angle. (, β Refractive index. - - - - - Crystallization trend. The data for the Skaergaard ferroaugites (Muir, 1951) have not been used in compilation.

comparing these optical properties with similar curves for the ferroaugite region (Hess, 1949, pl. I; Muir, 1951, fig. 4) it is important to consider the possible effects of the minor cations on the optical properties of the ferroaugites, assuming that their effect is approximately the same throughout the group of pyroxenes on which the curves are based.

When compared to the ferroaugite optical determinative curves of Hess (1949, pl. I), which are admittedly based on few analyses, and amongst which there are a few internal discrepancies, the new β refractive index curves (Fig. 3) are about 0·006 higher for equivalent compositions, whereas the new $2V_\gamma$ curves are, on average, 5° too low. However, three of the ferroaugites described by Hess (1949, Nos. 15, 17, 19, the latter having high soda) have exsolution lamellae which Hess (1949, p. 636) suggests may be corrected for by subtraction of 3° from the observed $2V_\gamma$. As the nature and extent of the exsolution product are largely unknown, this is not entirely satisfactory, especially as Brown (1957, p. 536) has indicated that for the Skaergaard augites 3° should, in fact, be added.

Muir has subsequently amended the determinative curves of Hess in the ferroaugite region, using the results of optical and chemical determinations on the Skaergaard ferroaugites which are devoid of exsolution lamellae (Muir, 1951,

fig. 4). When the curves of Fig. 3 were compared to Muir's suggested determinative curves, rather large differences were found. The $2V_\gamma$ curve for 50° (Fig. 3) is very near Muir's 50° curve, but is concave in the other direction with a maximum difference between the two of 2°. The 55° curve runs near Muir's 60° curve but falls with increase in iron to almost intersect Muir's 55° curve in the ferrohedenbergite region. The β refractive index curves are on average 0·004 higher than for corresponding compositions read off Muir's curves. Closer examination of Muir's optical data suggested that his curves do not always bear a close relation to his optical determinations (see Brown, 1957, p. 538). The Skaergaard ferroaugites (Muir, 1951, Nos. 10–17, 19) were plotted individually on Muir's suggested optical determinative curves and the discrepancies for $2V_\gamma$ and β refractive index about their relevant smoothed curves were noted. The same procedure was then followed using these determinative curves (Fig. 3) and the results also noted.

Thus compared to Muir's determinative curves, the Skaergaard ferroaugites indicated that $2V_\gamma$ showed an average displacement of 3·6° and equal scatter, while β refractive index had an average displacement of 0·0054 with a distinct tendency for the observed values to be higher, i.e. with a positive bias. Again, compared to the curves of Fig. 3, the Skaergaard ferroaugites indicated that $2V_\gamma$ had an average displacement of 2·7° and a possible slight negative bias. It is assumed that Nos. 10 and 11 (Muir, 1951, p. 693) define the position of the 45°-curve, which would then fall an equal distance below the 50°-curve of Fig. 3. β showed an average displacement of 0·0036 with a possible slight positive bias.

It would appear then that the determinative curves presented in Fig. 3 give a slightly better correspondence with the observed optical properties of the Skaergaard ferroaugites, with, however, no convincing systematic difference between the Skaergaard results and these new results.

If, as has been suggested above, the determinative curves of Fig. 3 are representative of the optics of the Skaergaard ferroaugites, then the deduced composition of the unanalysed hedenbergite of the Skaergaard transgressive granophyre (Muir, 1951, p. 694, No. 20) is of importance as it represents the possible termination of the Skaergaard ferroaugite trend. If the optical properties of the hedenbergite ($\beta = 1{\cdot}735$, $2V_\gamma = 56°$) are plotted on Muir's determinative curves (Muir, 1951, fig. 4), then the derived composition is near $Ca_{43}En_6Fs_{51}$, whereas the composition Muir (1951, fig. 1) suggests is about $Ca_{48}En_1Fs_{51}$. The composition of the hedenbergite deduced from Fig. 3 is $Ca_{46}En_8Fs_{46}$; it cannot be taken as established, therefore, that the Skaergaard calcic-pyroxene trend moves to the hedenbergite corner (Muir, 1951, p. 708; cf. Brown, 1957, p. 538, however).

Hori (1954) has suggested that the effect of a cation upon the optical properties of a clinopyroxene is dependent upon its lattice site, and that Al, Ti, and Fe''' in fourfold coordination decrease the refractive index and increase $2V$, whereas in octahedral coordination they have the opposite effect (marked in the case of Ti). It would be expected that, in view of the cation distribution of these

clinopyroxenes (Table 3), which contain less Al in the (Z) group and less Al and Ti in the (WXY) group than the Skaergaard ferroaugites, there would be a decrease of the β refractive index and an increase of $2V_\gamma$ in relation to the Skaergaard ferroaugites which, with the exception of Nos. 11 and 13 (Muir, 1951),[1] do not contain Ti in tetrahedral coordination. As the Skaergaard ferroaugites contain an average of 1·1 per cent TiO_2 which is accommodated in the octahedral position, it is surprising that there is so little difference in optics between these two groups of clinopyroxenes.

If the augite (Table 2, No. 1) is plotted in Hess's determinative curves (1949, pl. I), the composition corresponds to a 7°-excess in the observed $2V_\gamma$ and an excess of 0·005 in the observed β refractive index. The discrepancy in $2V$ is possibly due to the inclusion of Ti in the (Z) group, whereas if Hori's hypothesis is correct, the observed β refractive index should be less than that deduced from the curves. Perhaps the unusually high contents of Fe''' and Mn could account for this anomaly, for the regression coefficient for Fe''' in the equation for β refractive index is almost as high as for Ti, and that for Mn is also high (Hori, 1954, p. 76).

The author would like to reiterate Brown's comments (1957, p. 538) on the use of calcium-rich pyroxene optical determinative curves. These curves (Fig. 3) can only safely be applied to ferroaugites of similar environment and cooling history to those described in this paper.

The iron-rich olivines

The optical determinative curves for the iron-rich olivines rely almost completely on the data for the synthetic olivines prepared by Bowen & Schairer (1935, p. 196). Deer & Wager (1939) were subsequently able to show that four olivines from the Skaergaard intrusion had optical constants which fell on or near the curves of refractive index based on the synthetic material.

The variation of α, β, and γ refractive indices with composition for synthetic olivines (Bowen & Schairer, 1935) are shown in Fig. 4, together with data available from the literature and the new determinations (Table 4). In view of the probable error of determination of these high values of refractive index, it is considered that the synthetic curves are representative of the data for the naturally occurring iron-rich olivines with a moderate content of manganese. With regard to the variation of $2V$ with composition, Kennedy (1947, p. 567) has published a curve calculated from the optical constants of the synthetic olivines. It cannot be expected that this calculated curve will closely resemble a curve based on direct measurement of $2V$. This curve (Fig. 4), based on direct determination of $2V$, falls about 5° below Kennedy's curve, and for this restricted range of composition is probably straight. Smaller differences exist between this $2V$ curve and the one published by Poldervaart (1950, p. 1073).

[1] See footnote on p. 316.

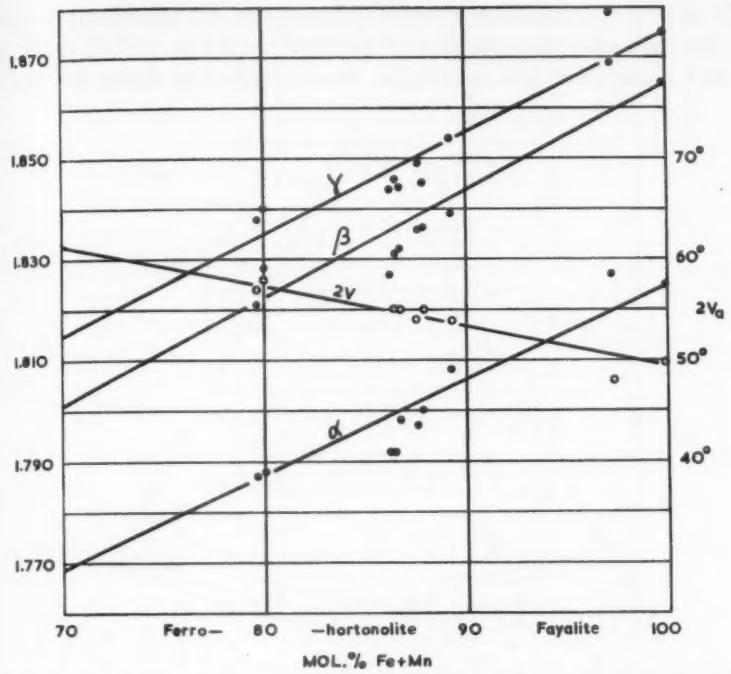

FIG. 4. Relationship between chemical composition and optical properties for the iron-rich olivines. The curves for α, β, and γ are for synthetic olivines (Bowen & Schairer, 1935). Refractive indices and optic axial angle of analysed natural olivines from the literature and Table 4 are represented by closed and open circles, respectively.

CHEMICAL ANALYSES OF PITCHSTONES AND RESIDUAL GLASSES

The residual glasses were separated from the phenocrysts on the Frantz isodynamic separator and by repeated centrifuging in methylene iodide. As some of the glasses enclose tiny felspar crystals, it was sometimes difficult to assess the purity of the glass fraction owing to composite grains of glass and fragments of felspar phenocrysts. However, it is believed that all the glasses were at least 98 per cent pure, and that most of them had less than 0·7 per cent impurity.

A rather different analytical scheme was used for the analysis of the pitchstones and residual glasses from that used for the minerals. Silica was determined colorimetrically as the molybdenum blue complex, the determination being made in duplicate or triplicate. Total iron was determined colorimetrically with thioglycollic acid, a method which gave highly reproducible results. Titania, manganese, and phosphorus were also determined colorimetrically, the alkalis by flame photometer, and alumina by subtraction of total iron as Fe_2O_3, TiO_2, MnO, and P_2O_5 from a weighed ammonia precipitate. Lime and magnesia were titrated with EDTA using Calcein and Eriochrome black T as indicators. Water and FeO were determined using the normal classical procedures. The estimation

of H_2O^- at 110° C caused considerable difficulty, for it is apparently not possible to dry the rock and glass powders to constant weight at 110° C, there being a small and continuous loss in weight. Accordingly, the figure for H_2O^- was

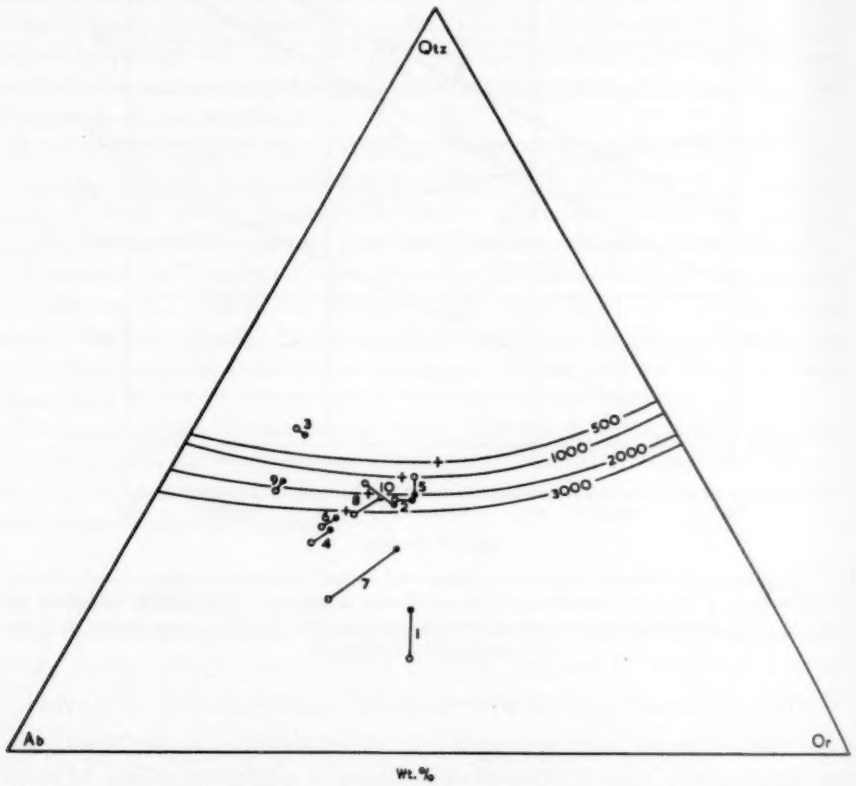

FIG. 5. Normative albite, orthoclase, and quartz of the analysed pitchstones and residual glasses are plotted in the system $NaAlSi_3O_8$–$KAlSi_3O_8$–SiO_2–H_2O. ○ Analysed pitchstones (Table 6). ● Analysed residual glasses (Table 6). The boundary curves for various water-vapour pressures (in kg/cm²) have been plotted. + Indicates position of the minimum on the boundary curves (Tuttle & Bowen, 1958). In the text an enumerated pitchstone–glass pair has been referred to as, for example, the pair 3R–3G.

derived from the loss in weight of 1 g of powder after an arbitary 2 hours in an oven at 110° C. The rather low average total of the pitchstone and residual glass analyses is believed to be due in part to the presence of BaO, which is noticeably present in all the pitchstones and residual glasses but which has not as yet been determined chemically. Nockolds & Allen (1956, Table 25, No. 4) report 1,500 p.p.m. Ba in the pitchstone from Glen Shurig, Arran (Table 6, No. 10R).

Although the pitchstone from Glen Shurig had previously been analysed (Tyrrell, 1928, p. 234), the content of MnO (0·50 per cent) seemed to the writer to be unusually high so that another analysis was made (Table 6, No. 10R). Con-

TABLE 6

Analyses of pitchstones and residual glasses

For the key to these analyses see p. 312, Table 1

	1R	1G	2R	2G	3R	3G	4R	4G	5R	5G	6R	6G	7R	7G	8R	8G	9R	9G	10R	10G
SiO_2	66·0	69·4	72·9	74·0	69·2	69·0	69·8	71·5	73·1	73·5	69·8	72·3	64·4	67·0	72·1	74·2	70·2	72·1	71·9	73·6
TiO_2	0·71	0·59	0·22	0·14	0·50	0·37	0·29	0·22	0·19	0·15	0·34	0·22	0·69	0·55	0·25	0·19	0·24	0·19	0·37	0·18
Al_2O_3	15·1	14·3	11·6	11·8	12·0	10·9	12·6	12·2	11·5	11·3	12·9	12·1	12·7	12·2	12·3	11·6	12·5	12·1	11·7	11·7
Fe_2O_3	1·5	1·3	0·52	0·39	2·2	1·2	1·2	0·9	0·49	0·32	0·7	0·4	1·7	1·2	0·9	0·6	1·0	0·7	0·6	0·4
FeO	1·2	1·0	0·89	0·84	1·4	1·8	1·7	1·7	0·96	0·93	2·4	1·4	3·8	3·9	1·4	1·0	1·7	1·5	2·1	1·1
MnO	0·11	0·11	0·04	0·03	0·12	0·11	0·10	0·09	0·04	0·03	0·08	0·05	0·21	0·20	0·06	0·05	0·10	0·08	0·07	0·02
MgO	0·69	0·41	0·12	0·10	0·59	0·40	0·32	0·21	0·08	0·07	0·21	0·09	0·66	0·32	0·13	0·04	0·10	0·09	0·38	0·14
CaO	1·2	0·92	0·75	0·62	2·2	1·6	0·92	0·62	0·77	0·58	1·7	1·0	1·9	1·4	1·0	0·71	1·8	1·3	1·4	0·70
Na_2O	4·9	4·7	4·0	3·9	4·1	4·1	5·2	5·0	3·6	3·8	4·8	4·9	4·9	3·9	4·6	4·3	5·0	5·1	4·0	4·1
K_2O	6·2	5·9	4·4	4·8	1·6	1·8	3·2	3·5	4·4	4·7	3·1	3·5	3·7	4·4	3·8	4·2	2·0	2·1	3·5	4·5
P_2O_5	0·11	0·10	0·02	0·02	0·08	0·06	0·04	0·02	0·02	0·02	0·07	0·04	0·11	0·11	0·02	0·04	0·02	0·04	0·05	0·03
H_2O^+	1·7	1·4	4·0	3·6	3·8	4·9	4·0	4·1	4·1	4·3	3·4	3·8	4·6	4·3	3·0	2·8	4·2	4·5	3·5	3·2
H_2O^-	0·4	0·2	0·5	0·1	2·1	3·7	0·3	0·1	0·6	0·1	0·4	0·1	0·6	0·1	0·2	0·1	0·7	0·2	0·3	0·1
TOTAL	99·8	100·3	100·0	100·3	99·9	99·9	99·7	100·2	99·9	99·8	99·9	99·9	100·0	99·6	99·8	99·8	99·6	100·0	99·9	99·8
$n_{20°}$	—	1·510	—	1·494	—	1·492	—	1·506	—	1·496	—	1·497	—	1·516	—	1·500	—	1·501	—	1·494
$d_{4°}$	2·472	—	2·344	—	2·318	—	2·426	—	2·360	—	2·443	—	2·470	—	2·397	—	2·380	—	2·422	—

TABLE 7. *Norms of pitchstones and residual glasses*

For the key to these analyses, see p. 312, Table 1

	1R	1G	2R	2G	3R	3G	4R	4G	5R	5G	6R	6G	7R	7G	8R	8G	9R	9G	10R	10G
Qz	11·3	17·8	31·0	31·6	34·0	34·0	24·7	27·0	33·4	32·0	25·6	28·3	16·3	22·3	28·7	31·9	29·2	31·4	30·9	31·0
Or	36·7	35·0	26·1	28·4	9·4	10·6	18·9	20·6	26·1	27·8	18·4	20·6	21·7	26·1	22·2	25·0	11·7	12·2	20·6	26·7
Ab	41·4	39·8	34·1	33·0	34·6	34·6	44·0	42·4	30·4	32·0	40·4	41·4	41·4	33·0	38·8	36·2	42·4	43·0	34·1	34·6
An	0·8	0·3	0·6	0·6	9·7	6·1	1·7	0·6	2·2	—	4·4	0·8	2·0	2·8	2·0	—	5·8	4·2	3·6	0·3
Wo	2·1	1·7	1·4	1·0	0·5	0·8	1·2	1·0	0·7	1·2	1·6	1·7	3·1	1·7	1·3	1·5	1·3	0·9	1·4	1·3
En	1·7	1·0	0·3	0·2	1·5	1·0	0·8	0·5	0·2	0·2	0·5	0·2	1·6	0·8	0·3	0·1	0·2	0·2	1·0	0·3
Fs	—	—	0·9	0·9	—	1·7	1·7	2·1	1·1	1·2	3·4	1·8	4·9	5·5	1·4	0·9	2·1	2·0	2·8	1·2
Il	1·4	1·2	0·5	0·2	0·9	0·8	0·6	0·5	0·5	0·3	0·6	0·5	1·4	1·1	0·5	0·5	0·5	0·5	0·8	0·5
Mt	2·1	1·6	0·7	0·7	3·2	1·9	1·9	1·4	0·7	0·5	0·9	0·7	2·6	1·9	1·4	0·9	1·4	0·9	0·9	0·7
Hm	—	0·2	—	—	—	—	—	—	—	—	—	—	—	—	—	—	—	—	—	—
H_2O	2·1	1·6	4·5	3·7	5·9	8·6	4·3	4·2	4·7	4·4	3·8	3·9	5·2	4·4	3·2	2·9	4·9	4·7	3·8	3·3
TOTAL	99·6	100·2	100·1	100·3	99·7	100·1	99·8	100·3	100·0	99·6	99·6	99·9	100·2	99·7	99·8	99·9	99·5	100·0	99·9	99·9
Total iron as Fe_2O_3	—	2·36	—	1·32	—	3·16	—	2·76	—	1·35	—	1·97	—	5·55	—	1·70	—	2·38	—	1·59
$\frac{Fe+Mn}{Fe+Mn+Mg}\times 100$	—	76	—	90	—	80	—	88	—	90	—	93	—	90	—	96	—	94	—	87

versely, the analysis of the Rauthaskritha dacite (Hawkes, 1924) shows no MnO and a trace of TiO_2, and the analysis was similarly repeated (Table 6, No. 9R). These two analyses were not made on the original powders. Harris & Brindley (1954, p. 820) give an analysis of the residual glass from the pitchstone from Judd's No. 1 dyke, Tormore, Arran. They state that the pitchstone has phenocrysts of quartz and fayalite (op. cit., p. 819), whereas the specimens the writer collected from the same dyke contain two pyroxenes (Fig. 1, Nos. 2, 2A), quartz and fayalite being absent.

The analyses of the pitchstones from which the analysed pyroxenes and olivines have been separated, together with the analyses of the residual glasses, are set down in Table 6 and their norms in Table 7. The pitchstone and residual glass analyses have been given the same numerical prefix as their contained pyroxenes and olivines (Fig. 1, Tables 2, 4).

It is proposed to confine this discussion of the residual glasses to those aspects of their chemistry which are believed to be related to the crystallization of the ferromagnesian silicates. The general relationship of the pitchstones to their residual glasses is shown in Fig. 5, where the normative salic constituents (less anorthite) have been plotted in the system $NaAlSi_3O_8$–$KAlSi_3O_8$–SiO_2, together with the position of the quartz–felspar boundary curves under various water-vapour pressures (Tuttle & Bowen, 1958, pp. 54–56). The trend of the tie-lines between the Icelandic pitchstones and their residual glasses is in distinct contrast to the more varied trends of the British pitchstone–glass tie-lines, and the possible reasons for this will be taken up in a later paper. The anomalous position of No. 3R–3G (fig. 5) is due to the low content of K_2O (Table 6, Nos. 3R, 3G) which is believed to be the result of subsequent hydrothermal alteration. No. 9 may be similarly affected, although the geological environment is less well known to the writer.

THE STATUS OF THE PYROXENE PHENOCRYSTS

The recognition of the exact relationship between the pyroxene phenocrysts and the residual glasses is not simple, as several alternatives exist. The pyroxene phenocrysts may be in equilibrium with one another if two exist; they may also be in equilibrium with the residual glass, or they may be xenocrysts which have become incorporated in the glass. It is also possible that they may be a metastable phase as was found experimentally on heating natural granite to its melting-point (Tuttle & Bowen, 1954, p. 83).

The tie-lines between the calcium-poor and the calcium-rich pyroxenes (Fig. 1, Nos. 1–1A, 2–2A) are parallel, or nearly so, to the pyroxene tie-lines of the slowly cooled tholeiitic rocks (Fig. 2) and indicate that the two calcium-rich pyroxenes (Fig. 1) are in equilibrium with the two calcium-poor pyroxenes. The trend of a tie-line between the orthopyroxene and the ferroaugite from the Glen Shurig, Arran, dyke (Fig. 1, Nos. 10, 10A), together with the mode of occurrence (p. 310), suggests that this orthopyroxene is xenocrystic, the crystals—which

may have been partially resorbed—later acting as nuclei for the precipitation of ferroaugite.

It is to be expected that enrichment in iron relative to magnesium in the pyroxenes will be matched or reflected by similar enrichment in the residual glasses. The iron-magnesium atomic ratios of the ferroaugites have been plotted in Fig. 6 together with those of the residual glasses. This ratio for the glasses is given at the bottom of Table 7 and is derived from the directly determined figure for total iron (Table 7). As the ferroaugite phenocrysts may be considered to represent a solidus, and the iron-magnesium components of the residual glasses a liquidus, a hypothetical solid solution series of these calcium-rich pyroxenes may be constructed.

It has been assumed as an approximation that a straight line drawn between the melting temperature of a component *A* and the lower melting temperature of the second component *B*, which form a complete solid solution series without a minimum, will lie in a mean position between the liquidus and the solidus. In other words, this line represents the mean ratio of the *A* to *B* ratio of the solid, and the *A* to *B* ratio of the liquid in equilibrium with the solid, at any given temperature. For the olivine solid solution series this approximation is reasonably precise, but it becomes less so in the plagioclase series. The temperatures used (Fig. 6) are the melting temperature of diopside (approximately 1,390° C) and the temperature of the solid solution minimum for the ferrosilite–hedenbergite series (950° C) (Bowen, Schairer & Posnjak, 1933, p. 213), and a line drawn between these two temperatures represents the mean Fe+Mn/Fe+Mn+Mg ratio of the solid (ferroaugite) and the liquid (glass). The temperature scale in this context has little meaning and was used solely to give a slope for the axial line.

In a general way, the relative iron-enrichment of the ferroaugites is matched by iron-enrichment in the residual glasses, and a curve may be drawn through the ferroaugites and is taken to represent a solidus, whereas the curve through the residual glasses represents a hypothetical liquidus (Fig. 6). As the scatter of points which define the liquidus is rather large, the recognition of anomalous ferroaugite–glass pairs is somewhat arbitrary. The ferroaugite–glass pair 2–2G (Fig. 6), however, lies off the general trend and this indicates that the pyroxene 'phenocrysts', although in equilibrium with one another (Fig. 1, Nos. 2, 2A), are either possible composite xenocrysts or are metastable. The remaining ferroaugite–glass pairs do not show any significant scatter, and it is concluded that the ferroaugites exist in equilibrium with their glasses. Two pitchstones (Tables 1, 6, Nos. 3R, 7R) contain frequent basaltic fragments in various stages of disintegration and digestion, which may have modified the original composition of the glasses, and hence their positions in Fig. 6 (Nos. 3G, 7G).

As the pyroxene–glass pair 1–1G (Fig. 6) lie so far away from the rest of the analyses, it is less easy to assess their relationship. If, however, the augite (and hence the orthopyroxene 1A (Fig. 1)) is in equilibrium with the glass, the solidus

develops a rather odd-shaped bulge which may be an indication of a plateau (Wyllie, 1960) and therefore a variable rate of fractionation (rate of iron-enrichment) with a constant cooling rate. Brown (1957, p. 522) has commented briefly on the increase in the rate of fractionation in the Skaergaard with respect to the iron-enrichment in the calcium-rich pyroxenes with increasing height in the layered series.

The essential features of Fig. 6 are shown in the relationship between the

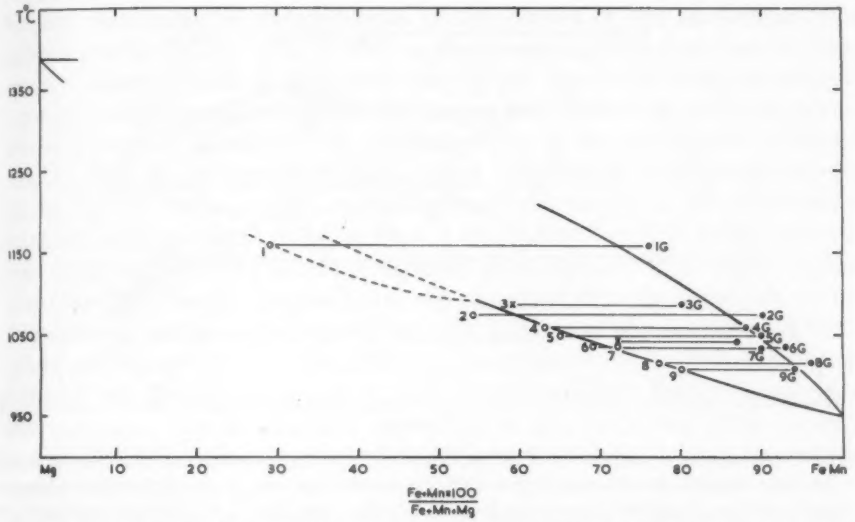

FIG. 6. Possible relationship between the calcium-rich pyroxenes and their residual glasses in respect of their relative iron enrichment. ○ Analysed calcium-rich pyroxenes (Table 2). × Optically determined ferroaugites. ● Analysed residual glasses (Table 6). The ferroaugite–glass pair 10–10G has not been labelled and lies between the pairs 5–5G and 6–6G.

ferrohortonolites and the residual glasses, and although the differences in the iron-magnesium ratios of the olivines and their glasses is very much smaller, the glasses show similar relative enrichment in iron.

THE PYROXENE COMPONENTS IN THE LIQUID

The general features of iron-enrichment of the residual glasses in relation to the calcium-rich pyroxene phenocrysts may also be shown in terms of the normative pyroxene components in these glasses. As the amount of normative pyroxene is very small (Table 7), and therefore the Ca:Mg:Fe ratio subject to great variation as a result of analytical error or subsequent alteration in the glass—as, for example, Nos. 1R and 1G (Tables 6, 7), where the occurrence of haematite in the norm indicates that the glass has been subsequently oxidized —it has been assumed that all the femic constituents other than ilmenite may be taken to represent the components of pyroxene in the liquid (glass). The directly

determined figure for total iron of the glasses (Table 7) has been converted to molecular proportions of ferrous iron, an equivalent to the molecular proportion of titania then subtracted, and finally the molecular proportions Ca:Mg:Fe″+Mn computed. Any potential components of iron-rich olivine or the iron–titanium oxides in the glasses have been neglected. It is difficult to assess the original amount of oxidized iron in the glass when liquid, and in view of possible subsequent oxidation it has been assumed that all the iron was present in the reduced state.

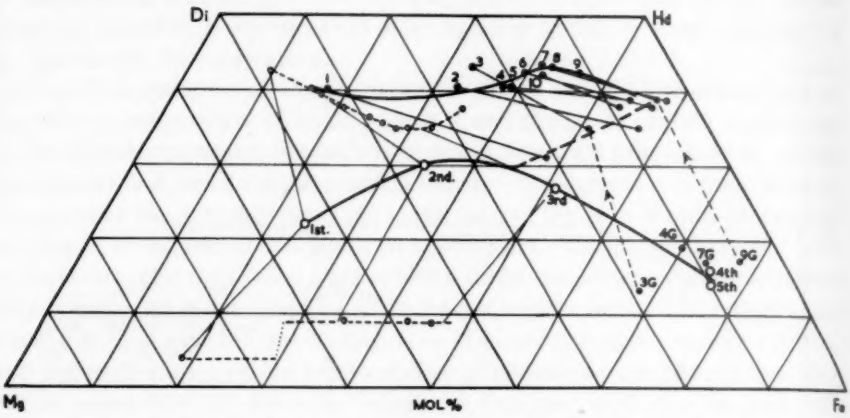

FIG. 7. The trend of crystallization of the pitchstone calcium-rich pyroxenes together with the Skaergaard calcium-rich and calcium-poor pyroxenes. The possible pyroxene components in their respective liquids are also plotted. ● Calcium-rich pyroxenes (Table 2 and Fig. 1). • Pyroxene components in the residual glasses with tie-lines connecting the relevant pairs. 3G– – –→ composition of the corrected pyroxene composition of two residual glasses (see text). – – – Possible trend of pyroxene components in the liquid (glasses). o - - o - - o Pyroxene trend of the Skaergaard intrusion with analysed specimens indicated (Brown, 1957, Table 1 and Fig. 2). o——o Normative pyroxene of the Skaergaard liquids (Wager & Deer, 1939) with tie-lines connecting the possible relevant pairs.

The femic components, less ilmenite, of the residual glasses have been plotted in Fig. 7, together with their respective calcium-rich pyroxenes. Two of the pitchstones and their residual glasses (Nos. 3R, 3G and 9R, 9G) fall outside the main field in Fig. 5, and the analyses and environment of one (Table 6, Nos. 3R, 3G) indicate an impoverishment in K_2O as a result of subsequent alteration. The undoubted alteration of No. 3G suggests the possible alteration of the other (No. 9G), and the normative pyroxene components of both have been recomputed so that only sufficient CaO combines with Al_2O_3 to form 1 per cent normative anorthite. These corrected molecular pyroxene components have been plotted in Fig. 7 together with the uncorrected compositions.

The pyroxene components of two of the residual glasses plot near the iron corner of the pyroxene diagram (Fig. 7, Nos. 4G, 7G) and the basaltic material contained by both pitchstones (Table 1, Nos. 4R, 7R) may have modified the compositions of the glasses and caused an increase in the content of iron and

possibly magnesia, which are particularly high in No. 7G but considerably less so in No. 4G (Table 6).

The Skaergaard liquids have also been plotted (Fig. 7), but only the normative pyroxene, which forms between 20 and 40 per cent of the liquids (Wager & Deer, 1939, p. 221), has been recomputed to Ca:Mg:Fe ratios. If normative olivine is taken into consideration, its effect will be to depress the first three liquids (Fig. 7) towards the enstatite–ferrosilite join.

The first liquid of the Skaergaard, the chilled margin, is assumed to have a similar relationship to the pyroxenes of the earliest crystal accumulate, the gabbro–picrite (Brown, 1957, p. 519), as the pyroxene phenocrysts have to their residual glasses. This is an approximation, for the liquid with which the earliest crystal fraction is in equilibrium has the composition of the original liquid minus the early formed crystals, and not the composition of the initial liquid. This will tend to alter the position of the first liquid very slightly towards the second liquid (Fig. 7). The second liquid developed after 60 per cent of the Skaergaard intrusion had solidified (Wager & Deer, 1939, p. 219), and the writer suggests that the first pyroxene fraction to separate at equilibrium from such a liquid may correspond to the composition of the pyroxenes from the lower part of the lower olivine–gabbros (Brown, 1957, Nos. 3, 4, 4A), and the tie-lines have been drawn accordingly (Fig. 7). The third liquid crystallized to give part of the lower ferrogabbros (Wager & Deer, 1939, p. 219), and the writer tentatively suggests that this liquid may have initially crystallized to give pyroxenes which lie very near the limit of the two-pyroxene field (Brown, 1957, Nos. 7, 7A, 8, 9) and the appropriate tie-lines have been drawn. The positions of the fourth and fifth liquids have been shown, but no estimate has been made of their initial pyroxene phases.

The tie-lines between the successive Skaergaard liquids and suggested first-formed pyroxenes form three-phase triangles whose apices may be generally considered to be slightly further from their bases than is shown (Fig. 7). Whether or not the tie-line between the calcium-rich pyroxene and the second liquid becomes nearly parallel to the tie-line between the augite (Fig. 7, No. 1) and its residual glass is unknown, so that the Skaergaard pyroxene–liquid relationships cannot reliably be used to assess the relationship of the augite (Fig. 6, 7, No. 1) to its residual glass. It has already been suggested that the calcium-poor pyroxene (Fig. 1, No. 1A) is in equilibrium with the calcium-rich pyroxene.

The later trend of the pyroxene components of these residual glasses towards $Ca_{40}Fe_{60}$ (Fig. 7) does not offer any convincing proof that the ferroaugite phenocrysts crystallized on a liquidus minimum (Muir, 1954, Fig. 4.), for it is to be expected that if this were so then the liquid pyroxene components would lead their respective ferroaugites along the pyroxene crystallization curve which, with the possible exception of Nos. 8 and 9, does not seem to be the case. The later trend of the Skaergaard liquids towards the Fe corner is due to the modal iron-rich olivine plus quartz occurring in the CIPW norm as

orthopyroxene; the calcium-rich pyroxene components of the fourth and fifth liquids lie almost midway between hedenbergite and ferrosilite (Wager & Deer, 1939, fig. 55).

The writer considers, in conclusion, that although the pyroxenes from one of the Arran dykes (Figs. 1, 6, Nos. 2, 2A,) may be xenocrystic, the lack of any petrographic evidence for the breakdown and incorporation of foreign material, which is so well depicted in many of the Icelandic glasses, together with the difficulty in providing a source for just these two pyroxenes of rather unusual composition, makes this distinction at the best tentative, and it must await further study.

ADDENDUM

After submission of the manuscript the writer discovered that two of the Arran dykes (Table 6, Nos. 5R, 10R) had previously been analysed and the results discussed by Vogt (1931, pp. 194–7). Vogt (p. 194) also remarks on the improbably high figure of MnO for the Glen Shurig dyke (Tyrrell, 1928) (cf. new analysis (Table 6, No. 10R)), and he also suggests that the determination of P_2O_5 may be in error. As the analyses made for Vogt by Kluver were presumably performed using almost entirely gravimetric techniques, the comparison between the two sets of results set down below is of interest, as these new results (Table 6) were obtained using almost entirely non-gravimetric techniques (see text). With the exception of CaO and MgO for Nos. 5R and 1 (Vogt, 1931, Table 44) there is satisfactory agreement, and the general measure of agreement between Nos. 10R and 2 (Vogt, 1931, Table 44) is encouraging.

	No. 5R (*Table* 6)	*No.* 1 (*Vogt, Table* 44)	*No.* 10R (*Table* 6)	*No.* 2 (*Vogt, Table* 44)
SiO_2	73·1	73·24	71·9	71·86
TiO_2	0·19	0·14	0·37	0·29
Al_2O_3	11·5	11·23	11·7	11·70
Fe_2O_3	0·49	0·54	0·6	0·80
FeO	0·96	1·08	2·1	2·15
MnO	0·04	0·04	0·07	0·07
MgO	0·08	0·36	0·38	0·41
CaO	0·77	0·37	1·4	1·35
Na_2O	3·6	3·40	4·0	3·74
K_2O	4·4	4·31	3·5	3·58
P_2O_5	0·02	0·008	0·05	0·043
H_2O^+	4·1	4·37	3·5	3·46
H_2O^-	0·6	0·63	0·3	0·42
TOTAL	99·9	99·91*	99·9	100·02†

* Includes BaO 0·11, CO_2 0·07, S 0·01.
† Includes BaO 0·12, CO_2 0·02, S 0·01.

ACKNOWLEDGEMENTS

The author wishes to thank Prof. J. Sutton and Dr. G. M. Brown for reading the manuscript and offering many valuable suggestions. The author is greatly

indebted to Mr. R. Curtis who laboriously handpicked some of the mineral concentrates before analysis. A grant from the Central Research Fund of the University of London, for travel to Iceland, is acknowledged.

REFERENCES

ANWAR, Y. M., 1955. A clinopyroxene from the granophyre of Meall Dearg, Skye. *Geol. Mag. Lond.* **92**, 367–73.

BELL, J. D., 1959. The geology of the northern end of the Blaven range, Isle of Skye. Unpublished thesis for D.Phil. degree, Univ. of Oxford.

BOWEN, N. L., SCHAIRER, J. F., & POSNJAK, E., 1933. The system CaO–FeO–SiO_2. *Amer. J. Sci.*, 5th ser., **26**, 193–284.

—— 1935. The system MgO–FeO–SiO_2. Ibid. **29**, 151–217.

BROWN, G. M., 1957. Pyroxenes from the early and middle stages of fractionation of the Skaergaard intrusion, East Greenland. *Miner. Mag.* **31**, 511–43.

DEER, W. A., & WAGER, L. R., 1939. Olivines from the Skaergaard intrusion, Kangerdlugssuaq, East Greenland. *Amer. Min.* **24**, 18–25.

HARKER, A., 1908. The geology of the small isles of Inverness-shire. *Mem. geol. Surv. Scotland*, 1–210.

HARRIS, P. G., & BRINDLEY, G. W., 1954. Mordenite as an alteration product of a pitchstone glass. *Amer. Min.* **39**, 819–24.

HAWKES, L., 1924. On an olivine–dacite in the Tertiary volcanic series of eastern Iceland: the Rauthaskritha (Hamerfjord). *Quart. J. geol. Soc. Lond.* **80**, 549–67.

HESS, H. H., 1949. Chemical composition and optical properties of common clinopyroxenes. Part 1. *Amer. Min.* **34**, 621–66.

HORI, F., 1954. Effects of constituent cations on the optical properties of clinopyroxenes. *Sci. Papers College Gen. Education, Univ. Tokyo*, **4**, No. 2, 71–83.

KENNEDY, G. C., 1947. Charts for correlation of optical properties with chemical composition of some common rock-forming minerals. *Amer. Min.* **32**, 561–73.

KUNO, H., 1950. Petrology of Hakone and the adjacent areas, Japan. *Bull. geol. Soc. Amer.* **61**, 957–1019.

—— 1954. Study of orthopyroxenes from volcanic rocks. *Amer. Min.* **39**, 30–46.

—— 1955. Ion substitution in the diopside-ferropigeonite series of clinopyroxenes. Ibid. **40**, 70–93.

—— & NAGASHIMA, K., 1952. Chemical compositions of hypersthene and pigeonite in equilibrium in magma. Ibid. **37**, 1000–6.

MUIR, I. D., 1951. The clinopyroxenes of the Skaergaard intrusion, eastern Greenland. *Miner. Mag.* **29**, 690–714.

—— 1954. Crystallization of pyroxenes in an iron-rich diabase from Minnesota. Ibid. **30**, 376–88.

—— & TILLEY, C. E., 1957. Contributions to the petrology of Hawaiian basalts. I. The picrite basalts of Kilauea. *Amer. J. Sci.* **255**, 241–53.

MURRAY, R. J., 1954. The clinopyroxenes of the Garbh Eilean Sill, Shiant Isles. *Geol. Mag. Lond.* **91**, 17–31.

NOCKOLDS, S. R., & ALLEN, R., 1956. The geochemistry of some igneous rock series. Part III. *Geochim. et Cosmoch. Acta*, **9**, 34–77.

OSBORN, E. F., 1959. Role of oxygen pressure in the crystallization and differentiation of basaltic magma. *Amer. J. Sci.* **259**, 609–47.

POLDERVAART, A., 1950. Correlation of physical properties and chemical composition in the plagioclase, olivine and orthopyroxene series. *Amer. Min.* **35**, 1067–79.

—— & HESS, H. H., 1951. Pyroxenes in the crystallization of basaltic magma. *J. Geol.* **59**, 472–89.

SAHAMA, TH. G., & HYTÖNEN, K., 1958. Calcium-bearing magnesian-iron olivines. *Amer. Min.* **43**, 862–71.

TILLEY, C. E., 1952. Some trends of basaltic magma in limestone syntexis. *Amer. J. Sci.*, Bowen vol., 529–45.

—— 1957. A note on the pitchstones of Arran. *Geol. Mag. Lond.* **94**, 329–33.

TUTTLE, O. F., & BOWEN, N. L., 1958. Origin of granite in the light of experimental studies. *Mem. geol. Soc. Amer.* **74**, 1–153.

TYRRELL, G. W., 1928. Geology of Arran. *Mem. geol. Surv. Scotland.*

VINCENT, E. A., 1954. Iron–titanium oxide minerals in layered gabbros of the Skaergaard intrusion, east Greenland. *Geochim. et Cosmoch. Acta*, **6**, 1–26.

VOGT, J. H. L., 1931. The physical chemistry of the magmatic differentiation of igneous rocks. III. Second half. *Skrifter Norske Vidensk-Akad. i. Oslo.* I. Mat.-Naturv. Klasse, Oslo, 1–101.

WAGER, L. R., & DEER, W. A., 1939. Geological investigations in east Greenland. Part III. The petrology of the Skaergaard intrusion, Kangerdlugssuaq. *Medd. Grønland*, **105**, No. 4, 1–352.

WALKER, G. P. L., 1959. Geology of the Reydarfjordur area, eastern Iceland. *Quart. J. geol. Soc. Lond.* **114**, 367–91.

WILKINSON, J. F. G., 1957. The clinopyroxenes of a differentiated teschenite sill near Gunnedah, New South Wales. *Geol. Mag. Lond.* **94**, 123–34.

WILSON, A. D., 1955. A method for the determination of ferrous iron in rocks and minerals. *Bull. G.S.G.B.*, No. 9, 56–58.

WYLLIE, P. J., 1960. The system CaO–MgO–FeO–SiO_2, and its bearing on the origin of basic and ultrabasic rocks. *Miner. Mag.* (in press).

YODER, H. S., & SAHAMA, TH. G., 1957. Olivine X-ray determinative curve. *Amer. Min.* **42**, 475–91.

—— & TILLEY, C. E., 1956. Natural tholeiite basalt-water system. *Ann. Rep. Geophys. Lab.*, Year Book No. 55, 169–71.

The Composition and Origin of the Striped Amphibolites of Connemara, Ireland

by BERNARD W. EVANS *and* BERNARD E. LEAKE

Department of Geology and Mineralogy, Oxford, and Department of Geology, Bristol, England

ABSTRACT

Major- and trace-element analyses, accompanied by modal analyses and mineralogical data, are given for thirty-three striped amphibolites from Connemara. It is concluded that prior to metamorphism these rocks were intrusions, lavas or tuffs of sodic basalt composition.

INTRODUCTION

THE Connemara Schists, in the west of Ireland (Fig. 1), consist of pelitic schists, semi-pelitic schists, siliceous granulites, quartzites, marbles, calc-magnesian metasediments, and amphibolites. The conditions of metamorphism correspond to the sillimanite–almandine–muscovite subfacies over most of Connemara, except in the north (staurolite–almandine subfacies) and in the south-west (quartz–albite–epidote–almandine subfacies). Folding along an east–west axis, following severe isoclinal folding and nappe formation, has given rise to the dominant structural feature of Connemara—the Connemara antiform (Fig. 1), the core of which is occupied by thick quartzites.

The amphibolites are mostly of two kinds, striped amphibolites and unstriped amphibolites, although gradations between the two are present. The former are fine-grained schistose hornblende–plagioclase rocks with a characteristic striped appearance, and the latter are coarse, poorly schistose or sometimes massive, homogeneous hornblende–plagioclase rocks. Mapping has revealed a close distributional association between striped amphibolite, quartzite, and marble (Fig. 2), and this fact, in conjunction with the striping, has suggested the possibility that the striped amphibolite might be of sedimentary origin. The present study of the chemistry of the striped amphibolites was carried out in an attempt to shed further light on their origin.

METHODS OF STUDY

Although the analysed samples came from various parts of Connemara (Fig. 1), rather more were collected from the central and south-western part because this area has recently been mapped in detail on the scale of 1:10,560 by both of us. The samples were chosen to cover the full range of modal variation within this group of amphibolites, so that BE 1082 is exceptional because it is a single pale stripe (see below) from an amphibolite and RB 659 is also unusual, being formed of more than 70 per cent of pale stripe and less than 30 per cent of amphibolite, with hornblende constituting only 12 per cent of the mode. Because

[Journal of Petrology, Vol. 1, Part 3, pp. 337–63, 1960

neither of these two samples is an average striped amphibolite, they cannot be directly compared with the remaining samples.

The major elements were determined by the method of Riley (1958) and the accuracy is believed to be rather better than that of classical silicate methods. Each sample was determined in duplicate.

The trace elements were determined by a quantitative spectrographic procedure, using anode excitation in a d.c. arc discharge, after Ahrens (1954).

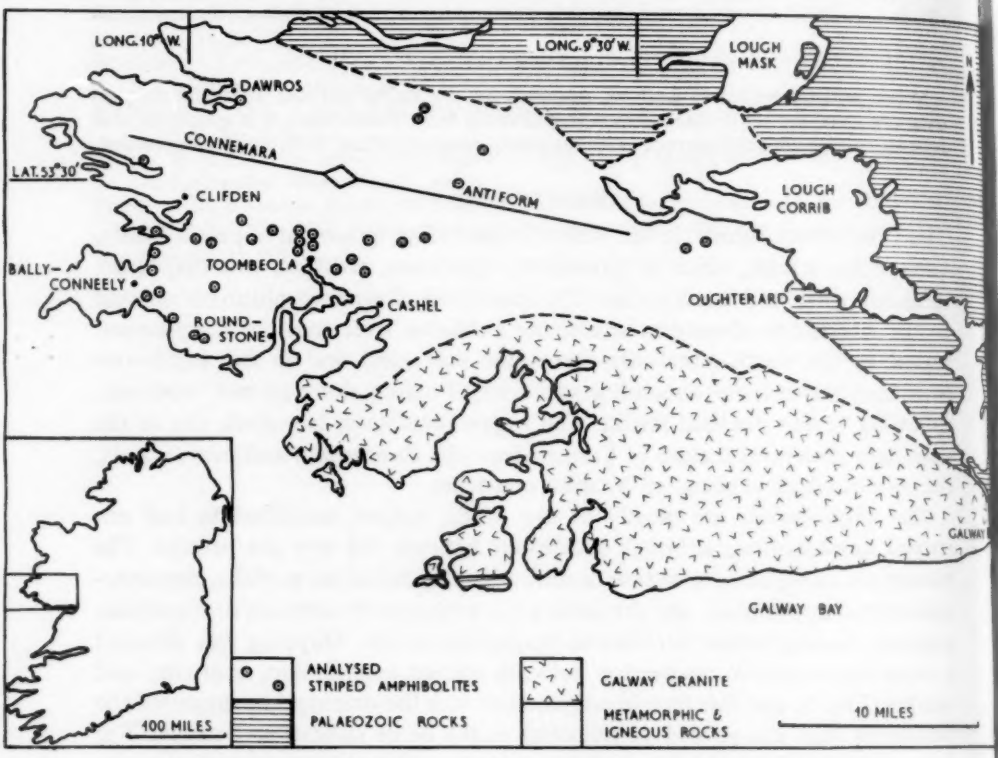

FIG. 1. Outline map of the geology of Connemara, Ireland, showing sample locations.

The sample was mixed with 2 parts by weight of a carbon–palladium mix, consisting of 1 per cent $(NH_3)_4Pd(NO_3)_2$ and 99 per cent Johnson–Matthey JM 9 carbon powder. The spectrograph was a Hilger large quartz and glass instrument, with a 7-step 2:1 rotating sector. The internal standard lines were Pd 3259 and Pd 3958 and the analysis lines Cu 3247, Ni 3414, Zr 3438, Co 3453, Sc 4246, Cr 4254, Sr 4607, and Ba 4934 Å. G–1 and W–1 were used as rock standards, with the following values:

	Cr	Ni	Co	Cu	Zr	Sc	Sr	Ba
G–1	20	5	4	13	200	3	260	1300
W–1	120	70	36	150	90	37	160	200

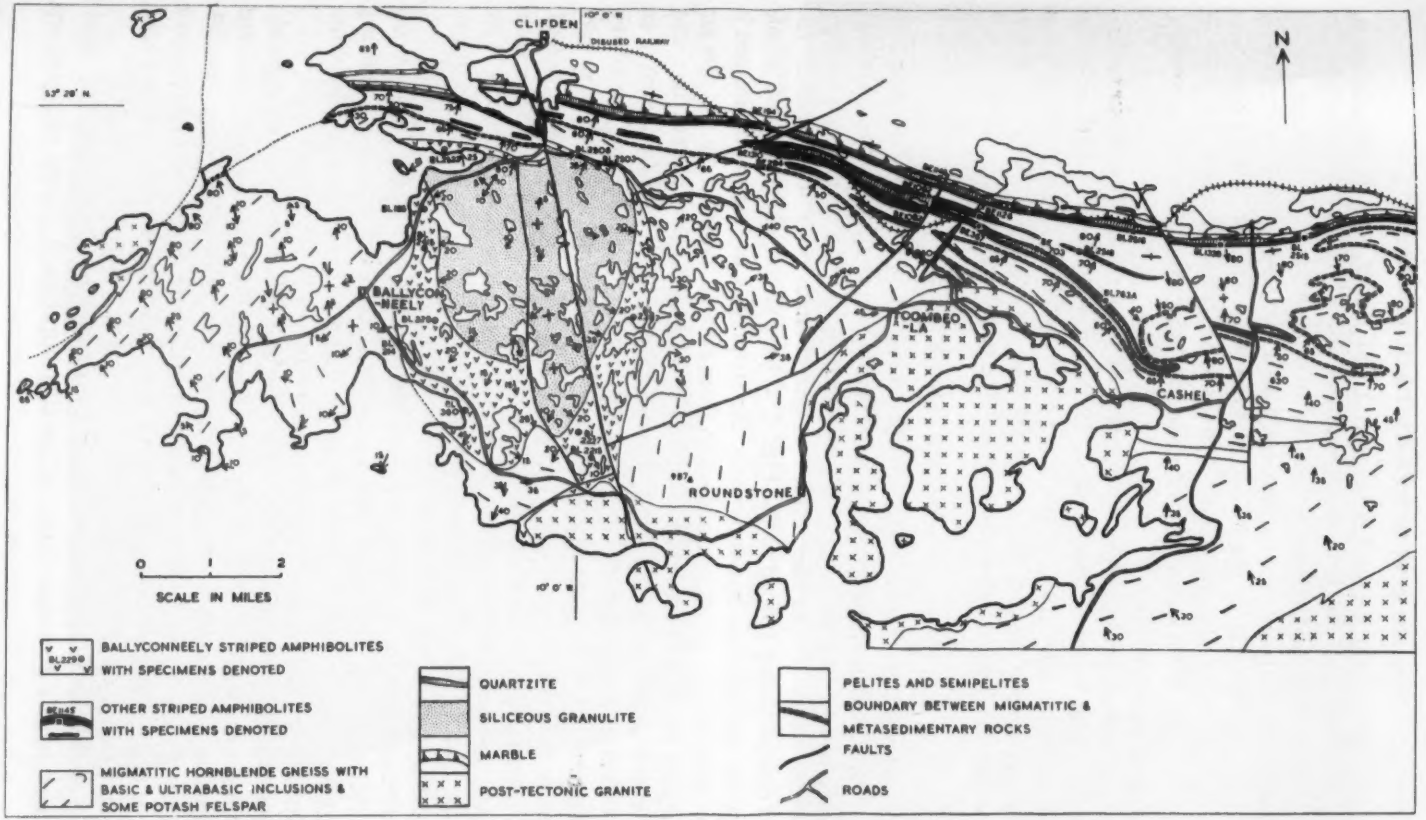

FIG. 2. Sketch-map of part of western Connemara showing structure and the field relationships between striped amphibolite, quartzite, and marble.

The precision of the method is between 5 and 10 per cent relative deviation. Because of the similarity between the samples and W–1, the accuracy should be rather high. Each sample was determined in duplicate.

The modal analyses were carried out with a Swift Automatic Point Counter on slides cut normal to the foliation. Between 1,500 and 7,000 points were counted per rock depending upon the degree of striping present. The Holmes effect (Chayes, 1956) will have given excessive values to the opaque minerals in the finer-grained schists.

Plagioclase compositions were estimated by the method of maximum extinction of albite twins in the zone $\perp$ (010) on a universal stage, using the curve of Poldervaart (1950, p. 1069). The optic angle ($\pm 2°$) of hornblende was measured directly between the optic axes, and the refractive index γ' ($\pm 0{\cdot}003$) represents the highest value obtained on cleavage fragments.

PETROGRAPHY

The striped appearance of the amphibolite is the result of variation in both the texture and the relative amounts of minerals—mostly the alternation of dark hornblende–plagioclase bands with off-white to pale green plagioclase–clinopyroxene bands or light plagioclase-rich quartz bands poor in hornblende. The most conspicuously striped rocks (Figs. 3, 4) have almost equal amounts of pale stripe to amphibolite, but commonly the striping is not so important and is often lacking. The bands range in width from about 1 mm to 2 cm and they are invariably parallel to the schistosity; individual bands can frequently be traced for several metres along the strike. The thicknesses of the different bands in an individual outcrop show no consistent relationship to each other. The amphibolites that are most persistent along the strike are generally the most striped, whereas boudinaged and discontinuous amphibolites tend to be unbanded. The heterogeneity of the rock may be accentuated by the presence of pale green masses, lenses or seams of epidotized amphibolite up to about $60 \times 15 \times 15$ cm in size, and by the occurrence of concordant veins or lenses of quartz–plagioclase–hornblende pegmatite (Fig. 3).

Although gradations between striped amphibolite and massive amphibolite can be observed, gradation between striped amphibolite and surrounding quartzite or pelite does not take place, the contacts being almost knife-sharp, except where shearing and boudinage have caused a little interdigitation.

Common hornblende and plagioclase are by far the most important minerals, forming more than 90 per cent of the rock in half the analysed specimens, and except for four specimens they always total more than 80 per cent. Very felspathic or very hornblendic rocks are extremely rare. Quartz does not exceed 15 per cent, clinopyroxene is frequently absent and never exceeds 25 per cent, and sphene is a notable accessory.

Texturally, the striped amphibolites are even-grained, schistose, and xenomorphic with a reticulate fabric of parallel hornblende prisms enclosing an-

FIG. 3. The typical outcrop appearance of the striped amphibolite. Striping is very conspicuous and a few concordant quartz–plagioclase pegmatite veinlets are present.

FIG. 4. Hand specimen of a conspicuously striped amphibolite (BE 1145). Clinopyroxene is restricted to the plagioclase-rich bands. The specimen measures 10 × 9 cm.

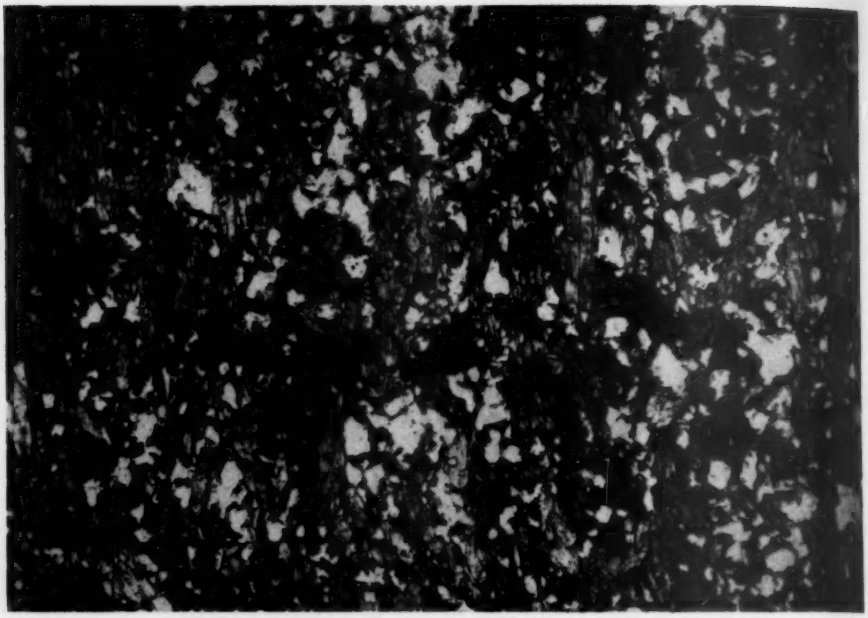

FIG. 5. Photomicrograph of homogeneous striped amphibolite BL 2404. Plagioclase is colourless, hornblende in shades of grey, and iron ore black. Magnification × 20.

FIG. 6. Photomicrograph of striped amphibolite BE 1145, consisting of alternation of the following bands from left to right: hornblende–plagioclase, plagioclase–clinopyroxene, hornblendite, hornblende–plagioclase, and plagioclase–hornblende–clinopyroxene. Magnification × 20.

hedral plagioclases which tend to be tabular parallel to the schistosity. The *a*-axes of the hornblendes often lie normal to the foliation and in many rocks a megascopic *b*-lineation results from the parallel alignment of the hornblende

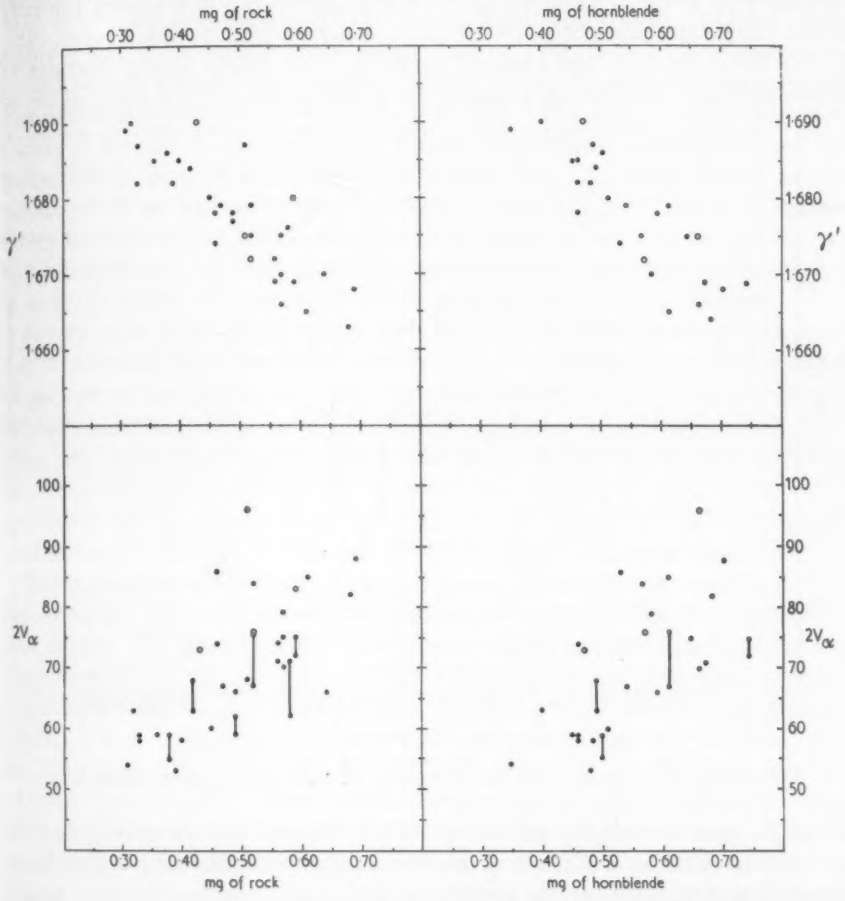

FIG. 7. Plot to show the relationship between the optical properties of the hornblende and the *mg* number of the rock and the calculated *mg* number of the hornblende (six hornblendes are omitted from the latter as they are associated with appreciable pyroxene whose composition is not precisely known). Circles represent brown hornblendes.

crystals in the schistosity plane. The plagioclase rich-clinopyroxene bands are usually granoblastic.

The amphibole is typically an ordinary green hornblende but greenish-brown and brown types are common and bluish-green varieties also occur. Elongation parallel to *c* is usually at least five times the *b* dimension. γ' ranges at least from 1·663 to 1·690 and the $2V$ (*-ve*) from 53° to 96°. Figs. 7 and 8 show the existence of a good correlation between γ', $2V$, the Niggli number *mg* of the

rock, and the estimated *mg* of the hornblendes as calculated from the chemical and modal analyses. This correlation of the more magnesium-rich hornblendes with higher $2V$s and lower refractive indices and of the more iron-rich hornblendes with lower $2V$s and higher refractive indices is a well-known property of the calciferous amphiboles (Winchell & Winchell, 1951, p. 434; Tröger, 1952, p. 77). Since many of the analysed rocks are very nearly simple mixtures of hornblende and plagioclase, a knowledge of the mode and the composition of

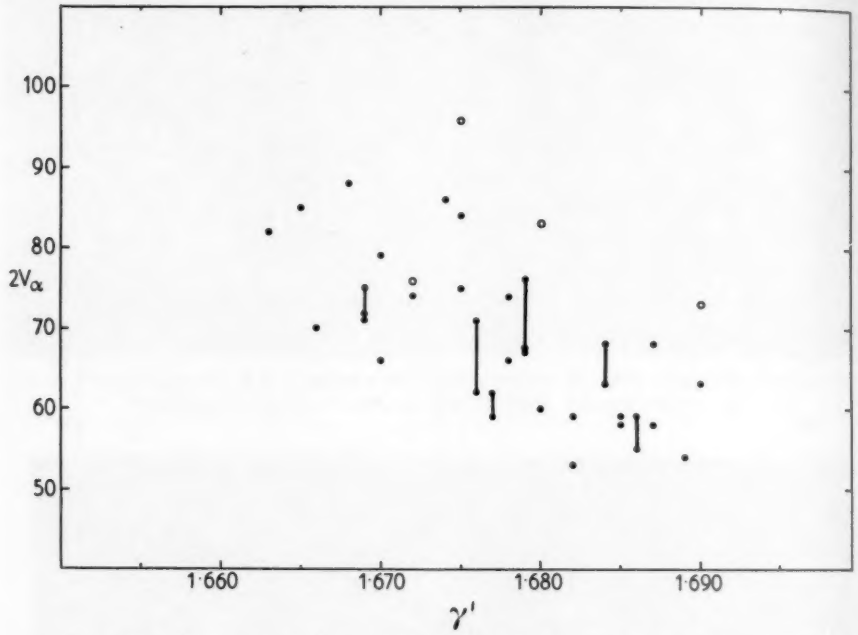

FIG. 8. Plot of $2V_\alpha$ against γ' for the hornblendes. Circles represent brown hornblendes.

the plagioclase permits the calculation of the approximate composition of the hornblende. The results for ten rocks which have more than 85 per cent hornblende plus plagioclase are as follows:[1]

BE 194: $(Si_{6\cdot3}Al_{1\cdot7}/Al_{0\cdot2}Fe^3_{0\cdot6}Ti_{0\cdot1}Fe^2_{1\cdot5}Mg_{3\cdot1})Ca_{1\cdot3}Na_{0\cdot6}K_{0\cdot1}$
BL 2516: $(Si_{6\cdot5}Al_{1\cdot5}/Al_{0\cdot4}Fe^3_{0\cdot3}Ti_{0\cdot1}Fe^2_{1\cdot2}Mg_{3\cdot5})Ca_{1\cdot5}Na_{0\cdot4}K_{0\cdot1}$
BL 2404: $(Si_{6\cdot3}Al_{1\cdot4}/Al_{1\cdot1}Fe^3_{0\cdot2}Ti_{0\cdot1}Fe^2_{1\cdot6}Mg_{2\cdot4})Ca_{1\cdot4}Na_{0\cdot6}K_{0\cdot1}$
BE 703: $(Si_{7\cdot2}Al_{0\cdot8}/Al_{0\cdot7}Fe^3_{0\cdot2}Ti_{0\cdot2}Fe^2_{1\cdot2}Mg_{2\cdot8})Ca_{1\cdot4}Na_{0\cdot7}K_{0\cdot2}$
RB 522: $(Si_{3\cdot4}Al_{1\cdot6}/Al_{0\cdot6}Fe^3_{0\cdot2}Ti_{0\cdot3}Fe^2_{1\cdot6}Mg_{2\cdot3})Ca_{1\cdot4}Na_{0\cdot5}K_{0\cdot2}$
BE 1126: $(Si_{7\cdot1}Al_{0\cdot9}/Al_{0\cdot4}Fe^3_{0\cdot3}Ti_{0\cdot0}Fe^2_{1\cdot2}Mg_{3\cdot5})Ca_{1\cdot6}Na_{0\cdot2}K_{0\cdot2}$
BE 1310: $(Si_{7\cdot0}Al_{1\cdot0}/Al_{0\cdot8}Fe^3_{0\cdot3}Ti_{0\cdot1}Fe^2_{0\cdot9}Mg_{3\cdot2})Ca_{1\cdot3}Na_{0\cdot7}K_{0\cdot1}$
BE 367: $(Si_{6\cdot8}Al_{1\cdot2}/Al_{0\cdot4}Fe^3_{0\cdot3}Ti_{0\cdot3}Fe^2_{2\cdot2}Mg_{2\cdot1})Ca_{1\cdot3}Na_{0\cdot5}K_{0\cdot5}$
BE 294: $(Si_{6\cdot5}Al_{1\cdot5}/Al_{0\cdot7}Fe^3_{0\cdot7}Ti_{0\cdot2}Fe^2_{1\cdot2}Mg_{2\cdot4})Ca_{1\cdot2}Na_{0\cdot3}K_{0\cdot4}$
BL 229: $(Si_{6\cdot8}Al_{1\cdot2}/Al_{0\cdot8}Fe^3_{0\cdot6}Ti_{0\cdot1}Fe^2_{1\cdot6}Mg_{2\cdot3})Ca_{1\cdot5}Na_{0\cdot5}K_{0\cdot2}$

[1] The unit of calculation is 15·5 cations which, within the range of common hornblende compositions considered, is approximately equivalent to 24 (O, OH, F). Corrections have been made for the small amounts of quartz, epidote, &c., and opaque ore (which is assumed to be two-thirds magnetite and one-third ilmenite).

It is notable that the two brown hornblendes calculated, RB 522 and BE 367, are both distinguished by their high titanium content. Correlation of brown coloration in some hornblendes with high titanium is well established (Deer, 1938, p. 74), as is also the tendency for brown hornblendes to be restricted to the higher-temperature metamorphic facies (Turner, 1948, p. 98; Miyashiro, 1958, p. 226). In the Connemara striped amphibolites brown hornblende always occurs with andesine or very calcic oligoclase, and often with clinopyroxene, while sillimanite is present in the associated pelites. The striped amphibolites of the Ballyconneely area in south-west Connemara (Fig. 2), which belong to the quartz–albite–epidote–almandine subfacies, never contain brown or green-brown hornblende but always a green or blue-green variety (e.g. BL 229 above). As a detailed study of the Connemara hornblendes is being undertaken by one of us (B. E. L.), further comment will be deferred for a later publication.

A very wide composition range, from An_6 to An_{56}, exists in the plagioclases. Albite is restricted to the Ballyconneely area, but for the rest of Connemara 84 per cent of the estimates of composition lie between An_{23} and An_{42} inclusive, the mean and frequency maximum of these determinations being coincident at An_{34}. The infrequent twinned plagioclases are not of a complex type, although the albite law is not always the dominant one. Zoning is rare, while partial decomposition to sericite is rather common, the plagioclase in three of the analysed rocks (JS 590, JS 626, and BE 1092) being completely sericitized.

The pyroxenes are colourless or pale green (never brown) stumpy prisms, averaging $0{\cdot}5\times0{\cdot}5\times1{\cdot}0$ mm in size, and are salites or ferrosalites of metamorphic origin. The clinopyroxene from an unanalysed specimen has the following properties: $2V_\gamma = 58°\pm1°$, $\beta = 1{\cdot}700\pm0{\cdot}002$; this corresponds approximately to a simple solid solution of 58 per cent diopside and 42 per cent hedenbergite (Hess, 1949, p. 634). Other $2V_\gamma$ measurements were as follows: BL 763A, 57°; BE 1145, 57½°; BL 1338, 57½°; BL 2515, 59°; RB 659, 57°; BE 1082, 56°; unanalysed specimen, 60°. These values are higher than those for the clinopyroxenes of basic igneous rocks (Hess, 1949). Clinopyroxene is distinctly concentrated in the clinopyroxene–plagioclase bands, where it sometimes tends to enclose the felspar poikiloblastically, being generally larger than the associated minerals. Only rarely does it occur as scattered grains amongst the hornblende; a sparse marginal growth of ragged or acicular pale bluish-green hornblende is rather common. Clinopyroxene is completely absent from the amphibolites of the Ballyconneely area.

The biotites are brown or red-brown, usually strongly orientated, and frequently altered to pale green pleochroic chlorite.

Garnetiferous striped amphibolite is most unusual in Connemara. Where present the garnets, in thin section, are pink, spongy, irregular in shape, and reach a diameter of about 1 mm. The properties of a garnet from an unanalysed hornblende schist BE 1164, believed to be closely comparable to that in BE 1092 (the only garnetiferous amphibolite analysed), are: $n = 1{\cdot}797\pm0{\cdot}003$, unit cell

TABLE 1

Chemical Analyses

For localities of the rocks see p. 347

	BL 2518	BE 194	BL 763A	BL 2516	BE 1145	BL 1338	BL 2404	JS 626	BE 1092	BL 2495	BE 703	RB 522	BL 2415	JS 590	BL 2494	BL 360
SiO_2	44·66	44·78	46·46	46·52	46·55	47·08	47·20	47·74	47·96	48·11	48·11	48·13	48·26	48·49	48·82	48·96
Al_2O_3	12·91	14·50	16·73	14·00	15·21	12·75	16·19	17·79	14·57	16·12	16·07	17·34	15·38	14·60	15·02	15·27
TiO_2	2·94	2·03	1·33	1·10	2·28	1·75	1·20	0·63	1·75	1·90	1·74	1·87	2·32	0·44	1·59	2·27
Fe_2O_3	3·21	5·90	2·56	2·42	3·15	4·08	2·71	1·38	4·40	2·63	2·90	2·51	4·70	1·68	2·59	5·11
FeO	13·93	9·17	8·06	8·00	8·31	8·43	10·35	7·47	10·20	9·10	7·97	8·18	10·43	7·27	8·39	9·18
MgO	10·02	8·94	8·37	12·88	6·50	9·55	8·12	7·81	6·18	5·56	7·97	6·58	5·47	10·67	8·09	5·13
CaO	6·09	7·21	9·60	9·78	11·18	10·20	7·94	9·41	9·10	9·83	8·35	8·09	6·45	10·51	9·96	7·17
Na_2O	1·95	3·80	3·36	2·45	3·36	2·70	3·60	1·76	1·56	3·37	3·55	3·95	4·25	1·88	2·65	4·30
K_2O	0·27	0·40	0·55	0·46	1·04	0·65	0·23	2·24	1·05	0·62	0·67	0·76	0·44	0·97	0·59	0·70
MnO	0·36	0·34	0·20	0·17	0·14	0 15	0·33	0·17	0·83	0·18	0·16	0·22	0·27	0·18	0·16	0·22
P_2O_5	0·30	0·29	0·16	0·08	0·32	0·16	0·04	0·04	0·44	0·20	0·19	0·24	0·36	0·04	0·18	0·32
H_2O	2·98	2·09	1·86	2·56	1·75	2·21	2·01	2·76	2·23	2·11	2·66	2·00	2·22	2·77	2·20	2·00
	99·62	99·45	99·64*	100·42	99·79†	99·84‡	99·92	99·20	100·27	99·73	100·34	99·87	100·55	99·50	100·24	100·63
Cr	12	130	300	1,080	160	560	210	320	180	85	300	255	32	305	410	37
Ni	24	50	210	465	115	340	92	115	84	54	122	72	18	205	120	32
Co	39	32	37	41	32	46	36	30	44	30	33	27	26	36	36	32
Cu	425	34	51	8	24	56	27	32	175	140	80	56	37	4½	140	9
Zr	210	130	100	60	180	145	185	34	150	125	115	170	185	31	100	210
Sc	50	30	23	25	25	23	37	33	30	32	25	35	36	27	38	45
Sr	110	275	630	275	670	350	250	400	180	615	315	370	90	200	370	165
Ba	220	94	350	140	360	230	140	475	245	265	70	270	240	240	150	180

	BL 214	BE 1126	BE 1310	BE 367	BL 2522	BL 2215	BL 165	BL 2387	BE 294	BL 2515	BL 229	BL 2227	BL 2506	BL 2419	BL 2503	RB 659	BE 1082
SiO_2	49·00	49·30	49·68	49·77	50·45	50·66	51·34	51·43	51·83	51·89	52·02	52·14	54·68	55·34	57·58	58·85	59·47
Al_2O_3	14·51	15·50	14·33	15·19	14·03	14·60	14·68	14·40	15·31	13·75	15·30	14·68	14·43	16·46	14·60	15·08	12·25
TiO_2	1·96	1·77	1·61	2·36	2·48	2·14	1·99	2·73	1·53	1·49	1·67	2·20	2·06	1·02	0·77	0·83	1·31
Fe_2O_3	4·92	3·06	4·39	1·88	5·54	5·09	5·37	7·06	4·50	2·82	3·89	5·24	4·91	2·44	2·56	1·92	1·85
FeO	8·13	8·05	6·59	9·90	9·22	10·10	9·03	8·50	6·80	6·20	7·90	8·65	8·10	8·04	4·91	3·49	3·94
MgO	6·34	7·79	8·68	5·04	4·89	3·74	4·40	4·17	5·98	6·25	5·25	3·68	3·50	4·95	5·38	2·96	5·72
CaO	6·86	6·96	6·66	7·60	6·56	8·71	6·91	5·17	6·66	9·98	5·79	7·02	4·02	6·04	5·15	7·74	9·06
Na_2O	4·04	4·05	4·66	4·30	4·32	2·58	3·85	4·16	2·90	4·22	5·53	4·43	5·55	3·69	5·33	2·68	3·02
K_2O	0·70	0·61	0·33	1·43	0·53	0·68	0·43	0·32	1·07	0·61	0·42	0·30	0·44	0·32	1·02	3·96	1·10
MnO	0·20	0·22	0·16	0·19	0·24	0·23	0·26	0·26	0·16	0·13	0·22	0·22	0·24	0·25	0·14	0·27	0·13
P_2O_5	0·21	0·25	0·22	0·35	0·29	0·27	0·27	0·35	0·19	0·21	0·25	0·39	0·45	0·09	0·10	0·24	0·18
H_2O	2·38	2·59	2·17	1·87	1·59	1·75	1·94	1·91	2·42	1·79	2·19	1·16	1·71	1·78	1·90	1·46	1·48
	99·25†	100·15	99·48	99·88	100·14	100·55	100·47	100·46	99·35†	99·34†	100·43	100·11	100·09	100·42	99·44	99·48	99·51
Cr	135	100	550	53	20	9	17	2	520	410	110	1	1	132	245	36	750
Ni	45	52	340	32	17	17	17	13	225	157	44	5½	7	65	115	27	285
Co	28	26	37	26	24	34	26	28	32	30	25	22	17	28	23	10	27
Cu	37	50	7	35	12	19	18	6½	46	21	44	12	8	190	39	60	135
Zr	140	145	165	180	160	175	140	260	105	115	255	215	400	120	165	280	80
Sc	44	29	20	26	38	43	42	38	26	26	35	33	26	28	27	11½	21
Sr	118	305	175	880	125	160	50	130	305	335	71	110	100	195	86	575	420
Ba	260	125	65	350	280	320	190	240	84	260	225	220	305	195	370	1,400	270

* $CO_2 = 0{\cdot}40$. † CO_2 present but not determined. ‡ $CO_2 = 0{\cdot}13$.

Localities of the rocks in Table 1

BL 2518 150 yd NW. of the NW. corner of Loughaunocary in NW. corner of 6-in. sheet 51, Co. Galway.
BE 194 South bank of Lough Fadda West at the SE end: one-fifth mile on a bearing of 355° from west end of Lough Croaghat. 6-in. sheet 36, Co. Galway.
BL 763A 780 yd east of the south point of Wood's Lough. 6-in. sheet 51, Co. Galway.
BL 2516 180 yd SSW. of the SW. corner of Lough Nabrucka: 870 yd on a bearing of 182° from Bulrush Island. 6-in. sheet 37, Co. Galway.
BE 1145 East end of Lough Fadda (by Ballinahinch). 6-in. sheet 36, Co. Galway.
BL 1338 240 yd SE. of the southern point of Nacoogarrow Lough (on 6-in. sheet 37). 6-in. sheet 51, Co. Galway.
BL 2404 400 yd NW. of Knockaunnabrone, Streamstown. 6-in. sheet 22, Co. Galway.
JS 626 190 yd west of the 1436 triangulation point, Knockaumbaum. 6-in. sheet 25, Co. Galway.
BE 1092 200 yd NE. of the north bank of Lough Aleen and 90 yd NNW. of the small unnamed lough. 6-in. sheet 36, Co. Galway.
BL 2495 1,000 ft at a bearing of 248° from 1436 triangulation point Tooreenacoona. 6-in. sheet 24, Co. Galway.
BE 703 On Derryadd West, 470 yd on a bearing of 348° from the northern edge of Lough Aderreen. 6-in. sheet 50, Co. Galway.
RB 522 1 mile and 60 yd on a bearing of 92° from the south point of Lough Beg. 6-in. sheet 39, Co. Galway.
BL 2415 20 yd NW. of north point of Lough Ascardaun. 6-in. sheet 49, Co. Galway.
JS 590 370 yd north of the T of Illion West, i.e. 990 yd on a bearing of 150° from the Knocknahillion 1993 triangulation point which is at the joining of the Illion West, Derryvoreada, and Poundcartuon townlands on 6-in. sheet 10, Co. Galway.
BL 2494 500 ft SE. of the last A of Tooreenacoona. 6-in. sheet 24, Co. Galway.
BL 360 150 yd WSW. of Callow Bridge. 6-in. sheet 49, Co. Galway.
BL 214 120 yd WNW. of the F of Foorglass on 6-in. sheet 49, Co. Galway.
BE 1126 Roadcutting on NW. side of the road about 50 yd NE. of Ballynahinch station. 6-in. sheet 36, Co. Galway.
BE 1310 330 yd at 265° from point where the small stream emerges from Knocknaferderg Lough. 6-in. sheet 36, Co. Galway.
BE 367 530 yd on a bearing of 155° from Ballynahinch station. 6-in. sheet 50, Co. Galway.
BL 2522 180 yd ESE. of bench mark 19·8, Maum, Errislannan promontory. 6-in. sheet 35, Co. Galway.
BL 2215 370 yd on a bearing of 85° from the northern point of Lough Rannaghaun. 6-in. sheet 49, Co. Galway.
BL 165 110 yd south of bench mark 21·8 on the Ballinaboy–Ballyconneely road. 6-in. sheet 35, Co. Galway.
BL 2387 North end of Lough Nasoodery on 6-in. sheet 49, Co. Galway.
BE 294 Exactly ½ mile due north of the northern end of the east branch of Lough Conga. 6-in. sheet 36, Co. Galway.
BL 2515 340 yd east of the eastern end of Loughyvangan, Garroman. 6-in. sheet 37, Co. Galway.
BL 229 750 yd on a bearing of 280° from the western end of Lough Nambrackkeagh, Ballyconneely. 6-in. sheet 49, Co. Galway.
BL 2227 450 yd east of the south point of Lough Drama, Dolan. 6-in. sheet 49, Co. Galway.
BL 2506 70 yd WSW. of bench mark 46·0 on the bridge between Beaghcauneen and Ardagh. 6-in. sheet 35, Co. Galway.
BL 2419 30 yd south of a quarry on the west side of the road, ¼ mile north of the Letterfrack Cross Roads. 6-in. sheet 23 Co. Galway.
BL 2503 150 yd east of bench mark 53·0 in Beaghcauneen. 6-in. sheet 35, Co. Galway.
RB 659 940 yd east of the centre of the east bank of Lough Beg. 6-in. sheet 39, Co. Galway.
BE 1082 75 yd south of the east end of the south bank of Lough Aleen. 6-in. sheet 36, Co. Galway.

TABLE 2

Niggli numbers and one-cation molecular norm

	BL 2518	BE 194	BL 763A	BL 2516	BE 1145	BL 1338	BL 2404	JS 626	BE 1092	BL 2495	BE 703	RB 522	BL 2415	JS 590	BL 2494	BL 360	BL 214
si	97	98	103	122	106	103	105	112	113	115	112	115	118	106	112	120	122
al	16·5	18·5	22	16·5	20·5	16·5	21	24·5	21	23	22	24·5	22	19	20	22	21
fm	64·5	56	47	56·5	43·5	53	51·5	45	51	43	48·5	44·5	50·5	51	48·5	47·5	50
c	14·5	17	23	21·5	27	24	19	23·5	23	25	21	20·5	17	24·5	24·5	19	18
alk	4·5	8·5	8	5·5	9	6·5	8·5	7	5	9	9	10·5	10·5	5·5	7	11·5	11
ti	4·85	3·27	2·23	1·68	3·90	2·87	2·00	1·13	3·09	3·43	3·03	3·36	4·25	0·67	2·74	4·19	3·65
p	0·28	0·26	0·15	0·07	0·31	0·15	0·04	0·03	0·44	0·20	0·19	0·24	0·37	0·03	0·17	0·32	0·22
k	0·08	0·06	0·10	0·11	0·17	0·14	0·08	0·46	0·31	0·11	0·11	0·11	0·06	0·25	0·13	0·10	0·10
mg	0·51	0·52	0·59	0·69	0·51	0·58	0·52	0·61	0·42	0·46	0·57	0·52	0·39	0·68	0·57	0·40	0·47
Q	—	—	—	—	—	—	—	—	3·71	—	—	—	—	—	—	—	—
Or	1·65	2·45	3·30	2·75	6·30	3·95	1·40	13·65	6·50	3·80	4·00	4·55	2·65	5·85	3·55	4·25	4·30
Ab	18·45	32·70	25·60	22·10	21·95	24·90	32·85	16·30	14·70	31·20	32·45	36·05	39·30	17·25	24·30	39·60	37·65
An	27·15	21·92	29·42	25·92	23·90	21·35	27·85	35·12	31·22	27·93	26·43	27·80	22·27	29·17	28·00	20·85	20·15
Ne	—	1·44	3·06	—	5·37	—	—	—	—	—	—	0·66	—	—	—	—	—
Di	2·32	10·60	14·48	17·88	24·76	23·76	9·60	10·24	10·84	16·96	11·68	9·28	6·84	19·12	17·16	10·96	11·16
Hy	33·64	—	—	—	—	4·98	0·82	6·50	24·74	3·88	3·50	—	11·78	12·84	13·34	7·66	13·78
Ol	8·31	21·09	19·17	27·13	10·44	13·86	22·83	15·72	—	10·26	16·02	16·98	8·05	13·26	7·77	6·42	4·35
Mt	3·54	6·34	2·73	2·53	3·37	4·38	2·88	1·48	4·83	2·83	3·03	2·67	5·07	1·80	3·26	5·47	5·34
Ilm	4·32	2·90	1·90	1·54	3·24	2·50	1·70	0·90	2·56	2·74	2·46	2·64	3·32	0·62	2·26	3·24	2·84
Ap	0·62	0·56	0·32	0·15	0·65	0·32	0·08	0·08	0·90	0·40	0·37	0·47	0·72	0·08	0·35	0·65	0·42
An%*	59·5	38	49	54	44	46	46	68	68	47	45	43	36	63	53·5	34·5	35
Fe/Mg in pyroxene and olivine	0·57	0·32	0·39	0·27	0·43	0·30	0·58	0·465	0·68	0·65	0·37	0·48	0·67	0·33	0·46	0·31	0·39

	BE 1126	BE 1310	BE 367	BL 2522	BL 2215	BL 165	BL 2387	BE 294	BL 2515	BL 229	BL 2227	BL 2506	BL 2419	BL 2503	RB 659	BE 1082
si	118[1]	118	126	129	130	140	138	137	130	136	139	159	153	168	188	176
al	22	20	22·5	21	22	18·5	23	24	20·5	23·5	23	25	27	25	28·5	21·5
fm	50	52	44	49·5	46·5	50	50·5	48	42	45·5	45	26	44·5	41·5	28·5	39
c	18	17	20·5	18	24	20	15	19	26·5	16	20	12·5	18	16	26·5	29
alk	10	11	13	11·5	7·5	11	11·5	9	11	15	12	16·5	10·5	17·5	16·5	10·5
ti	3·19	2·88	4·48	4·76	4·15	4·08	5·53	3·04	2·79	3·27	4·41	4·51	2·13	1·68	2·00	2·91
p	0·25	0·22	0·38	0·31	0·29	0·31	0·39	0·21	0·22	0·28	0·43	0·55	0·11	0·12	0·33	0·22
k	0·09	0·04	0·18	0·07	0·14	0·07	0·05	0·20	0·09	0·05	0·04	0·04	0·05	0·11	0·49	0·19
mg	0·56	0·59	0·43	0·38	0·31	0·36	0·33	0·49	0·56	0·45	0·32	0·33	0·46	0·57	0·49	0·64
Q	—	—	—	1·59	7·70	4·67	7·58	6·36	—	—	4·54	5·09	7·33	3·59	9·46	13·67
Or	3·70	2·00	8·65	3·25	4·20	2·60	1·95	6·60	3·70	2·50	1·85	2·65	1·95	6·10	24·05	6·65
Ab	37·00	42·40	37·40	40·05	24·30	35·80	35·80	27·15	38·65	50·30	40·95	51·15	33·80	48·35	24·75	27·80
An	22·72	17·45	18·35	17·90	27·52	22·33	20·52	26·75	17·12	15·92	19·87	13·55	27·97	13·05	17·92	17·06
Ne	—	—	1·28	—	—	—	—	—	—	—	—	—	—	—	—	—
Di	8·76	11·76	14·52	11·12	12·92	9·24	3·32	5·24	25·68	9·36	10·96	3·40	1·72	9·76	16·12	22·36
Hy	8·54	5·06	—	15·94	13·90	16·08	15·37	20·38	5·04	9·56	12·24	15·06	23·00	15·16	4·18	8·28
Ol	10·02	13·95	13·71	—	—	—	—	—	4·35	8·43	—	—	—	—	—	—
Mt	3·25	4·65	2·02	5·99	5·58	5·82	7·68	6·56	3·00	4·12	5·64	5·26	2·61	2·71	2·05	1·95
Ilm	2·52	2·28	3·36	3·56	3·12	2·88	3·96	2·20	2·12	2·36	3·16	2·94	1·46	1·08	1·18	1·88
Ap	0·50	0·45	0·70	0·60	0·55	0·55	0·70	0·40	0·43	0·50	0·80	0·90	0·17	0·20	0·47	0·35
An%	38	29	32	31	53	38	34·5	50	31	24	33	21	45	21	42	38
Fe/Mg in pyroxene and olivine	0·38	0·22	0·79	0·54	0·87	0·65	0·42	0·34	0·34	0·54	0·69	0·69	0·71	0·33	0·45	0·20

* Ne calculated as Ab.

TABLE 3

Modal analyses

	BL 2518	BE 194	BL 763A	BL 2516	BE 1145	BL 1338	BL 2404	JS 626	BE 1092	BL 2495	BE 703	RB 522	BL 2415	JS 590	BL 2494	BL 360	BL 214
Hornblende	59·8	63·0	49·4	79·5	48·0	39·1	73·0	60·0	55·4	58·3	55·0	55·3	48·4	73·5	69·8	47·8	54·9
Plagioclase*	19·0	32·0	36·5	19·7	32·0	35·8	25·0	—	—	31·8	34·5	42·2	40·9	—	24·5	42·7	40·4
Quartz	—	—	—	—	—	—	—	—	9·5	—	tr.	—	—	—	—	—	—
Clino-pyroxene	—	—	12·6	—	15·0	20·8	—	tr.	—	—	—	—	—	—	—	—	—
Chlorite	13·1	—	0·2	—	—	0·2	0·2	—	—	2·1	6·0	0·4	5·3	—	—	5·3	tr.
Sericite	—	—	—	—	—	—	—	40·0	25·8	—	—	—	—	26·5	—	—	—
Opaque	8·1	4·5	0·4	0·5	—	0·4	1·8	tr.	2·0	0·1	2·5	1·8	4·7	—	0·5	3·2	3·0
Biotite	tr.	—	—	—	—	—	—	—	—	1·2	—	tr.	—	—	—	tr.	—
Apatite	tr.	tr.	0·3	tr.	0·5	0·2	—	—	0·2	0·2	tr.	0·2	—	—	0·1	tr.	—
Sphene	—	—	0·6	0·2	4·5	2·4	—	—	1·0	6·2	tr.	0·1	tr.	—	5·2	—	0·9
Epidote	—	tr.	—	—	—	—	—	tr.	0·5	—	2·0	tr.	0·7	—	—	1·0	0·8
Calcite	—	—	tr.	—	—	tr.	—	—	—	—	—	—	—	—	—	—	—
Garnet	—	—	—	—	—	—	—	—	5·6	—	—	—	—	—	—	—	—
Microcline	—	—	—	—	—	—	—	—	—	—	—	—	—	—	—	—	—
An. of Plagioclase	42	29	41	42	29	36	27	—	—	—	40	36	—	—	—	—	—
γ' of hornblende.	1·675	1·679	1·680	1·668	1·687	1·676	1·675	1·665	1·684	1·678	1·675	1·672	1·682	1·663	1·670	1·685	1·679
$2V_\alpha$ of hornblende	96	67–76	83	88	68	62or71	84	85	63or68	74	75	76	53	82	79	58	67
Av. grain size in mm	0·1	0·2	0·2	0·2	0·2	0·1	0·2	0·03	0·1	0·08	0·2	0·08	0·02	0·1	0·1	0·03	0·1

	BE 1126	BE 1310	BE 367	BL 2522	BL 2215	BL 165	BL 2387	BE 294	BL 2515	BL 229	BL 2227	BL 2506	BL 2419	BL 2503	RB 659	BE 1082
Hornblende	44·0	57·0	49·0	48·8	56·1	43·8	36·8	48·0	36·6	49·9	41·6	20·9	35·7	35·5	12·1	25·5
Plagioclase*	46·0	38·0	45·0	41·0	40·8	36·9	51·2	37·5	50·0	47·1	45·6	66·7	60·9	48·6	40·7	37·0
Quartz	—	—	—	—				10·5	—	—					10·2	12·0
Clinopyroxene	—	—	1·0	—	—	—	—	—	11·6	—	—	—	—	—	15·8	23·0
Chlorite	5·5	—	—	3·9	—	0·2	5·0	—	—	—	—	7·1	0·7	2·3	—	—
Sericite	—	—	—	—	—	—	—	—	—	—	—	—	—	3·0	—	—
Opaque	4·5	5·0	2·0	5·4	2·3	1·9	7·0	3·5	1·0	3·0	1·9	5·3	2·6	0·8	0·4	0·5
Biotite	—	—	—	—	—	—	—	—	—	—	—	—	0·1	—	—	—
Apatite	tr.	tr.	0·5	—	0·2	—	tr.	tr.	0·1	—	—	—	tr.	—	0·3	tr.
Sphene	—	—	0·5	tr.	0·6	tr.	tr.	—	0·6	—	0·5	tr.	—	—	1·3	2·0
Epidote	—	tr.	tr.	0·9	—	17·2	—	0·5	tr.	—	10·5	—	—	9·8	0·3	tr.
Calcite	—	—	—	—	—	—	—	—	0·1	—	—	—	—	—	—	—
Garnet	—	—	—	—	—	—	—	—	—	—	—	—	—	—	—	—
Microcline	—	—	—	—	—	—	—	—	—	—	—	—	—	—	18·9	—
An. of Plagioclase	25	21–26	28	—	35	—	—	39	—	6–13	—	6	—	—	46	33
γ' of Hornblende	1·669	1·669	1·690	1·686	1·689	1·685	1·687	1·678	1·672	1·680	1·690	1·682	1·674	1·666	1·677	1·670
$2V_\alpha$ of hornblende	71	72–75	73	55or59	54	59	58	66	74	60	63	59	86	70	59–62	66
Av. grain size in mm	0·1	0·08	0·1	0·05	0·08	0·03	0·02	0·2	0·08	0·03	0·05	0·02	0·05	0·03	0·1	0·1

* Plagioclase is often partly altered to sericite and sometimes also to saussurite.

edge $a = 11{\cdot}645 \pm 0{\cdot}005$ Å, MnO = 10·25 wt per cent (i.e. wt per cent spessartite = 23·9). Calculation of its approximate composition gives (mol. prop.) almandine 50 per cent, grossularite 27 per cent, and spessartite 23 per cent. This is exceptionally rich in the spessartite component because, of the twenty garnets from amphibole schists compiled by Wright (1938, pp. 440–1), sixteen have spessartite contents below 5 per cent and the highest amount is only 12·5 per cent. BE 1092 (Table 1) has easily the highest MnO content (0·83 per cent) of all the analysed samples (average MnO = 0·22 per cent), which supports the belief in the spessartite-rich nature of the garnet of BE 1092 and also suggests that garnet probably formed only in those Connemara amphibolites rich in MnO.

Not infrequently the epidote-rich lenses, which are largely replacive in origin, also contain some garnet in irregular masses up to about 5 cm across, poikiloblastically enclosed by meagre replacive pistacite. These garnets, however, are grandites; one example, BE 1106, has $n = 1{\cdot}77 \pm 0{\cdot}01$ and $a = 11{\cdot}868 \pm 0{\cdot}0\,05$ Å, corresponding according to Sriramadas (1957) to 65–75 per cent grossularite, 15–25 per cent andradite, and 5–15 per cent pyralspite. It is suggested that this garnet formed when the supply of water for epidote formation was locally insufficient. Grandites in calcic lenses associated with amphibolites are also recorded by Miyashiro (1958, p. 244).

Small ellipsoidal sphenes occur either as isolated grains, in layers parallel to the schistosity, or mantling grains of iron ore. Sphene is especially common in the clinopyroxene–plagioclase bands. Ilmenite and magnetite are the chief opaque minerals, although pyrite is also common. In the striped pyroxene-bearing rocks it is usual to find the iron ore restricted to the pyroxene-free parts. Quartz is evenly distributed in the form of irregular, somewhat elongated, strained grains, of a size comparable to the associated plagioclase. Very small amounts of carbonate, probably calcite, are sometimes present in the clinopyroxene–plagioclase bands.

DISCUSSION

General

Much discussion has recently taken place concerning the differences, particularly chemical differences, between para- and ortho-amphibolites (Engel & Engel, 1951; Lapadu-Hargues, 1953; Poldervaart, 1953; Eckelmann & Poldervaart, 1957; Wilcox & Poldervaart, 1958), but underlying much of the analytical work has been the basic assumption that amphibolites are metasedimentary because they are banded or occur as thin bands within genuine metasediment. Thus, Poldervaart (1953, p. 268) states that 'the so-called "feather amphibolites" are usually of sedimentary origin', and Wilcox & Poldervaart (1958, p. 1363) say that para-amphibolites show 'intimate interlayering with other rock types and lack of uniformity in the hornblendic bands, whereas the latter (ortho-amphibolites) are more homogeneous'. Banding can occur in a rock because of original sedimentation differences or as a result of metamorphic segregation or shearing of one rock into another. We believe that the striping of the Conne-

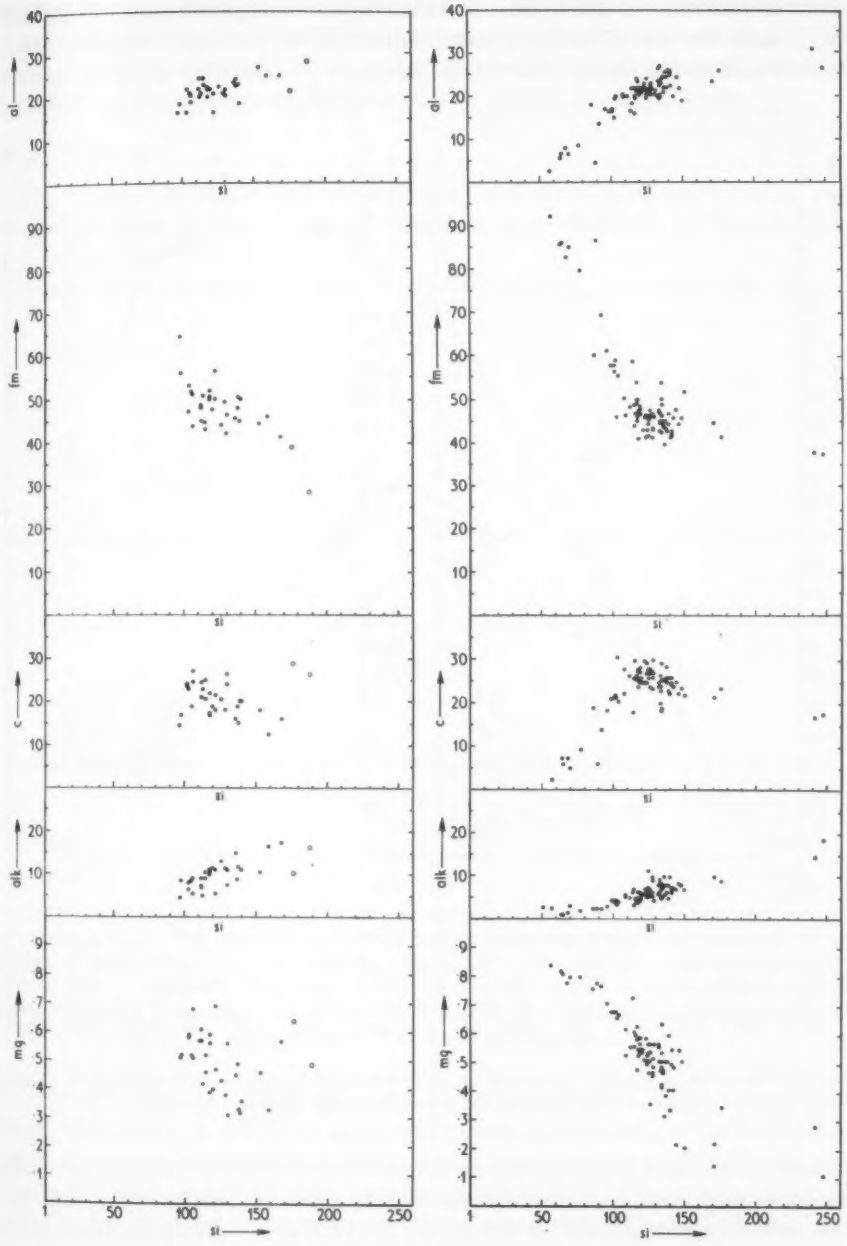

FIG. 9. Plot of *al*, *fm*, *c*, *alk*, and *mg* against *si* for the striped amphibolites (left column) and for the Karroo dolerites (right column). Data from Walker & Poldervaart (1949). Circles represent BE 1082 and RB 659.

mara amphibolites is due to intense metamorphic segregation along the schistosity planes, the only *S* surface present. Although the rocks are folded by major folds which extend for distances of not less than 20 miles (Fig. 2), the stripes are

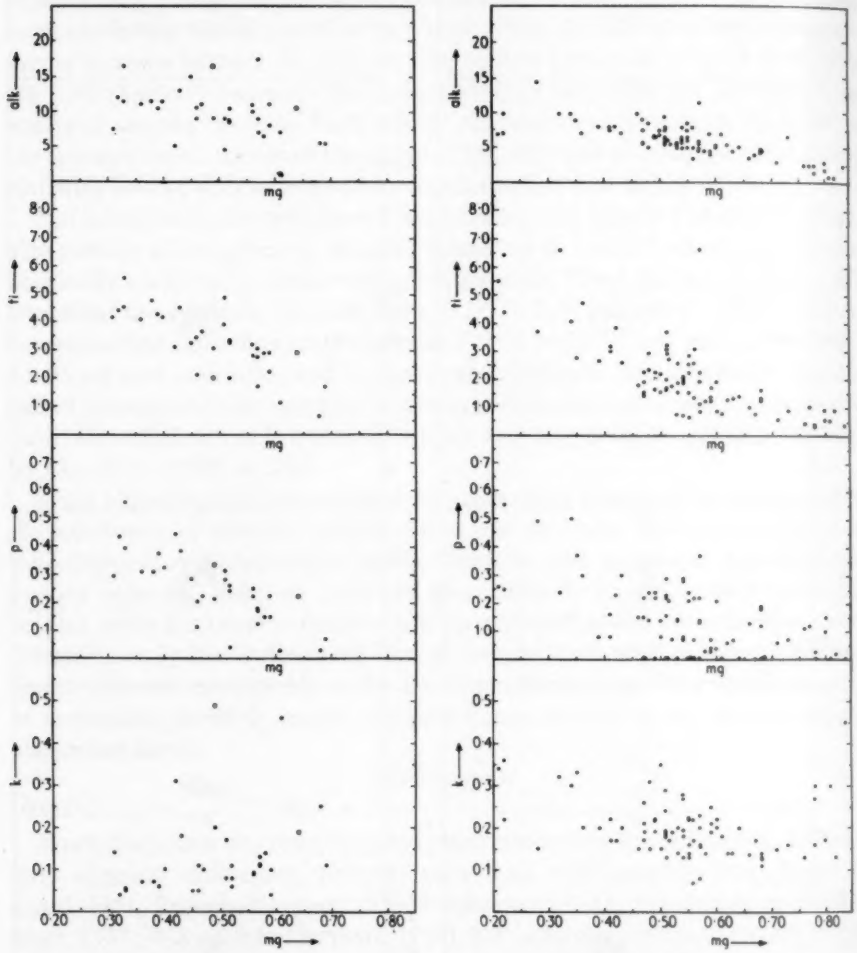

FIG. 10. Plot of *alk*, *ti*, *p*, and *k* against *mg* for the striped amphibolites (left column) and the Karroo dolerites (right column). Circles represent BE 1082 and RB 659.

scarcely ever folded, implying that deformation took place by means of slip along the schistosity. Such conditions would be favourable for metamorphic segregation to form bands parallel to the schistosity and, where gradation takes place from striped to unstriped rocks, this is interpreted as showing a change from suitable to unsuitable conditions for segregation. Small masses of amphibolite enclosed in quartzite or pelite are generally boudinaged and unstriped, indicating

that tectonic and metamorphic, rather than sedimentary, differences control the presence or absence of striping. The importance of segregation processes in these rocks is further suggested by the pegmatitic quartz–felspar material, which is frequently margined by amphibolite relatively enriched in hornblende.

Major elements

The variation in major-element composition of the striped amphibolites can be seen in Table 1. The average composition on a water-free basis, excluding

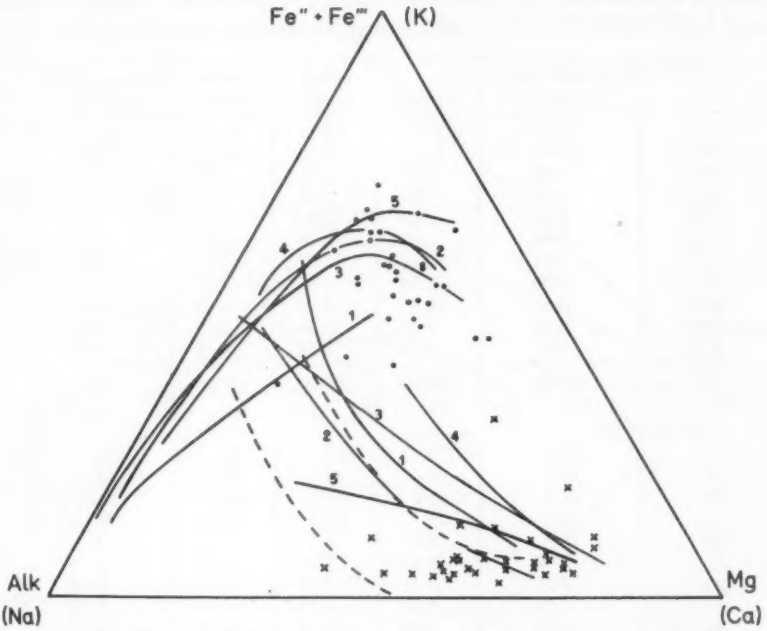

FIG. 11. Ternary plot of Mg: Fe″ + Fe‴: *Alk* (dots) and Ca: K: Na (crosses) by weight for the striped amphibolites. Lines 1–6 are some well-defined igneous rock series from Nockolds & Allen (1954–6), as follows: 1. Lassen Peak lavas (calc–alkaline), 1954, p. 107. 2. Scottish alkali basalt–trachyte trend, 1954, p. 246. 3. Polynesian alkali basalt–trachyte trend, 1954, p. 248. 4. Karroo dolerites (main trend), 1956, p. 36. 5. Hakone P lavas (tholeiitic), 1956, p. 35. The dashed lines enclose the Ca: K: Na field of spilites, after Battey (1956, p. 59).

RB 659, BE 1082, JS 590, JS 626, and BE 1092 (see below), is compared with Nockolds's (1954, p. 1021) averages for the three main basaltic types in Table 4, and the essential similarity is obvious. The average striped amphibolite can be matched in every respect by any number of analyses of alkali olivine basalt or andesine basalt in the literature; some of the Hawaiian 'andesine andesites' are particularly close.

The major elements (Fig. 9) show trends of increasing *al* and *alk* and decreasing *fm* with increasing *si*, similar to that of the Karroo dolerites (Walker &

Poldervaart, 1949). Although these trends could have resulted from a soda felspar-producing metasomatism, the fall of *mg* with increase in *si* suggests that magmatic differentiation has, in fact, played an important part. Some movement of alkalis clearly has taken place in three of the samples, namely JS 626, JS 590, and BE 1092, all hornblende–sericite (after plagioclase) schists, which must have suffered late K metasomatism with replacement of Na by K, while the

TABLE 4

Average composition of Connemara striped amphibolite, Normal Tholeiite, Normal Alkali Basalt, 'Central' Basalt, and 200 amphibolites, on a water-free basis

	Connemara striped amphibolite	*Tholeiite*	*Alkali basalt*	*Central basalt*	*Average of 200 amphibolites*
SiO_2	50·73	51·33	46·14	51·56	50·3
Al_2O_3	15·29	14·21	14·75	18·12	15·7
TiO_2	1·90	2·05	2·65	1·10	1·6
Fe_2O_3	3·94	2·91	3·18	3·42	3·6
FeO	8·74	9·09	8·80	5·73	7·8
MgO	6·69	6·40	9·46	6·04	7·0
CaO	7·73	10·52	10·82	10·12	9·5
Na_2O	3·90	2·25	2·65	2·27	2·9
K_2O	0·61	0·83	0·96	0·82	1·1
MnO	0·22	0·18	0·20	0·16	0·2
P_2O_5	0·25	0·23	0·39	0·16	0·3
	100·00	100·00	100·00	100·00	100·0
Niggli numbers					
si	121	123	97	126	118
al	21·5	20	18·5	26	21·5
fm	48·5	46·5	50·5	40·5	46·5
c	20	27	24·5	26·5	24
alk	10	6·5	6·5	7	8
ti	3·39	3·67	4·18	2·03	2·18
p	0·26	0·23	0·34	0·16	0·28
k	0·09	0·20	0·19	0·19	0·20
mg	0·49	0·49	0·59	0·55	0·53

Average amphibolite from Poldervaart (1955, p. 136).
Basalt averages from Nockolds (1954, p. 1021).

existence of over 20 per cent of microcline in the stripes of RB 659 also indicates movement of K. Systematic decrease in *mg* is probably the most reliable criterion of differentiation in basic magmas, and Fig. 10 is strong support for the view that the Connemara striped amphibolites, showing trends closely comparable to those of the Karroo dolerites, are of magmatic origin. The fact that the plots on the *alk* against *si* diagram (Fig. 9) lie consistently above those of the Karroo dolerites indicates alkaline tendencies, but this is due entirely to the very high soda contents of the amphibolites, the mean potassium content lying below that of all three of the basalt types (Table 4). On a triangular Ca : Na : K plot (Fig. 11), the amphibolites tend to fall in the spilite field, so that in fact the affinities of the amphibolites may be more with the spilites than the alkali basalts. Although a

few points scatter widely on the *alk* against *mg* plot (Fig. 10), there is in fact a good smooth trend of increasing *alk* (dominantly soda since most *k* values are below 0·2) with decreasing *mg*, and this is regarded as indicating that the high soda of the rocks is essentially a product of magmatic differentiation, introduced soda being unlikely to correlate with *mg*. The scatter of the points on the Fe:Mg:*Alk* plot (Fig. 11) is probably due to the combined effects of igneous cumulation, metamorphic differentiation, and the movement of alkalis.

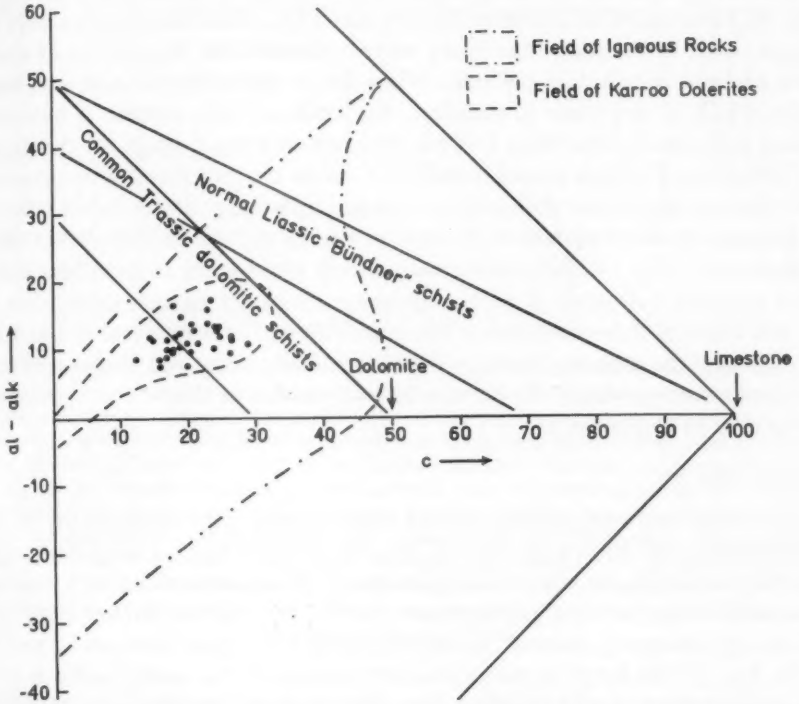

FIG. 12. Plot of *al–alk* against *c* for the striped amphibolites, after Niggli (1954, p. 24).

Wilcox & Poldervaart (1958, p. 1363) have suggested that some amphibolites might have been formed from metamorphosed dolomitic greywackes. Although the points on the *al–alk* against *c* diagram (Fig. 12) lie within the area of overlap of sedimentary and igneous rocks, it is important to note that they show no trend parallel to the line joining mixtures of clay and dolomite and, indeed, if any trend exists at all, it is more likely to be approximately at right angles to the clay–dolomite line, i.e. parallel to the trend found in igneous rocks, such as the Karroo dolerites.

It is highly significant that, except for JS 626, JS 590, and BE 1092, which are believed to have been late potash-metasomatized on account of the sericitization

of their plagioclase, none of the rocks has a k-value exceeding 0·20, whereas mixtures of clay and dolomite possess very much higher k-values ($> 0{\cdot}50$). Moreover, the Connemara pelites are quite rich in potassium and poor in sodium (Leake, 1958), the average k of seventeen analyses being 0·70 compared with Shaw's (1956, p. 928) average pelite which has $k = 0{\cdot}55$, so there is no evidence to suggest that the Connemara pelites were of greywacke origin with abundant detrital albite. In addition, although some pelites have TiO_2 contents of about 2 per cent, pelites are generally appreciably poorer in titanium; e.g. Shaw's (op. cit.) average pelite contains 0·82 per cent TiO_2.[1] The Connemara pelites are rather richer in titanium than many pelites; nevertheless, the average of seventeen analyses is only 1·35 per cent. When this is diluted by mixture with dolomite, which is very poor in titanium, the resultant TiO_2 content is obviously going to be much lower than 1·90 per cent, which is the average for the striped amphibolites. The high titanium and low k-values are therefore not in agreement with the hypothesis that the rocks are a metamorphosed pelite–dolomite mixture.

Because of the composition of the Connemara striped amphibolites a metasedimentary origin would require sodium-rich greywackes to have been mixed with iron-rich dolomites. If such a curious sedimentary mixture exists, then we do not know of it, and because of the quite different environments in which the two parts of the supposed mixture characteristically occur, the existence of such a mixture seems unlikely. So far as is known, neither of these rock types occurs separately in Connemara.

Minor elements

The range and mean values of each trace element determined in the striped amphibolites are shown on Fig. 13. Cr, Ni, and Cu show a large dispersion, but the remainder are not so widely scattered. Histograms of frequency against abundance show marked positive skew for Cr, Ni, and Cu, while Co, Zr, and Ba are approximately normal. An excellent coherence exists between Cr and Ni.

In Fig. 13 the range in minor-element content of the amphibolites is compared with that in basalts, shales, and carbonate rocks. In every case except Sc, both the arithmetic and geometric means of the striped amphibolites lie within the possible range of compositions for shale–carbonate rock mixtures. The mean Sc content exceeds that of any likely shale–dolomite mixture, although it must be remembered that the available data on Sc in sediments are scarce. The high contents of Cr and Ni in some of the amphibolites are noteworthy; in BL 2516 both elements exceed by a factor of two the maximum content of those

[1] Some typical TiO_2 contents are: average Mississippi silt, 0·6; fifty-one Palaeozoic shales, 0·8; average blue mud, 0·8; average shale, 0·7; seventy-eight clays from Norway, 0·8; average terrigenous mud, 1·4; twenty-seven Mesozoic and Cenozoic shales, 0·5; average mica schist from Finland, 0·3; twenty-two slates, Clarke, 0·9; 103 mica schists, Poldervaart, 1·0; sixty-one slates, Poldervaart, 0·7; thirty-three Precambrian slates, 0·8; fifty phyllites, Poldervaart, 1·1; all from Poldervaart, 1955, pp. 135–6. Average of 139 Scottish and Alpine pelitic and semi-pelitic schists computed by Leake (1958), 1·20.

elements possible in shale–dolomite combination. On the other hand, none of the eight trace elements examined in the amphibolites exceeds the span of possible compositions of basaltic rocks. Indeed, the mean values are closely comparable to the average basic igneous rock indicated by a cross on Fig. 13.

Figs. 14 and 15 show that where there is a pronounced trend for trace-element content against *mg*, as for Cr, Ni, and Co/Ni, the trend for the amphibolites is practically identical to that for the Karroo dolerites (Nockolds & Allen, 1956).

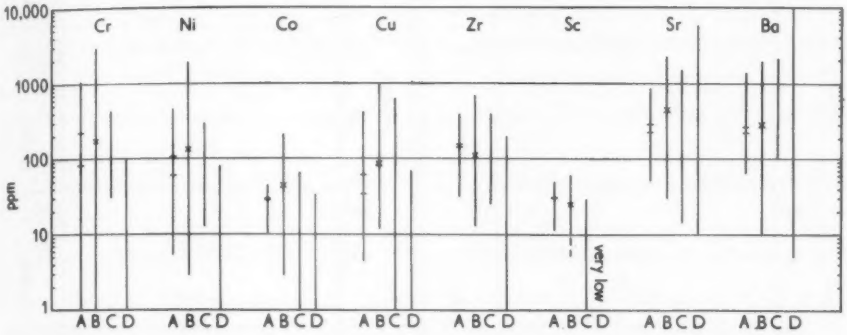

FIG. 13. The range in trace-element composition of the striped amphibolites (A), compared with the range in basalts (B), shales (C), and limestones and dolomites (D). Ticks on the amphibolite line represent the arithmetic and geometric means, the former in every case being higher than the latter. The average basic igneous rock is indicated by a cross, these values being obtained from Turekian (1956) for Cr, Ni, and Cu; Degenhardt (1957) for Zr; Turekian & Kulp (1956) for Sr; and Green (1959) for Co, Sc, and Ba. The abundance ranges were compiled from the following sources. For basalts: Amstutz (1953), Cornwall & Rose (1957), Degenhardt (1957), Fairbairn, Ahrens, & Gorfinkle (1953), Nockolds & Allen (1954–6), Patterson (1951), Patterson & Swaine (1955), Turekian & Kulp (1956), Wager & Mitchell (1953), and Young (1957). For shales: Krauskopf (1955), Macpherson (1958), Mohr (1959), Ostrom (1957), Rankama & Sahama (1950), Shaw (1954), and Turekian & Kulp (1956). For carbonate rocks: Hurst & Nicholls (1958), Krauskopf (1955), Ostrom (1957), Pugh (1956), and Rankama & Sahama (1950).

Zr increases with decreasing *mg* in both rock series, but for given *mg* values Zr is more abundant in the amphibolites. The behaviour of Sc is rather different for the two groups, but the slight increase over the comparable range of *mg* values is found for other igneous rock series, e.g. the Skaergaard intrusion (Wager & Mitchell, 1951). Co, Sr, and Ba cannot be said to define a trend in the amphibolites. When trace elements are plotted against *mg* for sediments, e.g. the Littleton pelites (Shaw, 1956, p. 922), which span the range from $mg = 0{\cdot}24$ to $0{\cdot}47$ (Figs. 14, 15), there is no systematic variation, except possibly for Zr.

Thus the minor-element content of the striped amphibolites is indistinguishable from that of a series of basic igneous rocks and very different from that of common shales, limestones, or dolomites, or any combination of these. Similar conclusions, based on trace-element analyses, were made for some New Zealand green schists by Taylor (1955).

Origin of the amphibolites

A sedimentary origin for the Connemara striped amphibolites raises numerous chemical difficulties which have been discussed above. In addition, both the lack of gradation between amphibolite and any metasediment and the general absence

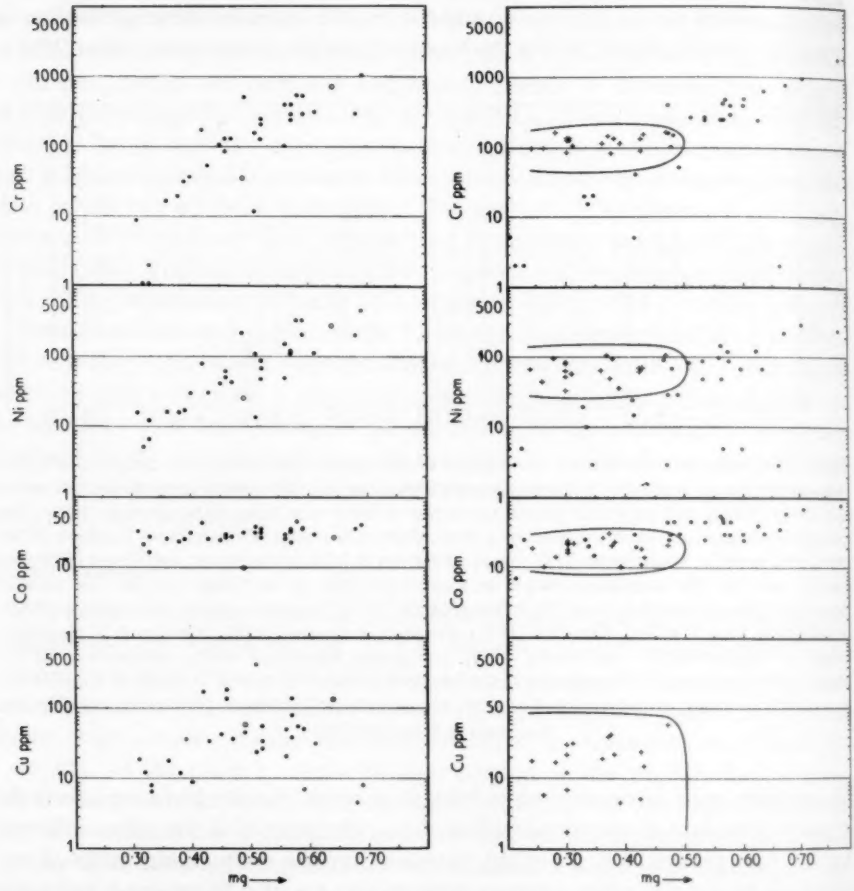

FIG. 14. Plot of Cr, Ni, Co, and Cu against *mg* for the striped amphibolites (left column) and the Karroo dolerites (Nockolds & Allen, 1956) (right column, dots) and the Littleton pelites (Shaw, 1956) (right column, crosses, ringed). BE 1082 and RB 659 are plotted as circles.

of carbonate in the amphibolites (despite the fairly common occurrence of marble in Connemara) fail to support any supposed origin by mixture of sediments. On the other hand, the remarkable coincidences in location on the *mg* plots, and to a lesser degree the *si* plots, together with the agreement in nature and degree of the trends for many of the elements between the amphibolites and a series of igneous rocks, the Karroo dolerites, can be regarded as

a clear indication of the igneous origin of the striped amphibolites. No evidence has been found to indicate whether these rocks formed lavas, tuffs, or minor intrusions. The field association of striped amphibolite and quartzite is probably the result of isoclinal folding causing repetition of a simple original sequence.

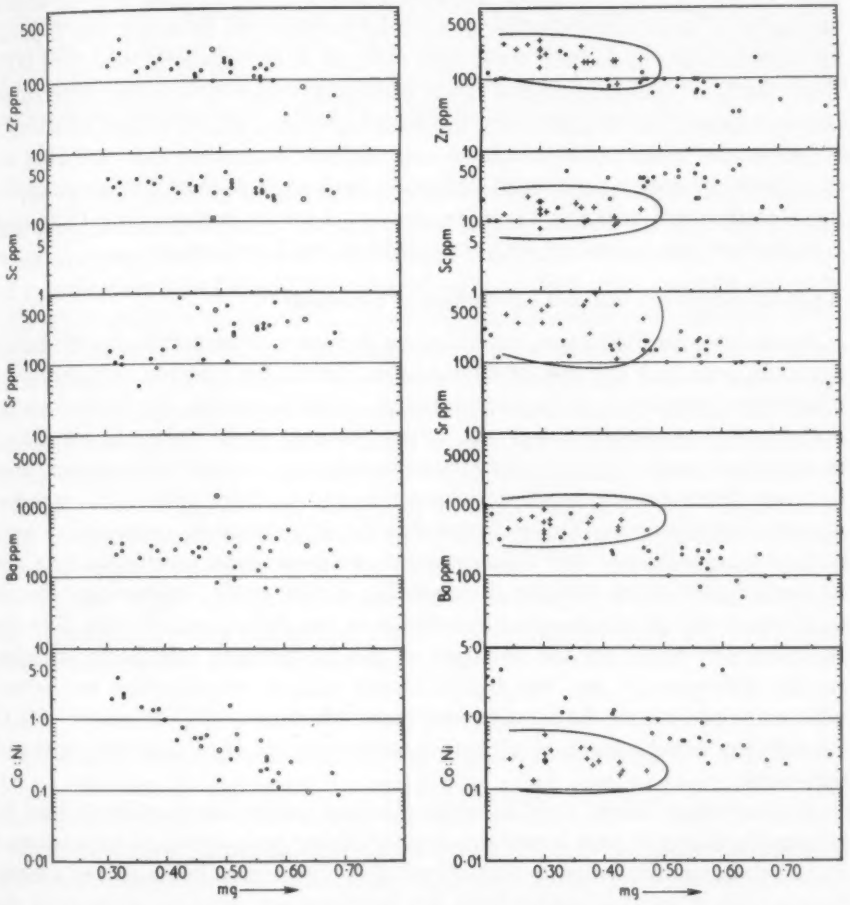

FIG. 15. Plot of Zr, Sc, Sr, Ba, and Co/Ni against *mg* for the striped amphibolites (left column) and the Karroo dolerites (right column, dots) and the Littleton pelites (right column, ringed crosses). BE 1082 and RB 659 are plotted as circles.

To judge from the norms (Table 2), the original rocks would appear to have been labradorite or basic andesine–olivine–augite–ilemenite assemblages or, especially in the Ballyconneely area, andesine–orthopyroxene–augite–ilmenite assemblages.

It is possible that metamorphic segregation and shearing of thin layers of rock into one another may have resulted in some ortho-amphibolites in other

parts of the world being considered metasedimentary, and consequently it is hardly surprising that no chemical differences are apparent between these rocks and known ortho-amphibolites. It is our view that the chemistry of the majority of amphibolites would reveal their origin and judging from Poldervaart's (1955, p. 136) average of 200 amphibolites (Table 4), most of these would appear to be ortho-amphibolites. It must be pointed out, however, that if para-amphibolites are to include mafic tuffs (Wilcox & Poldervaart, 1958, p. 1363), then clearly no chemical criteria can at present be expected to reveal differences between these para-amphibolites and ortho-amphibolites. It is not, of course, suggested that para-amphibolites do not exist. In Connemara there are what we consider to be proven para-amphibolites, because some of them contain graphite, have gradational contacts to pelite, possess *k*-values greater than 0·50, and contain less than 1 per cent TiO_2 (unpublished work by Leake).

Regional compositional and mineralogical variations

Apart from the differences in conditions of metamorphism between the Ballyconneely area and the rest of Connemara, there exist notable compositional differences between the striped amphibolites of the two areas. The Ballyconneely rocks have consistently lower *mg* values (average 0·39) than the remaining samples (average 0·54); only three out of the eleven from the Ballyconneely area have *mg* values greater than 0·42, whereas no sample from outside this area has *mg* less than this figure. This indicates that the Ballyconneely amphibolites were derived from a slightly later differentiate of the magma responsible for the Connemara amphibolites, and this is interesting in view of the independent deduction, based on the upside-down succession in the Ballyconneely area, that the Ballyconneely rocks are the youngest of the Connemara schists. In addition to the difference in *mg*, the Ballyconneely striped amphibolites are somewhat more sodic than the average rock from other parts of Connemara—Na_2O = 4·39 per cent and *alk* = 12·5 compared with Na_2O = 3·34 per cent and *alk* = 8·5.

Although high values (> 0·5) of the quotient-normative diopside divided by normative diopside plus hypersthene plus olivine (calculated as hypersthene) appear to be necessary for the occurrence of clinopyroxene in the striped amphibolites, this mineral is absent from the Ballyconneely area on account of the lower grade of metamorphism in that region, rather than because this number is not exceeded.

In the Scottish epidiorites, almandine appears at the same time as it does in the associated pelites (Wiseman, 1934, p. 378), that is, in rocks of the quartz–albite–epidote–almandine subfacies. The low *mg* values, or alternatively the high ratios of FeO:MgO, of the Ballyconneely amphibolites make them well suited for almandine formation (of six analyses of Highland epidiorites (Pantin, 1956, p. 61; Wiseman, 1934, p. 379) almandine-rich garnet occurs in rocks with *mg* values of 0·26, 0·33, and 0·47 and is absent from rocks with *mg* values of

0·60, 0·46, and 0·43), but almandine has not generally been produced in the Connemara amphibolites. This general absence of almandine in the basic rocks, while partly of course due to the high *mg* figures, is probably due to the Connemara metamorphisms being of a low-pressure type. Shidô (1958, p. 210) has pointed out that high pressures will favour garnet in amphibolites while lower pressures will favour amphibole. This view of the Connemara metamorphisms is in agreement with the virtual absence of kyanite in Connemara and with the widespread occurrence of cordierite, sillimanite, and andalusite.

CONCLUSIONS

The striped character of the rocks is believed to be purely the result of tectonic and metamorphic processes and not related to any original feature. The amphiboles are common hornblendes, showing a consistent relationship of increase of γ' and decrease of $2V$ with decrease of *mg*, and the brown varieties are probably significantly richer in titanium than the green varieties and occur only in the higher metamorphic facies. The plagioclases show a wide composition range from albite to sodic labradorite but, in most of Connemara, tend to concentrate about sodic andesine. The clinopyroxenes are metamorphic salites and ferrosalites, while garnet, which is only rarely present, is remarkable for its high spessartite content (e.g. 23 per cent) compared with most garnets from amphibolites. The major and minor element content of the striped amphibolites, together with their variation trends, have been shown to be similar to those of a differentiating basaltic magma, like that of the Karroo dolerites. The low *k*, high *ti*, lack of trend on an *al–alk* against *c* plot, and the abundance of certain trace elements are regarded as being inconsistent with a sedimentary origin for the striped amphibolites unless it be that of a mafic tuff.

ACKNOWLEDGEMENTS

We wish to thank Mr. R. Bradshaw of Bristol for supplying two samples and Mr. J. Starkey of Liverpool for permitting us to include two unpublished chemical analyses. The first author is indebted to Dr. S. R. Taylor for initial instruction in spectrographic analysis, and gratefully acknowledges the receipt of a D.S.I.R. maintenance award during which part of the work was carried out.

REFERENCES

AHRENS, L. H., 1954. *Quantitative spectrochemical analysis of silicates*. London: Pergamon Press.

AMSTUTZ, G. C., 1953. Geochemistry of Swiss lavas. *Geochim. et Cosmoch. Acta*, **3**, 157–68.

BATTEY, M. H., 1956. The petrogenesis of a spilitic rock series from New Zealand. *Geol. Mag. Lond.* **93**, 89–110.

CHAYES, F., 1956. *Petrographic modal analysis*. New York: John Wiley & Sons.

CORNWALL, H. R., & ROSE, H. J., 1957. Minor elements in Keweenawan lavas, Michigan. *Geochim. et Cosmoch Acta*, **12**, 209–24.

DEER, W. A., 1938. The composition and paragenesis of the hornblendes of the Glen Tilt complex, Perthshire. *Miner. Mag.* **25**, 56–74.

DEGENHARDT, H., 1957. Untersuchungun zur geochemischen Verteilung des Zirconiums in der Lithosphäre. *Geochim. et Cosmoch. Acta*, **11**, 279–309.

ECKELMANN, F. D., & POLDERVAART, A., 1957. Geologic evolution of Beartooth Mountains, Montana and Wyoming, Part 1: Archean history of the Quad Creek area. *Bull. geol. Soc. Amer.* **68**, 1225–62.

ENGEL, A. E. J., & ENGEL, C. G., 1951. Origin and evolution of hornblende–andesine amphibolites and kindred facies (Abstract). Ibid. **62**, 1435.

FAIRBAIRN, H. W., AHRENS, L. H., & GORFINKLE, L. G., 1953. Minor element content of Ontario diabase. *Geochim. Acta*, **3**, 34–46.

GREEN, J., 1959. Geochemical table of the elements for 1959. *Bull. geol. Soc. Amer.* **70**, 1127–84.

HESS, H. H., 1949. Chemical composition and optical properties of the common clinopyroxenes, Part 1. *Amer. Min.* **34**, 621–66.

HURST, D. M., & NICHOLLS, G. D., 1958. Techniques in sedimentary geochemistry: (1) separation of the detrital and non-detrital fractions of limestones. *J. sed. Pet.* **28**, 468–81.

KRAUSKOPF, K. B., 1955. Sedimentary deposits of rare metals. *Econ. Geol.*, 50th anniv. vol., Part 1, 411–63.

LAPADU-HARGUES, P., 1953. Sur la composition chimique moyenne des amphibolites. *Bull. Soc. géol. Fr.*, sér. 6, **3**, 153–73.

LEAKE, B. E., 1958. Composition of pelites from Connemara, Co. Galway, Ireland. *Geol. Mag. Lond.* **95**, 281–96.

MACPHERSON, H. G., 1958. A chemical and petrographic study of Precambrian sediments. *Geochim. et Cosmoch. Acta*, **14**, 73–92.

MIYASHIRO, A., 1953. Progressive metamorphism of calcium-rich rocks of the Gosaisyo–Takanuki district, Abukuma plateau, Japan. *Jap. J. Geol. Geog.* **23**, 81–107.

—— 1958. Regional Metamorphism of the Gosaisyo–Takanuki district in the central Abukuma Plateau. *J. Fac. Sci. Univ. Tokyo*, Sec. II, **11**, 219–72.

MOHR, P. A., 1959. A geochemical study of the shales of the Lower Cambrian Manganese Shale Group of the Harlech Dome, North Wales. *Geochim. et Cosmoch. Acta*, **17**, 186–200.

NIGGLI, P., 1954. Rocks and mineral deposits. W. H. Freeman & Co.: San Francisco.

NOCKOLDS, S. R., 1954. Average chemical composition of some igneous rocks. *Bull. geol. Soc. Amer.*, **65**, 1007–32.

—— & ALLEN, R., 1954–6. The geochemistry of some igneous rock series, Parts 1–3: *Geochim. et Cosmoch. Acta*, **4**, 105–42; **5**, 245–85; **9**, 34–57.

OSTROM, M. E., 1957. Trace elements in Illinois Pennsylvanian limestones. *Illinois State geological Survey*, Circular 243.

PANTIN, H. M., 1956. The petrology of the Ben Vrackie epidiorites and their contact rocks. *Trans. geol. Soc. Glasg.* **22**, 48–79.

PATTERSON, E. M., 1951. A petrochemical study of the Tertiary lavas of NE. Ireland. *Geochim. et Cosmoch. Acta*, **2**, 283–99.

—— & SWAINE, D. J., 1955. Petrochemical study of Tertiary tholeiitic basalts: middle lavas of the Antrim Plateau. *Geochim. et Cosmoch. Acta*, **8**, 173–81.

POLDERVAART, A., 1950. Correlation of optical properties and chemical composition in the plagioclase, olivine and orthopyroxene series. *Amer. Min.* **35**, 1067–79.

—— 1953. Metamorphism of basaltic rocks; a review. *Bull. geol. Soc. Amer.* **64**, 259–74.

—— 1955. Chemistry of the earth's crust. *Geol. Soc. Amer.*, Spec. Paper **62**, 119–44.

PUGH, W. J., 1956. The limestones of Scotland: Chemical analyses and petrography (Spectrographic determinations of trace elements by R. L. Mitchell). *Mem. geol. Surv. U.K.: Mineral Resources of Great Britain*, **37**.

RANKAMA, K., & SAHAMA, TH. D., 1950. *Geochemistry*. Chicago: Chicago University Press.

RILEY, J. P., 1958. The rapid analysis of silicate rocks and minerals. *Anal. Chim. Acta*, **19**, 413–28.

SHAW, D. M., 1954–6. Trace elements in pelitic rocks, Parts 1–3. *Bull. geol. Soc. Amer.* **65**, 1151–66, 1167–82; **67**, 919–34.

SHIDÔ, F., 1958. Plutonic and metamorphic rocks of the Nakoso and Iritôno districts in the Central Abukuma plateau. *J. Fac. Sci. Univ. Tokyo*, Sec. II, **11**, 131–217.

SRIRAMADAS, A., 1957. Diagrams for the correlation of unit cell edges and refractive indices of garnets with chemical composition. *Amer. Min.* **42**, 294–8.

TAYLOR, S. R., 1955. The origin of some New Zealand metamorphic rocks as shown by their major and trace element abundances. *Geochim. et Cosmoch. Acta*, **8**, 182–97.

TRÖGER, E., 1952. *Tabellen zur optischen Bestimmung der gesteinsbildenden Minerale*. Stuttgart: E. Schweizarbeit, Verlagsbuchhandlung.

TUREKIAN, K. K., 1956. The abundance of Cu, Ni, and Cr in basaltic rocks. *Trans. Amer. geophys. Un.* **37**, 361.

—— & KULP, J. L., 1956. The geochemistry of strontium. *Geochim. et Cosmoch. Acta*, **10**, 245–96.

TURNER, F. J., 1948. Mineralogical and structural evolution of the metamorphic rocks. *Mem. geol. Soc. Amer.* **30**.

WAGER, L. R., & MITCHELL, R. L., 1951. The distribution of trace elements during strong fractionation of basic magma—a further study of the Skaergaard intrusion, East Greenland. *Geochim. et Cosmoch. Acta*, **1**, 129–208.

—— —— 1953. Trace elements in a suite of Hawaii lavas. Ibid. **3**, 157–68.

WALKER, F., & POLDERVAART, A., 1949. Karroo dolerites of the Union of South Africa. *Bull. geol. Soc. Amer.* **60**, 591–706.

WILCOX, R. E., & POLDERVAART, A., 1958. Metadolerite dike swarm in Bakersville–Roan Mountain area, North Carolina. Ibid. **69**, 1323–68.

WINCHELL, A. N., & WINCHELL, H., 1951. *Elements of optical mineralogy. Part 1, Description of minerals.* New York: John Wiley & Sons.

WISEMAN, J. D. H., 1934. The central and south-west Highland epidiorites; a study in progressive metamorphism. *Quart. J. geol. Soc. Lond.* **90**, 354–417.

WRIGHT, W. I., 1938. The composition and occurrence of garnets. *Amer. Min.* **23**, 436–49.

YOUNG, R. S., 1957. The geochemistry of cobalt. *Geochim. et Cosmoch. Acta*, **13**, 28–41.

The Major Element Variation of the Layered Series of the Skaergaard Intrusion and a Re-estimation of the Average Composition of the Hidden Layered Series and of the Successive Residual Magmas

by L. R. WAGER

Department of Geology and Mineralogy, Oxford, England

ABSTRACT

Using variation diagrams for the major elements in the layered rocks, estimates are made of the average amounts of the various elements in the total rock separating at successive stages. From the analyses of the chilled marginal gabbro, taken to represent the composition of the initial magma, and with the further likely assumption that the Skaergaard intrusion is a closed system, at any rate for most of the elements, various hypotheses on the relative volumes of the different parts of the intrusion are tested to find the one best fitting the known distribution of the elements in the observable rocks. Estimates are then made of (1) the overall composition of the hidden part of the intrusion by subtracting the amounts of an element in the observed rocks from the total in the initial magma, and (2) the composition of the successive residual magmas formed as a result of the crystal fractionation.

In an igneous layered series the rocks usually show strong rhythmic variation in composition as a result of the differing assemblages of the accumulated crystals. Having obtained a general view of the changes in composition of the Skaergaard rocks from the early analyses by Dr. (now Professor) W. A. Deer (Wager & Deer, 1939), it seemed that further analysis of whole rocks would only be of limited value. The available analytical effort was therefore concentrated on the analysis of minerals separated from the rocks, e.g. plagioclase (in Wager & Mitchell, 1951), pyroxenes (Muir, 1951; Brown, 1957), iron oxides (Vincent & Phillips, 1954), sulphides (Wager, Vincent, & Smales, 1957), and olivines (in progress). Recently, however, further analyses of whole rocks have been made with the intention of deducing from them an improved estimate of the composition of the successive magmas developed by the crystal fractionation. The new analyses are mainly by Dr. E. A. Vincent and I am very grateful to him for making them.

It was hoped that the composition of the successive liquids might be obtained from rocks which were apparently plagioclase orthocumulates (for terminology see Wager, Brown, & Wadsworth, 1960) by subtracting from the bulk analysis the proper amount of plagioclase of the composition of the cumulus crystals as was done by Brown for an allivalite of Rhum (Brown, 1956, p. 43). Of the two most hopeful-looking rocks investigated one has given what seems a reasonable result and this is discussed below (pp. 387–91), but the other has not, probably

[Journal of Petrology, Vol. 1, Part 3, pp. 364–98, 1960]

because the assumption that it is a plagioclase ortho- or mesocumulate is not correct.

As this line of investigation was not found to be giving a satisfactory series of compositions for the successive residual liquids, a modification of the method used in the first paper on the Skaergaard intrusion (Wager & Deer, 1939, pp. 217–36) has been developed. In its original form the method consisted of estimating, from mapping and petrological investigation, the volume of the intrusion and of the various component rocks. Then from the established time sequence of types, and assuming that the intrusion was essentially a closed system, the composition of successive residual magmas was obtained by successive summation of the composition of the various rocks formed from the magma in reverse order to their sequence of formation. Thus the composition of a late liquid was obtained by averaging the composition of the rocks formed from it; the composition of the next earlier liquid by again averaging the composition of all rocks formed from it, including those previously used, and so on as far back as the evidence from the observable rocks allowed. In the present paper a graphical method of carrying out this process is used. From the same data, together with the composition of the initial magma, an improved estimate of the composition of the hidden layered rocks has also been obtained.

A REVISED CLASSIFICATION AND ESTIMATE OF THICKNESS OF THE LAYERED SERIES

During a fourth expedition to the Skaergaard intrusion in 1953, further mapping and collecting along measured traverses have resulted in small modifications in the estimated thicknesses of the various units of the layered series and an improvement in the subdivision and nomenclature of the layered series has been made (Fig. 1). As is customary for the Bushveld and other layered masses, the Skaergaard layered series is now divided into zones and subzones. The limits of the various divisions are based on the incoming and outgoing of the cumulus minerals. Thus the boundary between the lower zone (LZ) and the middle zone (MZ) is at the level where olivine, which is present in the LZ, ceased to form as a cumulus mineral. It is therefore the same dividing criterion as that between the so-called hypersthene olivine gabbros and the Middle Gabbros of the original paper. The boundary between the MZ and the upper zone (UZ) is put at the level where the olivine returns as a cumulus mineral, and thus it corresponds to the top of the old Middle Gabbros.

The lower zone has been divided into subzones; the boundary LZa–b is the level where augite first becomes a usual cumulus phase and the boundary LZb–c where magnetite does the same. The upper zone has also been divided into subzones; the boundary UZa–b is the level at which cumulus apatite comes in and UZb–c the level at which iron wollastonite, now inverted to a pyroxene, appears.

The incoming and outgoing of cumulus minerals is not found to occur at a

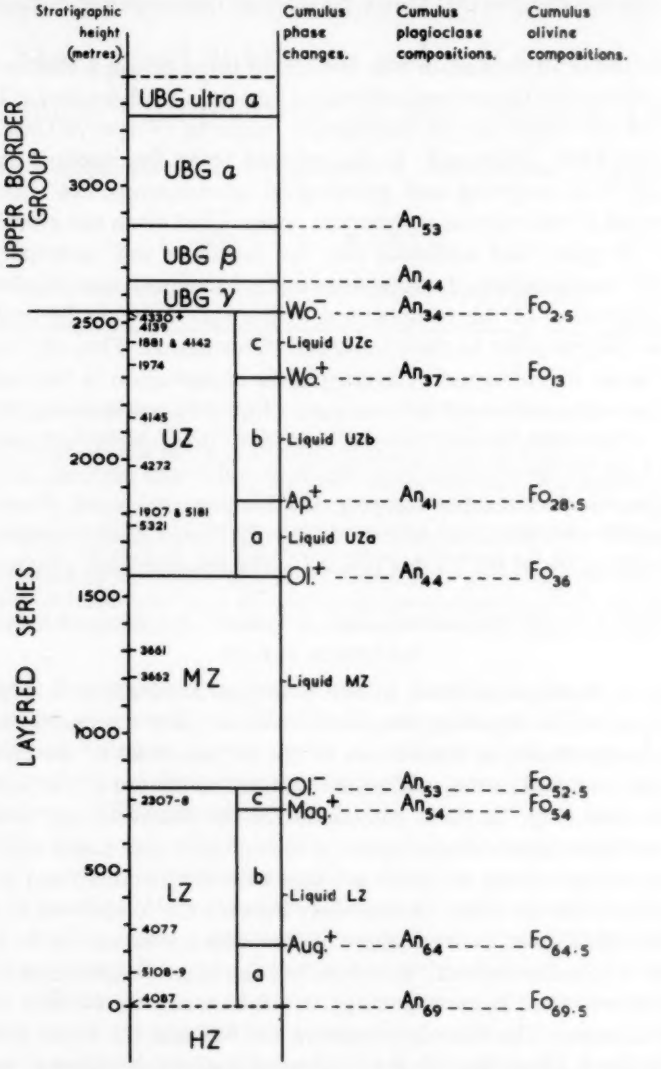

FIG. 1. Revised classification and thickness of the Skaergaard layered series and upper border group, with the heights of the analysed rocks.

precise level, but to be erratic over a considerable thickness, sometimes as much as 100 m. The boundary between two zones is drawn where the new phases have become a usual feature of the rocks, rather than where they first appear.

The compositions of the cumulus plagioclase and olivine at the various zone and subzone boundaries are indicated in Fig. 1. The compositions given are

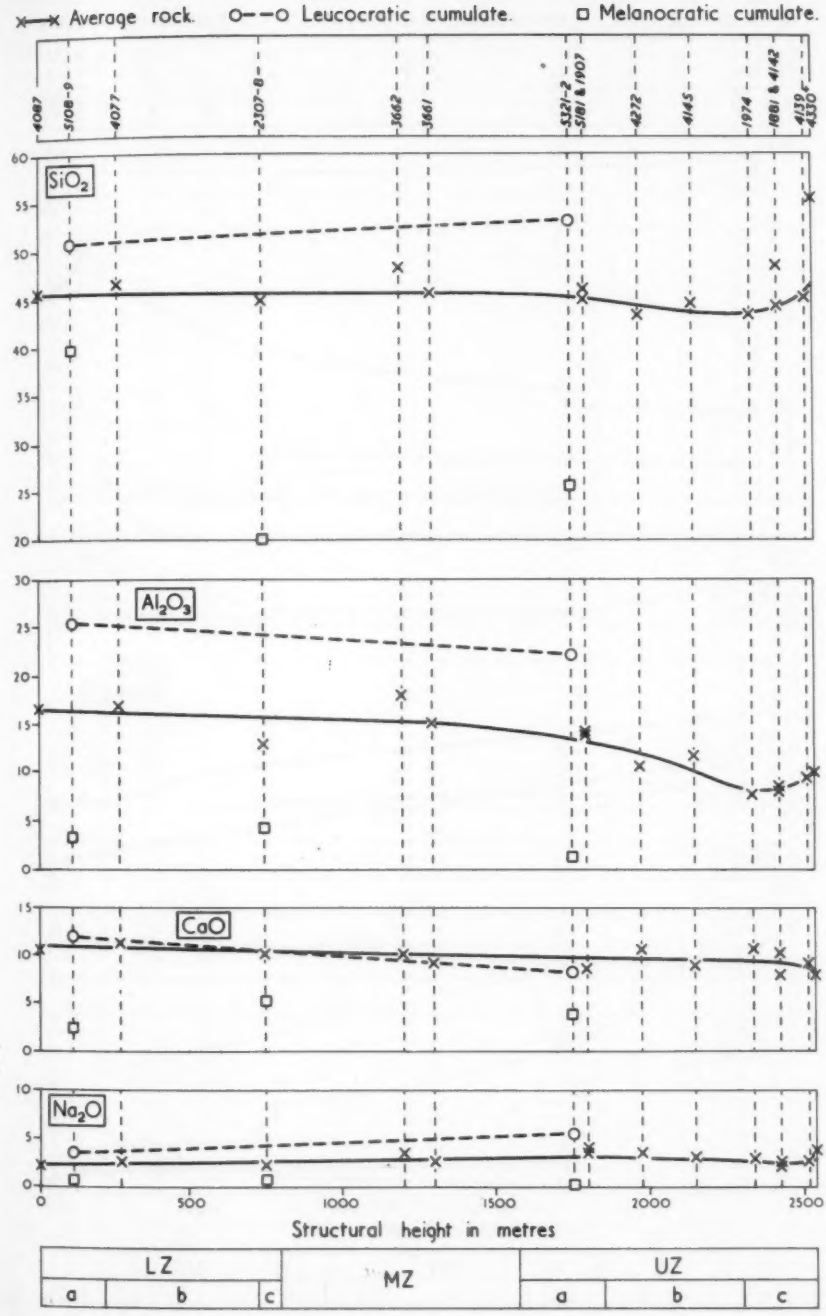

FIG. 2. Chemical variation of the observable layered series plotted against height for: SiO_2, Al_2O_3, CaO, and Na_2O.

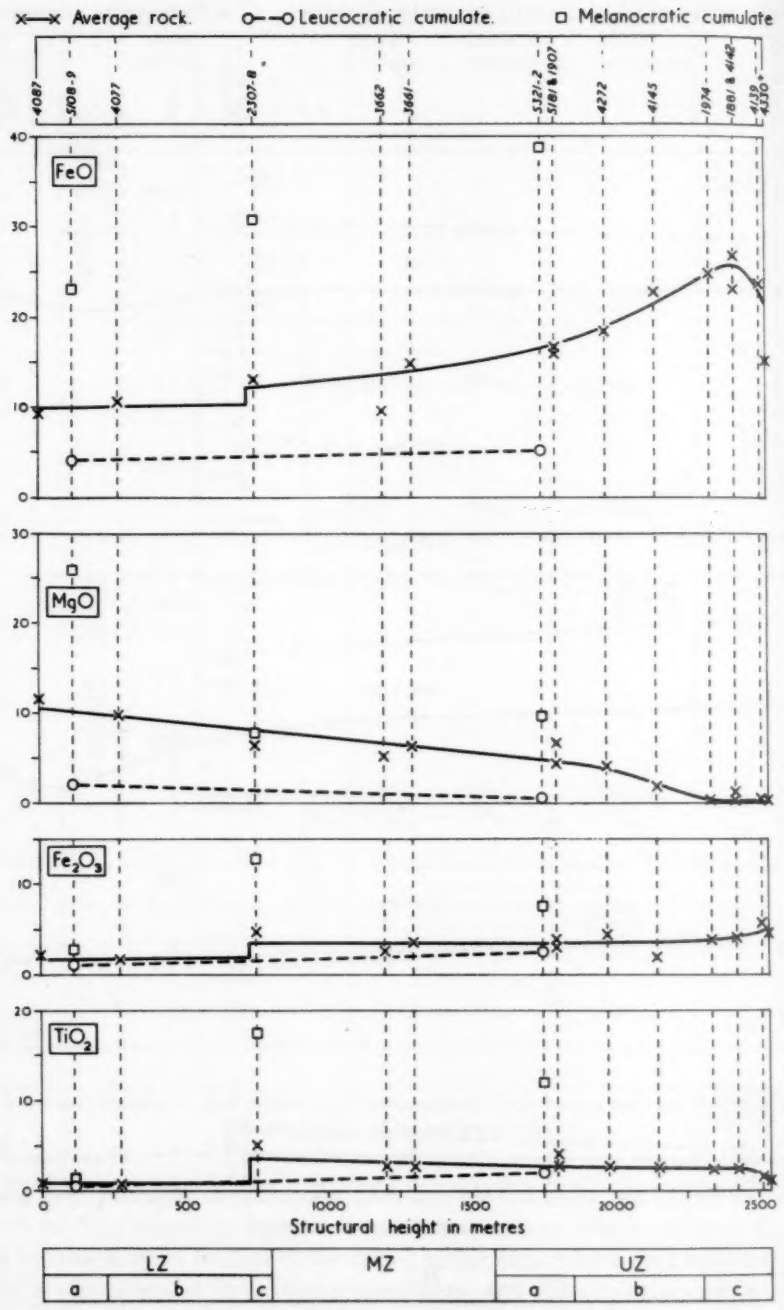

FIG. 3. Chemical variation of the observable layered series plotted against height for: FeO, MgO, Fe_2O_3, and TiO_2.

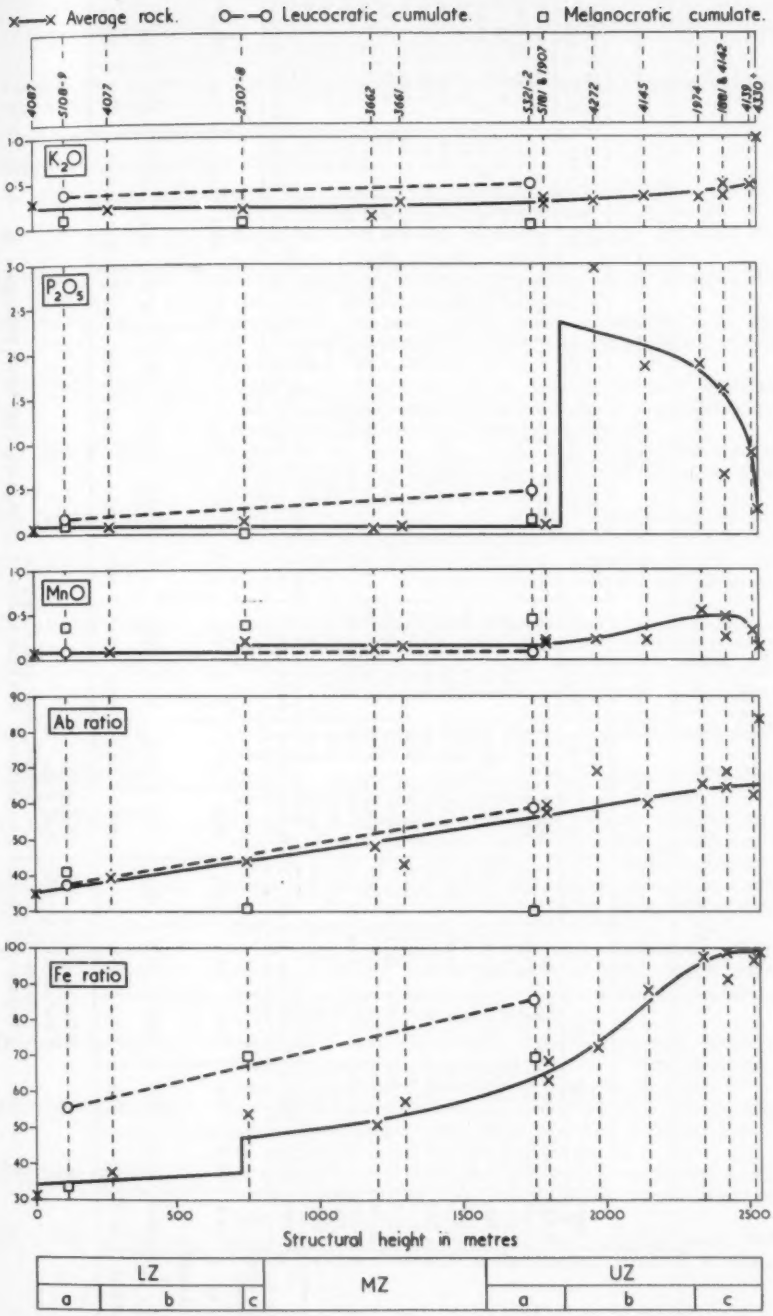

FIG. 4. Chemical variation of the observable layered series plotted against height for: K_2O, P_2O_5, MnO and the similarly plotted albite and iron ratios.

TABLE 1

Analyses of the rocks of the Skaergaard layered series

	LZ						MZ		UZ										
	a			b	c				a				b		c				
	I 4087	II 5108	III 5109	IV 4077	V 2307	VI 2308	VII 3662	VIII 3661	IX 5321	X 5322	XI 1907	XII 5181	XIII 4272	XIV 4145	XV 1974	XVI 4142	XVII 1881	XVIII 4139	XIX 4330+
SiO_2	45·48	39·65	50·65	46·37	44·75	19·95	48·15	45·65	53·17	25·67	44·81	45·73	43·05	44·1	43·24	44·13	48·27	45·19	55·10
Al_2O_3	16·41	3·29	25·54	16·82	13·00	4·60	18·02	15·08	21·83	1·49	13·96	14·68	10·58	11·70	7·62	7·88	8·58	9·37	9·90
Fe_2O_3	2·09	2·68	1·11	1·52	4·88	12·74	2·52	3·41	2·40	7·58	3·75	2·85	4·49	2·05	3·93	4·05	4·06	5·78	4·75
FeO	9·29	22·93	4·07	10·44	12·95	30·70	9·50	14·86	5·23	38·95	16·66	15·83	18·23	22·68	24·75	26·63	22·89	23·77	15·14
MgO	11·65	25·84	1·90	9·61	6·23	7·54	5·25	6·35	0·50	9·50	5·54	4·18	3·92	1·71	0·37	0·25	1·21	0·43	0·13
CaO	10·46	2·29	11·74	11·29	10·09	5·30	10·17	9·18	8·04	3·63	8·53	8·38	10·37	8·71	10·35	10·03	7·42	9·05	7·76
Na_2O	2·06	0·48	3·54	2·45	2·21	0·50	3·46	2·48	5·54	0·18	3·35	3·71	3·39	2·95	2·73	2·15	2·65	2·43	3·86
K_2O	0·27	0·08	0·36	0·20	0·22	0·06	0·14	0·28	0·49	0·05	0·33	0·27	0·30	0·35	0·31	0·47	0·34	0·49	1·00
H_2O^+	0·77	0·81	0·44	0·29	0·21	0·27	0·20	0·22	0·09	0·28	0·34	0·40	0·11	0·22	1·47	0·30	1·13	0·57	0·92
H_2O^-	0·26	0·18	0·04	0·09	0·04	0·04	0·02	0·08	0·02	0·08	0·19	0·15	0·16	0·20	0·13	0·19	0·37	0·31	0·20
TiO_2	0·94	1·30	0·50	0·79	5·04	17·36	2·64	2·59	2·07	11·92	2·55	3·90	2·54	2·43	2·23	2·48	2·20	1·67	1·16
P_2O_5	0·05	0·08	0·16	0·06	0·13	trace	0·05	0·08	0·48	0·14	0·08	0·09	2·95	1·85	1·87	1·61	0·65	0·91	0·24
MnO	0·06	0·34	0·09	0·09	0·20	0·37	0·12	0·15	0·08	0·45	0·17	0·22	0·22	0·21	0·55	0·48	0·26	0·32	0·14
TOTAL	99·79	99·95	100·14	100·02	100·14*	100·15†	100·50‡	100·41	99·94	99·92	100·26	100·39	100·31	100·15§	99·55	100·65	100·03	100·29	100·30
abratio(atomic) $\frac{2Na}{Na+Al-K}$	34·4	41·0	37·6	39·0	44·1	30·4	48·0	43·2	59·0	30·3	57·5	59·7	70·5	59·9	75·9	68·8	64·2	62·2	83·9
fe ratio (atomic) $\frac{Fe+Mn}{Fe+Mn+Mg}$	30·9	33·4	55·2	38·0	54·0	69·7	50·6	57·2	85·9	69·8	63·2	68·2	72·4	88·2	97·6	91·4	98·3	96·8	98·6
% solidified	70·0	71·8	71·8	74·3	81·6	81·6	88·5	90·0	96·3	96·3	96·6	96·6	97·8	98·7	99·0	99·3	99·3	99·4	99·5

* Includes: Cr_2O_3 0·008, V_2O_3 0·18.
† Includes: Cr_2O_3 0·037, V_2O_3 0·68.
‡ Includes: CO_2 0·03, S 0·14, SrO 0·07, BaO 0·01, CuO 0·006.
§ Includes: CO_2 0·04, S 0·31, ZrO_2 0·01, SrO 0·08, BaO 0·02, Cr_2O_3 trace, CuO 0·016, NiO trace.

Key to analysed rocks (Table 1)

The numbers refer to rocks in the Skaergaard intrusion collection in the Department of Geology and Mineralogy, Oxford.

Structural heights are given above the arbitrary base.

* indicates new analysis not previously published.

I.	4087 at 0 m.	Average rock (plagioclase-olivine cumulate) of LZa. 150 m from northern margin, Uttentals Plateau. Anal.: W. A. Deer.
II.*	5108 at 110 m.	Melanocratic layer (olivine cumulate) of LZa. Uttentals Plateau. Anal.: E. A. Vincent and B. A. Collett.
III.*	5109 at 110 m.	Leucocratic layer (Labradorite cumulate) of LZa. Uttentals Plateau. Anal.: E. A. Vincent and B. A. Collett.
IV.	4077 at 280 m.	Average rock (plagioclase, olivine, augite cumulate) of LZb. Junction of Uttentals Plateau and WNW. ridge of Peak 1,300 m of Gabbro-fjaeld. Anal.: W. A. Deer.
V.*	2307 at 750 m.	Average rock (plagioclase, augite, olivine, magnetite cumulate) of LZc. Near highest point of layered series on Kraemers Island and about 366 m from margin. Anal.: E. A. Vincent.
VI.*	2308 at 750 m.	Melanocratic band (magnetite, augite, olivine, plagioclase cumulate) of LZc. In 2307 near highest point of layered series on Kraemers Island. Anal.: E. A. Vincent.
VII.	3662 at 1205 m.	Olivine-free gabbro (plagioclase, augite, magnetite cumulate) of MZ. 25 m above sea-level at west foot of Pukugaqryggen. Anal.: W. A. Deer.
VIII.	3661 at 1295 m.	Olivine-free gabbro (augite, plagioclase, magnetite, inverted pigeonite cumulate) of MZ. 50 m above 3662 at west foot of Pukugaqryggen. Anal.: W. A. Deer.
IX.*	5321 at 1750 m.	Leucocratic band (plagioclase–magnetite cumulate) of UZa (=2568). Trough Band H, House Area. Anal.: E. A. Vincent and B. A. Collett.
X.*	5322 at 1750 m.	Melanocratic band (olivine, augite, magnetite cumulate) of UZa (=2569). Trough Band H, House Area. Anal.: E. A. Vincent and B. A. Collett.
XI.	1907 at 1800 m.	Ferrogabbro (plagioclase, augite, olivine, magnetite cumulate) of UZa. Basishusene. Anal.: W. A. Deer.
XII.*	5181 at 1800 m.	Ferrogabbro (plagioclase, augite, olivine, magnetite cumulate) of UZa. Basishusene. Anal.: E. A. Vincent and B. A. Collett.
XIII.*	4272 at 1975 m.	Ferrogabbro (plagioclase, olivine, augite, magnetite, apatite cumulate) of UZb. East of Skaergaard Bay, SE. of houses, approaching top of Raven's Rock. Anal.: I. D. Muir. (Alkalis by E. A. Vincent.)
XIV.	4145 at 2150. m.	Ferrogabbro (plagioclase, olivine, augite, magnetite, apatite cumulate) of UZb. West ridge of Basistoppen, 213 m below 'purple band' and 250 m above Basishusene. Anal.: W. A. Deer.
XV.*	1974 at 2340 m.	'Purple band' ferrogabbro (inverted iron wollastonite, plagioclase, olivine, magnetite, apatite cumulate) of UZc. 122 m above sea-level, SE. of head of small bay at NE. end of Skaergaard Bay. Anal.: I. D. Muir. (Alkalis by E. A. Vincent.)
XVI.	4142 at 2425 m.	'Purple band' ferrogabbro (inverted iron wollastonite, olivine, plagioclase, magnetite, apatite cumulate) of UZc. At 550 m above sea-level on west face of Basistoppen. Anal.: W. A. Deer.
XVII.	1881 at 2430 m.	Ferrogabbro (inverted iron wollastonite, plagioclase, olivine, magnetite, apatite cumulate) of UZc. 10 m from top of Nunatak II. Anal.: W. A. Deer.
XVIII.	4139 at 2510 m.	Ferrogabbro (olivine, plagioclase, inverted iron wollastonite, magnetite, apatite cumulate) of UZc. 100 m above 'purple band' on west face of Basistoppen. Anal.: W. A. Deer.
XIX.*	4330+ at 2540 m.	Ferrogabbro (plagioclase, augite, olivine, magnetite, apatite cumulate) of UZc. 152 m above 4139 on Basistoppen. Anal.: E. A. Vincent and B. A. Collett.

average values obtained by plotting well-determined minerals against height, drawing an average curve of the variation, and then reading off the compositions at the levels corresponding to the boundaries between zones.

The new classification of the layered series, although more logical, does not differ much from the original one (cf. fig. 25 of original paper). The limits of the zones and subzones will be discussed more fully when the layered series is re-described.

VARIATION IN COMPOSITION OF THE LAYERED ROCKS WITH HEIGHT

All satisfactory analyses of the layered series rocks are plotted against height in Figs. 2, 3, and 4, and the analyses themselves are presented in Table 1. The positions of the analysed rocks are shown on the vertical section (Fig. 1). The rocks analysed vary from leucocratic cumulates (5109, 5321) through roughly average rocks (the bulk of those plotted) to melanocratic cumulates (5108, 2308, 5322); these three groups are distinguished in the graphs and two sets of curves are drawn. The leucocratic cumulates consist of plagioclase and the products of crystallization of the trapped contemporary magma, i.e. the pore material; the average rocks consist of all the cumulus phases possible at the particular stage of fractionation together with pore material; and the melanocratic rocks consist of one or more of the melanocratic cumulus minerals together with pore material. The three melanocratic rocks do not form a coherent group. Thus 5108 is an olivine cumulate with a moderate amount of pore material; 2308 is a magnetite-ilmenite cumulate with only small amounts of pore material; and 5322 is an olivine magnetite augite cumulate with, again, only a small amount of pore material.

There is a precise meaning to be attached to the conception of average rock, namely, an assemblage of minerals in the proportions in which they were separating at the particular stage in the fractionation. The so-called average rocks are, however, only those which were selected as such by eye in the field. Since all the rocks show rhythmic layering, the so-called average rocks can only be expected to correspond very roughly to the ideal composition. The best approach to the composition of the true average material separating at successive stages has been obtained by drawing curves through the rather scattered points for the analyses of the so-called average rocks and reading off the amounts of the various constituents for particular levels on these curves.

The spread of points on the graphs emphasizes the wide range of composition of the layered rocks. The variation in amount of an element in the different rhythmic layers at any one horizon is often greater than its cryptic variation in the average rocks throughout the whole layered series.

After the deposition of the layered series had been completed there was a small amount of magma left over which underwent further fractionation, probably by filter press action, giving intermediate and acid rocks. At this very late stage the variation in the amount of most of the elements was rapid, but these changes

are not shown on the graphs, since they do not belong to the layered series, and in any case graphs drawn on the scale chosen would not permit the variation to be shown effectively.

The following are brief comments on the variation found in the layered series for each major oxide:

SiO_2. The variation for the average rock is slight, the amount lying between 43 and 46 per cent. The slight fall in the UZ is partly due to the average layered series at this stage having relatively small amounts of plagioclase and relatively large amounts of ferromagnesian minerals, especially olivine. The two plagioclase cumulates have 50 and 53 per cent silica, respectively, due to the relatively high percentages of silica in the abundant plagioclase of these rocks. The amount of SiO_2 in the three melanocratic rocks varies strongly from 20 to 40 per cent, as would be expected from their different contents of silicates and non-silicate minerals.

Al_2O_3. The variation is rather like that of silica except that the melanocratic rocks, in which both silicates and oxide minerals contain low Al_2O_3, are in this case similar. The average content in the LZ and MZ is between 15 and 16 per cent and falls in the UZ because the amount of felspar is less. The plagioclase cumulates have 25–22 per cent Al_2O_3 and the melanocratic rocks 2–5 per cent. Rocks covering the whole range from 2 to 25 per cent Al_2O_3 could, of course, be obtained from the rhythmically varying layered series.

Fe_2O_3. A step in the curve for the average rocks must occur at the level where magnetite becomes a cumulus mineral and the plotted points can reasonably be interpreted in this way. No step is to be expected for the leucocratic cumulates.

FeO. Where magnetite first appears there should be a slight step up in the curve for the average rock; such a step is shown although not necessitated by the rather limited number of points. Even in the average rocks there is an impressive change in amounts of FeO with height from 10 to 25 per cent FeO. The FeO in the labradorite cumulate 5109 is 4 per cent, and this is only present in the material crystallized from the trapped liquid. If the amount of trapped liquid be a third by weight of the total rock then the percentage FeO in the contemporaneous magma would be 12 per cent, and this is no doubt of the right order (cf. Table 4).

MgO. A smooth curve is drawn for the average rocks. The abrupt disappearance of olivine when the MZ is reached, and its return at the beginning of the UZ, must theoretically cause a step and change in direction of the curve. This effect, and similar changes for FeO, &c., are, however, not shown with the few data available and, in any case, would be slight. The low amount of MgO in the leucocratic cumulates is to be expected, as also the high, or average amounts in the melanocratic, depending on whether the dark cumulus crystals are largely olivine and pryoxene or iron ore.

CaO. Because lime occurs abundantly in both plagioclase and augite there is practically no difference in the curves for the leucocratic and average cumulates,

but the amount in the melanocratic rocks is low because they are relatively poor in calcium-bearing minerals.

Na_2O. The curve for the average rock shows first a rise due to increasing albite content of the plagioclase, then a fall in the UZ due to decrease in the amount of modal plagioclase which similarly affected the amounts of SiO_2 and Al_2O_3. The Na_2O in the melanocratic rocks is low, since it must be mainly in the products of crystallization of the trapped liquid; it is high in the plagioclase cumulates because of the abundant plagioclase.

K_2O. For the average rocks K_2O remains steady and low until the UZ, when it rises slowly in sympathy with increasing amounts of micropegmatite.

TiO_2. Until the LZc is reached TiO_2 is very low in the average rocks and also in the leucocratic and melanocratic layers, but when titaniferous magnetite and ilmenite appear as cumulus phases, TiO_2 rises abruptly. A step in the curve is shown for both average and melanocratic rocks. The TiO_2 in the labradorite cumulate is low as it is only present in the pore material (cf. FeO above).

P_2O_5. The average rock contains about 0·05 per cent P_2O_5 until apatite becomes a cumulus mineral at the UZb stage when P_2O_5 rises suddenly to 2 or 3 per cent. There is more P_2O_5 in the leucocratic cumulates than in the average rocks, which was unexpected. It was also not expected that the amount of P_2O_5 would be about the same in the average LZ, MZ, and UZa rocks. The P_2O_5 content will be considered more fully in a later paper as it is considered to be a useful indication of the amount of trapped liquid.

COMPOSITION OF THE HIDDEN ZONE OF THE LAYERED SERIES

The nature and composition of the hidden zone of the layered series could be obtained by observation if a deep bore-hole were drilled, but until such time its nature can only be deduced indirectly. If the amount of an element found in the observable rocks be subtracted from the amount in the whole mass of original magma, the total amount in the hidden rocks is obtained and this amount must be distributed in some definite way throughout the hidden rocks. Thus, to estimate the overall composition of the HZ it is necessary to know (1) the relative volume of the observable and hidden parts of the intrusion, (2) the overall composition of the observable rocks, and (3) the composition of the original liquid. The first of these may be roughly estimated from the mapping; the third is taken as the composition of the chilled olivine gabbro found at the margin. Three analyses of the chilled marginal gabbro have now been made and all the data are presented in Table 2. The specimen 1724 was collected rather far from the southern margin and 1825, which was much nearer, is a patchy rock, possibly slightly contaminated by acid gneiss of the basement complex. Thus 4507, 3 ft from the southern boundary, is regarded as the best specimen to represent the original magma. If all three analyses are averaged the figures obtained are not far removed from the preferred analysis (4507), and the

estimates of the composition of the HZ rocks presented here would not be essentially different if the average were used as the original magma composition.

In the original paper the total volume of the intrusion was roughly estimated by extrapolation of the boundaries both downwards, below the level of observation, and upwards, where erosion has removed them. This extrapolation was far from satisfactory and made the weakest link in the chain of argument. The

TABLE 2

Analyses of three specimens of chilled olivine gabbro from the marginal border group. The figures for EG4507 are taken as the composition of the original magma

	4507	1724	1825	*Average*
SiO_2	48·08	47·83	48·01	47·97
Al_2O_3	17·22	18·62	19·11	18·32
Fe_2O_3	1·32	1·16	1·20	1·23
FeO	8·44	8·87	8·44	8·58
MgO	8·62	7·92	7·72	8·09
CaO	11·38	10·59	10·33	10·77
Na_2O	2·37	2·54	2·34	2·42
K_2O	0·25	0·20	0·17	0·21
H_2O^+	1·01*	0·27	0·55	0·61
H_2O^-	0·05	0·16	0·05	0·09
TiO_2	1·17	1·29	1·51	1·32
P_2O_5	0·10	0·06	0·07	0·08
MnO	0·16	0·09	0·12	0·12
TOTAL	100·17†	99·00	99·62	99·81

4507. Southern margin near coast on east side of Skaergaard Bay. Specimen 3 ft from contact with lavas. Anal.: E. A. Vincent and B. A. Collett. Various trace constituents have been determined (see Wager, Vincent, & Smales, 1957).

1724. Southern margin near coast on east side of Skaergaard Bay. Specimen 25 m from contact with lavas. Anal.: W. A. Deer.

1825. South-eastern margin at head of Ųdlöberen. Specimen 3 m from contact with lavas. Anal.: W. A. Deer.

* Probably high due to slight alteration of olivine.

† Includes: S 0·0055, Cu 0·0126, Ni 0·0193, Co 0·0056, Pd 0·0000018, In 0·0000054, Au 0·0000005, as trace constituents.

original estimates of the ratio of the volume of observable to hidden layered rock, based on fig. 15 of the original paper, gave a ratio of about 3:2. With this estimate the amount of certain oxides in the HZ was reduced to vanishing point (Wager & Deer, p. 218). The intrusion was therefore assumed to have less inwardly inclined margins in depth, which could give a ratio of observable to hidden layered rocks of 2:3. Even with these proportions the amount of P_2O_5 in the HZ became negative and various possible explanations were offered (ibid., p. 220). Thus, in making the original estimates of the relative proportions of the observable and hidden layered series, chemical data were used in preference to extrapolation upwards and downwards of observed boundaries, and this method has again been adopted in the present paper.

The graphical procedure here developed for estimating the composition of the HZ is not different in principle from that of the original paper but is more convenient. It may be illustrated by considering TiO_2 (Fig. 5). Percentages of magma solidified are represented along the abscissa. In Fig. 5A the lowest exposed layered rock is assumed to have formed when 60 per cent of the total intrusion had solidified. The volume of each unit of the layered series is taken as directly proportional to its thickness and therefore the percentages solidified are proportional to the thickness (reserving a final one-half per cent for intermediate and acid rocks later than the highest layered material). To produce the graphs the amounts of TiO_2 in the average layered rock at the various stages, as read from the average curve of Fig. 3, have been plotted against the percentages solidified; this gives the curve on the right-hand side of Fig. 5A. The graphs, Fig. 5 B, C, are similar, but in B the lowest observable layered rock is assumed to have formed when 70 per cent of the whole had solidified and in C when 80 per cent had solidified.

The amount of TiO_2 in the original magma is 1·17 per cent (see Table 2) and the total TiO_2 in the whole intrusion is proportional to the area of the rectangle *oabc*. The amount of TiO_2 in the observable layered rock is proportional to the area between the abscissa and the curve *QRSTU*. For the moment it will be assumed that the effect of the marginal and upper border group rocks is slight and that the area *QRSTUCD* represents the total amount of TiO_2 in all the various observable rocks separating at successive stages from the magma. The curve defining the amount of TiO_2 in the rocks must continue on the left-hand side of the diagram giving the TiO_2 content of the rocks of the HZ. The position of the left-hand part of the curve is necessarily such that the area beneath the curve *PQRSTU*, which is proportional to the total amount of TiO_2 in the rocks of the whole intrusion, is equal to the area of the rectangle *oabc*, which is proportional to the amount in the original magma. The position of the part *PQ* of the curve has been established so as to satisfy this condition.[1] With the particular assumption which is made in Fig. 5A of the proportion of the observable layered series to the whole intrusion, the amount of TiO_2 in the earliest layered rocks drops below zero; this cannot be correct, and other assumptions have therefore been tried. Thus Fig. 5 B and C have been constructed assuming that the lowest observable layered rock was formed at 70 and 80 per cent solidified respectively. With the assumption of Fig. 5B (70 per cent magma crystallized) the first layered rock of the HZ contains 0·6 per cent TiO_2, and with the assumption of Fig. 5C (80 per cent magma crystallized), 0·9 per cent TiO_2. Of these three possibilities the most likely is represented by B and the following digression is required to explain this preference.

Evidence based on the nature of the gabbro picrite and the perpendicular

[1] The position of *P* has been fixed by trial and error, various positions of *P* being tried until finally the area *aVRQPO* equalled the area *VST*. When this is the case the condition that area *oabc* equals *PQRSTU* is also satisfied.

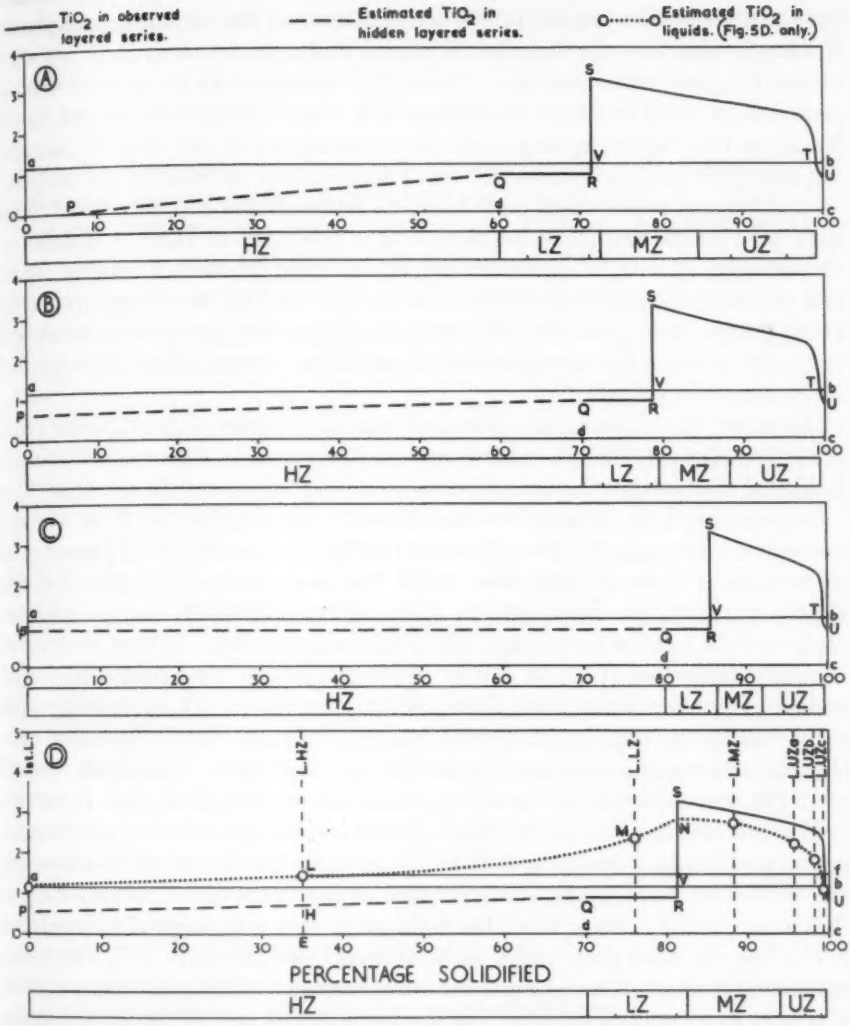

FIG. 5. The TiO_2 content of layered rocks, plotted against percentage solidified, with various assumptions about the relative volumes of the observed and hidden layered series, and deduction of TiO_2 composition of HZ rocks and of successive liquids (Fig. 5D only):

A, assuming lowest observed layered rock formed when 60 per cent of the intrusion was solidified.

B, assuming that the lowest layered rock formed at 70 per cent solidified.

C, assuming that the lowest layered rock formed at 80 per cent solidified.

D, the same as B with the additional assumption that the UZ rocks have, on the average, half the volume they would have had if the volume were proportional to thickness. On this graph the estimated composition of successive liquids is also shown.

felspar rock of the marginal border group (Wager & Deer, pp. 144–64, and further observations not yet published) indicate that the earliest crystal phases to have formed from the Skaergaard magma under equilibrium conditions were olivine Fo_{81} and plagioclase An_{77}. The earliest layered rocks are believed to have consisted of these minerals[1] together with a certain amount of trapped liquid which at this beginning-stage had the composition of the original magma. Assuming the formula compositions for Fo_{81} and An_{77}, estimates of the composition of various assemblages most likely to represent the earliest layered rocks have been made, and the most likely one is presented in Table 3, column *A*. The amount of TiO_2 is controlled by the assumed amount of trapped liquid and this was probably about 35 per cent, so that the TiO_2 percentage should be about 0·4 per cent. Thus for TiO_2 the preferable assumption is the case shown in Fig. 5B in which the first observable layered rock formed when 70 per cent of the magma had solidified.

A similar test of the most reasonable relative volumes of the different units of the complex may also be made using the P_2O_5 content of the rock. The usual analytical methods for the determination of phosphorus in rocks are apparently unprecise when P_2O_5 is much less than about 0·1 per cent, but Dr. E. A. Vincent has recently devised a neutron activation method for the analysis of phosphorus when present in small amounts, which has been successfully used for the Skaergaard rocks low in phosphorus. Using figures obtained by the new method, plots of P_2O_5 against percentage solidified, assuming that the first observable layered rock formed at 60, 70, and 80 per cent solidified, have been constructed and it has been found that in all three cases the amount of P_2O_5 in the observable rocks exceeds the total in the whole intrusion. Only one case is illustrated here (Fig. 6A) which is the one assuming that the first observable layered rock formed at 70 per cent solidified, the percentage satisfying best the TiO_2 data. However, even in this case the amount of P_2O_5 in the observable layered rocks, represented by the area beneath the curve *QRSTU*, is 1½ times that in the whole intrusion, represented by the area *oabc* which is based on the figure of 0·1 per cent P_2O_5 in the chilled olivine gabbro. When the Skaergaard data were originally considered in this way the same discrepancy arose as mentioned above (p. 375). The rocks containing the bulk of the phosphorus are of the zones UZ b and c where apatite is present as a cumulus mineral. The thickness of this part of the layered series is well established from the field work but it is not known from direct observation whether or not they spread over the whole area of the intrusion. A similar discrepancy between the large amount of sulphur found in certain bands of the UZc and the small amount in the initial magma was also shown in a recent paper on the Skaergaard sulphides (Wager *et al.*, 1957, pp. 883–4). To make the chemical picture for phosphorus and sulphur reasonable it is necessary to assume that the volume of the UZ rocks is indeed considerably less than in

[1] Possibly, however, enstatite may have replaced olivine at depth because of the high pressure (see p. 384).

direct proportion to their thickness. This implies that the lateral extent of the layered rocks at the UZ level is less than at the LZ and MZ levels, and this is

TABLE 3

Estimated composition of the earliest average layered rock assuming various amounts of cumulus crystals (A and B) and the composition of the earliest layered rock and of the average hidden zone material based on the graphs of Fig. 14 and from earlier data (C, D, and E)

	A	*B*	*C*	*D*	*E*
SiO_2	47·06	49·54	50·8	48·7	48·7
Al_2O_3	22·53	22·53	19·5	18·0	21·2
Fe_2O_3	0·46	0·46	—	0·7	—
FeO	4·98	4·42	4·5	6·8	5·8
MgO	9·94	7·70	9·3	9·5	9·0
CaO	11·98	12·27	13·0	12·0	10·8
Na_2O	2·23	2·23	2·1	2·2	2·2
K_2O	0·09	0·09	0·21	0·23	0·10
H_2O^+	0·35	0·35	—	—	—
H_2O^-	0·02	0·02	—	—	—
TiO_2	0·41	0·41	0·55	0·7	0·80
P_2O_5	0·04	0·04	0·04	0·03	0·05
MnO	0·06	0·06	0·16	0·13	—
			Norms		
Q			—	—	—
Or			1·11	1·11	0·56
Ab			17·82 62·03	18·34 58·07	18·34 66·72
An			43·10	38·62	47·82
Di			8·93	8·70	2·44
			6·10 17·14	5·50 16·84	1·60 4·70
			2·11	2·64	0·66
Hy			9·20 12·50	5·80 8·57	11·00 15·22
			3·30	2·77	4·22
Ol			5·39 7·53	8·47 12·85	7·00 9·86
			2·14	4·38	2·86
Mt			— 0·46	1·16 2·53	— 1·52
Il			0·46	1·37	1·52

A, estimated composition of earliest layered rock assuming that it is made up of 50 per cent ($An_{77}Ab_{23}$), 15 per cent (Fo_{81} Fa_{19}), and 35 per cent of the initial magma.

B, estimated composition of earliest layered rock assuming that it is made up of 50 per cent ($An_{77}Ab_{23}$), 15 per cent ($Ca_4Mg_{78}Fe_{18}$), and 35 per cent of the initial magma.

C, composition of the earliest layered rock read from the graphs of Fig. 14.

D, composition of the average hidden zone rock (i.e. rock at 35 per cent solidified) based on the graphs of Fig. 14.

E, composition of the average hidden zone taken from Wager & Deer, 1939, table xxxvi, p. 221.

not an unreasonable assumption. In Fig. 6B the assumption has been made that the volume of the successive UZ rocks became increasingly less than is implied by direct proportionality to thickness and that, overall, the volume of UZ rocks is half that implied by their thickness. This assumption is equivalent to saying

FIG. 6. The P_2O_5 content of layered rocks, plotted against percentage solidified, and deduction of the P_2O_5 composition of the HZ and of successive liquids: A, assuming that the lowest layered rocks were formed at 70 per cent solidified and that the volumes are proportional to thickness. With these assumptions the amount of P_2O_5 in the HZ is negative.

B, the same except that the UZ rocks, on the average, are assumed to have half the volume they would have had if the volume were proportional to thickness. With this assumption the amount of P_2O_5 in the HZ averages 0·03 per cent.

that the area originally covered by the successive UZ rocks decreased steadily so that on the average the area covered is only half that of the LZ and MZ rocks. No field evidence is opposed to this assumption, and certain general arguments can be used in its support which will be presented in a later paper, when the data on the uppermost layered rocks and the upper border group are revised.

With the assumption of the smaller volume of the UZ rocks (Fig. 6B) the amount of P_2O_5 in all the observable rocks is reduced and the curve for P_2O_5, satisfying the various assumptions, gives a P_2O_5 content for the earliest layered rock of 0·4 per cent. Referring to Table 3, column *A*, it will be seen that such an amount of P_2O_5 fits approximately with the assumption found satisfactory for TiO_2, namely, that the earliest layered rocks contained about 35 per cent of trapped liquid of the composition of the original magma.

In estimating the amounts of TiO_2 and P_2O_5 in the HZ rocks it has been assumed that the curves showing the amounts of these two elements in the layered rocks represents satisfactorily the whole of the TiO_2 and P_2O_5 separating, that is, the amount of these elements not only in the layered rocks but also in the simultaneously forming marginal and upper border groups. The bulk of the marginal border group is small and may be disregarded for the present purposes, but the bulk of the upper border group is about one-third the amount of the contemporary layered rocks (cf. Fig. 1) assuming general similarity in the areas covered by them. The composition of upper border group rocks must therefore be taken into consideration for those elements which differ considerably in amount in the simultaneously forming UBG and LS rocks. The UBG, when contemporaneous with the LZ rocks, have similar basic plagioclase and iron-poor ferromagnesian minerals, and when contemporaneous with MZ and UZ rocks they have, similarly, more sodic plagioclase and iron-rich ferrogmagnesian minerals. The overall proportions of the minerals present in the two groups are, however, rather different and result in certain compositional differences of significance. Thus the upper border group tends to be richer in plagioclase and poorer in ferromagnesian minerals and such analyses as are available show the effects of these differences in mineral proportions (Wager & Deer, 1939, table 42). The UBG rocks tend to be richer by about 3 per cent in silica, 2 per cent in Al_2O_3, and 0·5 per cent in Na_2O than the corresponding layered rocks. At the same time they are poorer by about 2 per cent in FeO and MgO. If the proportion between UBG and LS is about 1 to 2 or 3, then the total rock separating will be about 1 per cent richer in SiO_2, 0·5 per cent in Al_2O_3, and a variable but small amount richer in Na_2O. Similar adjustment for FeO and MgO is also necessary. In constructing graphs representing the composition of the overall material separating from the liquid, adjustments of the layered series graphs for SiO_2, Al_2O_3, FeO, MgO, Na_2O, and K_2O have been made (broken curves in Fig. 14). For the remaining elements here considered, Fe_2O_3, TiO_2, P_2O_5, and MnO, no modification seemed necessary, the curves for the layered series being taken as representing adequately the composition of the total material successively separating from

the magma. Knowledge of the upper border group rocks is unfortunately much less than of the layered series and the available analyses are few. Thus these adjustments are somewhat arbitrary but they are no doubt of the right order.

The assumptions fitting best the known facts for P_2O_5 and TiO_2 are (1) that the first observable layered rocks formed at 70 per cent solidified, and (2) that the area of the sheets of UZ rocks became gradually less, making their overall volume half that to be expected if the area had remained the same as for the LZ and MZ rocks. In obtaining the composition of the hidden layered rocks for the other elements the same assumptions have been made, and in addition the modified curves showing the estimated overall composition of the material separating at successive stages, based on the composition of the layered rocks and border group rocks, have been used where necessary (Fig. 14). The overall picture of the chemistry of the intrusion, with these assumptions, is an improvement upon that originally put forward, but it is interesting to note that the present estimate of the nature of the composition of the hidden rocks proves to be not much different from that originally given (Wager & Deer, 1939, p. 220).

From the graphs (Fig. 14) the composition of the average rocks of HZ, taken as the amounts at 35 per cent solidified, can be read and is given in Table 3, column *D*, along with the CIPW norm. It is compared in column *E* with the estimated average composition of the hidden layered rocks from the original paper. Rocks having the composition given in columns *D* and *E* could well be plagioclase pyroxene olivine cumulates rich in basic plagioclase. It was surmised in the original paper that the rock would be a felspar-rich olivine eucrite (Wager & Deer, p. 220), and the newly estimated composition would also be capable of producing a rock which could be described in those terms.

COMPOSITION OF SUCCESSIVE RESIDUAL MAGMAS

During the fractional crystallization of the Skaergaard magma to give the various rocks of the complex, there must have been a steady change in the composition of the liquid phase. Had some fortunate concurrence of circumstances provided samples of the magma, for instance as periodic extrusions of lavas or injection of dykes, then the composition of a representative series of liquids might have been known by direct observation. However, such samples are not available to be analysed except in the case of the initial magma which forms the chilled marginal olivine gabbro; the compositions of the successive, now vanished, contemporary liquids can only be obtained by an indirect method. The original estimates (Wager & Deer, 1939, pp. 217–24; Wager & Mitchell, 1951, pp. 174–7) have not infrequently been used as an example of the changing composition of a basic magma resulting from strong crystal fractionation. Using new field and chemical data, a revision of the estimate for the composition of successive liquids has been made and it is satisfactory to find that the revised figures are not very different from those presented earlier.

Once the proportions, compositions, and sequences of the various parts of the intrusion have been adequately established, no further data are necessary for the determination of the composition of the successive liquids. The graphical method by which the composition of the liquids may be obtained can be conveniently illustrated using the case of TiO_2. On the preferred graph giving the amount of TiO_2 separating in the successive rocks (Fig. 5D), the composition of the initial magma, 1·17 per cent TiO_2, is shown at point *a*. The amount of TiO_2 in the liquid at 35 per cent solidified, the average for HZ, is shown by point *L* which has been fixed by means of the following considerations: The amount of TiO_2 in the rocks from 35 to 100 per cent solidified is proportional to the area *HQRSUcE*. This was all present in the liquid at 35 per cent solidified so that *L*, fixed by trial and error, is the point which makes the area of the rectangle *LfcE* equal to the area *HQRSUcE*. Sufficient points, *LMN*, &c., have been fixed by this means to draw the general curve for TiO_2 in the liquid. The curve is concave upward to *N* where a maximum TiO_2 content for the liquid of 2·80 per cent is reached. At this stage, which is the beginning of the LZc, a titaniferous magnetite was precipitated and from then on the amount of TiO_2 in the liquid began to fall, at first gently but, in the latest stages, rapidly. In a similar way the curve for P_2O_5 in the liquid has been drawn in Fig. 6B.

The variation of all the major oxides in the successive residual liquids, determined as for TiO_2, is presented in Fig. 14. In making the estimates it is necessary to use the estimated composition of the total rock separating (continuous line). In some cases this is the same as the curve for the layered series while in other cases (SiO_2, Al_2O_3, FeO, MgO, Na_2O, K_2O) the curve is different from the layered series curve (broken line) for reasons explained earlier (p. 378). For most oxides the change in composition of the liquid during the last few per cent of the solidification process is rapid and is highly sensitive to the amount and composition of the last dregs of liquid believed to give rise to the intermediate and acid rocks in between the layered series and UBG, or injected into the UBG. The graphs are based on the assumption that the amount of the intermediate and acid rocks coming after the latest layered rocks is one-half per cent of the whole volume of rock; at this late stage the curves turn off towards the average composition of the intermediate and acid rocks. The rapidly changing composition cannot be adequately shown on graphs of the scale used here but will be considered in a future paper dealing with the highest layered rocks and the upper border group.

The variation for each oxide in the successive residual liquids, up to about 98 per cent solidified, will now be briefly discussed.

SiO_2. Silica in the liquid decreases slightly from 48 to 46 per cent during the fractionation from 0 to 98 per cent solidified. It is perhaps surprising that the SiO_2 content decreases with fractionation until the late stages; this was shown to be the case in the original paper (ibid., see fig. 43 and plate 27) and the present

results are not essentially different. The chief cause of this is believed to be the large amount of plagioclase precipitated. In the later stages of the fractionation the amount of SiO_2 precipitated in the various minerals of the rocks approximately equals the amount in the liquid, and the composition of the latter does not change appreciably until the latest stage of filter press fractionation, which is not dealt with here.

Unless SiO_2 is lost from the system it seems that the silica content of the HZ must be relatively high. It is true that if the silica in the later rocks separating has been underestimated, then the amount of silica in the HZ would be less, but this seems unlikely. The composition of the earliest layered rocks, calculated on the assumption that plagioclase and olivine were the cumulus crystals (Table 3, column *A*), has 3 per cent less silica than that obtained from the graph (Fig. 14). As Dr. G. M. Brown has pointed out in conversation, the only way in which rocks so rich in silica could reasonably be produced in the early stages of the layered series is by orthopyroxene being one of the cumulus minerals. The composition of the earliest rock, assuming it to have 15 per cent of bronzite instead of olivine, is given in Table 3, column *B*, and this has an SiO_2 content closer to the estimated figure than column *A* rock having olivine as a cumulus mineral. A bronzite, not produced from pigeonite by inversion, occurs in the outer part of the marginal border group and occasionally similar early grains of bronzite are found in the lowest observable layered series, which provide some slight support for the hypothesis that orthopyroxene may have been a cumulus mineral in the lowest and earliest layered rocks. Although the chilled marginal gabbro shows that at the higher levels the earliest phases to separate were plagioclase and olivine, it is possible that some orthopyroxene in place of olivine may have formed as an early phase in the deeper levels of the hidden zone as a result of higher hydrostatic pressure.

Al_2O_3. The behaviour of alumina in the successive liquids closely follows that of silica, the amount falling steadily until a late stage.

Fe_2O_3. The amount of Fe_2O_3 in the observable layered series is such that, with the accepted assumptions on relative volumes, the amount in the earliest layered rock is reduced to zero. The amount in the earliest rock is, however, likely to be about 0·5 per cent (Table 3, cols. *A*, *B*). There is $1\frac{1}{2}$ times too much Fe_2O_3 in the observable rock than there should be if the assumptions about relative volumes, &c., which fit all the other elements, are accepted. It seems possible that the high content of Fe_2O_3 in the observable rocks is due to a steady change of some of the ferrous to ferric iron during cooling. In the original paper (Wager & Deer, 1939, p. 183) it was suggested that loss of hydrogen from the system allowed some increase in ferric iron.

FeO. The FeO content of the magma increases until it reaches 18 per cent in the UZc, at which stage an iron wollastonite was precipitated instead of an iron-rich augite. The increase in iron in the liquid implies that the minerals separating were less rich in iron than the liquid, and this continued until iron

wollastonite began to form, after which a fall in FeO set in. When titaniferous magnetite first began to occur as a cumulus mineral at the LZb–c level there should have been a slight slowing up of the rate of increase of FeO in the liquid, and the graph changes slope slightly, as expected.

MgO. The amount of MgO separating exceeds the amount in the liquid, and the curve falls, slowly at first and then rapidly, until the amount is less than 0·8 per cent.

CaO. The first liquid contains 11 per cent of lime which compares with the usual basic magmas. The fall in lime content is slow and is still 7 per cent. in liquid UZc.

Na_2O. There is only a slight increase in Na_2O in the liquid until the beginning of the UZ (2·4 to 3·1 per cent), after which the change depends on the assumption made of the effect of the upper border group rocks on the composition of the overall material separating. Only in the case of Na_2O is the effect of the upper border rocks sufficient to alter the curve from a descending to an ascending one. The soda content of the analysed rocks of UBG β and γ is from 0·5 to 2 per cent greater than for the corresponding average layered rocks. The volume of the rocks of the UBG β and γ is probably considerably less than that of the corresponding layered rocks and the graph for total Na_2O separating has therefore been increased by a few tenths of a per cent. If these approximations are accepted, then the Na_2O content of the liquid increases throughout the differentiation.

K_2O. The graph for K_2O separating in the overall rocks in the later stages should be drawn higher than that for the layered rocks, but the difference is very small and has been ignored. The rate of increase of K_2O in the liquid is very slight over the first 98 per cent solidified.

TiO_2. The curve for TiO_2 in the liquid is concave upwards until the level at which titaniferous magnetite separates. This occurs when the TiO_2 content of the magma is about 2·8 per cent and the FeO and Fe_2O_3 contents are 14 and 3·5 per cent respectively. These are the percentages of TiO_2, FeO, and Fe_2O_3 when this particular magma is saturated for titaniferous magnetite. The amount of TiO_2 in the saturated liquid falls from 2·8 per cent to about 2 per cent with increasing fractionation and lowering temperature. It is interesting to note the big difference in the TiO_2 content of the rock and the liquid, 0·8 and 2·8 per cent respectively, immediately before cumulus titaniferous magnetite forms in the LZc.

P_2O_5. As for TiO_2, the curve for P_2O_5 in the liquid is concave upwards until apatite is precipitated as cumulus crystals at 97 per cent solidified. The percentage of P_2O_5 in the liquid, to cause precipitation of apatite, is 1·75 per cent. The unexpectedly low amount of P_2O_5 in the average layered rocks up to the end of UZa, compared with the increasing amount in the contemporaneous liquid, is interpreted to mean that the amount of trapped liquid in the layered rocks, on average, becomes less with ascent in the layered series. The P_2O_5 content of the

layered rocks can probably be used as a means of estimating the proportion of trapped liquid to the rest of the material of the rock.

MnO. The amount of manganese in the hidden zone is higher than would be expected. In the liquid the amount of MnO slowly rises, reaching a maximum of 0·35 per cent at about 98 per cent solidified.

TABLE 4

The composition of the liquids at the middle point of the various zones (L.HZ, L.LZ, &c.) *as read from the graph* (*Fig. 14*), *and comparisons with early estimates* (*Wager & Deer*, 1939, *p.* 221)

	First liquid (=4507)	L.HZ	L.LZ	L.MZ	L.UZa	L.UZb	L.UZc	*Earlier estimate of liquid compositions* (*Wager & Deer*, 1939, *p.* 221)	
Percentage solidified	0	35	76	88·2	95·7	98·2	99·3	*Second liquid corresponding to* 70%	*Third liquid corresponding to* 94%
SiO_2	48·1	47·3	46·8	46·9	47·5	49·8	55·0	46·7	45·7
Al_2O_3	17·2	16·4	15·2	14·1	12·5	11·8	11·8	15·3	12·7
Fe_2O_3	1·3	2·0	3·3	3·6	3·8	4·3	4·5	2·9	3·6
FeO	8·4	10·0	13·0	15·0	17·3	17·8	14·5	12·9	18·2
MgO	8·6	8·1	5·8	4·0	2·5	1·3	0·8	5·9	3·5
CaO	11·4	10·9	10·0	9·5	9·5	8·0	7·0	9·9	8·3
Na_2O	2·37	2·45	2·80	3·00	3·20	3·40	3·65	2·83	3·16
K_2O	0·25	0·29	0·33	0·40	0·65	1·00	1·40	0·29	0·44
TiO_2	1·17	1·42	2·37 (2·80*)	2·65	2·20	1·80	1·05	2·18	2·36
P_2O_5	0·10	0·13	0·28	0·50	1·25 (1·75*)	1·35	0·40	0·42	0·92
MnO	0·16	0·16	0·16	0·20	0·28	0·35	0·25	0·16	0·22
Fe ratio (atomic) $\frac{Fe+Mn}{Fe+Mn+Mg}$	35·8	41·2	55·9	68·1	79·6	83·8	91·2		
Ab ratio (atomic) $\frac{2Na}{Na+Al-K}$	37·2	39·6	47·2	52·8	62·0	68·3	73·8		

* Maximum reached at intermediate stages.

The composition of the Skaergaard liquids corresponding to the middle part of the various zones as read from Fig. 14 graphs, is given in Table 4. The calculated iron and albite ratios are also given. While in the UZc liquid at 99 per cent. solidified the iron ratio reaches 91 per cent corresponding to a fayalite, the albite ratio at the same percentage solidified has only reached 74 per cent corresponding to a calcic oligoclase. In the same table are given the calculated second and third liquid compositions from the original paper (Wager & Deer, 1939, p. 221) and these are close to the

revised compositions at the equivalent stages. The kind of double variation diagram for the rock fractions and the liquids from which the rocks formed, given in Fig. 14, is qualitatively rather similar to that given by Cornwall (1951, pp. 157–8) for the Greenstone flow of Michigan, although the intensity of the variation in the latter is much less. So far, it seems that no other intrusions provide enough data to be dealt with in this way.

A CROSS CHECK ON THE COMPOSITION OF THE SKAERGAARD LIQUID FROM THE COMPOSITION OF A LABRADORITE CUMULATE OF THE LOWER ZONE OF THE LAYERED SERIES

In the introduction it is stated that it was hoped to obtain the composition of the contemporary magma from certain layered rocks which had a simple make-up of cumulus crystals and intercumulus material. From one such rock, a labradorite cumulate of LZa, a composition for the contemporary magma has been obtained which is fairly close to that obtained from consideration of the successive rock compositions. The rock, 5109, at 110 m in the layered series, comes from a band about 24 in. thick showing only slight igneous lamination (Fig. 7). Plagioclase forms 83 per cent by volume of the rock and the remainder consists of poikilitic crystals of augite, pigeonite inverted to hypersthene, olivine, and iron ore, and there are in addition small patches of quartz or quartz–orthoclase micropegmatite, with rare small apatites and zircons. The poikilitic iron-ore crystals occur in patches separated by one or two centimetres from the next patch. Poikilitic olivine crystals are even more widely separated from their neighbours. Three slices, totalling 15 cm^2, were micrometrically measured on an integrating stage to obtain the mode given in Table 5; it would have been desirable to have measured even more had the specimens been sufficiently large.

The plagioclase of this rock, forming crystals 3 or 4 mm in length and having the shape of thin square tablets, shows considerable zoning; there is an inner core, determined by the maximum symmetrical extinction method on the universal stage as An_{66}, with a broad outer rim going down to about An_{55} with occasional thin outermost zones of even lower anorthite content. The normative plagioclase calculated from the analysis is $Or_{2{\cdot}6}Ab_{36{\cdot}6}An_{60{\cdot}8}$ (mol. per cent).

Augite is in skeletal poikilitic crystals up to 1·5 cm across and enclosing fifty or so plagioclase crystals. Inverted pigeonite occurs in essentially similar skeletal ophitic crystals now partly altered to bastite. There is probably rather more augite than inverted pigeonite. The two pyroxenes cannot be distinguished in the photomicrograph (Fig. 7). Olivine in skeletal poikilitic crystals is rather rare, only one such crystal occurring within the field of Fig. 7, at *a a*. When it occurs it is found in units 0·5 cm across and the nearest neighbouring olivine

may be 4 or 5 cm away. From optical data the composition is not fully established, but the Fo content is less than Fo_{42} mol. per cent. Iron ore occurs as skeletal ophitic crystals rather similar in size to the olivine but more frequent.

Quartz, and sometimes micropegmatite, are found sporadically between the felspars (Fig. 7, at *b b*). Apatite occurs in some abundance in a similar situation to the quartz and often associated with it; the crystals are of moderate size and

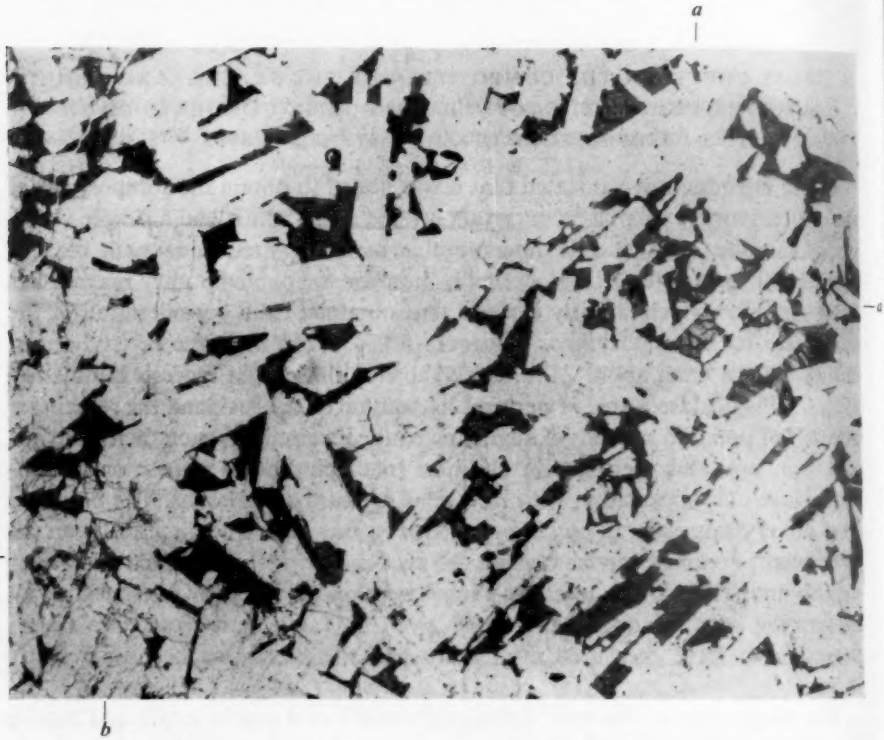

FIG. 7. Photomicrograph of labradorite cumulate 5109 showing poikilitic intercumulus crystals of pyroxene, titaniferous magnetite, olivine (*a a*) and micropegmatite (*b b*). Magnification ×7.

are sometimes seen to be allotriomorphic to the early felspar. Small zircon crystals are occasionally to be seen in association with the quartz and apatite. Hydrothermal alteration is liable to occur in the neighbourhood of the late crystallizing quartz and apatite; the hydrothermal minerals formed are bastite from the hypersthene, hornblende, chlorite, epidote, and considerable amounts of a micaceous mineral replacing plagioclase.

Quartz is not present in the average rocks of the layered series at these low horizons, where abundant olivine, about Fo_{65}, occurs; its presence in the leucocratic bands had not been discovered when the original paper was published in 1939, but it now proves to be a standard feature of the leucocratic rock. Apparently

TABLE 5

Composition, norm, and mode of the labradorite cumulate (5109) *and two different estimates of the composition of the contemporaneous liquid*

		Liquid at 5109 *horizon* (72% *solidified*)	
	Rock analysis of 5109* (110 *m*)	*By subtraction of cumulus plagioclase* An_{64} (*see Fig.* 8)	*Calculated from successive rock compositions* (*see Fig.* 14)
SiO_2	50·65	47·3	46·8
Al_2O_3	25·54	15·3	15·4
Fe_2O_3	1·11	3·5	3·2
FeO	4·07	12·4	12·4
MgO	1·90	5·9	6·2
CaO	11·74	9·4	10·2
Na_2O	3·54	2·55	2·72
K_2O	0·36	0·20	0·33
H_2O^+	0·44	1·6	
H_2O^-	0·04		
TiO_2	0·50	1·6	2·15
P_2O_5	0·16	0·70	0·26
MnO	0·09	0·25	0·18
TOTAL	100·14	100·70	99·94

Norm of 5109			*Weight% Mode of* 5109	
Qz	—		Quartz and orthoclase	1·3
Or	2·22	84·61	Plagioclase	79·3
Ab	29·87		Pyroxene	16·1
An	52·52		Olivine	0·4
	1·97		Iron ore	2·3
Di	0·90	3·93	Apatite, Chlorite, &c.	0·7
	1·06			
Hy	2·80	6·36		
	3·56			
Ol	0·70	1·72		
	1·02			
Mγ	1·62	2·53		
Il	0·91			
Ap	0·34			
Water	0·48			
TOTAL	99·97			

* New analysis by E. A. Vincent and B. A. Collett.

quartz crystallized from the intercumulus liquid only where there was no cumulus magnesian olivine with which the excess silica could react.

This rock is interpreted as consisting of plagioclase crystals, about An_{66}, perhaps slightly enlarged by adcumulate growth and surrounded by material which has crystallized from the trapped liquid. If from the bulk analyses the amount of the oxides present in the (extended cumulus) plagioclase be subtracted, the composition of the trapped liquid should be obtained. This process has been carried out graphically, as shown in Fig. 8. The composition of the

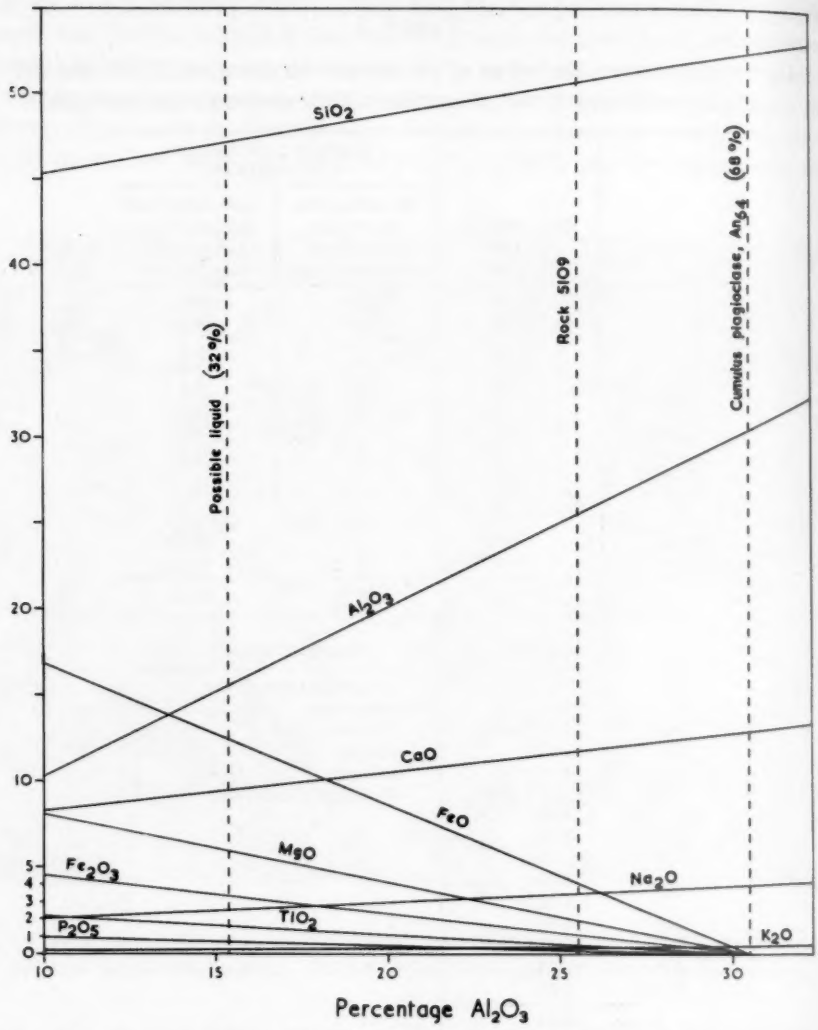

FIG. 8. Plot of the compositions of the labradorite cumulate (EG5109) and of the cumulus felspar An_{64} with the deduced composition of the trapped liquid.

rock and of plagioclase $Or_{2\cdot5}Ab_{33\cdot5}An_{64}$ are plotted against the percentage of Al_2O_3, and the possible liquid having 15·3 per cent Al_2O_3 (the amount found in the liquid at this horizon by the consideration of successive rock compositions) is obtained. Plagioclase of this particular composition is subtracted, although the optical determinations indicated $An_{66}\pm2$, as it gives a rather closer approach to the composition of the liquid obtained by the other method. The orthoclase percentage assumed is based on the analysis of a similar plagioclase by W. A.

Deer (Wager & Mitchell, 1951, p. 146). With these assumptions the amount of plagioclase which has to be subtracted to give the presumed pore liquid composition is 68 per cent. The composition of the liquid obtained by subtraction of the cumulus plagioclase is compared with that from consideration of the successive rock compositions in Table 5. A range of compositions for the pore liquid could, of course, be obtained by subtracting different amounts of cumulus plagioclase and the range might at no point correspond to that obtained graphically from the successive rock composition method. The fact, however, that at one point, when 68 per cent of plagioclase is subtracted, there is good agreement, suggests that the various assumptions are well founded. The mode and texture of the rock make it reasonable that it should consist of 68 per cent of extended plagioclase cumulus crystals of An_{64} composition. In another case estimates of the composition of the contemporary liquid from what was believed to be a plagioclase cumulate have not given reasonable results; it is likely that the make-up of this rock is more complex than assumed and that the rock is actually a heteradcumulate. The method of obtaining the composition of the trapped liquid by subtracting the composition of the presumed cumulus material is likely to be more valuable as a means of deciding on the make-up of a particular cumulate, assuming the composition of the contemporary magma obtained by the successive rock composition method, than as a means of obtaining the composition of trapped liquid by assumptions about the nature of the cumulate.

SOME RELATIONSHIPS AND COMPARISONS CONCERNING THE SKAERGAARD LIQUID LINE OF DESCENT

One of the methods of defining the stage of fractionation of basic magma is based on the use of the albite and iron ratios, the two most significant ratios for ordinary basic magma. This was done *inter alia* for the estimated composition of the changing Skaergaard magma in a recent paper (Wager, 1955, fig. 1), and it is repeated here using the revised estimate of composition (Fig. 9). The plotting shows that, with these criteria, the original Skaergaard magma belongs to the early fractionation stage, the LZ liquid to the middle stage, and the UZb liquid to the late stage. It is worth noting that the LZ liquid of a middle fractionation stage formed at 76 per cent solidified, while the UZb liquid of a late fractionation stage formed when 98 per cent of the original magma had solidified. On the diagram the positions of certain rocks of the layered series are also indicated and tied to the contemporary magma composition. The spread on the diagram of the contemporaneous rocks is very great, but their situation is reasonable when their make-up is considered. The average rocks, 4087 and 5181, have lower Ab ratios because they contain a considerable amount of cumulus plagioclase which is more basic than the normative plagioclase of the liquid. They also have a lower iron ratio because they contain a considerable amount of cumulus ferromagnesian minerals which are more

magnesium-rich than the normative ferromagnesian minerals of the liquid. For the same reason the leucocratic rocks should have a lower albite ratio than the liquid but they should have the same iron ratio, since that ratio should be due solely to the trapped liquid; the position of the plotted points fits these con-

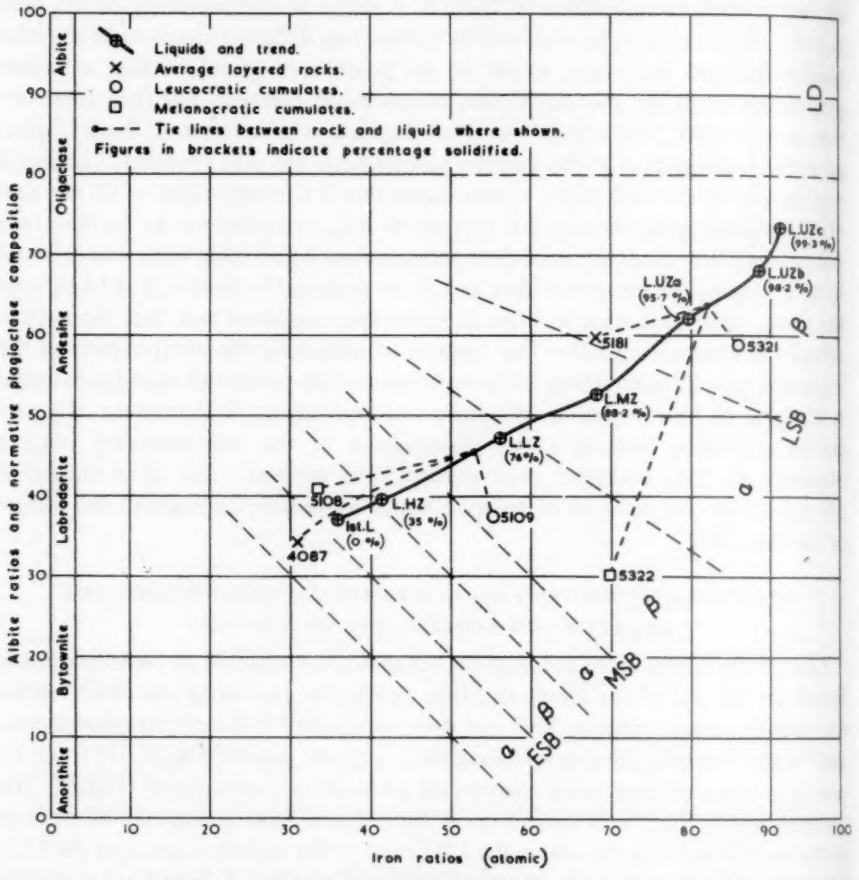

FIG. 9. Skaergaard liquid compositions plotted to show fractionation stages. Points for certain layered rocks are shown tied to the corresponding liquid.

siderations. Similarly, the melanocratic rocks should have lower iron ratios than the corresponding liquid, and, ideally, the same albite ratios as the latter should be due solely to there being intercumulus material with the albite ratio of the contemporary magma. The melanocratic rock 5108 plots in the expected position, but the other melanocratic rock has so little plagioclase in it that the albite ratio based on the norm is not significant since all Al is formally allotted to the An molecule, whereas in fact most is in the pyroxene. The iron ratio is also higher than would be expected because it is much affected by the abundant

iron ore and not merely by the iron to magnesium ratio of the ferromagnesian minerals.

The trend in composition of the Skaergaard liquid and corresponding rocks was shown in the original paper (Wager & Deer, 1939, p. 231) by plotting on a triangular diagram the amounts of three groups of normative constituents: (1) the most refractory, i.e. anorthite, wollastonite, enstatite, and forsterite; (2) the medium refractory, ferrosilite, fayalite, ilmenite, and magnetite; (3) the least refractory, orthoclase and albite. The plots showed that fractionation produced a trend from the most refractory towards the medium refractory and finally towards the least refractory. To save the effort of calculating norms when extensive comparisons were to be made, the more significant oxides in the three groups of normative minerals, namely, MgO, FeO, and Na_2O+K_2O were used instead (Wager & Deer, 1939, pp. 313–14). This simplified type of diagram, which preserves many of the useful features of the original, has been used since by Walker & Poldervaart (1949), Kuno *et al.* (1957), and others. It has sometimes been modified by using atomic proportions of Mg, Fe^{2+}, and Na+K, and this is without doubt an improvement. Often, however, it has also been modified by adding Fe_2O_3 to the FeO. To bring in Fe_2O_3 may suit rocks in which oxidation of iron has occurred extensively during or after fractionation, but it makes it more difficult to understand the meaning of the distribution of points in terms of fractionation, although the implications will ultimately have to be faced. On the diagram given here (Fig. 10), in which atomic percentages are used, the trend of the Skaergaard liquid is seen to lead to extreme richness in iron. Since various assumptions have had to be made in obtaining the liquid composition it might be argued that such an extreme iron-rich liquid composition was the result of errors in these assumptions, but this is believed not to be the case, because the precipitation of iron wollastonite at a late stage of the fractionation is indicative of an exceptionally iron-rich liquid. From 0 to 99 per cent solidified the trend shows only a 5 per cent increase in Na_2O+K_2O. It is only after this stage that the trend is strongly towards the Na_2O+K_2O corner, and this part of the differentiation is not being considered here. Points are also shown on the graph for some of the rocks of the layered series with tie-lines to the corresponding liquid. The points for rocks at the same level but from different rhythmic layers are widely separated from the liquid composition, but their positions are again generally understandable when the make-up of the rocks is kept in mind. The inset to Fig. 10 shows the same liquid compositions in terms of weight percentages of the oxides and indicates the spread of points for Mull and Ardnamurchan lavas and dyke rocks taken from the original paper (Wager & Deer, 1939, fig. 62). The successive liquids, tied to the corresponding average rocks as read from Fig. 14, are shown in Fig. 11. Over the first 80 per cent of the solidification process the composition of the average rock in terms of Mg, Fe, and Na+K is closely similar to the liquid trend, but lags behind it.

The relation between the composition of the cumulus plagioclase in the layered rocks, as determined optically, and the albite ratio of the liquid, which is the same as the normative plagioclase composition, is shown in Fig. 12. On this diagram is also indicated the albite ratio of the melt for the two-component anorthite–albite system (Bowen, 1913) with which the plagioclase cumulus

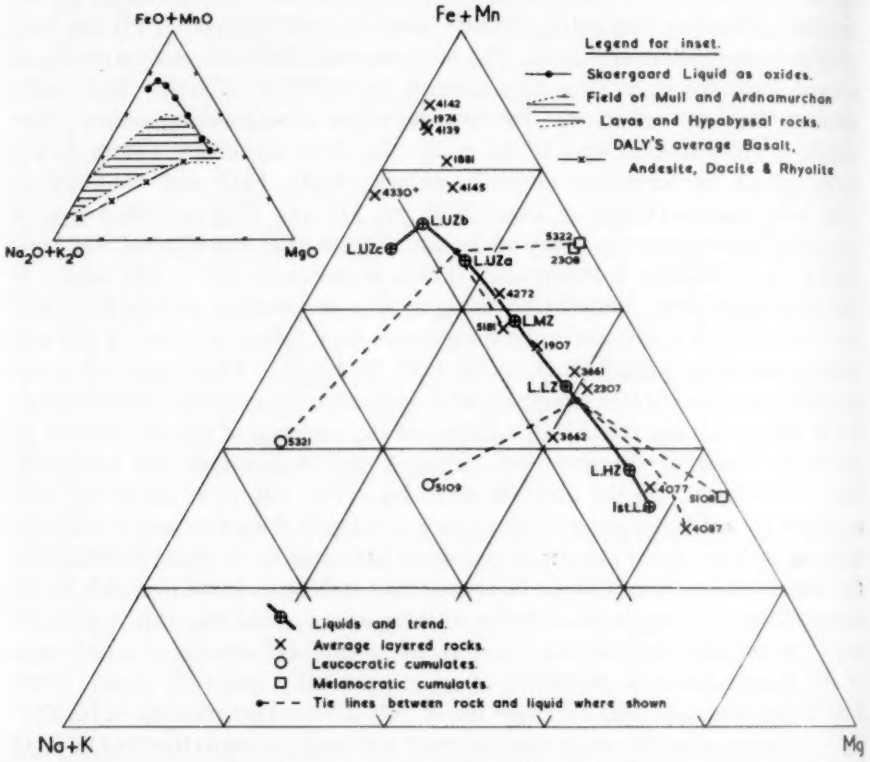

FIG. 10. Successive Skaergaard liquids and selected layered rocks plotted on a triangular diagram showing at the three corners the chief elements of high-, medium-, and low-temperature minerals.

would be in equilibrium. In the natural system there is much less difference in composition between the precipitated plagioclase and normative melt plagioclase than there is between solid and liquid phases in the synthetic two-component system. An essentially similar result was found by Matthews (1957) when comparing the composition of plagioclase phenocrysts and the normative plagioclase of a series of Quaternary lavas from Mount Garibaldi, British Columbia.

The relationship between the iron to magnesium ratio of the successive liquids and the same ratio for the cumulus olivines in equilibrium with them are similarly shown in Fig. 13 and compared with the iron ratio of the liquid

in the Mg_2SiO_4:Fe_2SiO_4 system (Bowen & Schairer, 1935, fig. 7). As for plagioclase, there is less difference in the natural system between the composition of the precipitated olivine and the normative melt olivine than in the synthetic two-component system.

The trend in composition which has been established for the successive residual liquids of the Skaergaard intrusion leads to more extreme compositions than are found among basalts. The trend among basalt lavas often shows a

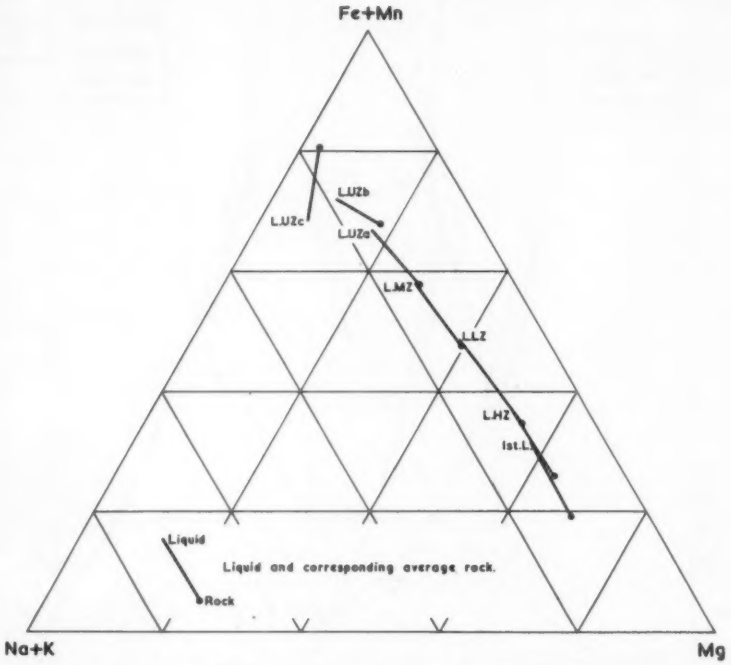

FIG. 11. Triangular diagram of Skaergaard liquids and corresponding average rocks taken from graphs of Fig. 14.

tendency to start off in the direction of the Skaergaard magma trend (cf. fig. 7 in Wager, 1956) but then something intervenes and a very different final result is produced. Sufficiently high enrichment of the magma in ferrous iron to produce the precipitation of iron wollastonite has so far not been described from other rock series. Among various possible reasons for the apparently unusual trend of the Skaergaard liquid line of descent may be the composition of the initial Skaergaard magma which has slight differences from the usual basalt composition and this may possibly lead to big differences in late fractions. Thus the initial Skaergaard magma differs from the commoner basaltic magmas, at a comparable fractionation stage, in being a little poorer in silica, richer in alumina and highly reduced in terms of the ferrous to ferric ratio. The early

stage Medicine Lake Highlands basalt which is beginning to be described as a high-alumina type is very close in composition to the Skaergaard magma (cf. Tilley, 1950). In making a comparison of basalt analyses some such device as a division into fractionation stages is a desideratum. The cursory consideration

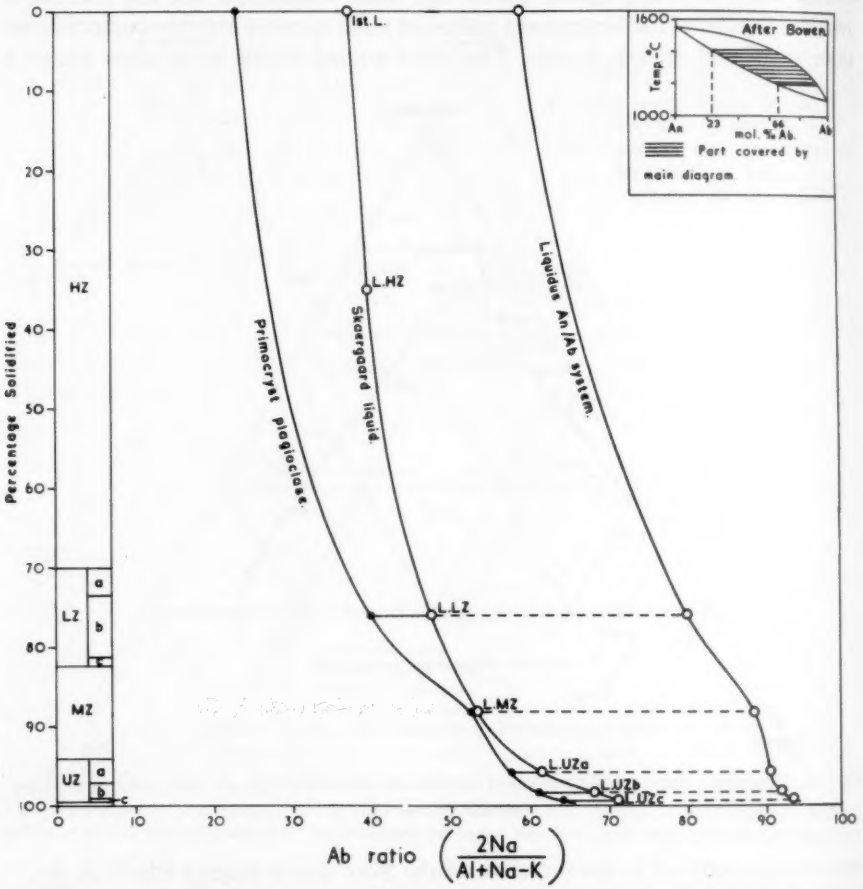

FIG. 12. Plot of the albite ratios of (1) the Skaergaard liquid, (2) the corresponding primocryst plagioclase, and (3) the corresponding liquid in the An/Ab system.

of selected provinces after division into fractionation stages (cf. Wager, 1956, fig. 8) indicates that there are probably many real, but small, variations in the proportion of the oxides in various groups of basalts although no statistical evaluation has been attempted or would be of much value with so few data. High alumina in basalt magma, by producing abundant early plagioclase, should keep silica and soda low in the residual liquid. Low oxidation should delay the formation of cumulus magnetite and encourage the ultimate formation of

ferrous-rich olivine and pyroxene. Thus certain of the special features of the original Skaergaard magma should tend to lead to some of the features characteristic of the fractionation. However, it still seems to be an entirely open question whether the slightly unusual composition of the original Skaergaard

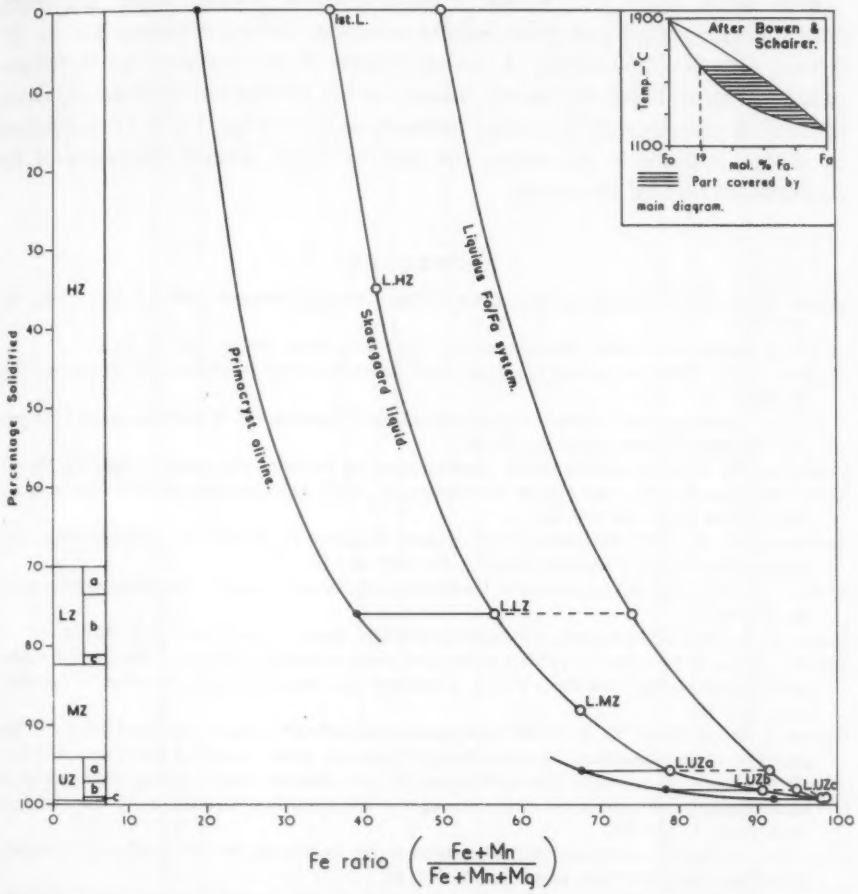

FIG. 13. Plot of the iron ratios of (1) the Skaergaard liquid, (2) the corresponding primocryst olivine, and (3) the corresponding liquid in the Fo/Fa system.

magma is a sufficient cause for the Skaergaard fractionation trend, which differs so notably from the trends usually obtained from studies of the varying composition of groups of consanguineous basaltic lavas.

ACKNOWLEDGEMENTS

The new analyses for this paper have been carried out by my colleague Dr. E. A. Vincent or by Mr. Brian Collett under the direction of Dr. Vincent; to

both I express my thanks. The radioactivation method of analysis for P_2O_5 was devised by Dr. Vincent and the work was carried out by Mr. W. D. Curren and Mr. R. P. C. Pockley; I am very grateful to all three. I wish also to thank Mrs. J. Cooke for her careful calculations and graphing of the data.

Prof. W. A. Deer, joint author of the original Skaergaard paper, has kindly read the manuscript and given helpful criticism. To my colleague Dr. G. M. Brown, who is collaborating in various aspects of the new work on the Skaergaard intrusion, I also express my thanks; he has carried out the determinations of mineral composition by optical methods used for Figs. 1 and 12 and helped by critical reading of the manuscript and by much general discussion of the problems of layered intrusions.

REFERENCES

BOWEN, N. L., 1913. The melting phenomena of the plagioclase feldspars. *Amer. J. Sci.*, 4th ser. **35**, 577–99.

—— & SCHAIRER, J. F., 1935. The system MgO–FeO–SiO_2. Ibid., 5th ser. **29**, 151–217.

BROWN, G. M., 1956. The layered ultrabasic rocks of Rhum, Inner Hebrides. *Phil. Trans. roy. Soc.* B, **240**, 1–53.

—— 1957. Pyroxenes from the early and middle stages of fractionation of the Skaergaard intrusion, East Greenland. *Miner Mag.* **31**, 511–43.

CORNWALL, H. R., 1951. Differentiation in magmas of the Keweenawan series. *J. Geol.* **59**, 151–72.

KUNO, H., YAMASAKI, K., IIDA, C., & NAGASHIMA, K., 1957. Differentiation of Hawaiian magmas *Jap. J. Geol. Geog.* **28**, 179–218.

MATHEWS, W. H., 1957. Petrology of Quaternary volcanics of the Mount Garibaldi map-area, southwestern British Columbia. *Amer. J. Sci.* **255**, 400–15.

MUIR, I. D., 1951. The clinopyroxenes of the Skaergaard intrusion, eastern Greenland. *Miner. Mag.* **29**, 690–714.

TILLEY, C. E., 1950. Some aspects of magmatic evolution. *Quart. J. geol. Soc. Lond.* **106**, 37–61.

VINCENT, E. A., & PHILLIPS, R., 1954. Iron-titanium oxide minerals in layered gabbros of the Skaergaard intrusion, East Greenland. Part 1. Chemistry and ore-microscopy. *Geochim. et Cosmoch. Acta*, **6**, 1–26.

WAGER, L. R., & DEER, W. A., 1939. Geological investigations in East Greenland. Part III. The petrology of the Skaergaard intrusion, Kangerdlugssuak. *Medd. Grønland*, **105**, No. 4, 1–352.

—— & MITCHELL, R. L., 1951. The distribution of trace elements during strong fractionation of basic magma—a further study of the Skaergaard intrusion, East Greenland. *Geochim. et Cosmoch. Acta*, **1**, 129–208.

—— 1956. A chemical definition of fractionation stages as a basis for comparison of Hawaiian, Hebridean, and other basic lavas. Ibid. **9**, 217–48.

—— VINCENT, E. A., & SMALES, A. A., 1957. Sulphides in the Skaergaard intrusion, East Greenland. *Econ. Geol.* **52**, 855–903.

—— BROWN, G. M., & WADSWORTH, W. J., 1960. Types of igneous cumulates. *J. Petrol.* **1**, No. 1, 71–85.

WALKER, F., & POLDERVAART, A., 1949. Karroo dolerites of the Union of South Africa. *Bull. geol. Soc. Amer.* **60**, 591–706.

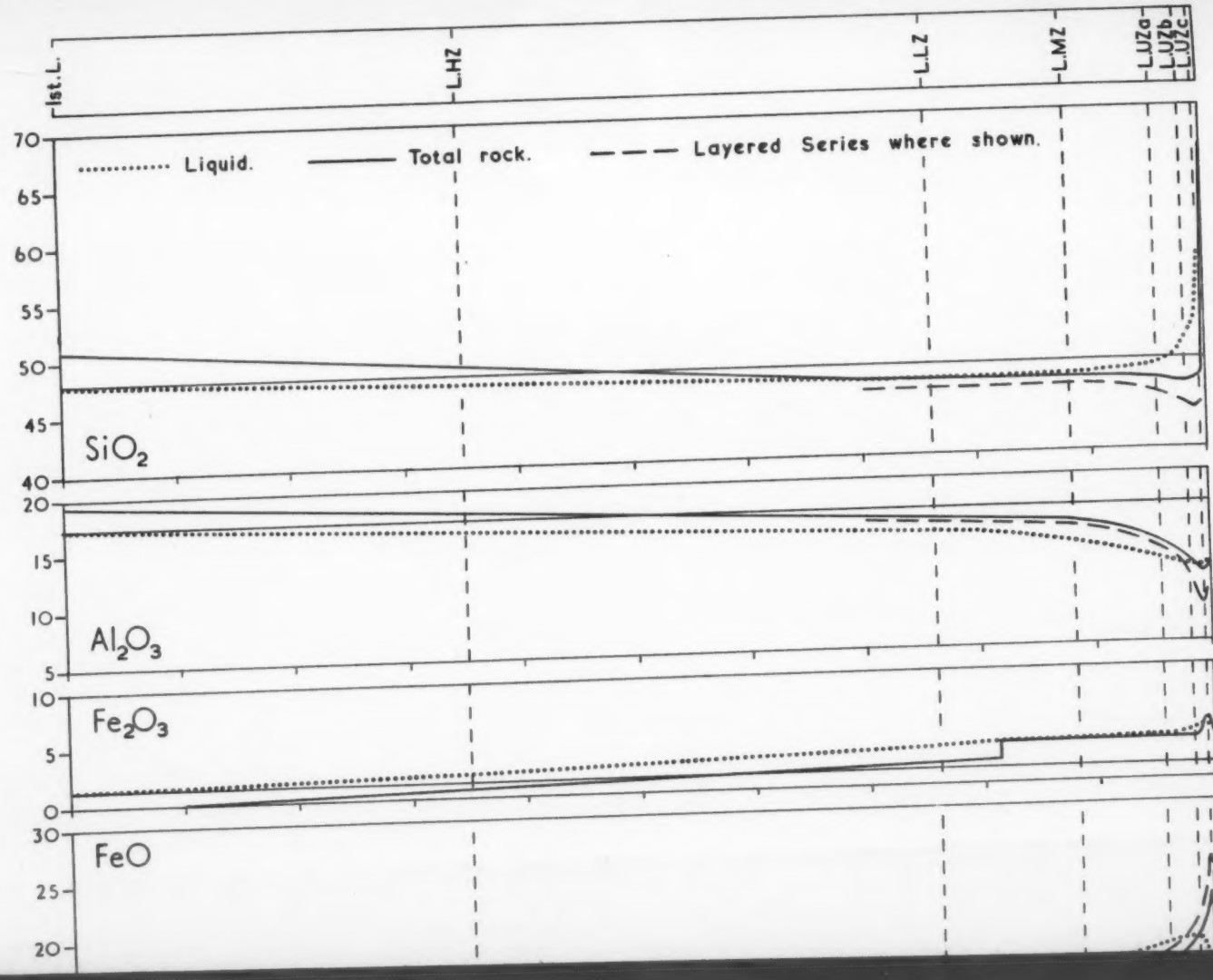
Ist.L.
L.HZ
L.L.Z
L.M.Z
L.U.Z.a
L.U.Z.b
L.U.Z.c
..... Liquid.
——— Total rock.
— — — Layered Series where shown.
70
65
60
55
50
45
40
SiO_2
20
15
10
5
Al_2O_3
10
5
0
Fe_2O_3
30
25
20
FeO

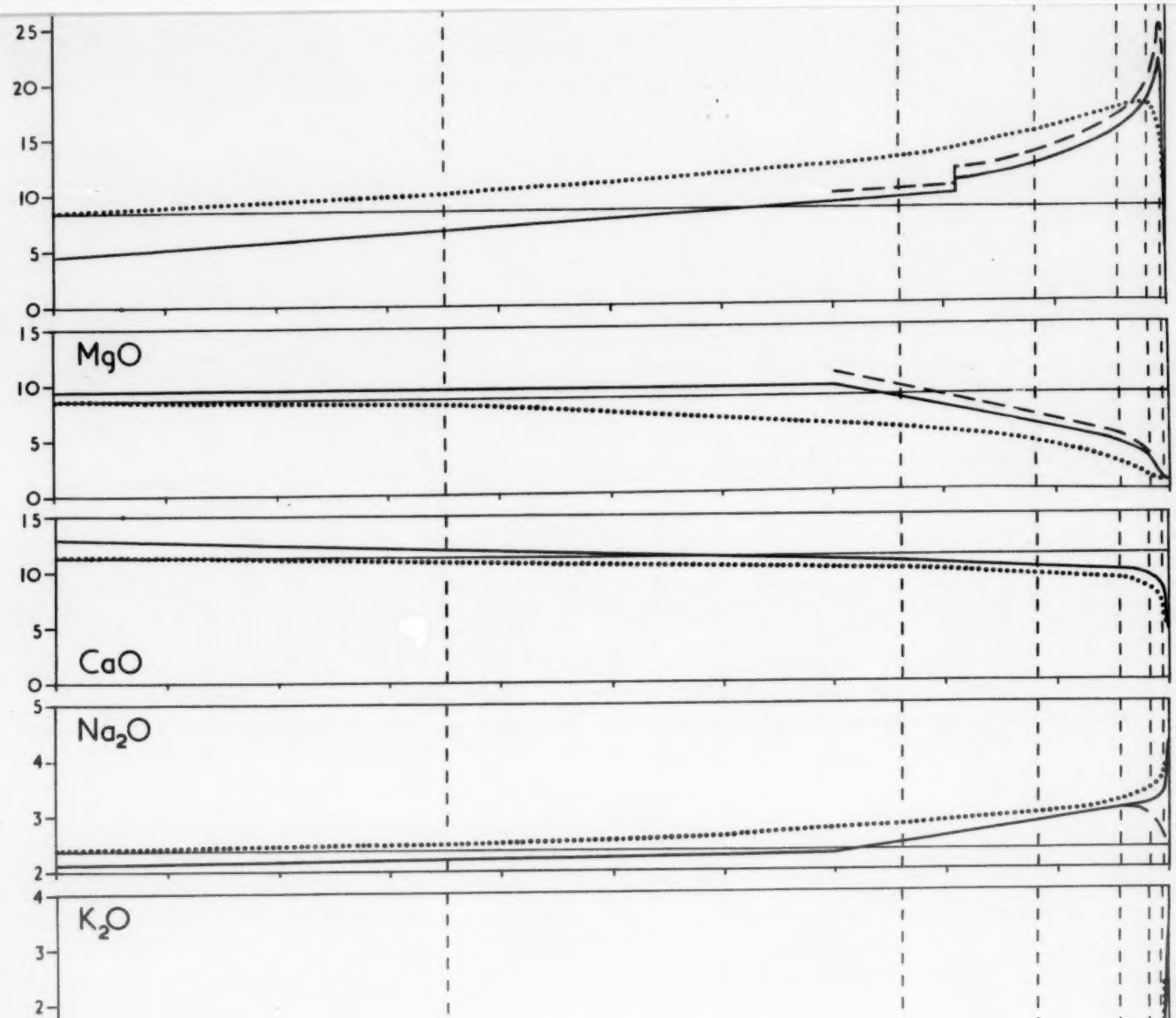
25
20
15
10
5
0
MgO
15
10
5
0
CaO
15
10
5
0
Na2O
5
4
3
2
K2O
4
3
2

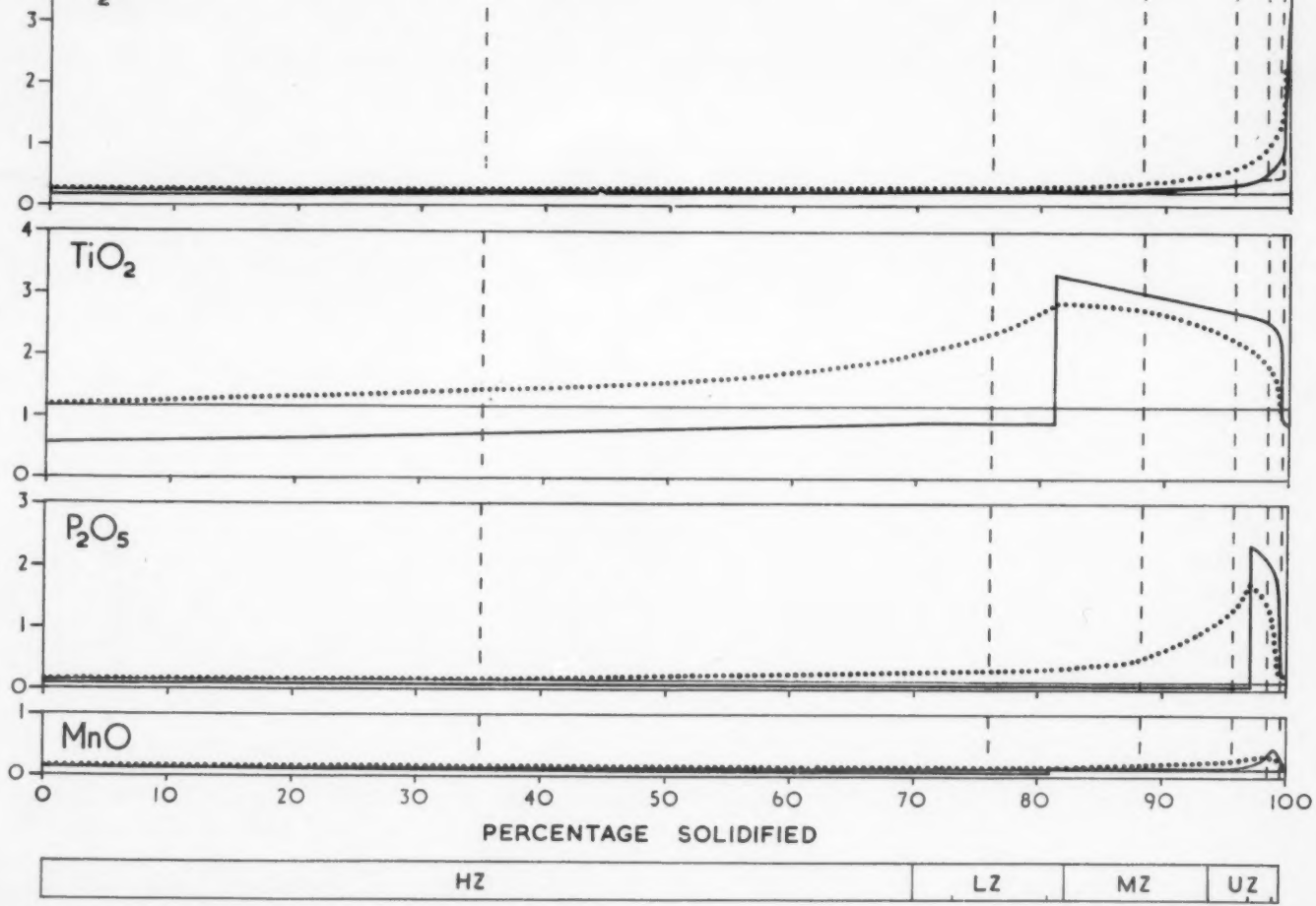

FIG. 14. Variation in the amounts of the major elements in the total rock separating from the Skaergaard liquid at successive stages and the corresponding variation in these liquids. Amounts in the average layered rocks are shown where differing significantly from that in the total rock.